

**Canterbury Earthquakes 2010/11 Port Hills Slope
Stability: Risk assessment for Quarry Road**

C. I. Massey
B. Lukovic

F. Della Pasqua
W. Ries

T. Taig
D. Heron

**GNS Science Consultancy Report 2014/75
August 2014 FINAL**



DISCLAIMER

This report has been prepared by the Institute of Geological and Nuclear Sciences Limited (GNS Science) exclusively for and under contract to Christchurch City Council.

The report considers the risk associated with geological hazards. As there is always uncertainty inherent within the nature of natural events GNS Science gives no warranties of any kind concerning its assessment and estimates, including accuracy, completeness, timeliness or fitness for purpose and accepts no responsibility for any actions taken based on, or reliance placed on them by any person or organisation other than Christchurch City Council.

GNS Science excludes to the full extent permitted by law any liability to any person or organisation other than Christchurch City Council for any loss, damage or expense, direct or indirect, and however caused, whether through negligence or otherwise, resulting from any person or organisation's use of, or reliance on this report.

The data presented in this Report are available to GNS Science for other use after the public release of this document.

BIBLIOGRAPHIC REFERENCE

Massey, C. I.; Della Pasqua, F.; Taig, T.; Lukovic, B.; Ries, W.; Heron, D. 2014. Canterbury Earthquakes 2010/11 Port Hills Slope Stability: Risk assessment for Quarry Road. *GNS Science Consultancy Report 2014/75*. 115 p.+ Appendices

REVIEW DETAILS

This report in draft form was independently reviewed by Dr L. Richards and Dr J. Wartman. Internal GNS Science reviews of drafts were provided by N. Litchfield, M. McSaveney, D. Mieler and R. Buxton.

Risk calculations were checked by R. Buxton (GNS Science).

CONTENTS

EXECUTIVE SUMMARY	VIII
ES 1 INTRODUCTION.....	VIII
ES 2 INVESTIGATION PROCESS AND FINDINGS	IX
ES 3 CONCLUSIONS	XI
ES3.1 Hazard	xi
ES3.2 Risk.....	xi
ES3.3 Risk management	xii
ES 4 RECOMMENDATIONS.....	XII
ES4.1 Policy and planning	xii
ES4.2 Short-term actions	xii
ES4.3 Long-term actions.....	xiii
1.0 INTRODUCTION	1
1.1 BACKGROUND	1
1.2 THE QUARRY ROAD MASS MOVEMENTS.....	5
1.3 PREVIOUS WORK AT THE QUARRY ROAD SITE	9
1.4 SCOPE OF THIS REPORT.....	11
1.5 REPORT STRUCTURE	12
1.6 METHODS OF ASSESSMENT	12
1.6.1 Engineering geology assessment methodology.....	12
1.6.2 Hazard assessment.....	12
1.6.3 Estimation of landslide volumes	13
1.6.4 Risk assessment	13
2.0 DATA USED	15
3.0 SITE ASSESSMENT RESULTS	17
3.1 SITE HISTORY.....	17
3.1.1 Before the 2010/11 Canterbury earthquakes	17
3.1.2 During the 2010/11 Canterbury earthquakes	17
3.1.3 After the 2010/11 Canterbury earthquakes	17
3.2 SITE INVESTIGATIONS	21
3.2.1 Geomorphological mapping	21
3.2.2 Subsurface trenching and drilling	21
3.2.3 Surface movement	21
3.2.4 Subsurface movement	22
3.2.5 Groundwater	22
3.3 ENGINEERING GEOLOGICAL MODEL.....	23
3.3.1 Slope materials.....	23
3.3.2 Geotechnical properties	24
3.3.3 Rainfall and groundwater response.....	29
3.4 SLOPE FAILURE MODELS	33
4.0 HAZARD ASSESSMENT RESULTS	35

4.1	SLOPE STABILITY – STATIC CONDITIONS	35
4.1.1	Source area 11A (cross-section 2).....	35
4.1.2	Source area 11B (cross-section 1).....	37
4.1.3	Source area 11C (cross-section 3).....	40
4.2	SLOPE STABILITY – DYNAMIC CONDITIONS.....	47
4.2.1	Amplification of ground shaking	47
4.2.2	Back-analysis of permanent slope deformation	48
4.2.3	Slope stability – summary of results.....	61
4.3	RUNOUT DISTANCE	62
4.3.1	Potential source volume estimation	62
4.3.2	Runout modelling	65
4.3.3	Forecast runout modelling.....	70
5.0	RISK ASSESSMENT RESULTS	75
5.1	TRIGGERING EVENT FREQUENCIES	75
5.1.1	Frequency of earthquake triggers	75
5.1.2	Frequency of rainfall triggers.....	76
5.2	EARTH/DEBRIS FLOWS (SOURCE AREAS 11A AND 11C).....	76
5.2.1	Peak ground acceleration and permanent slope displacement	76
5.2.2	Overall triggering event frequency	77
5.3	CLIFF COLLAPSE (SOURCE AREA 11B)	78
5.3.1	Peak ground acceleration and permanent slope displacement	78
5.3.2	Permanent slope displacement and likelihood of catastrophic slope failure	78
5.4	DEAGGREGATION OF THE PROBABILISTIC SEISMIC HAZARD MODEL.....	79
5.5	DWELLING OCCUPANT RISK.....	80
5.5.1	Variables adopted for the risk assessment	80
5.5.2	Source areas 11A and 11C.....	87
5.5.3	Source area 11B.....	89
5.5.4	Source area 11E.....	90
5.6	ROAD USER RISK.....	90
6.0	DISCUSSION.....	99
6.1	DWELLING OCCUPANT RISK.....	99
6.2	ROAD USER RISK.....	100
6.3	ANNUAL FREQUENCY OF THE EVENT	100
6.3.1	Source areas 11A and 11C (earth/debris flows)	100
6.3.2	Source areas 11B and 11E (cliff collapses)	101
6.4	RISK ASSESSMENT SENSITIVITY TO UNCERTAINTIES	102
6.4.1	Source volumes.....	102
6.4.2	Annual frequency of the triggering event	102
6.4.3	Other key uncertainties	103
6.4.4	How reliable are the results?.....	103
7.0	CONCLUSIONS	107
7.1	HAZARD.....	107

7.2	RISK.....	107
7.2.1	Dwelling occupant	107
7.2.2	Road user	107
7.2.3	Risk management	108
8.0	RECOMMENDATIONS.....	109
8.1	POLICY AND PLANNING.....	109
8.2	SHORT-TERM ACTIONS.....	109
8.2.1	Hazard monitoring strategy	109
8.2.2	Risk monitoring strategy.....	109
8.2.3	Surface/subsurface water control.....	109
8.3	LONG-TERM ACTIONS.....	110
8.3.1	Engineering measures	110
8.3.2	Reassessment.....	110
9.0	REFERENCES	111
10.0	ACKNOWLEDGEMENTS.....	115

FIGURES

Figure 1	Location map	3
Figure 2	Mass movement location map showing assessed source area locations.....	7
Figure 3	Aerial view of the Quarry Road source areas 11A and 11C (within the yellow dashed lines). Photograph taken by M. Yetton (2012).	10
Figure 4	Aerial view of the Quarry Road source area 11B (within the yellow dashed line). Photograph taken by M. Yetton (2012).....	11
Figure 5	Engineering geological map (reproduced from Yetton and Engel, 2014).	19
Figure 6	Engineering geological cross-sections (reproduced from Yetton and Engel, 2014).	20
Figure 7	Numerical slope stability back-analysis of the fill material for cross-section 2, representing source area 11A.	25
Figure 8	Geological strength index plot for volcanic breccia at Quarry Road (modified after Hoek, 1999).	26
Figure 9	Daily rainfalls at Christchurch Botanic Gardens and landslides in the Port Hills.....	30
Figure 10	Rainfall depth-duration-return period relations estimated by Griffiths et al. (2009) using recorded rainfall data. Error limits of 20% are shown by dotted lines for the 1/2 and 1/100 AEP curves.....	32
Figure 11	Sensitivity assessment of the slope factor of safety (source area 11A) in response to changing piezometric head levels and tension crack conditions. Variable tension crack depths have been used.	37
Figure 12	Numerical slope stability back-analysis of the fill/buried top soil material for cross-section 3, representing source area 11C.	41
Figure 13	Example of limit equilibrium and finite element modelling results for cross-section 2, representing source area 11A.	42
Figure 14	Example of limit equilibrium and finite element modelling results for cross-section 1, representing source area 11B, for failure mechanism 1 through the loess.....	43

Figure 15	Example of limit equilibrium and finite element modelling results for cross-section 1, representing source area 11B, for failure mechanism 2 through the rock.	44
Figure 16	Example of limit equilibrium and finite element modelling results for cross-section 1, representing source area 11B, for failure mechanism 3 through the weak layer.	45
Figure 17	Example of limit equilibrium and finite element modelling results for cross-section 3, representing source area 11C, for a failure mechanism through the fill and loess.	46
Figure 18	22 February 2011 earthquake, modelled Slope/W decoupled displacements for source area 11A (cross-section 2), adopting variable estimates of the material strength of the fill.	50
Figure 19	13 June 2011 earthquake, modelled Slope/W decoupled displacements for source area 11A (cross-section 2), adopting variable estimates of the material strength of the fill.	51
Figure 20	Source area 11A (cross-section 2) seismic slope stability assessment for the 22 February 2011 earthquake. The slide surface, and associated slide mass, with the lowest yield acceleration is shown bright green in colour.	51
Figure 21	Source area 11B (cross-section 1) seismic slope stability assessment for the 22 February 2011 earthquake.	52
Figure 22	Source area 11B (cross-section 1) seismic slope stability assessment for the 22 February 2011 earthquake.	53
Figure 23	Source area 11B (cross-section 1) seismic slope stability assessment for the 22 February 2011 earthquake.	53
Figure 24	22 February 2011 earthquake, modelled Slope/W decoupled displacements for source area 11B (cross-section 1), adopting variable estimates of the material strength of the loess and rock.	54
Figure 25	22 February and 13 June 2011 earthquakes, modelled Slope/W decoupled displacements for source area 11B (cross-section 1), adopting variable estimates of the material strength of the rock.	55
Figure 26	Yield acceleration of the slope based on variable fill parameters and loess parameters shown in Table 11. Yield acceleration calculated adopting the pseudostatic method (Kramer, 1996).	56
Figure 27	Source area 11A (cross-section 2), decoupled Slope/W displacements calculated for different ratios of yield acceleration to maximum average acceleration of the mass (K_y/K_{MAX}), and maximum acceleration of the mass (K_y/A_{FF}), for selected slide-surface geometries, and given material shear strength parameters.	58
Figure 28	Source area 11B (cross-section 1), decoupled Slope/W displacements calculated for different ratios of yield acceleration to maximum average acceleration of the mass (K_y/K_{MAX}), and maximum acceleration of the mass (K_y/A_{FF}), for selected slide-surface geometries, and given material shear strength parameters.	59
Figure 29	Estimation of landslide volume assuming a quarter-ellipsoid shape.	63
Figure 30	Proportion of volume from debris avalanches in the Port Hills greater than or equal to a given volume.	64
Figure 31	Estimation of landslide volumes in the Port Hills loess from Townsend and Rosser (2012) adopting the area depth relationships of Larsen et al. (2010).	64
Figure 32	Empirical fahrboeschung angle measurements. The empirical fahrboeschung relationships, expressed as the ratio of height (H) to length (L) for debris avalanche talus and boulder roll (rockfalls), recorded in the Port Hills. N = 45 sections. Errors are expressed as the mean \pm one standard deviation (STD).	65
Figure 33	Estimation of boulder roll and talus fahrboeschung angles based on empirical runout data.	66

Figure 34	Estimation of debris flow fahrboeschung angles based on empirical runout data presented in Massey and Carey (2012).....	67
Figure 35	Range of parameters used to back-analyse the runout of debris avalanches in the Port Hills triggered by the recent earthquakes using the RAMMS software (RAMMS, 2011).	68
Figure 36	Range of parameters for different mass movement processes: a) debris flows, b) snow avalanches, c) snow avalanches, d) ice avalanches, e) debris floods.....	68
Figure 37	Mean volume difference between the RAMMS modelled volumes and the actual recorded volumes per 1 m ² grid cell. N = 23 debris avalanches triggered by 22 February and 13 June 2011 earthquakes.	69
Figure 38	Comparison between the RAMMS modelled and the empirical-modelled debris runout (Figure 36) and the actual recorded runout for debris avalanches triggered by the 22 February and 13 June 2011 earthquakes. N = 23 debris avalanches.	70
Figure 39	Earth/debris flow and debris avalanche hazard maps.	71
Figure 40	Dwelling occupant risk maps.	83
Figure 41	Sensitivity of the risk estimates for source area 11A, upper volume estimates, for triggering event return periods of 20, 50, 100 and 200 years.	88
Figure 42	Road user risk maps.	91
Figure 43	Maximum calculated road user risk per journey, source area 11A.	95
Figure 44	Maximum calculated road user risk per journey, source area 11B.	95

TABLES

Table 1	Assessed mass movement relative hazard exposure matrix (from the Stage 1 report, Massey et al., 2013).	5
Table 2	Summary of the main data used in the analysis. LiDAR is Light Detecting and Ranging.	15
Table 3	Measured cumulate crack apertures, which formed mainly during the 22 February, and less so during the 13 June, 2011 earthquakes, measured by the Port Hills Geotechnical Group (Yetton and Engel, 2014).....	21
Table 4	Range of bulk geotechnical material parameters adopted for Quarry Road soils.....	27
Table 5	Range of adopted rock strength parameters.	28
Table 6	Annual frequencies of given rainfall in the Christchurch for four main events following the 2010/11 Canterbury earthquakes (rainfalls are calculated daily from 09:00 to 09:00 NZST).....	31
Table 7	Example results from slope stability assessment of source area 11A (cross-section 2).....	35
Table 8	Example results from slope analysis of source area 11B across cross-section 1.....	39
Table 9	Example results from slope stability assessment of source area 11C across cross-section 3.	40
Table 10	Material strength parameters used for modelling permanent coseismic displacements for cross-sections 1 and 2. Coseismic displacements are inferred from survey records and field mapping of cracks.....	49
Table 11	Forecast modelling results from the dynamic slope stability assessment for source areas 11A and 11B. Estimated displacements are rounded to the nearest 0.1 m.....	60
Table 12	Example of estimated source volumes (the first digit in the number is significant) and Fahrboeschung angles.....	63

Table 13	The annual frequency of a given peak ground acceleration (PGA) band occurring on rock (site class B) for different years from the 2012 seismic hazard model for Christchurch (G. McVerry, personal communication 2014).	75
Table 14	Probability of failure for source area 11A. Estimated displacements are rounded to the nearest 0.1 m, and are based on the relationship between K_y/K_{MAX} shown in Figure 27.	77
Table 15	Probability of failure for source area 11B. Estimated displacements are rounded to the nearest 0.1 m, and are based on the relationship between K_y/K_{MAX} shown in Figure 28.	79
Table 16	Main Road usage assumptions.	97
Table 17	Uncertainties and their implications for risk.	104

APPENDICES

A1	APPENDIX 1: METHODS OF ASSESSMENT	A1-1
A1.1	ENGINEERING GEOLOGY ASSESSMENT METHODOLOGY	A1-1
A1.2	HAZARD ASSESSMENT METHODOLOGY	A1-1
	A1.2.1 Slope stability modelling	A1-2
	A1.2.2 Estimation of slope failure volumes	A1-5
	A1.2.3 Debris runout modelling	A1-6
A1.3	RISK ASSESSMENT	A1-7
	A1.3.1 Fatality risk for dwelling occupants	A1-8
	A1.3.2 Probability of inundation	A1-11
	A1.3.3 Probability of a person being present	A1-12
	A1.3.4 Probability of the person being killed if inundated by debris	A1-13
	A1.3.5 Road-user risk assessment	A1-15
	A1.3.6 Road user risk assessment illustration	A1-22
	A1.3.7 Road user risk – Additional discussion on main assumptions	A1-25
A2	APPENDIX 2: PAST LANDSLIDES IN THE PORT HILLS AND BANKS PENINSULA	A2-1
A3	APPENDIX 3: RESULTS FROM THE TWO-DIMENSIONAL SITE RESPONSE ASSESSMENT FOR CROSS-SECTIONS 1 AND 2	A3-1
A4	APPENDIX 4: RAMMS MODELLING RESULTS FOR SOURCE AREAS 1 AND 2. ESTIMATED LANDSLIDE RUNOUT HEIGHT	A4-1
A5	APPENDIX 5: RAMMS MODELLING RESULTS FOR SOURCE AREAS 1 AND 2. ESTIMATED LANDSLIDE RUNOUT VELOCITY	A5-1

APPENDIX FIGURES

Figure A1.1	Event tree model for road user risk assessment.	A1-16
Figure A3.1	Amplification relationship between the synthetic free-field rock outcrop input motions (A_{FF}) and the modelled cliff crest maximum accelerations (A_{MAX}) for cross-sections 1 and 2.	A3-2
Figure A3.2	Modelled peak horizontal ground acceleration contours for the 22 February 2011 earthquake at Quarry Road, source area 11A (cross-section 2). Note: the high peak horizontal ground accelerations shown at the left of the drawing are not thought realistic as the geological boundary conditions in this area are unknown and have been inferred.....	A3-4
Figure A3.3	Relationship between the modelled horizontal and vertical maximum accelerations modelled at the slope crest (A_{MAX}) for cross-sections 1 and 2, using the synthetic free-field rock outcrop motions for the Quarry Road site by Holden et al. (2014) as inputs to the assessment.	A3-5

APPENDIX TABLES

Table A1.1	Failure mechanisms and landslide hazard types included in this risk assessment.....	A1-8
Table A1.2	Vulnerability factors for different debris velocities used in the risk assessment.....	A1-14
Table A1.3	Definition and derivation of key road risk parameters.....	A1-17
Table A1.4	Assumptions used in quantifying road user risk for Quarry Road.....	A1-19
Table A1.5	Calculation process for risk from hazard 1 (single cell, per journey).	A1-23
Table A1.6	Calculation process for risk from hazard 2 (single cell, per journey).	A1-24
Table A1.7	Calculation of risk parameters of interest from single cell risk per journey.	A1-25
Table A1.8	Traffic volumes for Main Road (from Rantatira Terrace to The Brae), interpolated from Causeway and Ferrymead Road/Main Road junction values.	A1-27
Table A1.9	Traffic density and average journey speeds along Main Road.....	A1-29
Table A1.10	Vulnerabilities estimated for different road users, for loess inundation and for rockfall.	A1-31
Table A3.1	Results from the two-dimensional site response assessment for cross-section 1 (source area 11B) and cross-section 2 (source area 11A), using the synthetic free-field rock outcrop motions for the Quarry Road site by Holden et al. (2014) as inputs to the assessment. PGA is peak ground acceleration.	A3-2

EXECUTIVE SUMMARY

ES 1 INTRODUCTION

This report combines recent field information collected from the Cliff Street site with numerical slope-stability modelling to assess the risk to people in dwellings and users of Main Road from mass movements at the site. The results in this report supersede those in an earlier cliff-collapse study (Massey et al., 2012a).

Following the 22 February 2011 earthquakes, extensive cracking of the ground had occurred in some areas of the Port Hills. In many areas, the cracks were thought to represent only localised relatively shallow ground deformation in response to shaking. In other areas however, the density and pattern of cracking and the amounts of displacement across cracks clearly indicated large mass movements.

Christchurch City Council contracted GNS Science to carry out further detailed investigations of these areas of systematic cracking, in order to assess the nature of the hazard, the frequency of the hazard occurring, and whether the hazard could pose a risk to life, a risk to existing dwellings and/or a risk to critical infrastructure. This work on what are termed mass movements is being undertaken in stages. Stage 1 is now complete (Massey et al., 2013) and stages 2 and 3 are detailed investigations of mass movements from highest to lowest priority.

The Stage 1 report identified 36 mass movements of concern in the Port Hills project area. Four of these were further subdivided based on failure type, giving a total of 46 mass movements including their sub areas. Fifteen of these were assessed as being in the Class I (highest) relative hazard-exposure category. Mass movements in the Class I category could cause loss of life, if the hazard were to occur, as well as severe damage to dwellings and/or critical infrastructure, which may lead to the loss of services for many people.

Quarry Road mass movement area comprises eight localised sites affected by mass-movement processes (11A–H in Figures 1 and 2). Five of these sites (11A–E) were assessed in the Stage 1 report (Massey et al., 2013) as being in the highest relative hazard exposure category (Class I, involving potential risk to life), while the other three sites (11F, G and H) were assessed as being in Class II and III (not a life-safety risk).

This report presents the risk assessment results for four of the Quarry Road Class I mass movements: numbers 11A, 11B, 11C and 11E. Mass movement 11D was removed from the GNS Science assessment as instructed by Council, because the slope in this area had been engineered and a large retaining wall constructed with the work being approved and signed off by Council.

ES 2 INVESTIGATION PROCESS AND FINDINGS

Detailed investigations of the site and its history were carried out by URS Ltd. (Yetton and Engel, 2014). These investigations show evidence of past landslides in the assessment area, from the time of European settlement (about 1840 AD) to present.

The slopes were significantly cracked in the 22 February 2011 earthquakes, and again during the 13 June 2011 earthquakes. Relatively little movement was observed in the other moderate-sized earthquakes. Overall ground displacement through the 2010/11 Canterbury earthquakes is not known as there were no survey markers installed in the main areas where displacement had been identified, to enable before and after measurements to be made.

The present condition of the slopes is that they are significantly cracked, with numerous open cracks in the loess covering and in the rock-slope face, allowing rapid water ingress into the ground. By mapping cracks and relating these to the results of stability assessments, four potential landslide sources (areas 11A, 11B, 11C and 11E) have been identified, which were not addressed in the earlier cliff-collapse study. These landslide hazards are: 1) earth/debris flows occurring in the loess and fill (soil) materials; and 2) larger cliff collapses (comprising debris avalanches and cliff-top recession volumes that are larger than those previously assessed) occurring in the volcanic rock.

Two main types of landslide hazard are identified at the site: 1) earth/debris flows originating from the fill and loess slopes (source areas 11A and 11C); and 2) larger cliff collapses (comprising debris avalanches and cliff-top recession volumes that are larger than those previously assessed) occurring in the volcanic rock (source areas 11B and 11E).

Numerical models have been used to assess the stability of the Quarry Road slopes, in particular the two potential landslide hazard types. Analyses have considered both:

- static (without earthquake shaking); and
- dynamic (with earthquake shaking) conditions.

Earth/debris flows (source areas 11A and 11C)

The main triggering mechanism for source areas 11A and 11C is thought to be rain, although earthquake shaking could induce failure, especially if it occurs when the slope is wet. Rainfall-induced failures pose the greatest risk because the landslides are likely to be more mobile due to their fluid nature and ability to run-out further, and rainfall occurs more frequently than strong earthquakes.

Source areas 11A and 11C are primarily formed of fill, mainly comprising re-worked loess. Based on published laboratory test results on loess, cohesion can reduce to near zero when the water content is increased. Should the water content of the fill/loess increase, then the fill/loess would become much weaker and the static stability analysis indicates that failure would be possible. The water content of the fill at the critical failure surfaces has not been monitored, and so it is not known how long or how heavy the rainfall would need to be to create such a condition at the failure surface. It is known that there have been numerous past Port Hills landslides triggered by rain, that the probability of triggering a given landslide increases with rainfall intensity and duration, and that the slopes in their present condition are particularly vulnerable to substantial water ingress via the numerous open cracks in the fill.

For the assessed earth/debris flow source areas, the likely volume of material mobilised during a slope failure event and the frequency of the slope failure triggering event are both uncertain. Nonetheless, the slopes have remained stable during earthquake aftershocks since the 22 February 2011 earthquake. Although movement of the slope (source area 11A) was noted during the winter of 2012 and several small (less than 50 m³) earth/debris flows occurred from both sites (Yetton and Engel, 2014).

Cliff collapse (debris avalanches and cliff-top recession, source areas 11B and 11E)

The main triggering mechanism for the assessed cliff collapses is considered to be earthquakes, although rainfall could trigger smaller volumes of rock to fall from the slopes (source areas 11B and 11E). Failure under static conditions (non-earthquake) is possible and has also been modelled in the risk assessment.

For source area 11B, the dynamic analysis used the proprietary Quake/W and Slope/W models to calibrate the slope material parameters, by simulating the 22 February and 13 June 2011 earthquakes. Approximate parameters were adjusted to give the best fit with the observed slope movement and cracking. These best-fit parameters were then used in the model to explore the susceptibility of each of the newly identified potential sources to different levels of ground shaking.

The dynamic analyses showed that failure of the slope would be limited to relatively small volumes of material, unless subjected to very large ground accelerations (similar to those associated with the 22 February 2011 earthquake).

Given the lack of detailed site-specific information relating to the abandoned quarry slope at source area 11E, GNS Science has applied the generic cliff collapse risk model developed for a selection of Port Hills sites (Massey et al., 2012a) to this steep rock slope. The risk assessment by Massey et al. (2012a) was revised using the input parameters presented in this report.

Failure volumes and triggering frequencies

For the assessed landslide hazards, the likely volume of material mobilised during a slope failure event and the frequency of the slope failure triggering event are both uncertain.

The volumes of material involved in, and the frequency of, slope failure events from the newly identified sources have been assessed. Both are highly uncertain; the frequency particularly so. On the one hand the slopes have survived some substantial aftershocks and two substantial rainfall episodes since the 22 February 2011 earthquake without major failure. On the other hand:

- a. the strength of the slopes has been weakened by cracking; and in particular
- b. the cracking has made the slopes more vulnerable to water ingress, which would be expected to weaken them further (possibly critically so in a severe weather episode).

A risk assessment was carried out for each of the newly-identified potential source areas, using a range of triggering frequencies and landslide volumes (upper, middle and lower source volume estimates) to reflect the associated uncertainties, and the overall annual individual fatality risk for a nearby resident or users of Main Road has been assessed.

ES 3 CONCLUSIONS

With reference to source area boundaries as show in Figure 2, the conclusions of this report are:

ES3.1 Hazard

1. There is potential for volumes ranging from several hundreds to thousands of cubic metres of:
 - a. Earth/debris flows (source areas 11A and 11C) of mixed soil, mainly fill (re-worked loess); and
 - b. Cliff collapses of mixed soil and rock, mainly rock (source areas 11B and 11E), which are potentially larger than those cliff collapse failures previously assessed at the site (Massey et al., 2012a).
2. The most likely triggers for these newly identified landslide sources are earthquake ground shaking for the cliff collapses and prolonged heavy rainfall for the earth/debris flows.
3. The frequency of landslide events from these sources is difficult to estimate and could be anything from once in a few tens to once in many hundreds of years.

ES3.2 Risk

ES3.2.1 Dwelling occupant

1. Source area 11A: The risk associated with this earth/debris flow hazard affects the greatest number of dwellings, where the annual individual fatality risks are assessed as being 10^{-4} or greater, for some of these dwellings.
2. Source area 11B: The results from the risk assessment, taking into account the cliff collapse hazard assessed in this report, have increased the level of risk (from cliff-top recession) to an annual individual fatality risk of greater than 10^{-4} , at the dwelling that was already within the original cliff-top recession risk area (Massey et al., 2012a).
3. Source area 11C: The hazard associated with this earth/debris flow affects dwellings at the slope crest and at the toe, where the annual individual fatality risks are greater than 10^{-4} .
4. Source area 11E: The hazard associated with this debris avalanche affects a dwelling at the cliff toe, where the risk is assessed as being greater than 10^{-4} .

ES3.2.2 Road user

1. Source areas 11A and 11B are the only source areas putting users of the road (Main Road, one of Christchurch's busiest lifeline routes) at risk.
2. Source area 11A (upper source volume assumptions): the individual risk per journey or per year from earth/debris flows is substantially higher than the risk from motor vehicle crashes for all motor vehicles and pedestrians. The risk is similar for cyclists but is substantially lower than the crash risk for motorcyclists.

3. Source area 11B (for any assessed source volume assumptions): the individual risk per journey or per year from debris avalanches onto the southern side of the road (closer to the slope) is significantly higher than the corresponding motor vehicle crash risk for the same journeys for bus and truck occupants. The risk is comparable to the crash risk for car occupants, cyclists and pedestrians, but is significantly lower than the corresponding crash risk for motorcyclists. The risk falls rapidly with distance from the slope, reaching zero on the far (seaward) side of the road.

ES3.3 Risk management

1. A risk-management option of monitoring rainfall, soil moisture and pore-pressure in the source areas may be of some value in providing warning of conditions approaching critical levels, but:
 - a. Such early warning could not be assured, as experience in the Port Hills and elsewhere is that water levels in open tension cracks can rise very rapidly to critical values.
 - b. There would be little time to evacuate potentially at-risk residents given the rapid nature of the hazard.
 - c. There is currently no precedent data for rates of change of groundwater or water content of loess to provide reliable alert criteria.
2. It should be noted that slope material strengths, and thus factors of safety, may be expected to deteriorate with time, weathering and any further earthquakes.

ES 4 RECOMMENDATIONS

GNS Science recommends that based on the results of this study, Christchurch City Council:

ES4.1 Policy and planning

1. Decide what levels of life risk to dwelling occupants will be regarded as tolerable.
2. Decide how Council will manage risk on land and roads where life risk is assessed to be at the defined threshold of intolerable risk and where the level of risk is greater than the threshold.
3. Prepare policies and other planning provisions to address risk lesser than the intolerable threshold in the higher risk range of tolerable risk.

ES4.2 Short-term actions

ES4.2.1 Hazard monitoring strategy

1. Include the report findings in a slope stability monitoring strategy with clearly stated aims and objectives, and list how these would be achieved, aligning with the procedures described by McSaveney et al. (2014). In the meantime, establish a survey network on the slope (particularly on source area 11A), so as to maintain awareness of changes in the behaviour of the slope.
2. Ensure that the existing emergency management response plan for the area identifies the dwellings that could be affected by movement and runout, and outlines a process to manage a response.

ES4.2.2 Risk monitoring strategy

Monitoring the slope for early warning of potentially dangerous trends in groundwater, or slope movement as part of a hazard warning system, is not recommended as it is currently not thought to be feasible. Monitoring alerts for slope deformation and groundwater changes cannot be relied upon to provide adequate early warning as experience from Port Hills and elsewhere shows that deformation and groundwater changes can occur rapidly, with little warning, and there is little site-specific information on which to build such a warning system.

ES4.2.3 Surface/subsurface water control

Reduce water ingress into the slopes, where safe and practicable to do so, by:

- a. Identifying and relocating all water-reticulation services (water mains, sewer pipes and storm water) inside the identified mass-movement boundaries to locations outside the boundary, in order to control water seepage into the slope. In particular, a sewer main currently crosses the edge of source area 11A, and should if possible be relocated away from this area; and
- b. Control surface water seepage by filling the accessible cracks on the slope and providing an impermeable surface cover to minimise water ingress. However, it is not thought that such works alone are sufficient to reduce the risk.

ES4.3 Long-term actions

ES4.3.1 Engineering measures

Assess the cost, technical feasibility and effectiveness of alternative longer term engineering and relocation solutions, for example (but not limited to):

- a. Removal/stabilisation of the slopes in the assessed source areas;
- b. Installation of drainage works;
- c. Relocation of houses to alternative locations within existing property boundaries;
- d. Withdrawal and rezoning of the land for non-residential use; or
- e. Any proposed engineering works would require a detailed assessment and design and be carried out under the direction of a certified engineer, and should be independently verified in terms of their risk reduction effectiveness by appropriately qualified and experienced people.

ES4.3.2 Reassessment

Reassess the risk and revise and update the findings of this report in a timely fashion, for example:

- a. in the event of any changes in ground conditions; or
- b. in anticipation of further development or land use decisions.

1.0 INTRODUCTION

This report combines recent field information collected from the Quarry Road site with numerical slope-stability modelling to assess the risk to people in dwellings and users of Main Road from mass movements at the site. The results in this report supersede those in an earlier cliff collapse study (Massey et al., 2012a).

1.1 BACKGROUND

Following the 22 February 2011 earthquakes, members of the Port Hills Geotechnical Group (a consortium of geotechnical engineers contracted to Christchurch City Council to assess slope instability in the Port Hills) identified some areas in the Port Hills where extensive cracking of the ground had occurred. In many areas cracks were thought to represent only localised relatively shallow ground deformation in response to shaking. In other areas however, the density and pattern of cracking and the amounts of displacement across cracks clearly indicated that larger areas had moved systematically *en masse* as a mass movement.

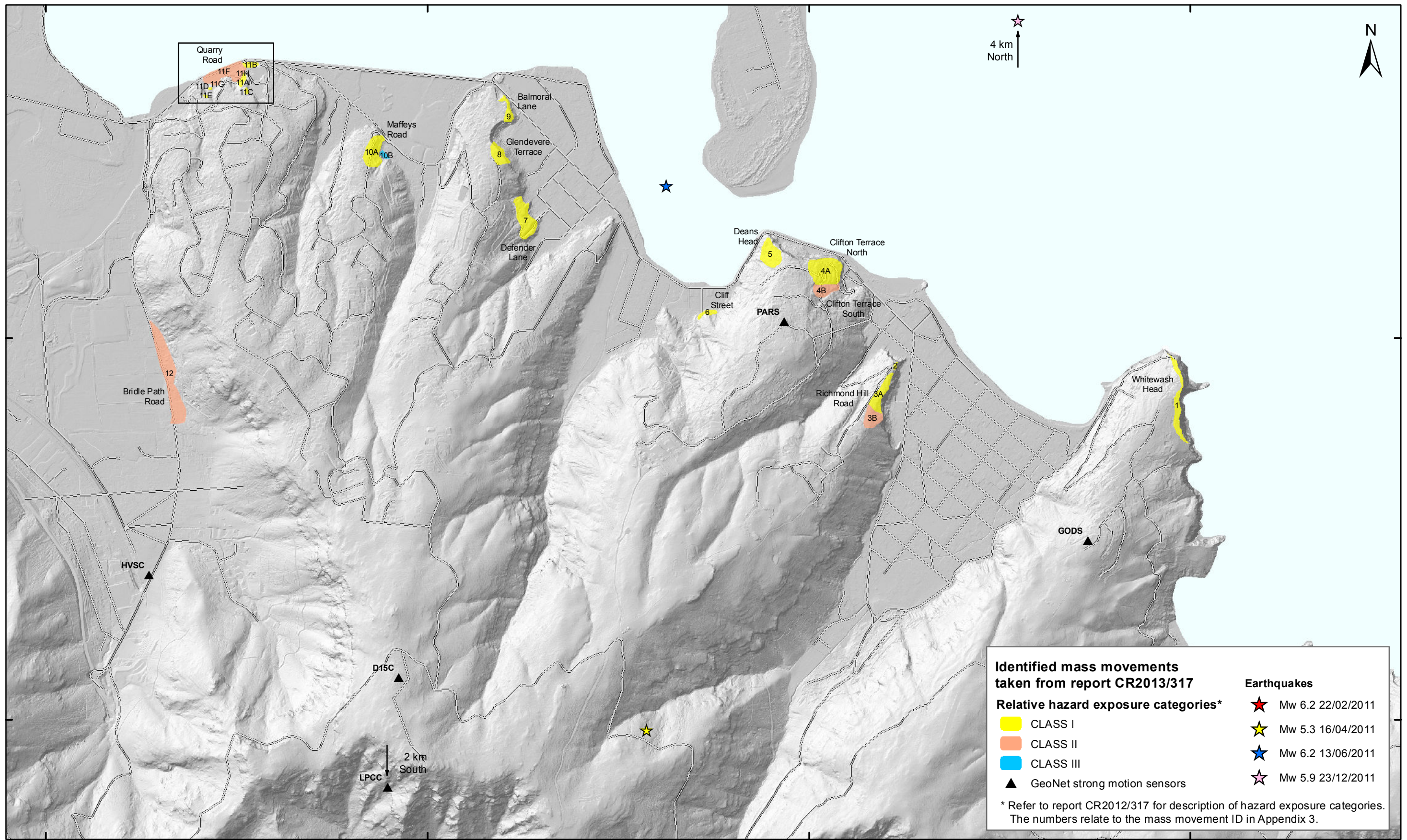
Christchurch City Council contracted GNS Science to carry out detailed investigations of the identified areas of mass movement, in order to assess the nature of the hazard, the frequency of the hazard occurring, and whether the hazard could pose a risk to life, a risk to existing dwellings and/or a risk to critical infrastructure (defined as water mains, sewer mains, pump stations, electrical substations and transport routes). This work is carried out under Task 4 of contract No. 4600000886 (December 2011).

The main purpose of the Task 4 work is to provide information on slope-stability hazards in the Port Hills, which were initiated by the 2010/11 Canterbury earthquakes. This is to assist Christchurch City Council land-use and infrastructure planning and management in the areas, as well as to establish procedures to manage on-going monitoring and investigation of the hazards and for civil defence emergency management procedures.

The Task 4 work is being undertaken in stages. Stage 1 is now complete (Massey et al., 2013; hereafter referred to as the Stage 1 report) and comprised: 1) a list of the areas susceptible to significant mass movement; 2) the interpreted boundaries of these areas (as understood at the time of reporting); and 3) an initial “hazard-exposure” assessment (Table 1) to prioritise the areas with regards to future investigations and what type of investigations could be appropriate. Stages 2 and 3 comprise detailed assessments of individual mass movements in order of decreasing priority.

The Stage 1 report identified 36 mass movements of concern in the Port Hills project area. Four of these were further subdivided based on failure type, giving a total of 46 mass movements including their sub areas (Figure 1). Fifteen of these were assessed as being in the Class I (highest) relative hazard exposure category, and the results of their detailed investigation and assessment are presented in Stages 2 and 3, which includes this Stage 3 report on the Quarry Road Class I mass movements. Mass movements assessed as being in the Class I category could cause loss of life, if the hazard were to occur, as well as severe damage to dwellings and/or critical infrastructure, which may lead to the loss of services for many people.

The Stage 1 report recommended that mass movements in the Class I relative hazard-exposure category should be given a high priority by Christchurch City Council for detailed investigations and assessment.



1576000

1578000

1580000

1582000

SCALE BAR: 0 0.5 1 km

EXPLANATION:
 Refer to Appendices 2 and 3 of report CR2012/317 for maps and more details of each mass movement.
 Background shade model derived from NZAM post earthquake 2011c (July 2011) LiDAR survey resampled to a 1 m ground resolution.
 Roads provided by Christchurch City Council (20/02/2012).
 PROJECTION: New Zealand Transverse Mercator 2000

DRW:
BL
 CHK:
CM



LOCATION MAP

**Port Hills
Christchurch**

FIGURE 1

Map 1

FINAL

REPORT:
CR2014/75

DATE:
June 2014

5176000

5174000

Table 1 Assessed mass movement relative hazard exposure matrix (from the Stage 1 report, Massey et al., 2013).

		Hazard Class		
		1. Displacement* greater than 0.3 m and debris runout	2. Displacement* greater than 0.3 m; no runout	3. Displacement* less than 0.3 m; no runout
Consequence Class	1. Life – potential to cause loss of life if the hazard occurs	CLASS I	CLASS III	CLASS III
	2. Critical infrastructure ¹ – potential to disrupt critical infrastructure if the hazard occurs	CLASS I	CLASS II ²	CLASS II
	3. Dwellings – potential to destroy dwellings if the hazard occurs	CLASS I	CLASS II	CLASS III

*Note: Displacements for each assessed mass movements are inferred by adding together the mapped crack apertures (openings) along cross-sections through the assessed mass movements. They are a lower bound estimate of the total displacement, as no account is given for plastic deformation of the mass and not every crack has been mapped.

¹ Critical infrastructure is defined, for the purpose of this report, as infrastructure vital to public health and safety. It includes transport routes (where there is only one route to a particular destination), telecommunication networks, all water related mains and power networks (where there is no redundancy in the network), and key medical and emergency service facilities. Networks include both linear features such as power lines or pipes and point features such as transformers and pump stations.

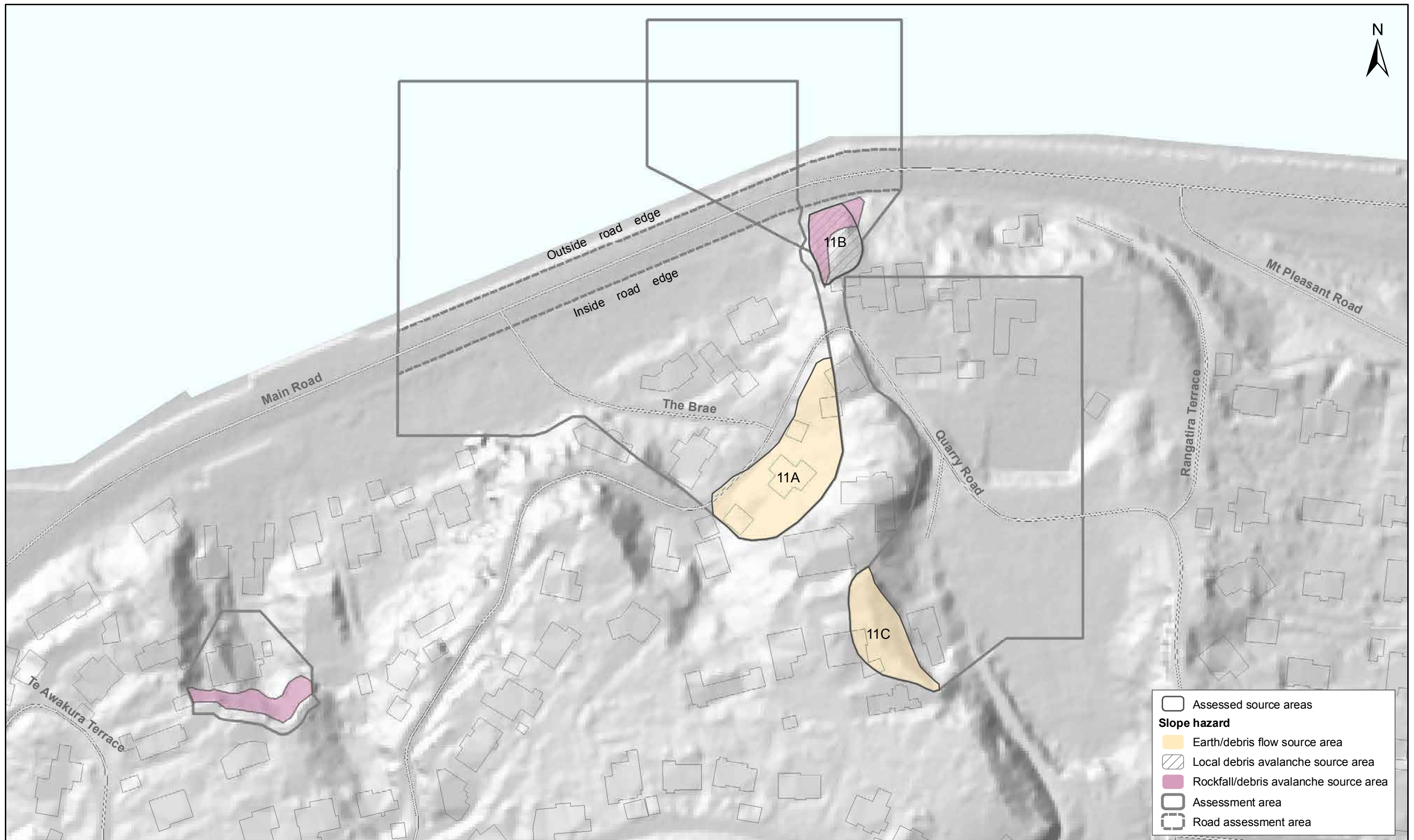
² This relative hazard exposure category is based largely on an assumption that 'critical infrastructure' exists within these areas. Until further assessments are made on the nature of toe slumps and the existence of critical infrastructure in these areas, the relative hazard exposure category of these assessed mass movements has been appropriately assessed as "Class II". It is likely that many of the assessed mass movements in the Class II relative hazard exposure category (where the hazard class is 2 and the consequence class is 2) would be more appropriately classified as "Class III" following further assessments.

1.2 THE QUARRY ROAD MASS MOVEMENTS

The Quarry Road mass movements comprise eight localised source areas (11A–H in Figures 1 and 2). Five of these source areas (11A–E) were assessed in the Stage 1 report (Massey et al., 2013) as being in the highest relative hazard exposure category (Class I), while the other three areas (11F, G and H) were assessed as being in Class II and III.

This report presents the risk assessment results for four of the Class I source areas: numbers 11A, 11B, 11C and 11E. Source area 11D was removed from the GNS Science assessment under Council instruction because a large retaining wall has been constructed there, which mitigated the hazard and the work was approved and signed off by Council.

The map (Figure 2) outlines the assessed potential landslide source areas associated with each of the assessed Class I mass movements.



SCALE BAR: 0 50 100 m

EXPLANATION:
 Background shade model derived from NZAM post earthquake 2011c (July 2011) LiDAR survey resampled to a 1 m ground resolution.
 Roads provided by Christchurch City Council (20/02/2012).
 PROJECTION: New Zealand Transverse Mercator 2000

DRW:
BL
 CHK:
CM, FDP



MASS MOVEMENT LOCATION MAP

**Quarry Road
Christchurch**

FIGURE 2

FINAL

REPORT: CR2014/75 DATE: June 2014

1.3 PREVIOUS WORK AT THE QUARRY ROAD SITE

Following the 22 February 2011 earthquakes significant localised cracking was noted in the fill slopes (source areas 11A and 11C, Figure 3) and above the steep rock slope at assessed source area 11B (Figure 4).

1. For source area 11B, the risk to life of people in dwellings at the slope crest from debris avalanche and cliff top recession hazards associated with the steep rock slope (collectively termed cliff collapse) has already been estimated and is contained in Massey et al. (2012a).
2. The Christchurch City Council engaged URS New Zealand Ltd. (hereafter referred to as URS Ltd.) to provide further geotechnical data to allow GNS Science to fully assess any potential life risks and lifeline impacts from mass movement at Quarry Road. The URS Ltd. work commenced in mid-August 2013 and results were delivered to GNS Science in October–November 2013. The results are presented in the report by Yetton and Engel (2014).
3. The purpose of the URS Ltd. investigation works comprised: 1) engineering geological and geomorphological mapping of the site at a scale of 1:1,000; 2) construction of geological cross-sections through the site area at a scale of 1:500; 3) interpretation of aerial photographs from 1946–2011; and 4) assessment of available LiDAR data for the site and the construction of a digital terrain model. Other investigations included review and assessment of movement monitored since 6 June 2013 (by M. Yetton at the request of Christchurch City Council).



Figure 3 Aerial view of the Quarry Road source areas 11A and 11C (within the yellow dashed lines). Photograph taken by M. Yetton (2012).



Figure 4 Aerial view of the Quarry Road source area 11B (within the yellow dashed line). Photograph taken by M. Yetton (2012).

1.4 SCOPE OF THIS REPORT

The scope of this report as per Appendix A of contract No. 4600000886 (December 2011) is to:

1. Estimate the annual individual fatality risk for affected dwelling occupants and users of Main Road from the assessed landslide hazards, within the shown assessment areas in Figure 2.
2. Provide recommendations to assist Christchurch City Council with considered options to mitigate life risks, associated with the assessed source areas.

For the purpose of this risk assessment, dwellings are defined as timber framed single-storey dwellings of building importance category 2a (AS/NZS 1170.0.2002). The consequences of the hazards discussed in this report on other building types, such as commercial buildings, have not been assessed.

The risk assessments contained in this report supersede the preliminary risk assessments contained in the Working Note 2013/09 (Massey and Della Pasqua, 2014).

1.5 REPORT STRUCTURE

- Section 1.6 of the report details the methodology.
- Section 2 details the data used in the assessments.
- Sections 3–5 contain the results from the engineering geological, hazard and risk assessments respectively.
- Section 6 discusses the results of the risk assessment and explores the uncertainties associated with the estimated risks.
- Section 7 summarises the assessment findings.
- Section 8 presents recommendations for Christchurch City Council to consider.

1.6 METHODS OF ASSESSMENT

The site assessment comprised three stages: 1) Engineering geology assessment; 2) Hazard assessment; and 3) Risk assessment. This was followed by analysis of the results.

1.6.1 Engineering geology assessment methodology

The findings presented in this report are based on engineering geological models of the site developed by URS New Zealand Ltd. (Yetton and Engel, 2014), in consultation with GNS Science.

1.6.2 Hazard assessment

The hazard assessment method followed three main steps:

Step 1 comprises assessment of the stability of the slope under non-earthquake (static) conditions, and an assessment of the dynamic (earthquake) stability of the slope, adopting selected cross-sections, to determine how likely landslides are to occur, and whether these can/cannot be triggered under static and/or dynamic conditions.

Step 2 uses the results from step 1 to define the likely failure geometries (source areas) of potential landslides, which are combined with the crack patterns and slope morphology and engineering geology mapping to estimate their likely volume. Three volumes are defined for each source area (upper, middle and lower volumes), which represent the range of potential source areas that could occur within the assessment area.

Step 3 involves the use of models to determine: 1) the distance the debris travels down the slope (runout); and 2) the volume of debris passing a given location, should the landslide occur. Modelling is done for each representative source area, and for the upper, middle and lower volume estimates.

The results from this characterisation are then used in the risk assessment.

1.6.3 Estimation of landslide volumes

The results of the engineering geological assessments and the slope stability modelling carried out by GNS Science have been used to define four potential landslide source areas associated with two main types of landslide:

1. Fill slope failure of source area 11A (earth/debris flow hazard);
2. Rock slope failure (with minor loess and fill) of source area 11B (cliff collapse hazard);
3. Fill and loess slope failure (of cut slope) of source area 11C (earth/debris flow hazard);
and
4. Rock slope failure (with minor loess and fill of an abandoned quarry) of source area 11E (cliff collapse hazard).

These are located in areas where the bulk strength of the slope could have been degraded as a result of earthquake-induced cracking. The assessed source areas (shown in Figure 2) represent the potential locations of the source areas for the assessed hazards that could occur in the assessment areas. For source area 11B these are additional to the smaller volume cliff collapses previously assessed by Massey et al. (2012a).

For the assessed landslide hazards:

- The most likely locations and volumes of potential failures were estimated based on the numerical analyses, current surveyed displacement magnitudes, material exposures, crack distributions and slope morphology. The purpose of this was to constrain the likely depth, width and length of any future failures. This was done by linking the main cracks and pertinent morphological features, in combination with the width, length and depth of the failure surfaces derived from the finite element and limit equilibrium modelling.
- Three failure volumes (upper, middle and lower) were estimated for each potential source area to represent a range of source volumes. The variation in failure volume reflected the uncertainty in the results from the modelling and mapping, e.g. the depth, width and length dimensions.

1.6.4 Risk assessment

The risk metric assessed is the annual individual fatality risk and this is assessed for dwelling from the earth/debris flows and cliff collapses assessed in this report. Cliff-collapse hazards (comprising debris avalanches and cliff-top recession) within the assessment area were previously assessed by Massey et al. (2012a) and these results are combined (where appropriate) with the results in this report, to present combined risk estimates for all of the assessed landslide hazards.

The quantitative risk assessment uses risk-estimation methods that follow appropriate parts of the Australian Geomechanics Society framework for landslide risk management (Australian Geomechanics Society, 2007). It provides risk estimates suitable for use under SA/SNZ ISO1000: 2009.

Using the Australian Geomechanics Society (2007) guidelines for landslide risk management, the annual fatality risk to an individual is calculated from:

$$R_{(LOL)} = P_{(H)} \times P_{(S:H)} \times P_{(T:S)} \times V_{(D:T)} \quad \text{Equation 1}$$

where:

$R_{(LOL)}$ is the risk (annual probability of loss of life (death) of a person) from debris/earth flows/avalanches;

$P_{(H)}$ is the annual probability of the initiating event;

$P_{(S:H)}$ is the probability that a person, if present, is in the path of the debris at a given location;

$P_{(T:S)}$ is the probability that a person is present at that location;

$V_{(D:T)}$ is the vulnerability, or probability that a person is killed if present and hit by debris.

The details relating to each of the above input parameters used in the risk assessments are discussed in Appendix 1.

1.6.4.1 Event annual frequencies

The frequency of occurrence of the events that could trigger the assessed landslide failure volumes is unknown.

- For non-earthquake triggers such as rainfall, a range of event annual frequencies ($P_{(H)}$) of 0.05, 0.02, 0.01, and 0.005 corresponding to return periods of 20, 50, 100 and 200 years, were used for the assessment to represent the likely return period of the event that could trigger failure of the assessed source areas.
- For earthquake events, the annual frequency of a given magnitude of permanent displacement of the slope, in the assessment area has been estimated by using:
 - a. The relationship between the yield acceleration (K_y) and the maximum average acceleration of the mass (K_{MAX}), derived from back-analysing the permanent displacement of the slope during the 2010/11 earthquakes; and
 - b. The New Zealand probabilistic National Seismic Hazard Model (Stirling et al., 2012) to provide the annual frequencies (return periods) of free-field rock outcrop peak horizontal ground accelerations (A_{FF}) and therefore the annual frequencies of the equivalent maximum average acceleration of the mass (K_{MAX}).

The methods adopted are discussed in detail in Appendix 1.

1.6.4.2 Scenarios assessed

Three scenarios for each source area were assessed in the risk assessment. This was done to take into account the main uncertainty relating to estimated source volumes used in the risk assessment. Uncertainties relating to the other input parameters used in the risk assessment and their impacts on the estimated risk are discussed in Section 6.

2.0 DATA USED

The data and the sources of the data used in this report are listed in Table 2.

Table 2 Summary of the main data used in the analysis. LiDAR is Light Detecting and Ranging.

Data	Description	Data source	Date	Use in this report
Post-22 February 2011 earthquake digital aerial photographs	Aerial photographs were taken on 24 February 2011 by NZ Aerial Mapping and were orthorectified by GNS Science (10 cm ground resolution).	NZ Aerial Mapping	Last updated 24 February 2011	Used for base maps and to map extents of landslides and deformation triggered by the 22 February 2011 earthquakes.
Post-13 June 2011 earthquake digital aerial photographs	Aerial photographs were taken between 18 July and 26 August 2011, and orthorectified by NZ Aerial Mapping (0.5 m ground resolution).	NZ Aerial Mapping	18 July–26 August 2011	Used to map extents of landslides and deformation triggered by the 13 June 2011 earthquakes.
Historical aerial photographs	Photographs taken in 1940, 1946, 1975, 1975 and 1984 by multiple sources and orthorectified by NZ Aerial Mapping and GNS Science (at variable ground resolutions).	NZ Aerial mapping and GNS Science	1946, 1975, 1975 and 1984	Used to assess the site history before the 2010/11 Canterbury earthquakes.
LiDAR digital elevation model (2011c)	Digital Elevation Model derived from post-13 June 2011 earthquake LiDAR survey; re-sampled to 1 m ground resolution.	NZ Aerial Mapping	18 July–26 August 2011	Used to generate contours and shade models for the maps and cross-sections used in the report.
Christchurch building footprints	Footprints are derived from aerial photographs. The data originate from 2006 but have been updated at the site by CCC using the post-earthquake aerial photos.	Christchurch City Council	Unknown	Used to identify the locations of residential buildings in the site.
GNS Science landslide database	Approximate location, date, and probably trigger of newsworthy landslides	GNS Science	Updated monthly	Used to estimate the likely numbers and volumes of pre-earthquake landslides in the areas of interest.
Earthquake Commission claims database	Location, date and brief cause of claims made in the Port Hills of Christchurch since 1993.	Earthquake Commission	1993–August 2010	Used to estimate the likely numbers and volumes of pre-earthquake landslides in the areas of interest.

Data	Description	Data source	Date	Use in this report
Synthetic earthquake time/ accelerations	Earthquake time acceleration history's for the four main 2011 earthquakes: 22 February, 16 April, 13 June and 23 December.	GNS Science	February 2014	Used as inputs for the seismic site response analysis.
Rainfall records for Christchurch	Rainfall records for Christchurch from various sources, extending back to 1873.	NIWA	1873– present	Used to assess the return periods of past storms triggering landslides of known magnitudes in the Port Hills.
Downhole shear wave surveys	Downhole shear wave velocity surveys carried out in the URS Ltd. drillholes.	Southern Geophysical Ltd. (2013)	February 2014	Used to determine the dynamic properties of the materials in the slope for the seismic site response analysis.
Geotechnical laboratory data	Geotechnical strength parameters for selected soil and rocks in the Port Hills.	GNS Science	February 2014	Used for static and dynamic slope stability analysis.
Field work	Field mapping of slope cracking and engineering geology and ground truthing of the risk analyses.	GNS Science and the Port Hills Geotechnical group	22 February 2011– present	Used in generating the engineering geological models of the site. Results from field checks used to update risk maps.
Port Hills Land Damage Studies Quarry Road Field Investigations	Field mapping, aerial photograph interpretation, interpretation of drillholes and assessment of engineering geological slope hazards present at the site	URS Ltd.	Final report April 2014 (Yetton and Engel, 2014)	Used as the basis for the hazard and risk assessments.
Traffic counts for Main Road (Causeway, to the East of the study area) and the Ferrymead/Main Road junction (to the West)	Detailed motor vehicle counts at 2-year intervals, by hour of day and day of week, are available for the Causeway. Junction data is more sparse but provides a valuable breakdown into heavy and light vehicles	Christchurch City Council	2008, 2010 and 2012 surveys	Used to assess total numbers of road users, and to model likely average extent and frequency of delays (and hence extended average time at risk) on Main Road.

3.0 SITE ASSESSMENT RESULTS

The site assessment and engineering geological conceptual models for the site were developed by URS Ltd. in consultation with GNS Science. The URS Ltd. engineering geological map, cross-sections and conceptual model for the site are presented in Figure 5 and Figure 6. These figures are reproduced from Yetton and Engel (2014), and the main results are summarised below.

3.1 SITE HISTORY

3.1.1 Before the 2010/11 Canterbury earthquakes

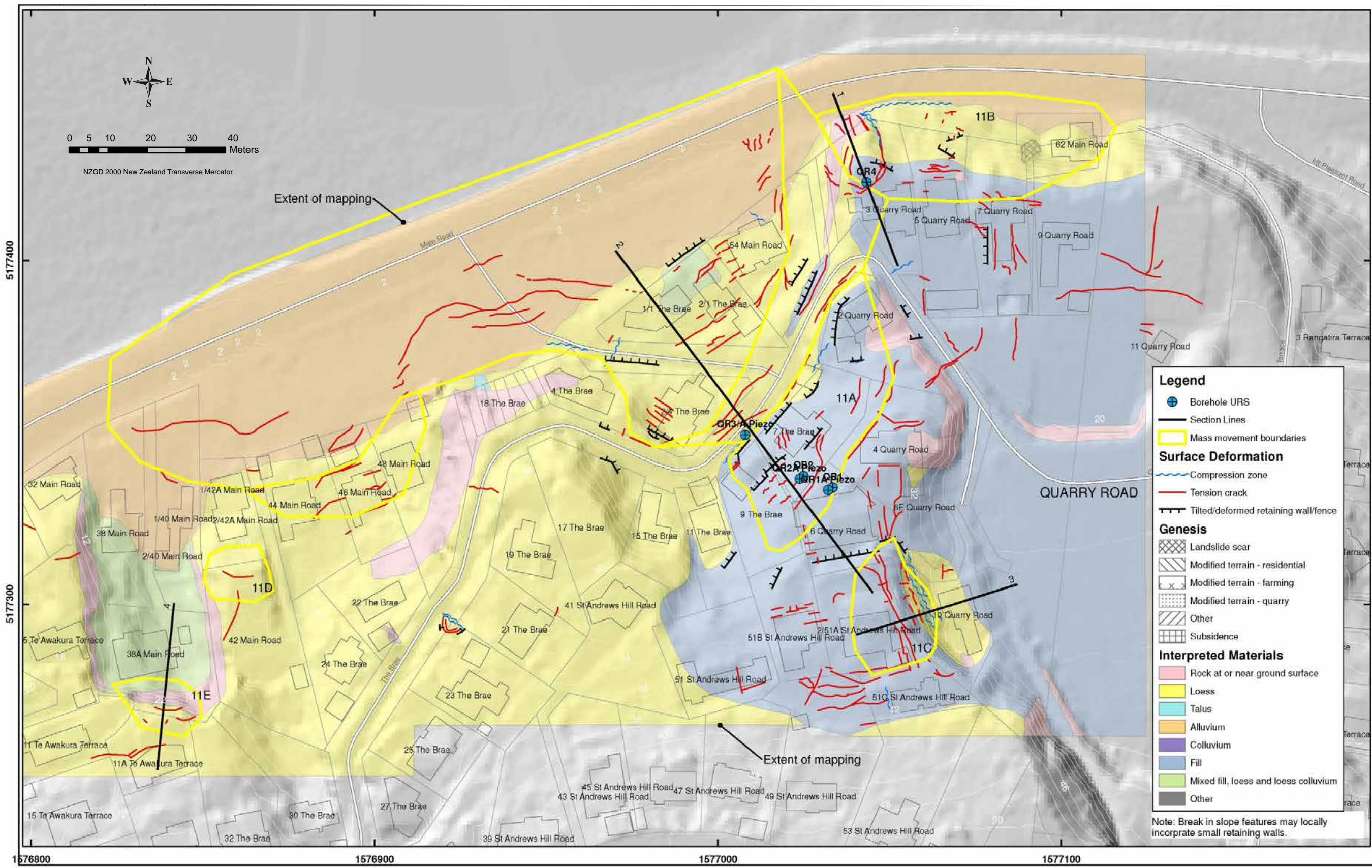
- No large-scale slope deformation has been recorded since European settlement.
- Geomorphic expression of old small scale landslide scars along the steep slopes beside Main Road and forward of 3, 5, 7, and 9 Quarry Road prior to 1946.
- Reports of subsidence damage to a former swimming pool at 6 Quarry Road in the early 1980's where leakage created deep subsurface erosion and collapse of the deep loess fill.
- A rainstorm in August 2000 triggered collapse of part of the former quarry face above 10 Quarry Road.
- No cracking reported or observed following 4 September 2010 earthquake.

3.1.2 During the 2010/11 Canterbury earthquakes

- The main cracks developed during the 22 February 2011 earthquake (Table 3). The retaining wall in front of 2 The Brae collapsed onto Quarry Road.
- Minor movement may have occurred due to the 13 June 2011 earthquakes, but this is not confirmed.

3.1.3 After the 2010/11 Canterbury earthquakes

- Post-earthquake movement of the fill slope at 7 The Brae occurred in the winter of 2012 with wet slide debris spilling over the deck area and locally collapsing various retaining walls. Compression is also now more apparent than it was in 2012 at the toe of the fill slope near drillhole QR4.
- During this same wet period in 2012 a small landslide occurred at the head of the toe slump area in the road shoulder, near the sharp bend in Quarry Road directly in front of 2 Quarry Road.
- A small debris flow developed from a landslide in the steep slope above 62 Main Road.
- No known further movement has occurred at the 3 Quarry Road rock spur or at 38A Main Road in the western quarry area, but neither of these sites is currently routinely monitored.



The drawing is reproduced from URS (2014), Port Hills land damage studies Quarry Road field investigations. Report prepared for Christchurch City Council. (Yetton, M. and Engel, M. 2014).

DRW:
PC
CHK:
CM



**URS LTD. ENGINEERING GEOLOGY MAP
Reproduced from Yetton and Engel (2014)**

**Quarry Road
Christchurch**

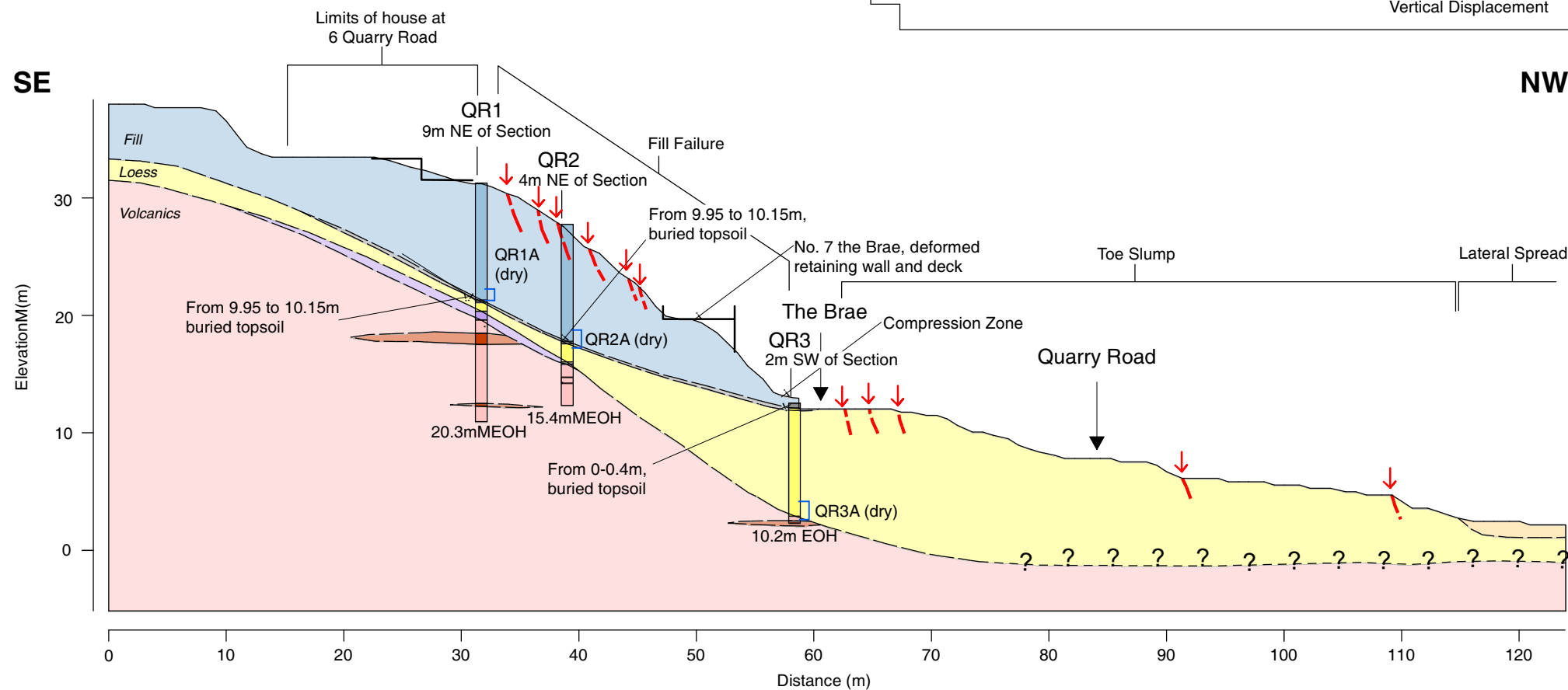
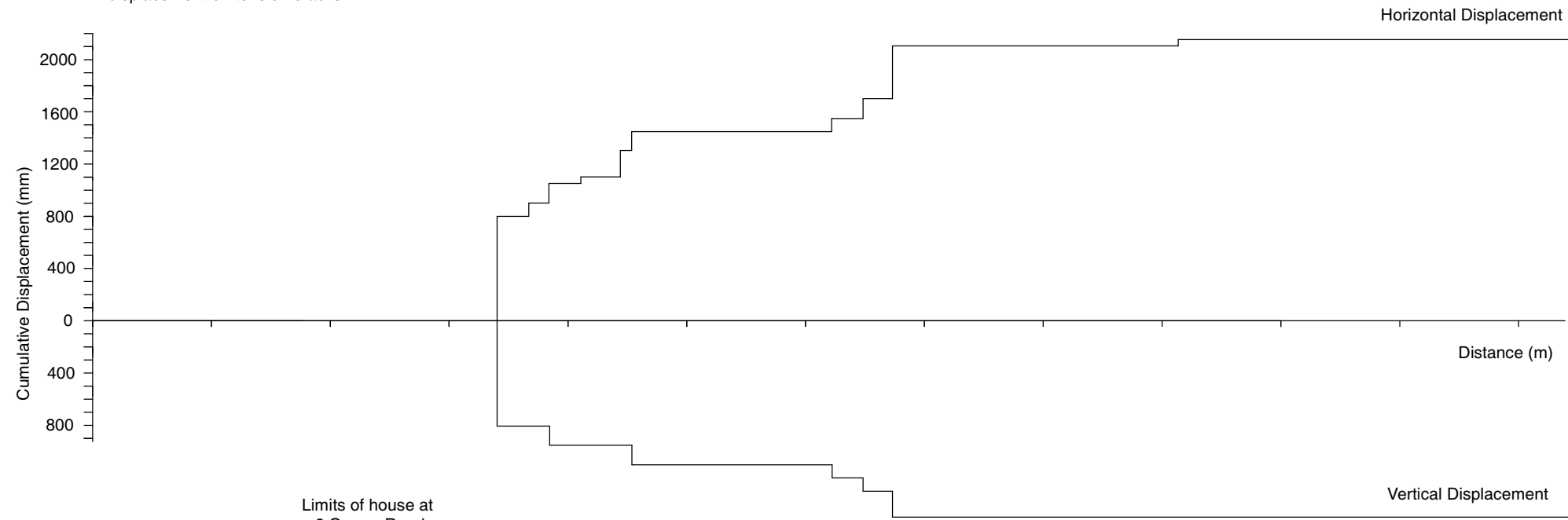
FIGURE 5

FINAL

REPORT: CR2014/75 DATE: June 2014

Cumulative Displacement Plot

Note: Cumulative displacement calculated from mapped displacement on tension cracks.



Cross Section 2



Legend

Contacts

- Contact Accurate
- - - Contact Inferred
- - - ? Contact Uncertain
- - - ? Downridge Cracking Inferred (On section)
- ↓ Tension crack inferred to contribute to movement along section

Interpreted Materials

- Fill
- Topsoil
- Basalt
- Basalt Breccia
- Loess and loess colluvium
- Alluvium
- Volcanic Colluvium
- Mixed Fill
- Tuff and epiclastics

The drawing is reproduced from URS (2014), Port Hills land damage studies Quarry Road field investigations. Report prepared for Christchurch City Council. (Yetton, M. and Engel, M. 2014).

DRW:
PC
CHK:
CM



**URS LTD. ENGINEERING GEOLOGY CROSS SECTION 2
Reproduced from Yetton and Engel (2014)**

**Quarry Road
Christchurch**

FIGURE 6A

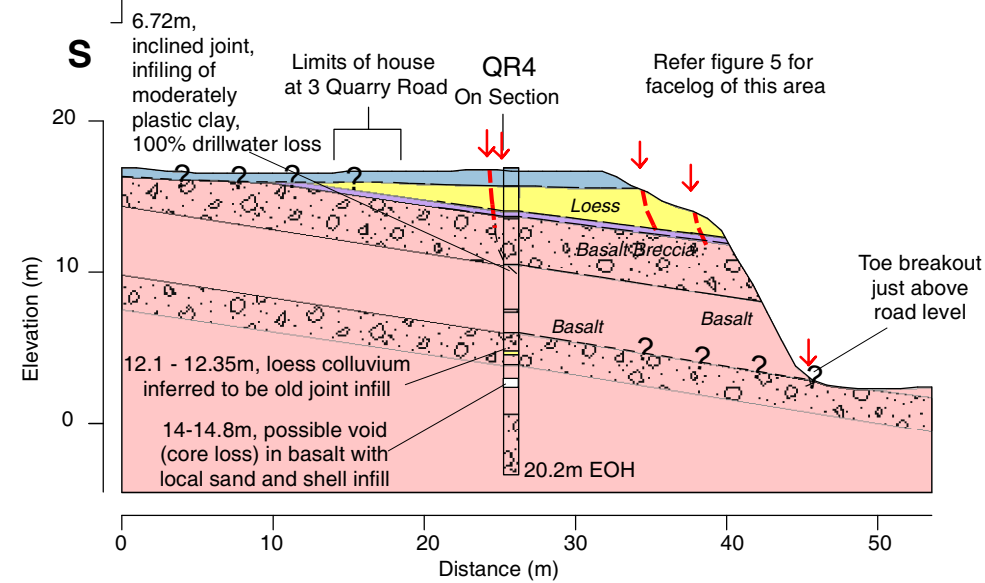
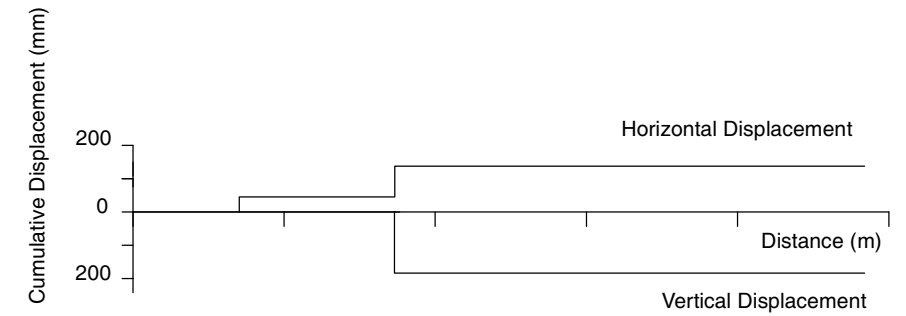
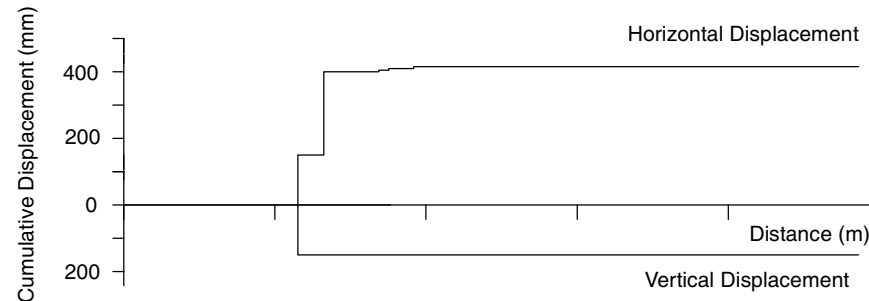
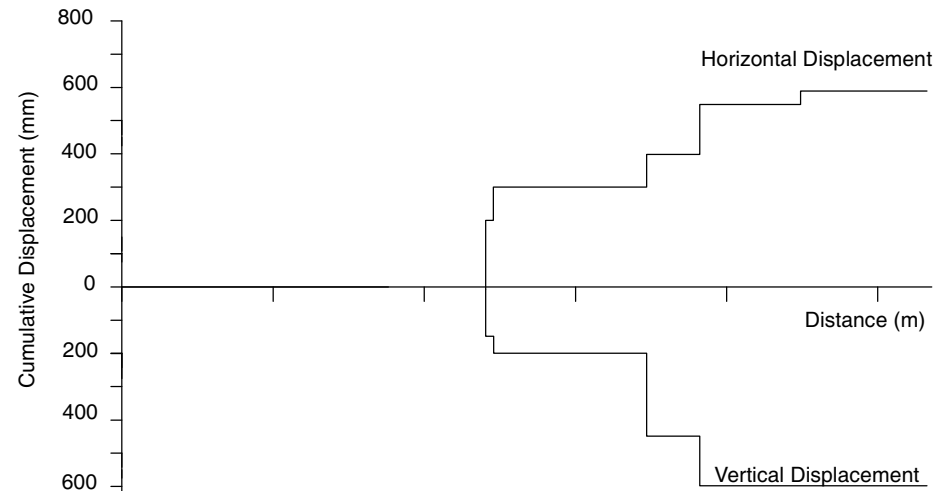
FINAL

REPORT:
CR2014/75

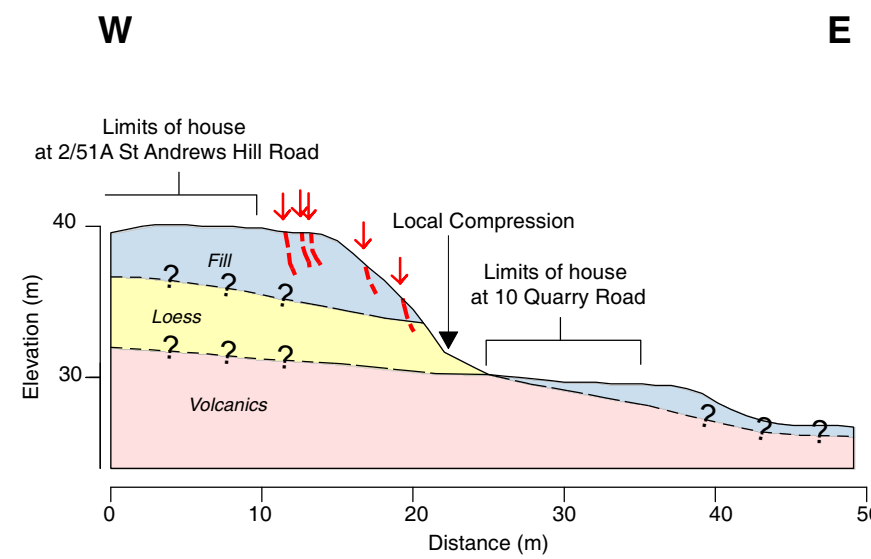
DATE:
June 2014

Cumulative Displacement Plots

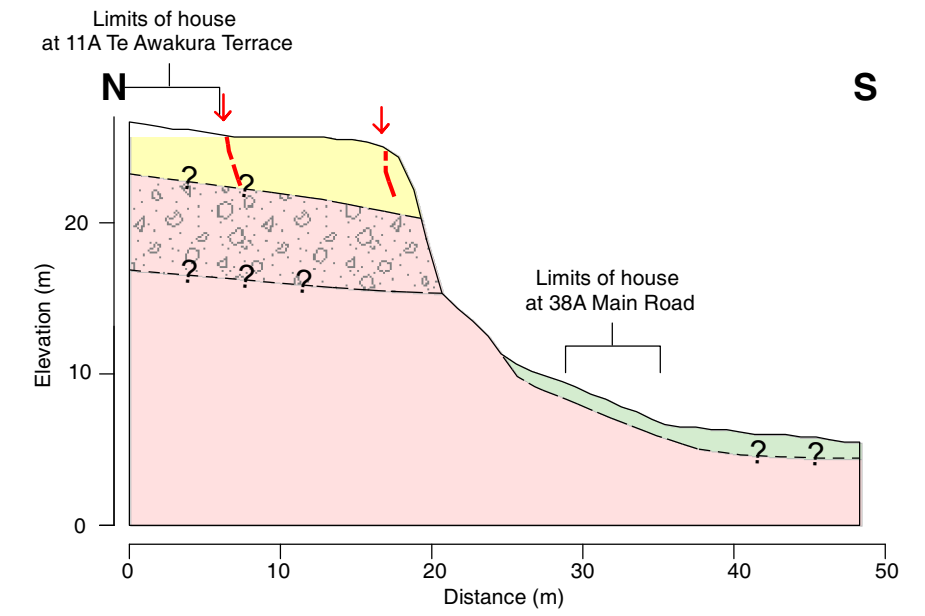
Note: Cumulative displacement calculated from mapped displacement on tension cracks.



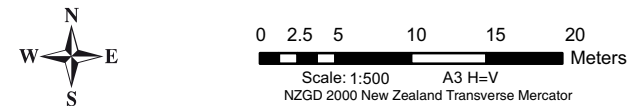
Cross Section 1: 3 Quarry Road



Cross Section 3: 10 Quarry Road



Cross Section 4: 38A Main Road



Legend	
Contacts	Interpreted Materials
----- Shear	Fill
———— Contact Accurate	Basalt
- - - - Contact Inferred	Basalt Breccia
- - - ? Contact Uncertain	Loess and loess colluvium
- - - - ? Downridge Cracking Inferred	Alluvium
↓ Tension crack inferred to contribute to movement along section	Volcanic Colluvium
	Mixed Fill
	Tuff and epiclastics

The drawing is reproduced from URS (2014), Port Hills land damage studies Quarry Road field investigations. Report prepared for Christchurch City Council. (Yetton, M. and Engel, M. 2014).

DRW:
PC
CHK:
CM



URS LTD. ENGINEERING GEOLOGY CROSS SECTIONS 1, 3 & 4, Reproduced from Yetton and Engel (2014)

**Quarry Road
Christchurch**

FIGURE 6B

FINAL

REPORT:
CR2014/75

DATE:
June 2014

3.2 SITE INVESTIGATIONS

3.2.1 Geomorphological mapping

The results from field mapping of slope morphology, interpreted surface materials and their genesis and surface deformation mapping carried out by URS Ltd. (Yetton and Engel, 2014) are shown in Figure 5 and Figure 6.

3.2.2 Subsurface trenching and drilling

The following site investigations have been undertaken by URS Ltd. (Yetton and Engel, 2014) for this report (see Figure 5 for locations):

- Diamond core drilling with core recovery (drillholes QR1, 2, 3 and 4);
- Non-core drilling (drillholes QR1A, QR2A);
- Installation of three standpipe piezometers in three drillholes (QR1, 2 and 3); and
- Installation of three inclinometer tubes in drillholes (QR1A, 2A and 4).

Drillholes QR1, QR1A, QR2, QR2A, QR3 and QR3A were located in source area 11A. Drillhole QR4 was located in source area 11B.

3.2.3 Surface movement

3.2.3.1 Inferred slope displacement from crack apertures

Total cumulative displacement of the slope inferred from crack apertures along cross-sections 1–4, in response to the 2010/11 Canterbury earthquakes, is in the order of about 0.3–2.6 m (Table 3).

Table 3 Measured cumulate crack apertures, which formed mainly during the 22 February, and less so during the 13 June, 2011 earthquakes, measured by the Port Hills Geotechnical Group (Yetton and Engel, 2014). Displacements are obtained from field mapping of tension crack apertures along survey lines. Errors are nominally estimated as being ± 0.01 m.

Cross-section (Yetton and Engel, 2014) (Figure 6)	Vertical component (mm)	Horizontal component (mm)	Resultant vector		Apparent dip of loess/rock interface from the horizontal (°)
			Magnitude (mm)	Dip (°)	
1 (source area 11B)	650	590	878	48	~9
2 (source area 11A)	1,500	2,150	2,622	35	~30
3 (source area 11C)	150	415	441	20	Not known
4 (source area 11E)	200	150	250	53	~5

The vector of displacement (direction and angle of movement from the horizontal, inferred from crack apertures) for cross-sections 1 and 4 are significantly steeper than the dip of the fill/loess/colluvium and rock interface (Figure 6B), suggesting displacement occurred through the underlying rock mass.

The vector of displacement for cross-section 2 is only slightly steeper than the dip of the loess/colluvium and rock interface (Figure 6A), suggesting displacement of the mass occurred along this interface.

3.2.3.2 Surface movement monitoring

No surface movement monitoring network has currently been installed in any of the assessed areas.

3.2.4 Subsurface movement

Drillhole inclinometer tubes are used to monitor displacements at depth, assess whether movement is occurring along single or multiple slide-surfaces, and to independently verify the results of surface monitoring. Monitoring is undertaken manually by commercial contract (Geotechnics Ltd.).

Inclinometer tubes were installed in the three URS Ltd., drillholes (QR1A, QR2A and QR4; Yetton and Engel, 2014) in October 2013. Displacements of the slope indicator 85 mm diameter, plastic inclinometer casings (installed to the base of the drillholes), are measured based on test method ASTM D6230:05, using probe-type inclinometers with readings at 0.5 m intervals. Inclinometer accuracy is quoted as ± 6 mm over 25 m of tubing (Slope Indicator, 2005). Initial readings were conducted on 5 November 2013, when each inclinometer was read twice.

The results from the survey are presented in Geotechnics (2014). No subsurface displacements outside of error have been identified to date.

3.2.5 Groundwater

The main findings reported by Yetton and Engel (2014) are:

- The groundwater levels in the area appear to be generally low.
- Drill water was lost in all, or large parts of, QR1, QR2 and QR4. Piezometers installed in QR1 and QR2 at the base of the fill, where the drill water return was the best, have been dry since their installation. No piezometer was installed in QR4 in source area 11B.
- QR3, located at the bottom of the fill slope (source 11A), had good water return during drilling but the piezometer that was been installed at the base of the hole at approximately 2 m above mean sea level remains dry.

It should be noted that the standpipe piezometers are measured manually and measurements are infrequent, and therefore it is possible that elevated transient piezometric levels, linked to rainfall, could be present but they are not being recorded.

3.3 ENGINEERING GEOLOGICAL MODEL

3.3.1 Slope materials

3.3.1.1 Fill

In some areas – particularly in source areas 11A and 11C the slope crest has been backfilled for construction of residential homes. The subsurface extent of the fill is not accurately known, although its inferred boundaries are shown in cross-sections in Figure 6. In source area 11A the fill material in drillholes QR1 and QR2 is loess derived spoil and it is described as being “soft and relatively weak” (Yetton and Engel, 2014). Based on drillhole intersections, the thickness of the fill varies from a few metres to over 10 m in places.

3.3.1.2 Buried topsoil (palaeosol)

Yetton and Engel (2014) identified a “buried topsoil layer” underlying the fill material in source area 11A. Reported core intersections of this unit in drillholes QR1 and QR2 were approximately 20 cm and 10 cm in thickness respectively, and the material was described as moist.

3.3.1.3 Loess

The loess mantling the cliff at the Quarry Road assessed source area is similar to other areas of the Port Hills. It is a relatively cohesive silt dominated soil with only minor clay mineral content. Its strength is largely controlled by the soil moisture content and this has been well studied, e.g. Bell et al. (1986), Bell and Trangmar (1987), McDowell (1989), Goldwater, (1990), Yetton (1992) and Carey et al. (2014). In some places the loess appears to have been reworked by construction activities for the residential dwellings. The loess forms recessive slopes above the underlying volcanic breccia of varying slope angle. The loess is highly hydrophyllic and when exposed to water (rain) it quickly disintegrates into muddy silt.

3.3.1.4 Colluvium

A layer (up to 50 cm recorded in drillhole QR1) of volcanic colluvium (“sandy silt with some clay and gravel”) is reported by Yetton and Engel (2014).

3.3.1.5 Bedrock (volcanic tuff)

The Quarry Road slopes are underlain by weak volcanic basalt breccia material. Drilling records of drillhole QR4 in source area 11B describe the underlying volcanic material as weak to very weak with rock quality designation as low as 30%, with loss of water circulation and core loss intervals of up to 0.85 m in length (Yetton and Engel, 2014). Clay infill, inclined open joints and ancient sand/shell infill are also reported in this hole. Also noted in drillhole QR4 is an approximately 0.25 m thick layer of loess colluvium (at 12.15 m drillhole depth, which is at an elevation of about 4.7 m above mean sea level), and is inferred to represent a lava cave infill.

3.3.2 Geotechnical properties

No materials from source areas 11A, 11B, 11C and 11E have been tested in the laboratory. Material strength parameters have instead been assigned to the materials forming the slope based on the results from in-house (GNS Science) laboratory tests and the published results of testing of similar materials by others from elsewhere in the Port Hills. For the purpose of stability assessment, material strength parameters for the main materials were selected as shown in Table 4.

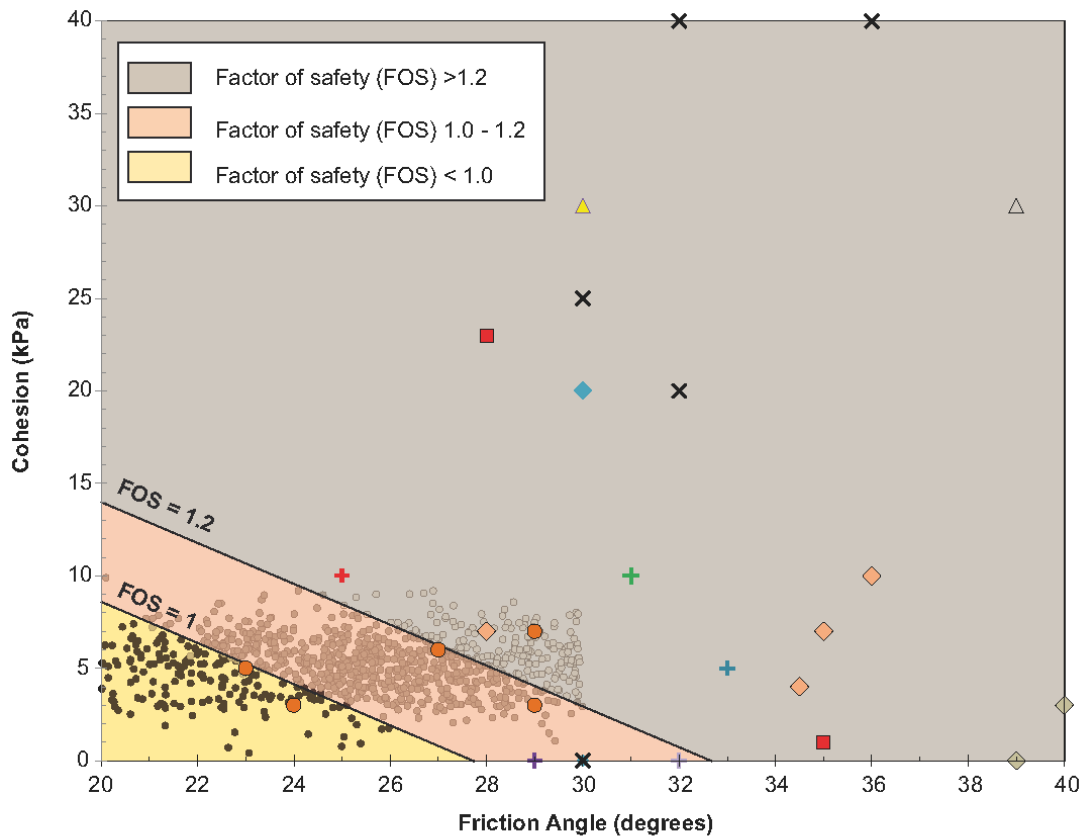
3.3.2.1 Fill (reworked loess)

Material parameters adopted for the fill material in source areas 11A and 11C are shown in Table 4. These are based on: 1) descriptions of the drillcore materials by Yetton and Engel (2014); 2) Port Hills loess strength test results reported by Carey et al. (2014) and others; and 3) numerical slope stability back-analysis of cross-section 2 (Figure 6).

Figure 7 shows the results from the numerical slope stability back-analysis of the fill, for cross-section 2 (Figure 6), representing source area 11A. A reasonable lower estimate of the shear strength of the fill, needed to derive a static factor of safety for the slope of 1.0, was friction (ϕ) of 25° and cohesion (c) of 5 kPa, or any combination of friction and cohesion that would yield a static factor of safety of 1.0. A similar result was obtained for the fill from numerical slope stability back-analysis of cross-section 3 (Figure 6), representing source area 11C.

The static factor of safety of these slopes is likely to be higher than 1.0 for at least the part of the year when the slopes are dry. Movement of source area 11A was noted by Yetton and Engel (2014) during the winter of 2012, indicating that the static factor of safety was marginally less than one at this time. The range of shear strengths derived for the fill from the numerical slope stability back-analysis – assuming a factor of safety for the slope of around one, are as expected, at the lower end of those derived from laboratory testing of loess materials from elsewhere in the Port Hills (Carey et al., 2014; Della Pasqua et al., 2014). As the fill is thought to predominantly comprise re-worked loess it is reasonable to assume that the cohesion of the fill, like the loess, is susceptible to changes in water content (Della Pasqua et al., 2014).

Results from slope stability back-analysis show that the factor of safety is sensitive to relatively small changes in cohesion. For example, a change in cohesion from 5 to 3 kPa would result in a drop in the factor of safety to below 1.0. Such changes in cohesion can be caused by changes in suction caused by changes in the bulk water content of the fill. Bulk water content is therefore likely to play a critical role in the overall static stability of the fill slope.



- FOS<1.0 BackAnalysis
- FOS>1.0 BackAnalysis ($\phi=30^\circ$, $c=0\text{kPa}$)
- FOS>1.2 BackAnalysis ($\phi=30^\circ$, $c=0\text{kPa}$)
- Carey et al. (2014) DIRECT SHEAR RESIDUAL 16 wt% water content
- Carey et al. (2014) RING SHEAR RESIDUAL 16 to 19 wt% water content
- ◆ Goldwater 1990 RESIDUAL water content unknown
- ▲ Tehrani (1988) DIRECT SHEAR PEAK 7wt% water content
- △ Tehrani (1988) DIRECT SHEAR PEAK dry water content
- × MCDowell (1989) TRIAXIAL PEAK 8 - 19 wt% water content
- + Tonkin and Taylor & Geotechnics RING SHEAR RESIDUAL 15-20 wt% water content

Figure 7 Numerical slope stability back-analysis of the fill material for cross-section 2, representing source area 11A. Note: each data point represents a modelled slide surface at a given combination of cohesion and friction adopted for the fill. Those slide surfaces shown as crosses, represent those combinations of cohesion and friction that would yield a static factor of safety of less than 1. The results from the dynamic back-analysis are also shown and are discussed in Section 4.

3.3.2.2 Volcanic bedrock

In order to derive rock mass strength parameters for the volcanic breccia and lava that take into account the nature of the discontinuities as well as the intact strength of the breccia and lava, the geological strength index (Hoek, 1999) was adopted using Rocscience RocLab software.

Given the anisotropic nature of the materials, especially with regards to the lateral and vertical extent of the lava sequences within the predominant volcanic breccia, and the generally low shear wave velocities derived from the down-hole surveys, it was decided to treat the volcanic materials as one unit, comprised mainly of breccia.

The geological strength index values adopted for the breccia are shown in Figure 8. In the absence of strength tests of Quarry Road rock samples, the results from testing of similar materials carried out on rock samples from Redcliffs (Carey et al., 2014) were used as a basis for the numerical models. The field strength and down-hole shear wave velocities of the tested samples from Redcliffs were compared to the materials in the drillcores and field exposures at Quarry Road, to ensure that they represented the materials at Quarry Road (Table 5).

For the modelling, the *in situ* shear-wave velocity and shear modulus for the volcanic breccia were derived from the downhole (within the drillhole) shear-wave surveys carried out by Southern Geophysical Ltd. (Southern Geophysical Ltd., 2013) in drillhole QR1 (source area 11A) and QR4 (source area 11B). Mohr-Coulomb parameters (cohesion and friction) were derived from RockLab by line fitting over the appropriate stress range of the slope.

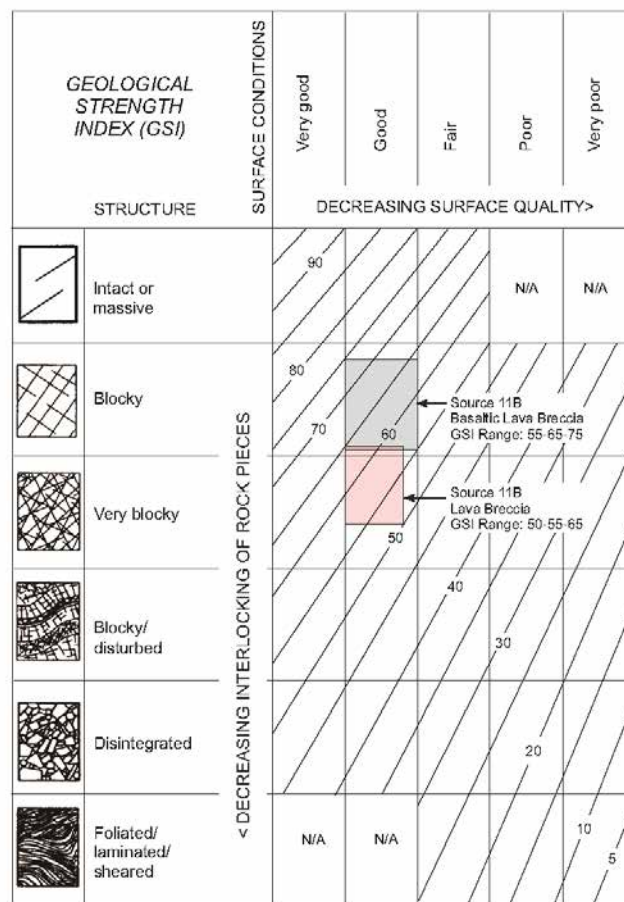


Figure 8 Geological strength index plot for volcanic breccia at Quarry Road (modified after Hoek, 1999).

Table 4 Range of bulk geotechnical material parameters adopted for Quarry Road soils.

Soil unit	Unit weight (kN/m ³)	Intact Young's modulus E _i (MPa)	Poisson's ratio	Cohesion c (KPa)	Friction φ (°)	Tensile strength (KPa)	Shear wave velocity (m/sec)	Shear modulus G _s (MPa)
							200	68
Fill	17	30	0.3	0–10	25–30	0	300	153
							400	272
Buried topsoil	17	30	0.3	0–10	25–30	0	200	68
Loess colluvium	17	30	0.3	0	28	0	200	68
Loess	17	30	0.3	10	30	10	200	68

Loess and colluvium strength parameters are as derived for Quarry Road source areas. Shear Modulus G_s (MPa) derived from down-hole shear wave velocity survey of drillhole QR1 (fill) and QR4 (loess). Where $G_s = \rho \cdot V_s^2$. Where ρ = density (Kg/m³) and V_s = shear wave velocity (m/s).

Table 5 Range of adopted rock strength parameters.

Unit		Lab UCS (MPa)	Bulk unit weight (kN/m ³)	Tensile (MPa)	Intact modulus E _i (MPa)	Poisson's ratio	Slope Height (m)	GSI	m _i ²	Cohesion ³ c (KPa)	Friction ³ φ (°)	Tensile strength (KPa)	Rock mass modulus E _M (MPa)	QR4 Shear wave velocity (m/sec)	Shear modulus G _s ⁴ (MPa)
	MIN ¹	1.3	18	0.2	310	0.1	15	55	6.5	44	27	15	127	300	162
Basalt lava breccia	AV	1.9	18	0.3	824	0.2		65	6.3	78	38	23	520	600	648
	MAX	2.9	19	0.5	1,500	0.3		75	5.8	140	49	44	1225	800	1216

¹ MIN, AV and MAX represent the range of test results and field measurements.

² m_i= The m_i values shown, represent the range in the ratio of unconfined compressive strength to tensile strength, derived from tested samples of basalt lavas and basalt lava breccias (Carey et al., 2014), and not the ratio of unconfined compressive strength to tensile values shown in the table.

³ Mohr-Coulomb parameters (cohesion and friction) were derived from RocLab by line fitting over the appropriate stress range of the slope.

⁴ Shear Modulus (G_s) is derived from down-hole shear wave velocity survey of drillhole QR4, where $G_s = \rho \cdot V_s^2$ and ρ =density (Kg/m³) and V_s = shear wave velocity (m/s).

3.3.3 Rainfall and groundwater response

In general there are two main effects that groundwater has on the stability of slopes that need to be considered: 1) rising groundwater within the slope leading to an increase in pore pressures and a reduction in the effective stress of the materials; and 2) infiltration from prolonged rainfall, leading to the deepening of the wetting band accompanied by a decrease in matric suction (e.g. Kim et al., 2004) and corresponding loss of cohesion. Owing to the lack of monitoring data, it is not known which mechanism could be the main contributor to rainfall-induced slope failures in the Port Hills. Loss of cohesion during long duration rainfall is a known cause of instability in fine grained, non-cohesive soils and therefore is likely to be a significant contributory factor to landslides in loess and loess derived materials (fill). Rapid increases in pore pressure within open tension cracks is thought to be the most important for rock slope stability, as the open tension cracks in the overlying loess would allow water to readily infiltrate any open cracks in the underlying rock mass. It should be noted that there is currently no systematic monitoring of groundwater levels at the site.

The relationship between rainfall and landslides in the Port Hills has been summarised by McSaveney et al. (2014). Heavy rain and long-duration rainfall have been recognised as potential landslide triggers on the Port Hills for many years. Loess earth/debris flows were noted frequently, even before the era of wider urban development in the Port Hills. A long historical landslide record has been gathered by searching “Paperspast” (<http://paperspast.natlib.govt.nz>). This electronically searchable record of daily and weekly newspapers in New Zealand has been searched over the period 1860–1926, but its landslide information is very incomplete, being only what newspapers of those times considered to be “newsworthy”. A summary of past landslides in the Port Hills and Banks Peninsula is contained in Appendix 2.

McSaveney et al. (2014) examined a list of Earthquake Commission claims for landslide damage for the period 1997–2010, and a Geotechnical Consulting Ltd. landslide investigations list, which covers much of the period 1992–2009. Any duplicate records for the period 1997–2009 contained in the data sets were removed. These records, though incomplete with respect to all of the landslides that occurred over those intervals, may be approximately complete with respect to the episodes of rain associated with landslide occurrences that damaged homes and urban properties (Figure 9).

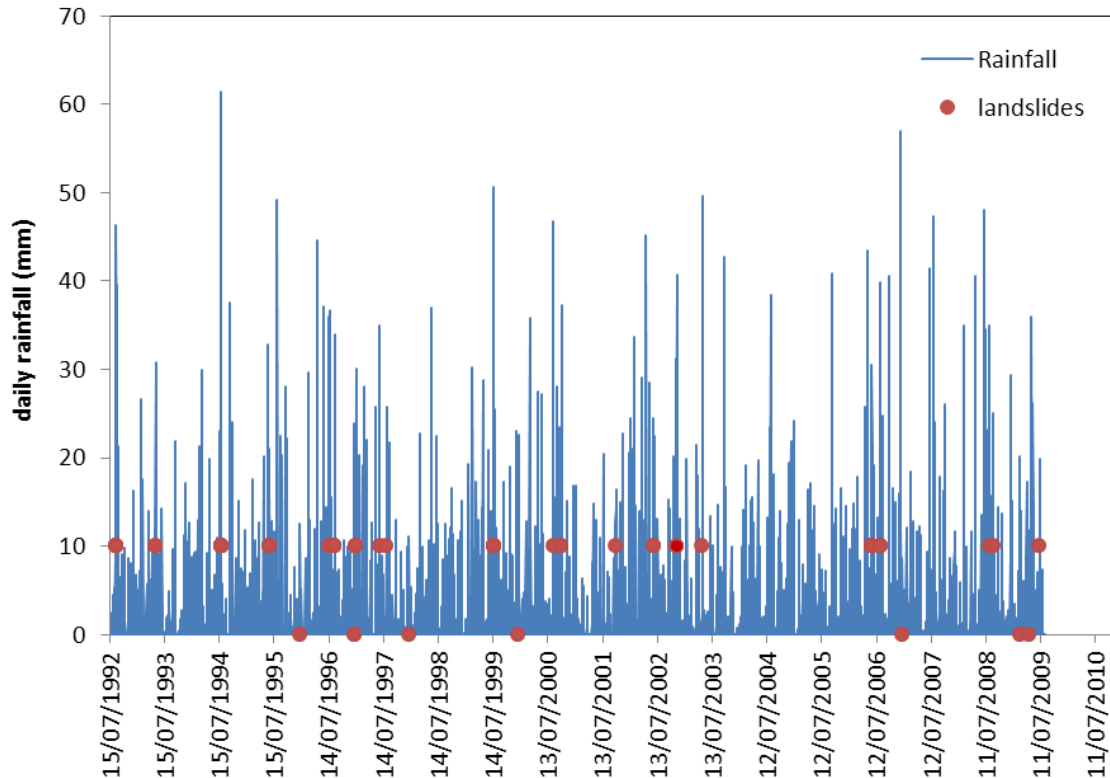


Figure 9 Daily rainfalls at Christchurch Botanic Gardens and landslides in the Port Hills. Daily rainfalls at Christchurch Botanic Gardens and landslides in the Port Hills investigated by Geotechnical Consulting Ltd, or listed by the Earthquake Commission as causing damage to homes. Landslides without rain are plotted at 0 mm, all others are plotted at 10 mm of rain (the minimum rainfall for triggered landslides).

McSaveney et al. (2014) conclude that comparison of the record of damaging landslides and daily rainfall for the period 1992–2010 shows that:

1. Landslides can occur without rain, but the probability of landslides occurring increases with increasing intensity of rainfall;
2. Landslides occurred much more frequently on days with rain, but there were many rainy days when no landslides were recorded; and
3. As the amount of daily rainfall increased, a higher proportion of the rainy days had recorded landslides.

Following the 2010/11 Canterbury earthquakes there have been two notable rainfall events (Table 6):

- 11–17 August 2012: occurred at the end of winter following a long period of wet weather. During this period a total of 92 mm of rainfall was recorded at the Christchurch Botanic Gardens. The maximum daily rainfall (24 hourly rainfall recorded 9 am–9 am) during this period occurred on 13 August 2012 and totalled 61 mm.
- 3–5 March 2014: occurred at the end of a period of dry weather. During these three days, a total of 118 mm of rain was recorded at the GNS Science rain gauge installed at Clifton Terrace in the Port Hills (approximately 4 km west of Cliff Street). The maximum daily rainfall (24 hourly rainfall recorded 9 am–9 am) during this period occurred on 5 March 2014 and totalled 85.4 mm.

The frequency of high-intensity rainfalls in Christchurch has been well studied (e.g. Griffiths et al., 2009, Figure 10, and McSaveney et al., 2014). Griffiths et al. (2009) use rainfall records for the period 1917–2008 from gauges all over Christchurch. McSaveney et al. (2014) use a composite rainfall record, for the period 1873–2013, mainly from the Christchurch Gardens gauge, but substituting averages for other nearby stations where gaps in the Christchurch Gardens data exist.

The annual frequencies for four rain events, including the two notable events are given in Table 6. Rainfall depth-duration-return period relations for Christchurch Gardens and Van Asch St, Sumner are taken from Griffiths et al. (2009) and for Christchurch Gardens from McSaveney et al. (2014).

Table 6 Annual frequencies of given rainfall in the Christchurch for four main events following the 2010/11 Canterbury earthquakes (rainfalls are calculated daily from 09:00 to 09:00 NZST).

Date	Total rainfall (mm)	Station	Max daily rainfall/date	Annual frequency Christchurch Gardens Griffiths et al. (2009)	Annual frequency Christchurch Gardens McSaveney et al. (2014)	Annual frequency Van Asch, Sumner Griffiths et al. (2009)
11–17 August 2012	92	Christchurch Gardens (CCC/NIWA)	61 mm 13 August 2011	92 mm = no data available 61 mm = 0.5 (once every 2 years)	92 mm = 0.4 (once every 2.7 years) 61 mm = 5 (5 times per year)	N/A
3–5 March 2014	118	Clifton Terrace (GNS Science)	89 mm 5 March 2014	N/A	N/A	118 mm = 0.1 (once every 10 years) 89 mm = 0.1 (once every 10 years)
3–5 March 2014	141	Christchurch Gardens (NIWA)	130 mm 5 March 2014	141 mm = 0.05–0.02 (once every 20–50 years) 130 mm = 0.02–0.01 (once every 50–100 years)	141 mm = 0.05 (once every 20 years) 130 mm = (>0.01) less than once every 100 years	N/A
18 April 2014	68	Lyttelton (NIWA)	68 mm	N/A	N/A	68 mm = 0.5 (once every 2 years)
29 April 2014	20	Clifton Terrace (GNS Science)	20 mm	N/A	N/A	Greater than 0.5 (occurs frequently every year)

Regardless of the dataset used, both suggest that the heavy rainfalls recorded in the Port Hills following the 2010/11 Canterbury earthquakes are unexceptional. Although the three-day rainfall of 118 mm had an annual frequency of 0.05–0.1 (once every 10 years), it occurred at the end of summer when the ground would have had a seasonally low water content.

The post-earthquake movement of source area 11A, collapse of retaining walls and small earth/debris flows were noted near the end of winter in 2012, following the 11–17 August 2012 rain. However, no movement or landslides were noted following the larger 3–5 March 2014 rainfall. These observations suggest that antecedent water conditions are also important as an indicator of slope instability. For example, large daily rainfalls occurring during periods of wet weather are more likely to trigger movement and landslides than very high daily rainfalls during long periods of dry weather.

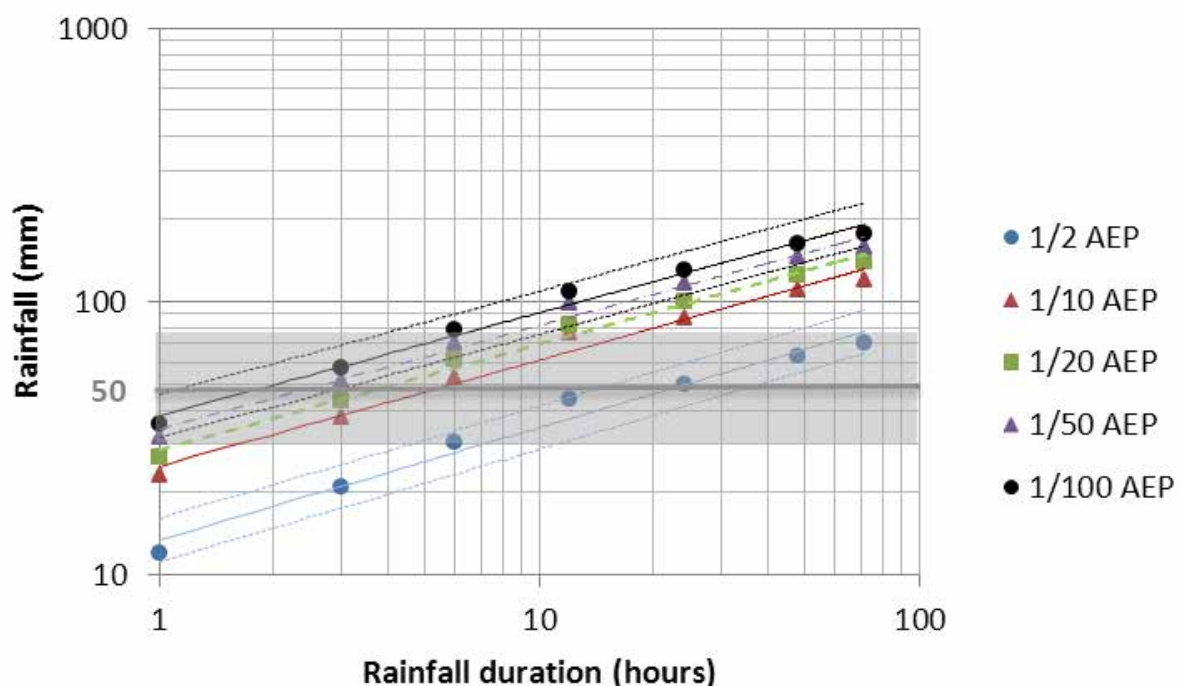


Figure 10 Rainfall depth-duration-return period relations estimated by Griffiths et al. (2009) using recorded rainfall data. Error limits of 20% are shown by dotted lines for the 1/2 and 1/100 AEP curves. Shaded area covers the range of 30–75 mm of rainfall over which the expected number of soil landslides in the Port Hills rises from very few to many. Rockfalls can occur without rain, but the probability of rockfalls occurring increases with increasing intensity of rainfall.

There is significant variation in rainfall across Christchurch in individual storms. The return period of the 89 mm of rain recorded at the GNS Science rain gauge at Clifton Terrace on the 5 March 2014 was about 10 years (using the data from Griffiths et al. (2009) for Van Asch Street in Sumner). The return period of the 130 mm of rain recorded at Christchurch Gardens for the same storm on the same day, was between 50 and 100 year (using the data from Griffiths et al. (2009) for the Christchurch Gardens).

At Lyttelton about 135 mm of rain was recorded on the 5 March 2014, which is considerably higher than the 89 mm recorded at Clifton Terrace, which is only about 5 km north of Lyttelton.

3.4 SLOPE FAILURE MODELS

The engineering geological models of the site presented by Yetton and Engel (2014), have formed the basis for numerical modelling of the static and dynamic stability of the slopes within the identified source areas 11A, 11B, 11C and 11E.

These are summarised below:

3.4.1.1 Source area 11A (cross-section 2)

- A steeply inclined fill slope failure between 7 The Brae and 6 Quarry Road. Landslide movement may be occurring close to the base of, or just under, the 10 m thick loess-derived quarry spoil that underlies this 30–35° slope;
- Static and dynamic conditions assessed.

3.4.1.2 Source area 11B (cross-section 1)

- Source area 11B: A deep-seated bedrock failure in volcanic materials (breccia) at the bluff in front of 3 Quarry Road extending from the spur crest to Main Road level. This has generated ground cracking on the spur crest and compression and local collapse in the toe at road level. This has been assessed as source area 11B under static and dynamic conditions.
- Further east along Main Road there are shallow failures in soils, possibly with some volcanic materials involved, including the recent small failure that generated the debris flow that hit 62 Main Road. The risk from these types of cliff collapse has been assessed by Massey et al. (2012a). No further assessment of these has been carried out in this report.

3.4.1.3 Source area 11C (cross-section 3)

- A potential cut slope collapse in loess fill and loess at 10 Quarry Road that involves the cracking and spalling of soil from the un-retained former quarry cut.
- Stability under static conditions assessed only.

3.4.1.4 Source area 11E (cross-section 4)

- Cracking and potential for slope collapse in bedrock and loess in an un-retained former quarry cut face at 38A Main Road.
- Stability under static or dynamic conditions have not been assessed as the risk has been estimated adopting the empirical model contained in Massey et al. (2012a).

3.4.1.5 Source area (no cross-section)

- Lateral spreading of the alluvium between the estuary and the toe slumps. This has not been assessed in this report. These were classified by Massey et al. (2013) as being in the Class II relative hazard exposure category.

3.4.1.6 Source areas 11G and 11H (no cross-sections)

- Two independent toe slump failures (eastern and western toe slumps) in loess soils in the lowest slope toe areas, the largest being the eastern toe slump near 1 The Brae. The head of this toe slump is overlain by fill at the sharp bend in Quarry Road. These have not been assessed in this report. These were classified in Massey et al. (2013) as being in the Class II relative hazard exposure category.

3.4.1.7 Slumping and cracking

In addition to the source areas 11A–H, an area of slumping and cracking has been identified at the crest of the slope, above (up slope) of source areas 11A and 11C. The density and pattern of cracking and the amounts of displacement across these cracks clearly indicated that this area had moved systematically, where the cracks are thought to be related to movement of the loess/fill, possibly along rockhead.

This area has not been assessed in this report. The origin of the cracking is therefore unknown and the depth of the materials in this area is also unknown as no ground investigation has been carried out.

4.0 HAZARD ASSESSMENT RESULTS

4.1 SLOPE STABILITY – STATIC CONDITIONS

For source areas 11A, 11B and 11C, the appropriate engineering geological cross-sections in Yetton and Engel (2014) (Figure 6) were used as the basis of the numerical slope stability modelling. Geotechnical material strength parameters used in the modelling are from Table 4 and Table 5 and models using variable shear strength parameters for the key materials were run to assess the sensitivity of the slope – along a given cross-section – to failure.

4.1.1 Source area 11A (cross-section 2)

Examples of results from the static limit equilibrium modelling and finite element modelling for a range of fill strength conditions are shown in Table 11. Three different failure mechanisms were adopted: 1) failure through the loess; 2) where the failure is through the fill; and 3) where failure is through a weak buried topsoil layer at the base of the fill. The results are summarised in Table 7.

Table 7 Example results from slope stability assessment of source area 11A (cross-section 2). Those values highlighted in red are for factors of safety less than 1.

Simulated failure mechanism	LOESS	FILL	TOP SOIL	Water level	FoS ¹ SLIDE	Search surface	SRF ² PHASE2
	Cohesion (kPa) / Friction (°)	Cohesion (kPa) / Friction (°)	Cohesion (kPa) / Friction (°)				
Failure through loess	10 / 30	10 / 30	Not simulated	Drained	1.5	CIRC	1.6
Through the fill	10 / 30	10 / 30	Not	Drained	1.5	CIRC	1.6
		5 / 30	Simulated		1.3	CIRC	
		0 / 30			0.9	CIRC	
		10 / 25	Not		1.3	CIRC	
		5 / 25	Simulated		1.1	CIRC	1.2
		0 / 25			0.7	CIRC	
Through the buried topsoil	10 / 30	10 / 30	0 / 28	Drained	1.3	BLOCK	
			0 / 20		1.0	BLOCK	1.0
		10 / 25	10 / 25		1.3	CIRC	
			0 / 28		1.2	BLOCK	
			0 / 25		1.1	CIRC	
			0 / 20		0.9	BLOCK	
		10 / 30	10 / 30		1.5	CIRC	
		5 / 25	5 / 25		1.1	CIRC	
			0 / 25		1.0	CIRC	
			0 / 28		1.1	BLOCK	
		0 / 20		0.9	BLOCK		

¹ FoS is the factor of safety derived using the general limit equilibrium method of Morgenstern and Price (1965).

² The finite element model was also used for comparison. Where the slope has been assessed using the finite element model, the stability of the slope is assessed in terms of the Stress Reduction Factor. Note the shear strength reduction method is used to determine the Stress Reduction Factor (SRF) or factor of safety value that brings a slope to the verge of failure (Dawson et al., 1999).

The results suggest that over the range of parameters assessed, the static factor of safety of the slope is in the order of 1.0–1.3. If fill parameters of friction (ϕ) 30° and cohesion (c) 10 kPa were adopted, the factor of safety would be in the order of about 1.5. However, these parameters are more typical of *in situ* loess and not fill or top soil (Carey et al., 2014; Della Pasqua et al., 2014), indicating the upper bound factor of safety is likely to be less than 1.5.

The sensitivity of the slope factor of safety to changes in transient pore pressure has been simulated by modelling: 1) a piezometric line at the base of the fill and increasing the level of this line (and therefore pore pressures within the fill) at given increments above the base of the fill and buried top soil; and 2) the in-filling of tension cracks in the slope by increasing the level of water acting with the tension cracks by given amounts.

The results are shown in Figure 11 for fill shear strengths of friction (ϕ) of 30° and cohesion (c) of between 5 and 10 kPa, representing the range of fill parameters thought to be reasonable. Models were run assuming: a) no tension cracks; b) with tension cracks; and c) with water in-filled tension cracks. The depth of the tension cracks are assumed to be 1.5 m deep based on the relationship in Craig (1997).

The results show that an increase in piezometric head levels of 2 m above the base of the fill reduces the factor of safety by about 0.1, indicating the slope is relatively sensitive to increases in piezometric head levels. Increases in piezometric head levels of about 3–4 m (over the range of fill shear strength parameters modelled and the different tension crack conditions) would reduce the slope factor of safety to below 1. At fill shear strengths of friction (ϕ) of 30° and cohesion (c) of 5 kPa, the factor of safety reduces by about 0.1 between filled and un-filled tension crack conditions, at the same piezometric head level. Conversely, significant water loess was noted during drilling suggesting the fill has a high permeability, therefore piezometric heads of 2 m may not be realistic.

The results from the assessment, adopting a failure mechanism through the buried top soil layer, give the lowest factors of safety (adopting the given range of parameters) of all of the modelled failure mechanisms. Drilling fluid circulation was reported as being “good” at the depth of the buried top soil (Yetton and Engel). It is therefore, possible that the topsoil could act as a relatively impermeable boundary above which pore pressures could develop.

The results from the slope stability back-analysis show that the factor of safety is sensitive to relatively small changes in cohesion of the fill and buried top soil (Figure 7). Results shown in Figure 11 show that the static factor of safety would decrease by 0.2 with a reduction in cohesion of 5 kPa – at piezometric head levels of 2 m above the base of the buried topsoil, and assuming filled tension cracks.

In reality, it is probably more reasonable to assume that the shear strength parameters of the buried topsoil/fill would reduce in response to increasing water content linked to rainfall, rather than the development of a continuous pore pressure surface within the slope leading to a reduction in the effective stress within the saturated buried topsoil/fill.

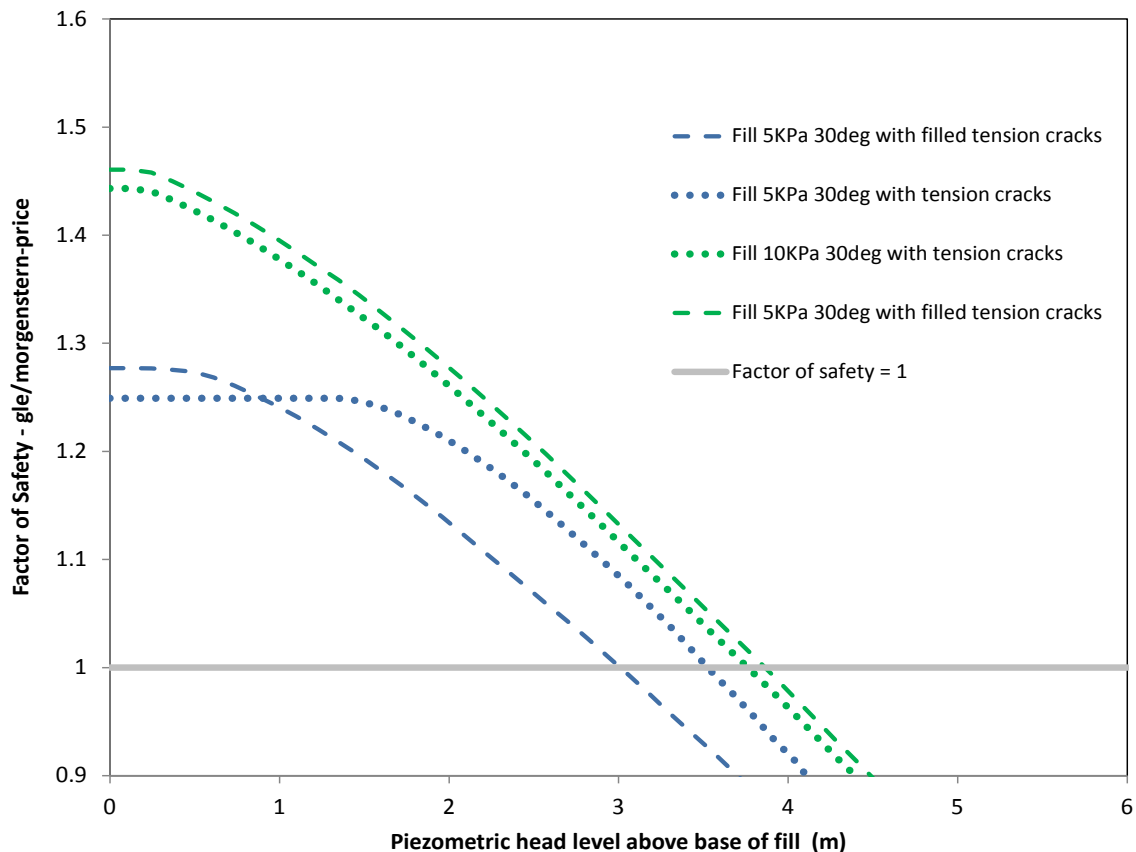


Figure 11 Sensitivity assessment of the slope factor of safety (source area 11A) in response to changing piezometric head levels and tension crack conditions. Variable tension crack depths have been used.

4.1.2 Source area 11B (cross-section 1)

This slope comprises a thin (<5 m) loess cover overlying volcanic breccia. Three static failure mechanisms were assessed:

1. *Failure through the loess:* The results from the assessment, adopting loess shear strength parameters of friction angle (ϕ) 30° cohesion (c) 10 kPa suggest that the slope factor of safety is above 1.5 (Table 8). These results suggest that the loess slope is relatively stable under static conditions. However, water ingress into the slope via the open tension cracks could cause washout failures to develop, but given the slope geometry these are unlikely to be large in volume.
2. *Failure of the rock slope through the breccia:* The factor of safety ranges from 1.9 to 5 for the range of adopted shear strength parameters given in Table 8.

3. *Failure of the rock slope by sliding along a weak basal layer:* The sensitivity of the slope to the presence of the 0.3 m layer of colluvium (Yetton and Engel, 2014) intercepted in drillhole QR4 within the volcanic breccia sequence and near the current elevation of the cliff toe has been assessed. The origin and lateral extent of this layer is unknown and may represent either a relict in-filled cave complex, or a paleo-surface in between the volcanic lava sequences. A failure mechanism involving block sliding through this weak layer was investigated, assuming that it is persistent within the slope and dips at the same angle from the horizontal as the overall volcanic sequence (about 15°). The results of the static assessment are summarised in Table 8, with factors of safety between 1.9 and 2.4. There is no evidence presented by Yetton and Engel (2014) to suggest groundwater levels could increase to critical levels. This appears consistent with the very small catchment area above the slope. Therefore the sensitivity of the slope to changes in groundwater was not assessed. The steeply-dipping (about 45°) clay slickensides reported by Yetton and Engel (2014) coating a defect in the breccia, are consistent with a block failure mechanism sliding on a lower angle basal surface.

Table 8 Example results from slope analysis of source area 11B across cross-section 1.

Simulated failure mechanism	Loess	Fill	Colluvium	Volcanic breccia	Weak layer	FOS ¹ SLIDE	Search surface ²	SRF ³ PHASE
	Cohesion (kPa) / Friction (°)	Cohesion (kPa) / Friction (°)						
1) Loess slope	10 / 30	10 / 30	0 / 23			1.7	Block	1.9
						1.8	Circular	
2) Rock slope	10 / 30		0 / 2	44 / 27 78 / 38 140 / 49		1.9	Circular	2.3
						3.0	Circular	4.2
						5.0	Circular	7.4
3) Rock slope with weak layer	10 / 30			44 / 27 78 / 8	10 / 30	1.9	Block	2.1
					10 / 30	2.4	Block	3.7

¹ FoS is the factor of safety derived using the general limit equilibrium method of Morgenstern and Price (1965).

² Block refers to the block slide surface method and CIRC refers to the circular slide surface method.

³ The finite element model was also used for comparison. Where the slope has been assessed using the finite element model, the stability of the slope is assessed in terms of the stress reduction factor. Note the shear strength reduction method is used to determine the Stress Reduction Factor (SRF) or factor of safety value that brings a slope to the verge of failure (Dawson et al., 1999).

4.1.3 Source area 11C (cross-section 3)

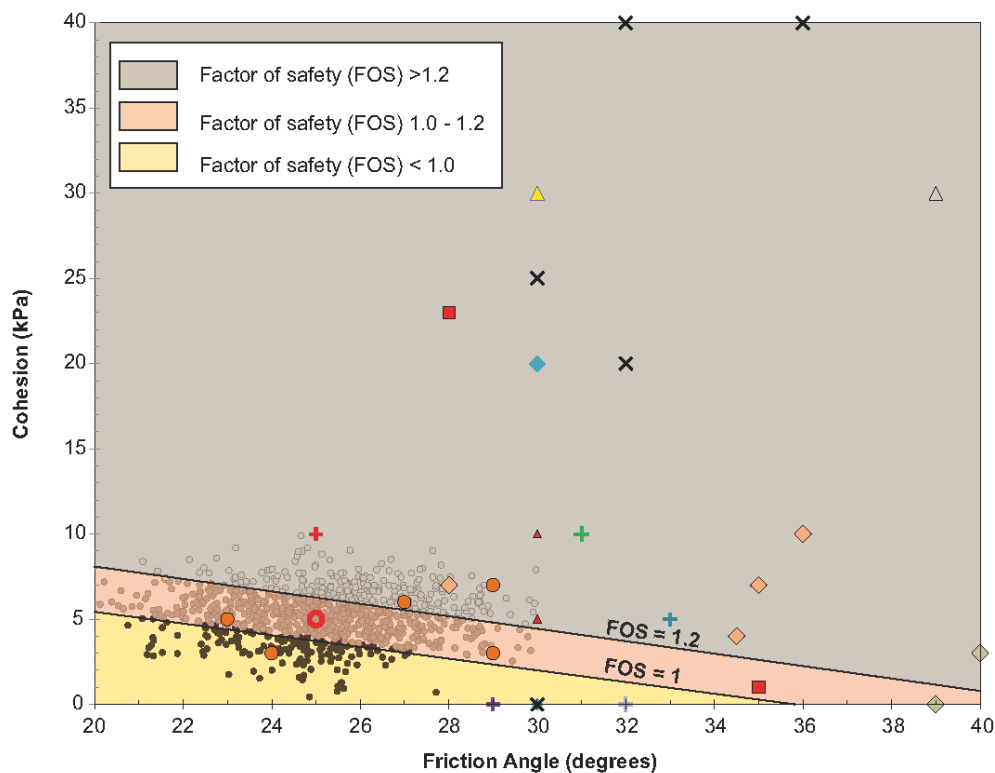
Source area 11C comprises fill material overlying loess. There are no drillholes to constrain the fill/loess boundary in the slope. The inferred geology of the slope is summarised in cross-section 3 (Figure 6). A considerable portion of this slope has been protected by an engineered structure comprising soil nails, shotcrete and mesh that was installed before the 2010/11 Canterbury earthquakes. The earthquake damaged this structure considerably. The effects of the soil nails, shotcrete and mesh installed on this slope have not been assessed or simulated, as they are assumed to now be damaged and of little benefit to the overall stability.

The dominant failure mechanism is thought to be failure through the fill or buried topsoil layer above the underlying loess. The result of back-analysis through cross-section 3 is shown in Table 9 and Figure 12. The results suggest that over the range of parameters thought to be reasonable (Figure 12) the static factor of safety of the slope is in the order of 1.1–1.3.

A small rise in groundwater levels of about 1 m above the buried topsoil layer, and within the fill, would reduce the factor of safety to about 1.0, indicating the slope is very sensitive to changes in pore pressure.

Table 9 Example results from slope stability assessment of source area 11C across cross-section 3.

Simulated failure mechanism	LOESS	FILL	TOP SOIL	Water level	FoS ¹ SLIDE	Search surface	SRF ² PHASE2
	Cohesion (kPa) / Friction (°)						
Failure through loess and fill	10 / 30	5–10 / 25–30	Assumed to be the same as the fill	Drained	1.1–1.3	Circular	1.3 (for fill cohesion of 5 kPa and friction 25°)
Failure through topsoil/fill	10 / 30	5 / 25	Assumed to be the same as the fill	1.0 m above topsoil	1.0	Circular and block	



- FOS<1.0 BackAnalysis
- FOS>1.0 BackAnalysis ($\phi=30^\circ$, $c=0\text{kPa}$)
- FOS>1.2 BackAnalysis ($\phi=30^\circ$, $c=0\text{kPa}$)
- Carey et al. (2014) DIRECT SHEAR RESIDUAL 16 wt% water content
- Carey et al. (2014) RING SHEAR RESIDUAL 16 to 19 wt% water content
- ◆ Goldwater 1990 RESIDUAL water content unknown
- ▲ Tehrani (1988) DIRECT SHEAR PEAK 7wt% water content
- △ Tehrani (1988) DIRECT SHEAR PEAK dry water content
- × MCDowell (1989) TRIAXIAL PEAK 8 - 19 wt% water content
- ⊕ Tonkin and Taylor & Geotechnics RING SHEAR RESIDUAL 15-20 wt% water content
- ⊕ Tonkin and Taylor & Geotechnics TRIAXIAL PEAK 21 wt% water content
- ⊕ Tonkin and Taylor & Geotechnics RING SHEAR RESIDUAL 19-21 wt% water content
- ◆ Jowett (1995) DIRECT SHEAR PEAK 10.1-11.5 wt% water content
- ◆ Jowett (1995) DIRECT SHEAR PEAK 12.8-21.5 wt% water content
- ▲ Dynamic Back Analysis
- Static Back Analysis

Figure 12 Numerical slope stability back-analysis of the fill/buried top soil material for cross-section 3, representing source area 11C. Note: each data point represents a modelled slide surface at a given combination of cohesion and friction adopted for the fill/buried top soil. Those slide surfaces shown as crosses, represent those combinations of cohesion and friction that would yield a static factor of safety of less than 1, assuming no groundwater.

Figure 13–Figure 17 are example limit equilibrium and finite element results for the modelled slope cross-sections 1–3 (Figure 6).

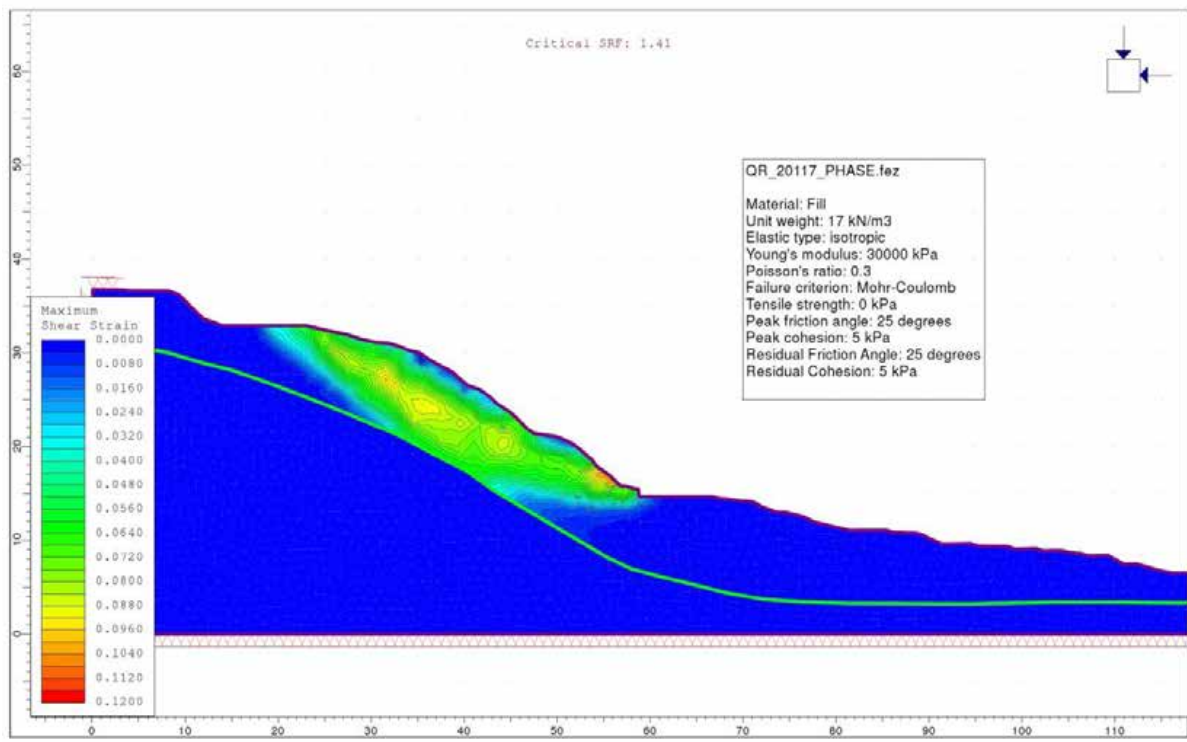
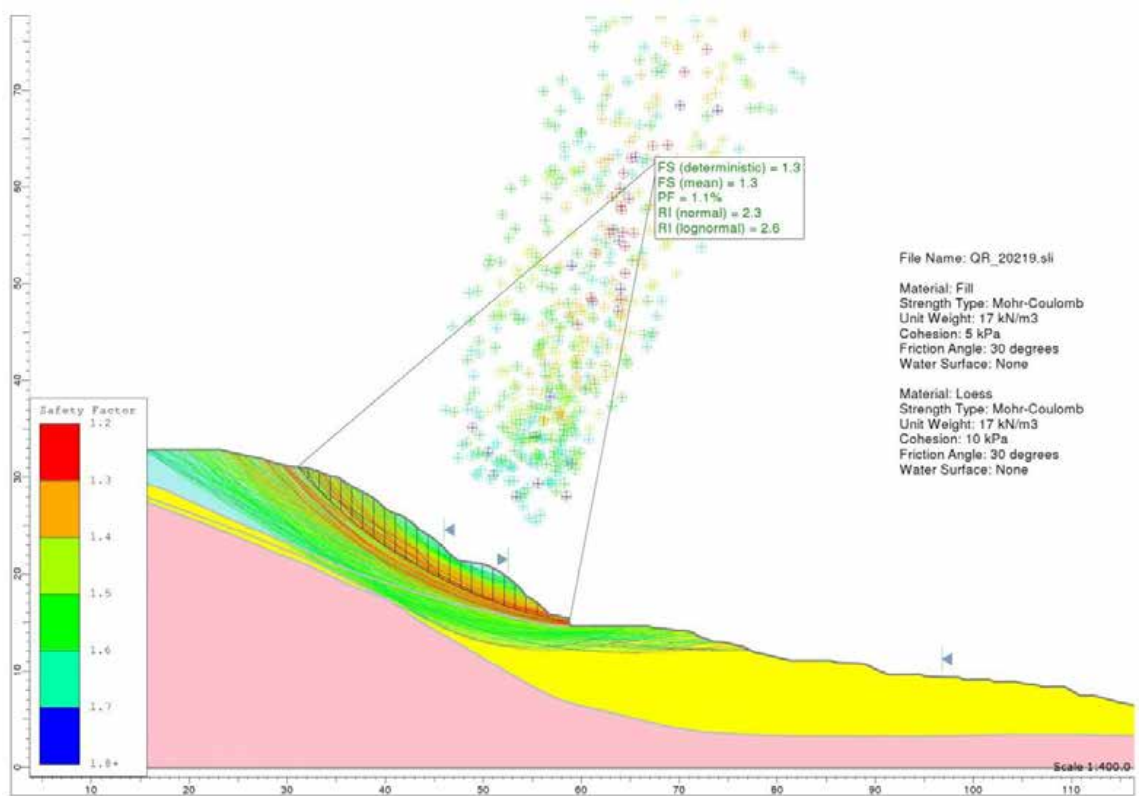


Figure 13 Example of limit equilibrium and finite element modelling results for cross-section 2, representing source area 11A.

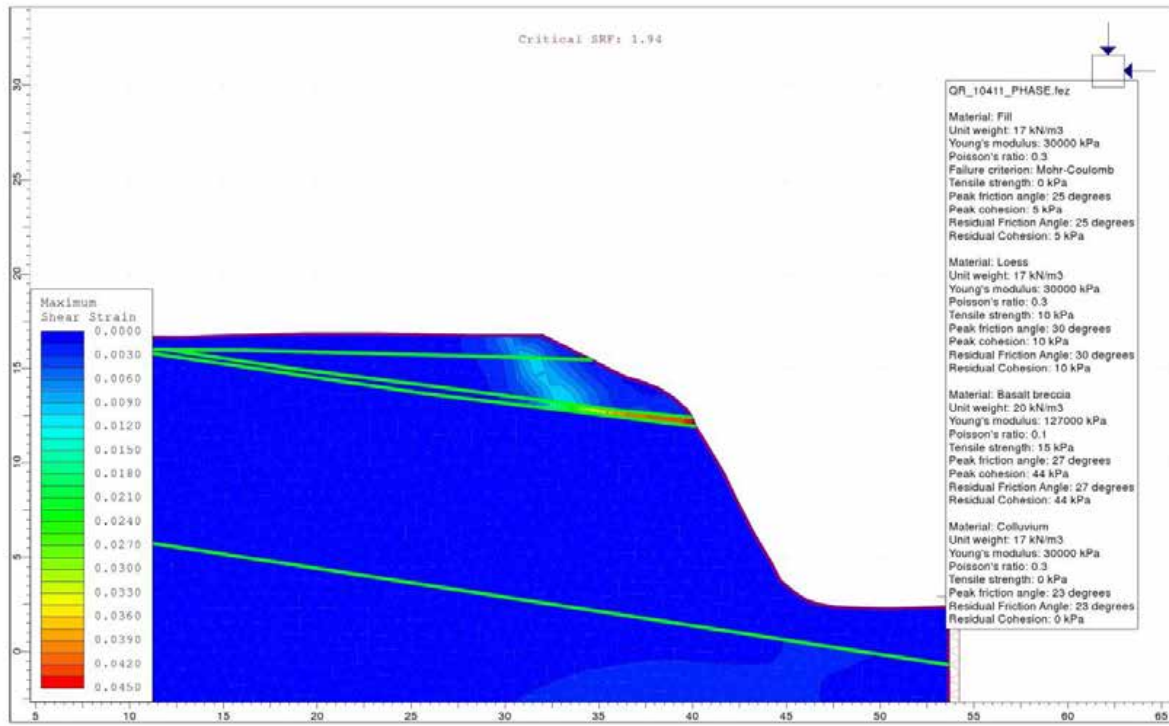
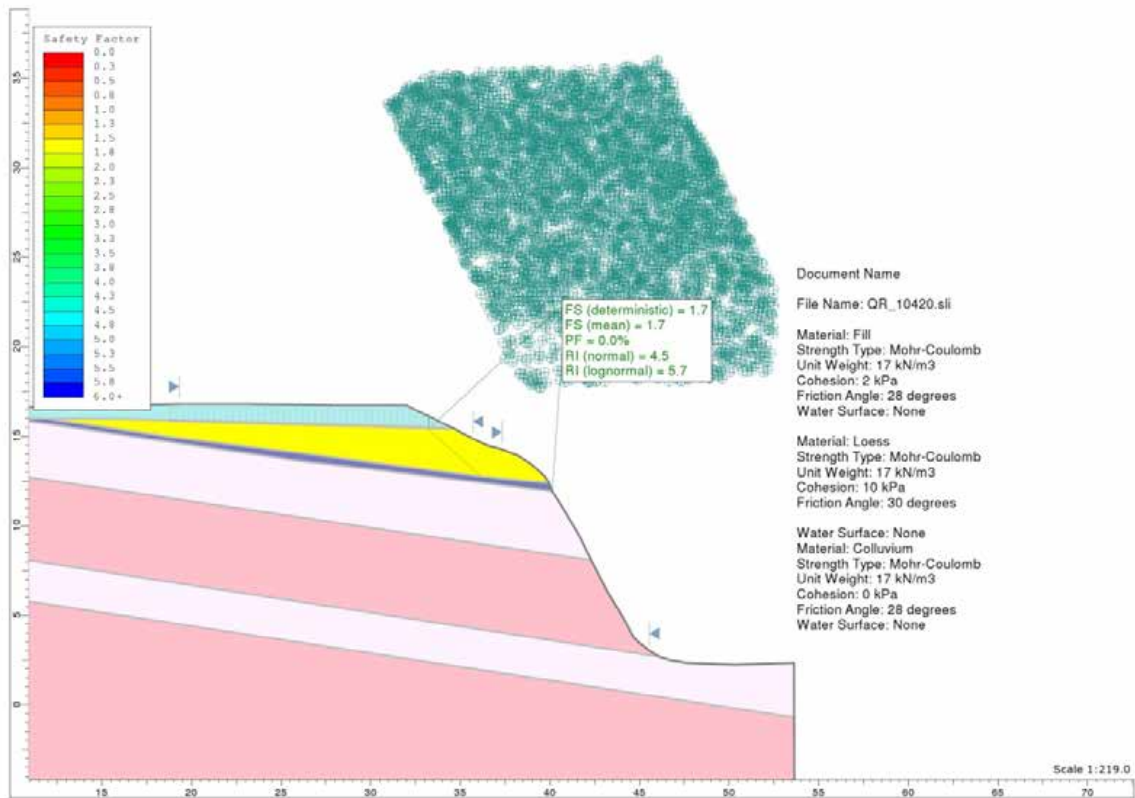


Figure 14 Example of limit equilibrium and finite element modelling results for cross-section 1, representing source area 11B, for failure mechanism 1 through the loess.

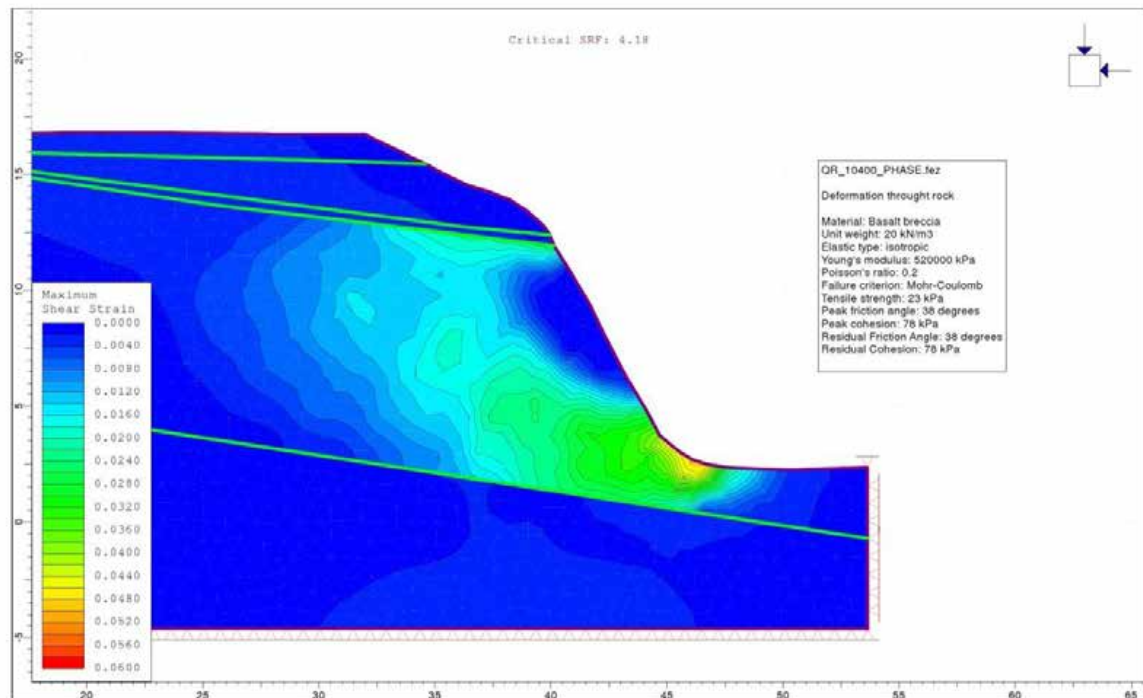
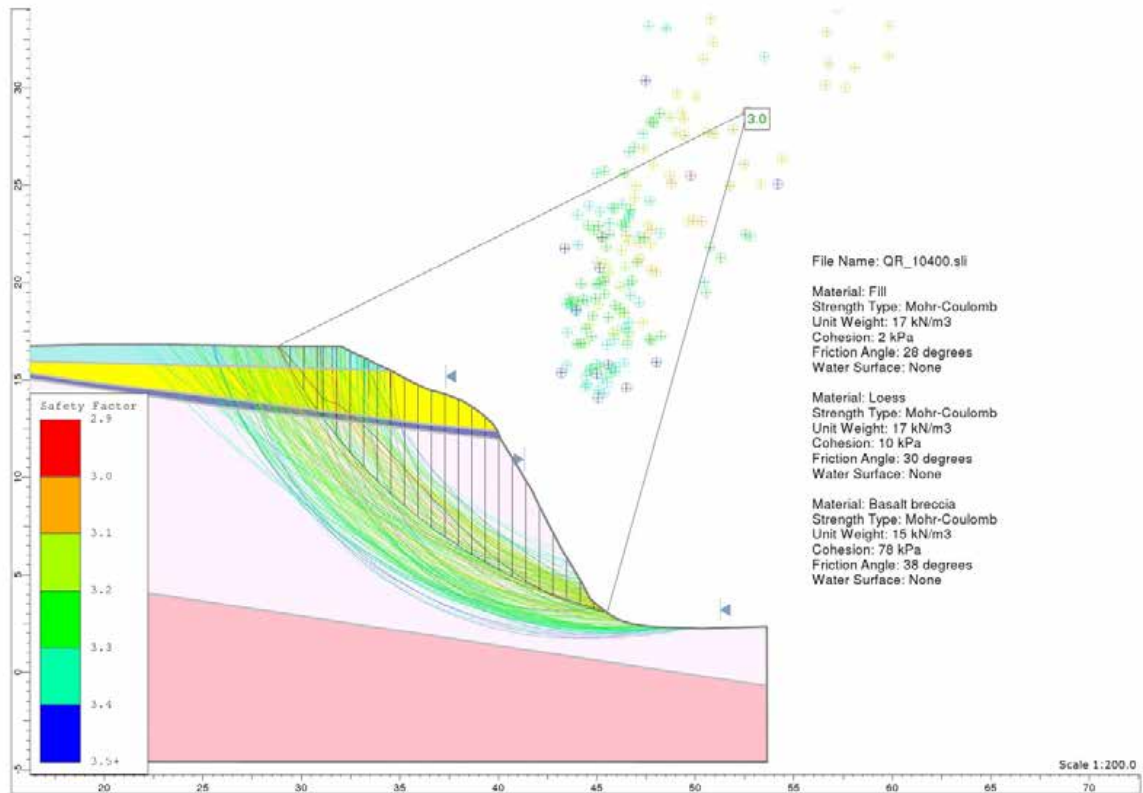


Figure 15 Example of limit equilibrium and finite element modelling results for cross-section 1, representing source area 11B, for failure mechanism 2 through the rock.

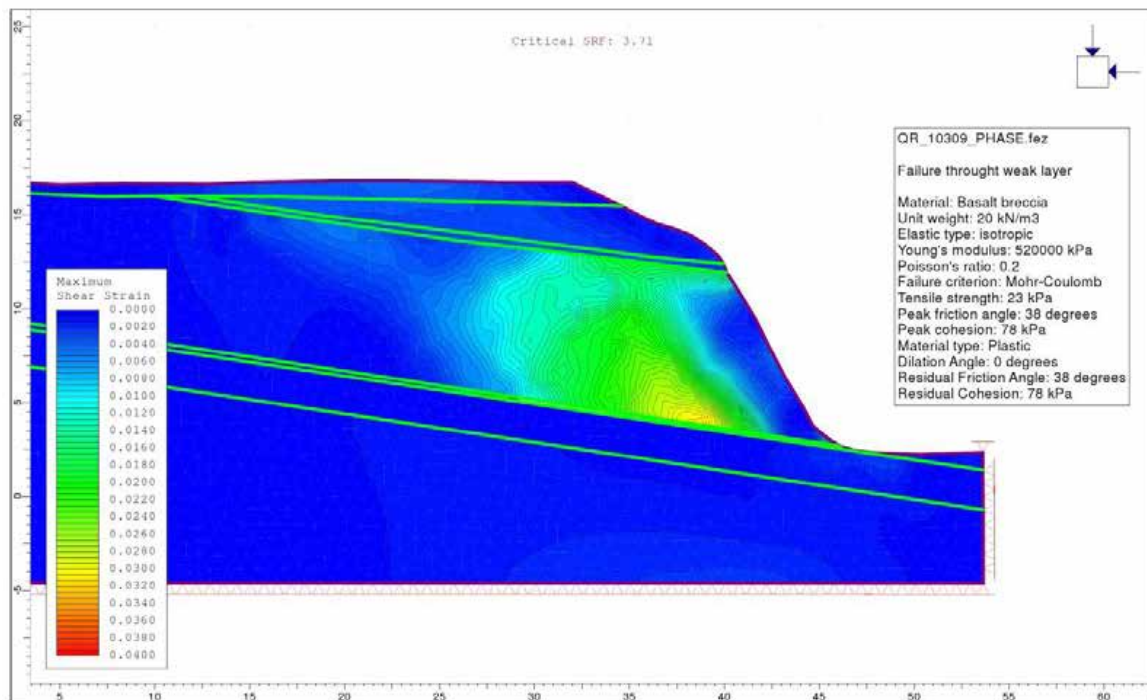
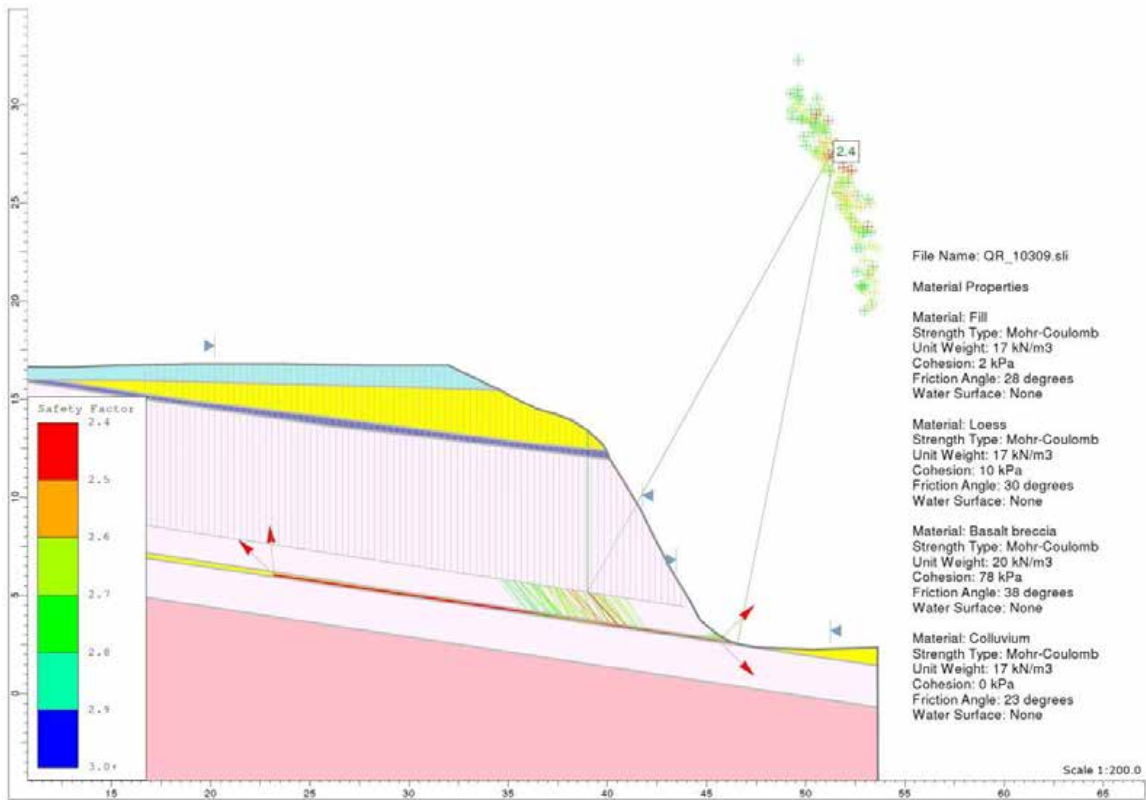


Figure 16 Example of limit equilibrium and finite element modelling results for cross-section 1, representing source area 11B, for failure mechanism 3 through the weak layer.

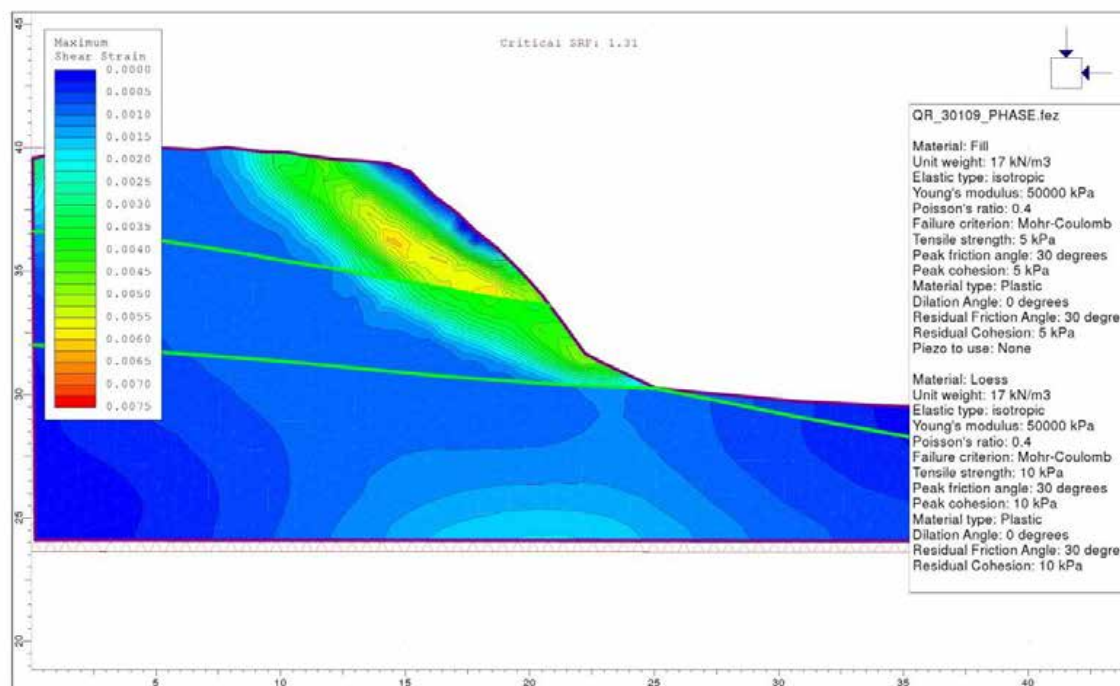
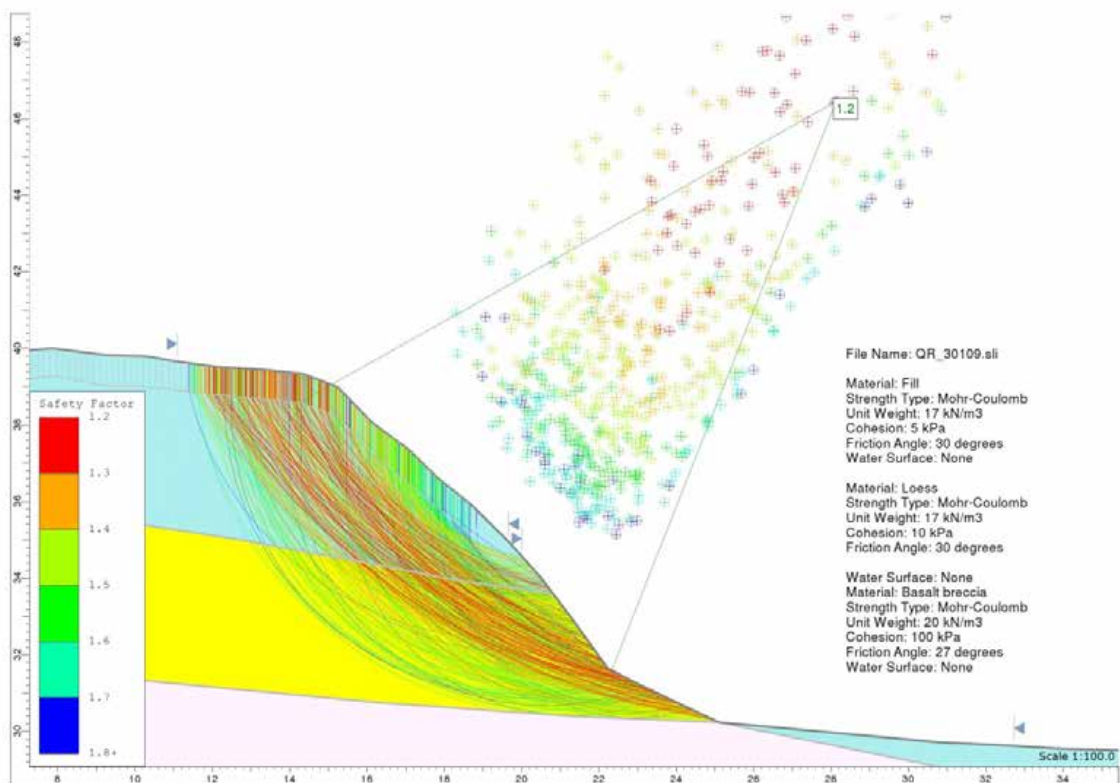


Figure 17 Example of limit equilibrium and finite element modelling results for cross-section 3, representing source area 11C, for a failure mechanism through the fill and loess.

4.2 SLOPE STABILITY – DYNAMIC CONDITIONS

Dynamic stability assessment comprised: 1) back-analysing the performance of the slope during the 2010/11 Canterbury earthquakes to calibrate the models and verify that the calculated displacements are consistent with those recorded during the earthquakes; and 2) using the calibrated models to forecast the likely magnitudes of future displacements under potential future peak ground acceleration scenarios.

Two cross-sections have been assessed representing source area 11A (cross-section 2) and 11B (cross-section 1). The dynamic stability of source area 11C has not been dynamically assessed as the main trigger is thought to be rain given its low static factor of safety. The slope stability of source areas 11A and 11B under dynamic conditions is assessed by assuming a drained slope with no permanent water table.

4.2.1 Amplification of ground shaking

The first stage of the assessment was to calculate the maximum acceleration at the slope crest (A_{MAX}) to quantify any amplification effects caused by topography and/or contrasting materials between the peak ground acceleration of the free field rock input motion and the peak acceleration at the slope crest (A_{MAX}). The slope crest is defined as the convex break in slope between the lower steeper slope and the upper less steep slope. Results from the dynamic site response assessment are contained in Appendix 3.

Results from this assessment show that the relationship between the peak ground acceleration of the free-field input motion (A_{FF}) and the corresponding modelled peak acceleration at the cliff crest (A_{MAX}) is approximately linear. The mean amplification factor (S_T) between A_{FF} and A_{MAX} (all modelled earthquakes) is 2.6 (± 0.2) for horizontal motions and 3.7 (± 0.2) for vertical motions. However, over the range of modelled peak horizontal accelerations, the peak ground acceleration amplification factors (S_T) for source area 11A (cross-section 2) at lower peak input accelerations are 4.4–4.5 (for the 16 April and 23 December 2011 earthquakes). At higher peak input accelerations (associated with 22 February and 13 June 2011 earthquakes) the amplification factors are 1.9–2.7, indicating the relationship is non-linear.

For source area 11B (cross-section 1) the relationship between the peak ground acceleration of the free-field input motion (A_{FF}) and the corresponding modelled peak acceleration at the cliff crest (A_{MAX}), is approximately linear, and range from 2.2 to 3.0 for horizontal motions and 0.6 to 1.6 for vertical motions. The mean amplification factor is 2.8 (± 0.2) for horizontal motions and 2.4 (± 0.1) for vertical motions. Errors, shown in brackets, are at one standard deviation.

The input peak accelerations are those derived from the synthetic free-field rock outcrop earthquake time acceleration histories described by Holden et al. (2014).

For cross-section 2 (source area 11A) these factors are at the upper end of those reported in the literature. This may be due to the impedance contrasts between the loess/fill and rock being so high leading to the trapping of seismic waves. However, in experimental data, as the slope displaces, the shear surface “base isolates” the mass above, resulting in lower levels of shaking and displacement. Assessment of this is outside the scope of this report.

4.2.2 Back-analysis of permanent slope deformation

Earthquake-induced permanent displacements were calculated using the decoupled method (Makdisi and Seed, 1978) and the Slope/W software. This was done for a range of slide surfaces, with: 1) different yield accelerations (K_y); and 2) different ratios of yield acceleration (K_y) to the maximum average acceleration of the slide mass (K_{MAX}). Permanent displacements were estimated along the slide surface, where the displacing mass was treated as rigid-plastic body and no internal plastic deformation of the mass was accounted for. Also, the mass accrued no displacement at accelerations below the yield acceleration.

The synthetic rock outcrop earthquake time acceleration histories from the 22 February and 13 June 2011 earthquakes were used as inputs for the modelling, as permanent coseismic displacement of the Quarry Road source areas were recorded or inferred (from site observations) during these events. The synthetic rock outcrop earthquake time acceleration histories from the 16 April and 23 December 2011 earthquakes were also modelled to confirm that either no modelled movement or very minor (undetectable) movement of the slopes occurred. Variable material strength parameters were used for the critical materials present in each source area. The different parameters used in the modelling are listed in Table 10.

For these assessments, the displacements inferred from crack apertures are assumed to represent the coseismic permanent displacement of the slopes during the 22 February and 13 June 2011 earthquakes. It should be noted that the displacements estimated from crack apertures could be lower bound estimates as not every crack was mapped and no account for plastic deformation of the soil mass (without cracking) has been taken into account. Conversely they could also be upper bound estimates, especially in locations where loess covers the rock mass, and where displacement of the rock mass is inferred from crack apertures in the covering soil (loess).

The results from each modelled scenario were then compared to the recorded coseismic permanent slope displacements for each earthquake, for each cross-section.

Table 10 Material strength parameters used for modelling permanent coseismic displacements for cross-sections 1 and 2. Coseismic displacements are inferred from survey records and field mapping of cracks.

Source area	Earthquake	Critical material	Cohesion c (kPa)	Friction ϕ (°)	Total inferred coseismic displacement (m)
11A Cross-section 2	22 February and 13 June 2011	Fill	5	25	1.8 (22 Feb). < 0.01 (13 Jun).
		Fill	5	30	
		Fill	10	30	
		Fill	20	30	
		Loess	10	30	
		Mixed basalt lava and breccia	38	78	
11A Cross-section 2	16 April and 23 December 2011	Fill	5	30	< 0.05 (no recorded displacement but not monitored)
		Fill	10	30	
		Loess	10	30	
		Mixed basalt lava and breccia	38	78	
11B Cross-section 1	22 February and 13 June 2011	Loess	5	30	0.9 (crack apertures) and 0.1 (toe breakout) (22 Feb). < 0.1 (13 Jun)
		Loess	10	30	
		Loess	20	30	
		Mixed basalt lava and breccia	44	27	
		Mixed basalt lava and breccia	78	38	
		Weak zone within volcanic sequence	10	30	
11B Cross-section 1	16 April and 23 December 2011	Loess	10	30	No recorded displacement
		Mixed basalt lava and breccia	44	27	
		Weak zone within volcanic sequence	10	30	

4.2.2.1 Source area 11A (cross-section 2)

The results from the modelling of the 22 February and 13 June 2011 earthquakes, adopting the parameters listed in Table 10, are shown in Figure 18 and Figure 19 respectively. The results show that:

- A good correlation between the recorded permanent coseismic displacements and modelled displacements for the 22 February and 13 June 2011 earthquakes was obtained for modelled slide surfaces adopting shear strength parameters for the fill of cohesion (c) 10 kPa and friction (ϕ) of 30°.
- The lowest yield acceleration for the modelled slide-surface geometries (adopting strength parameters for the fill of cohesion 10 kPa and friction (ϕ) of 30°) is about 0.2 g.
- Modelled permanent displacements for the 16 April and 23 December 2011 earthquakes were less than 0.01 m, adopting shear strength parameters for the fill of cohesion (c) 10 kPa and friction (ϕ) of 30°.

- There is a good correlation between the locations of the modelled slide surfaces with the lowest yield accelerations and the locations of the mapped cracks and slope toe deformation (Figure 20). There is also a good correlation between the locations and shape of the slide surfaces derived from the limit equilibrium and finite element static stability modelling, and those from the dynamic modelling.
- Given the low strength of the fill and the magnitude of inferred displacements under drained conditions, it is possible that larger permanent displacements of the fill could occur under dynamic conditions if:
 - i. the shear strength of the fill were to reduce in response to increased water content and or reduction in effective stress caused by elevated pore pressures.
 - ii. the duration of shaking in future earthquakes was longer than that experienced at the site during the 2010/11 for example an earthquake of a far-field fault such as the Porters Pass Fault.

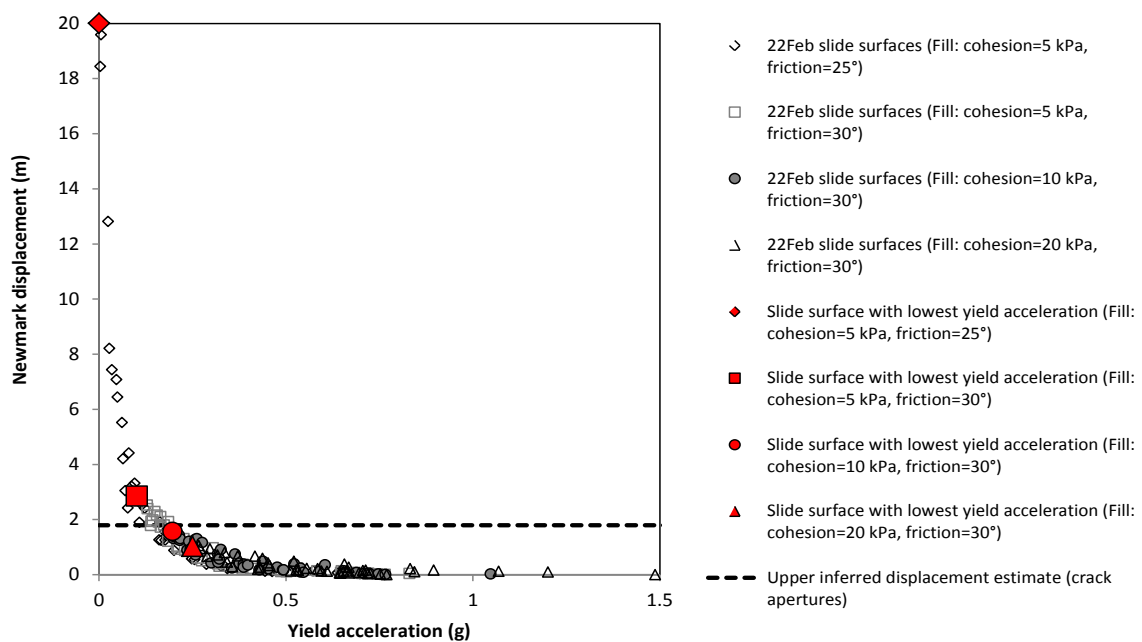


Figure 18 22 February 2011 earthquake, modelled Slope/W decoupled displacements for source area 11A (cross-section 2), adopting variable estimates of the material strength of the fill. Each data point represents a modelled slide surface and the corresponding estimate of its displacement as a result of the 22 February 2011 earthquake – adopting the synthetic free-field rock outcrop earthquake acceleration time histories. Data points are for slide surfaces mainly in fill. The dashed lines represent the total inferred coseismic permanent displacement for the cross-section during the given earthquake.

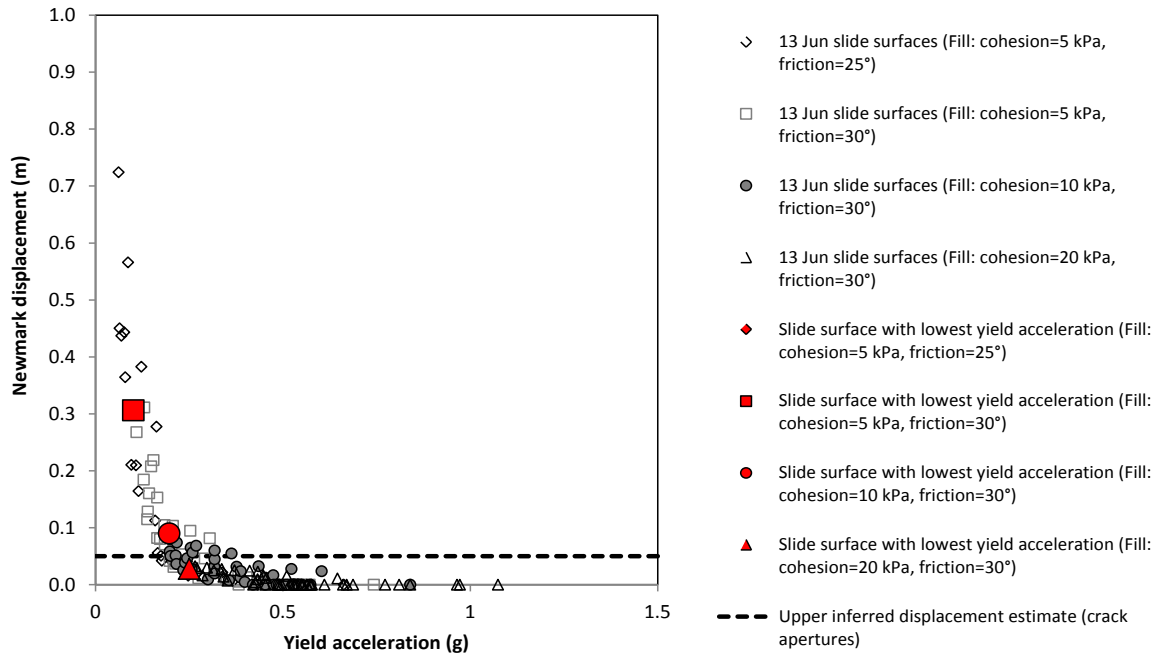


Figure 19 13 June 2011 earthquake, modelled Slope/W decoupled displacements for source area 11A (cross-section 2), adopting variable estimates of the material strength of the fill. Each data point represents a modelled slide surface and the corresponding estimate of its displacement as a result of the 13 June 2011 earthquake – adopting the synthetic free-field rock outcrop earthquake acceleration time histories. Data points are for slide surfaces mainly in fill. The dashed lines represent the inferred coseismic permanent displacement for the cross-section during the given earthquake.

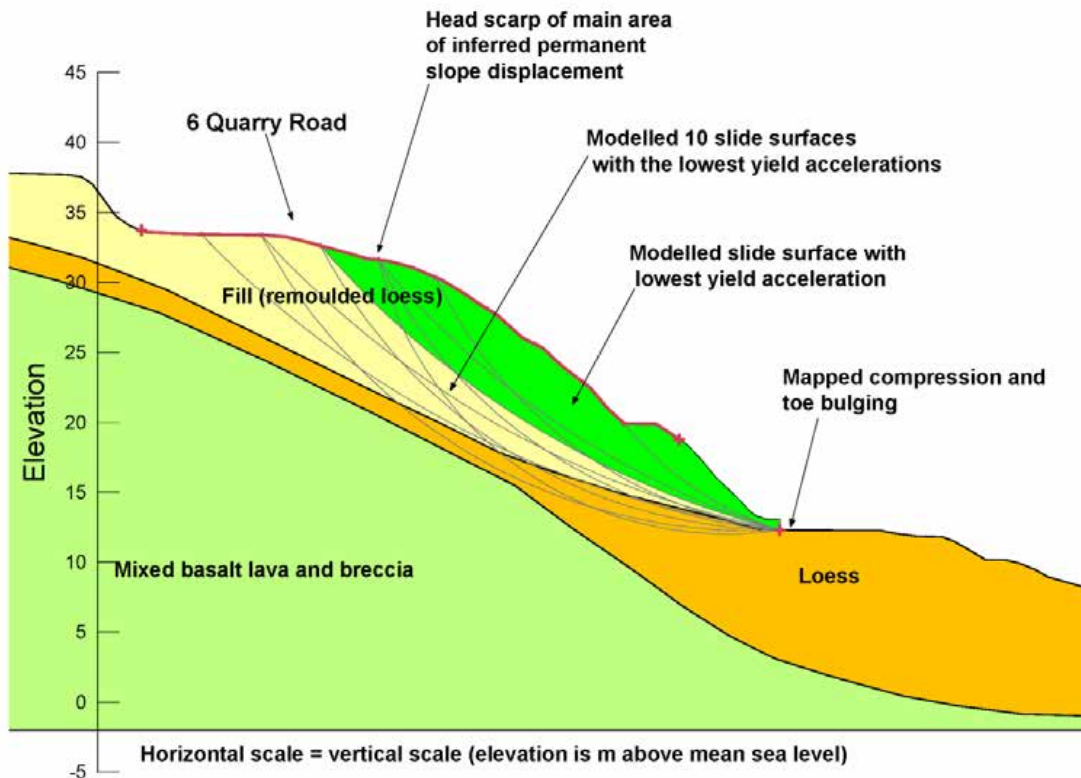


Figure 20 Source area 11A (cross-section 2) seismic slope stability assessment for the 22 February 2011 earthquake. The slide surface, and associated slide mass, with the lowest yield acceleration is shown bright green in colour.

4.2.2.2 Source area 11B (cross-section 1)

The results from the modelling of the 22 February and 13 June 2011 earthquakes, adopting the parameters listed in Table 10, are shown for the different modelled slope failure mechanisms:

- Mechanism 1 – failure through the loess only
- Mechanism 2 – failure through the rock
- Mechanism 3 – deep-seated failure of rock through the weak layer within the rock mass.

Figure 21, Figure 22 and Figure 23 show the modelled slide surfaces for the different assessed failure mechanisms. Figure 24 and Figure 25 show the estimated displacements for each assessed failure mechanism.

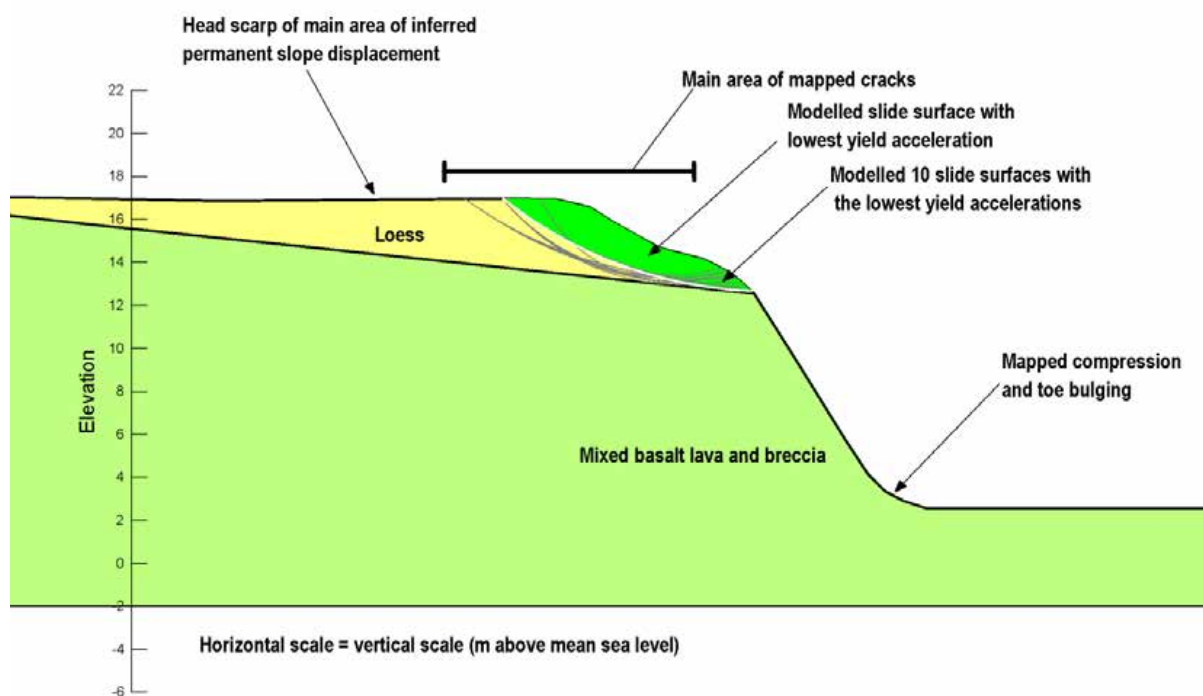


Figure 21 Source area 11B (cross-section 1) seismic slope stability assessment for the 22 February 2011 earthquake. Failure mechanism 1, failure through the loess only. The slide surface, and associated slide mass, with the lowest yield acceleration is shown bright green in colour.

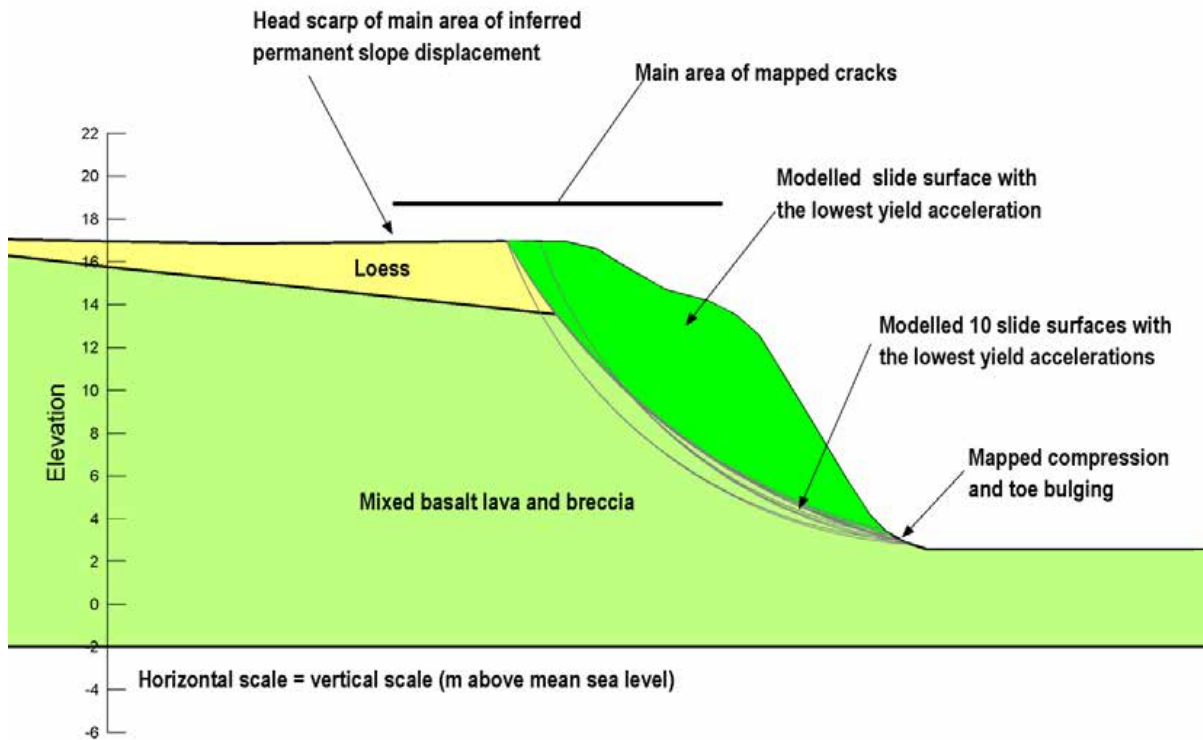


Figure 22 Source area 11B (cross-section 1) seismic slope stability assessment for the 22 February 2011 earthquake. Failure mechanism 2, relatively shallow failure through the rock. The slide surface, and associated slide mass, with the lowest yield acceleration is shown bright green in colour.

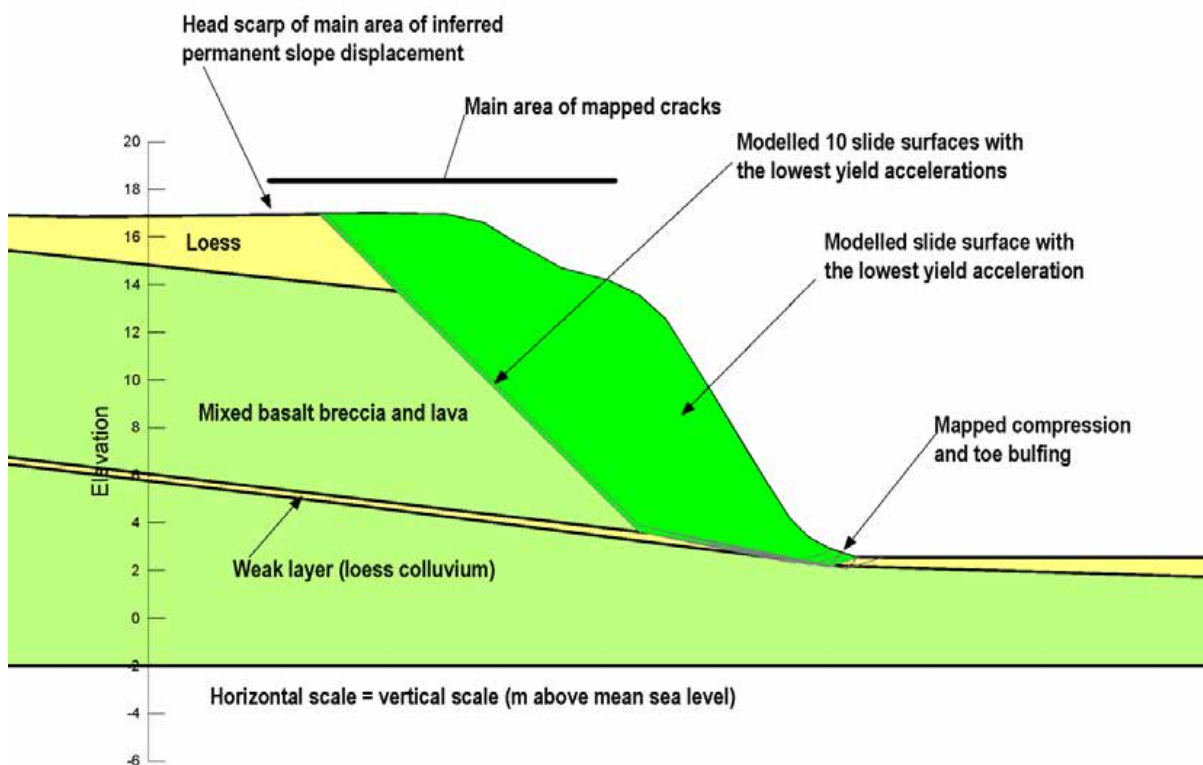


Figure 23 Source area 11B (cross-section 1) seismic slope stability assessment for the 22 February 2011 earthquake. Failure mechanism 3, failure of rock through the weak layer within the rock mass. The slide surface, and associated slide mass, with the lowest yield acceleration is shown bright green in colour.

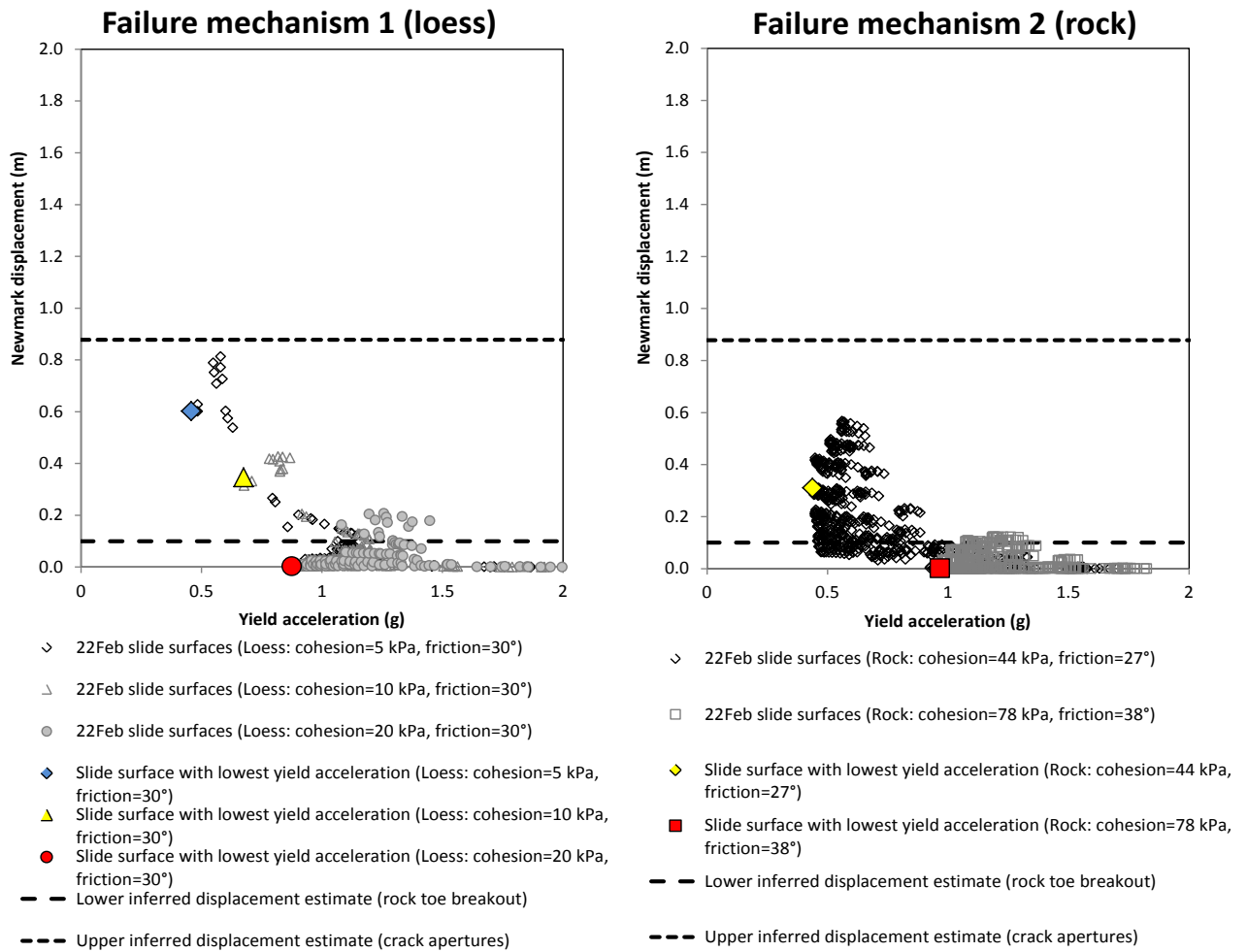


Figure 24 22 February 2011 earthquake, modelled Slope/W decoupled displacements for source area 11B (cross-section 1), adopting variable estimates of the material strength of the loess and rock. Each datapoint represents a modelled slide surface and the corresponding estimate of its displacement as a result of the 22 February 2011 earthquake – adopting the synthetic free-field rock outcrop earthquake acceleration time histories. Data points are for failure mechanisms 1 and 2. The dashed lines represent the total inferred coseismic permanent displacement for the cross-section during the given earthquake.

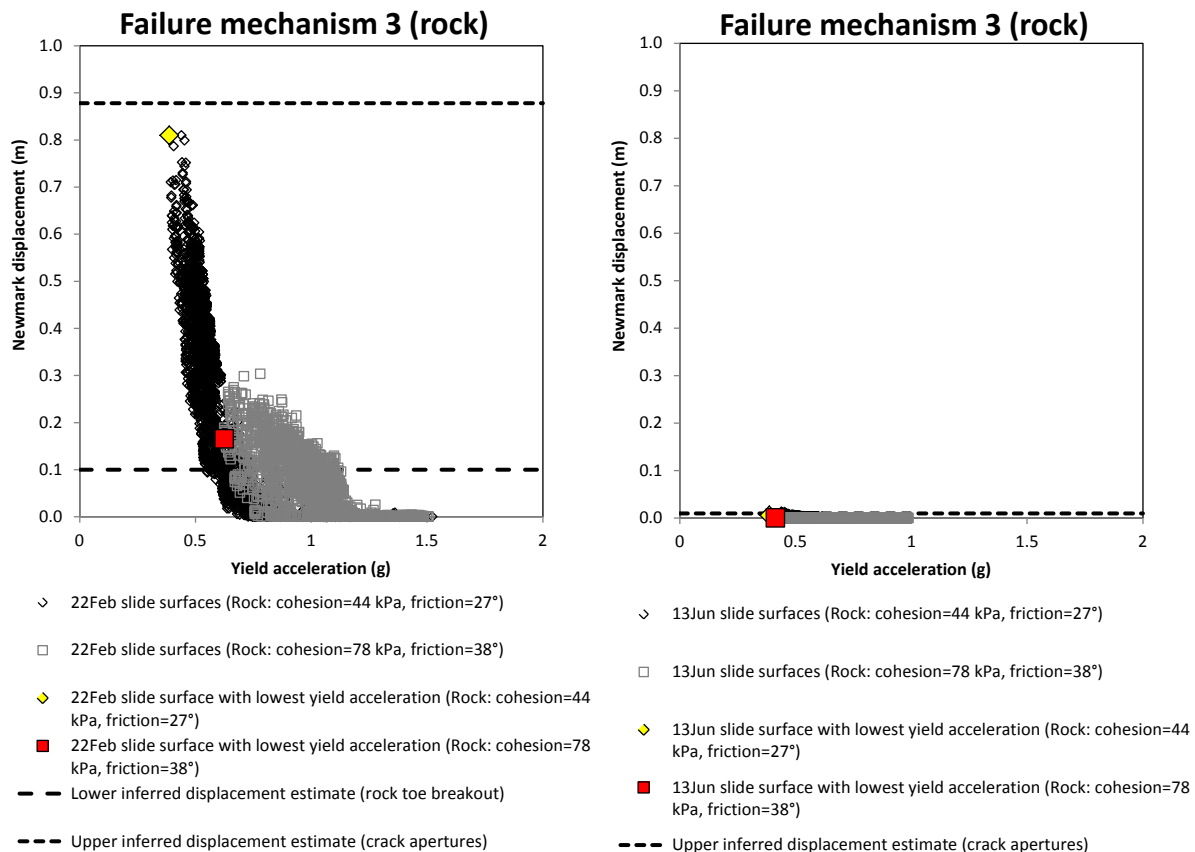


Figure 25 22 February and 13 June 2011 earthquakes, modelled Slope/W decoupled displacements for source area 11B (cross-section 1), adopting variable estimates of the material strength of the rock. Each datapoint represents a modelled slide surface and the corresponding estimate of its displacement as a result of the 22 February and 13 June 2011 earthquakes – adopting the synthetic free-field rock outcrop earthquake acceleration time histories. Data points are for slide surfaces through the weak layer within the rock (mechanism 3). The dashed lines represent the total inferred coseismic permanent displacement for the cross-section during the given earthquake.

The results from the assessment show that:

- The best correlation between the recorded permanent coseismic displacements and modelled displacements for the 22 February and 13 June 2011 earthquakes was obtained for modelled slide surfaces adopting mechanisms 1 (through the loess) and 3 (through the weak layer within the rock).
- Mechanism 1 however, cannot account for the mapped compression and bulging in rock at the toe of the slope. It also cannot account for the angle of displacement, inferred from crack apertures, which is about 48° from the horizontal, and much steeper than the loess/rock boundary, which is dipping at about 10° from the horizontal.
- Mechanism 2 on its own cannot account for the total inferred displacement of the slope, even when adopting the lower rock shear strength parameters are adopted of cohesion 44 kPa and friction (ϕ) 27° (which are at the lower end of the range thought to be credible and probably represent the shear strength of defects within the rock mass rather than the intact strength). However, it is possible that mechanisms 1 and 2 could, when combined, yield the inferred permanent slope displacements relating to the 22 February 2011 earthquake.
- Modelled permanent displacements for mechanisms 1 and 2 in response to the modelled 16 April, 13 June and 23 December 2011 earthquakes were less than 0.01 m, adopting the range of shear strength parameters given in Figure 23.

- Although mechanism 3 gives a good correlation, its credibility is uncertain, as the movement is inferred to be deep-seated and through the logged (in the drillhole) weak layer within the rock mass. The lateral persistence and strength of such a layer is uncertain and cannot be constrained from the current field mapping and drillhole alone.
- The lowest yield accelerations for the modelled slide-surface geometries (adopting the lower estimates of the strength parameters for the loess and rock mass, Figure 23 and 24) are between 0.4 and 0.5 g, for all failure mechanisms.
- It is therefore possible that future permanent displacements of the slope could occur, under dynamic conditions, via all three failure mechanisms. However, the probability of catastrophic failure (where the mass breaks down to form a debris avalanche) will be a function of the magnitude of any future permanent coseismic displacements of the mass.

4.2.2.3 Source area 11C (cross-section 3)

Given the relatively small size of the slope and lack of subsurface information, a simple assessment of the stability of the slope under dynamic conditions was carried out, adopting the pseudostatic method of assessment to determine the critical yield acceleration of the slope. The critical yield acceleration of a given slide mass is the minimum pseudostatic acceleration required to produce instability of the mass (Kramer, 1996).

The results are shown in Figure 26, for various fill (including topsoil) shear strength parameters. The critical yield acceleration of the slope varies between about 0.05 and 0.2 for the range of parameters assessed.

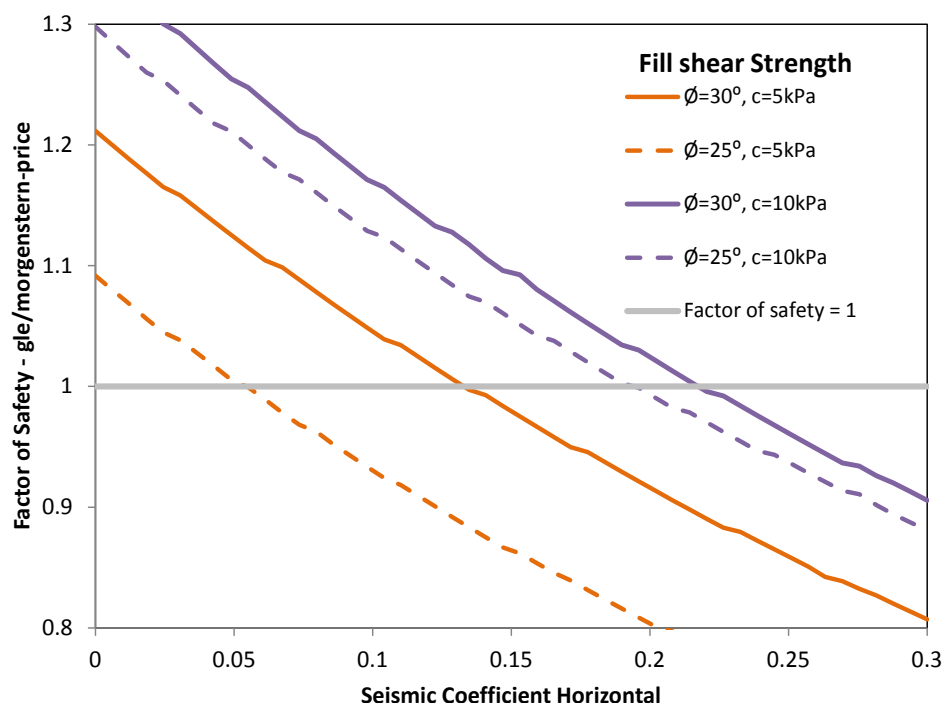


Figure 26 Yield acceleration of the slope based on variable fill parameters and loess parameters shown in Table 11. Yield acceleration calculated adopting the pseudostatic method (Kramer, 1996).

4.2.2.4 Forecast modelling of slope deformation

Permanent displacements, from the decoupled assessment results from the 22 February and 13 June 2011 modelled earthquakes, were calculated for a range of slide-surface geometries with different ratios of yield acceleration (K_y) to the maximum average acceleration of the failure mass (K_{MAX}). The maximum average acceleration (K_{MAX}) was calculated for each selected slide surface by taking the maximum value of the average acceleration time history from the response to the synthetic earthquake. About 10 slide surfaces were chosen to represent the results from each earthquake input motion, adopting different estimates of the shear strength of the key materials (listed in Table 10).

Source area 11A (cross-section 2)

The results from the assessment are shown in Figure 27 for those slide surface shown in Figure 19. The results show that between K_y/K_{MAX} values of 0.05 and 0.4, and K_y/A_{FF} values of 0.1 and 0.6, the data are well fitted to a straight line (exponential trend line) in semi-log space. The coefficient of determination (R^2) is 0.94 for K_y/K_{MAX} and 0.86 for K_y/A_{FF} , and includes all of the plotted data ($N = 31$). The gradients of the fitted lines are different, with the K_y/K_{MAX} line having a slightly steeper gradient, indicating, as expected, that for the same magnitude of displacement the ratio of K_y/K_{MAX} is lower than the corresponding K_y/A_{FF} ratio. The poorer coefficient of determination for ratios of K_y/A_{FF} is not unusual as Newmark (1965) displacements are highly sensitive to the high frequency components of the input motions, which can vary from event to event. By comparison, K_{MAX} “filters” the higher frequency components, and thus is less sensitive to the input motion characteristics.

The peak ground acceleration of the input motion (A_{FF}) does not take into account amplification effects caused by the slope geometry, and at this site, the material contrasts within the slope, between the fill and underlying rock. From the data in Figure 27, the mean ratio of K_{MAX} to A_{FF} for source area 11A is 1.7 (± 0.4 at one standard deviation), meaning that K_{MAX} is on average 1.7 times greater than the peak horizontal ground acceleration of the input motion.

For ratios of K_y/K_{MAX} in Figure 27, the estimated magnitudes of displacement are consistent with those reported by Jibson (2007), where the data plot between the ranges of data for earthquakes of M6.5–7.5 reported by Makdisi and Seed (1978) and plotted by Jibson (2007).

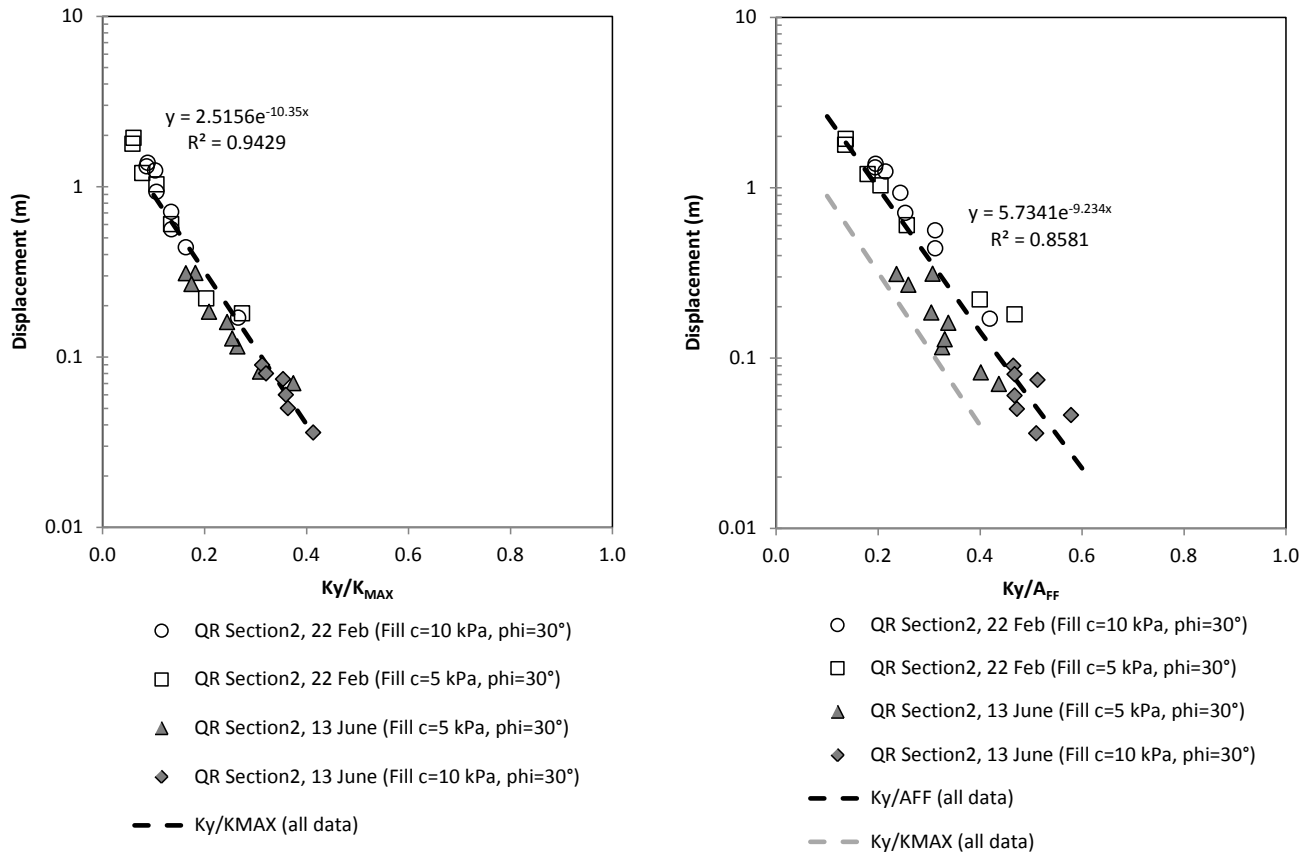


Figure 27 Source area 11A (cross-section 2), decoupled Slope/W displacements calculated for different ratios of yield acceleration to maximum average acceleration of the mass (Ky/K_{MAX}), and maximum acceleration of the mass (Ky/A_{FF}), for selected slide-surface geometries, and given material shear strength parameters. A_{FF} is the peak acceleration of the input earthquake time acceleration history. Synthetic rock outcrop time acceleration histories for the 22 February and 13 June 2011 earthquakes were used as inputs for the assessment. ($N = 31$). The dashed lines are exponential trend lines fitted to the semi-log data. The formula and the coefficient of determination (R^2) for the trend lines are shown.

Source area 11B (cross-section 1)

The results from the assessment are shown in Figure 28 for those slide surface shown in Figure 22 and Figure 23, for failure mechanisms 2 and 3 only. Failures through the loess (mechanism 1) have been discounted as they are likely to be relatively small in volume, in comparison to those that could be generated by failures through the rock mass.

The results show that between Ky/K_{MAX} values of 0.1 and 0.6 and Ky/A_{FF} values of 0.4 and 1.3, the data are well fitted to a straight line (exponential trend line) in semi-log space. The coefficient of determination (R^2) is 0.77 for Ky/K_{MAX} and 0.50 for Ky/A_{FF} , and includes all of the plotted data ($N = 40$). The gradients of the fitted lines are different, with the Ky/K_{MAX} line having a steeper gradient, indicating, as expected, that for the same magnitude of displacement the ratio of Ky/K_{MAX} is lower than the corresponding Ky/A_{FF} ratio.

For some slide surfaces in Figure 21 and Figure 22 the yield accelerations are larger than the peak horizontal acceleration of the input motion. In such cases permanent coseismic displacement should not occur. However, the peak horizontal acceleration of the input motion (A_{FF}) does not take into account amplification effects caused by the slope geometry, which at this site is relatively steep with a sharp convex break in slope at the crest. From the data in

Figure 28, the mean ratio of K_{MAX} to A_{FF} for source area 11B is 1.9 (± 0.4 at one standard deviation), meaning that K_{MAX} is on average 1.9 times greater than the peak horizontal ground acceleration of the input motion.

For ratios of K_y/A_{FF} in Figure 28, the estimated magnitudes of displacement are consistent with those reported by Jibson (2007), where the data plot between the ranges of data for earthquakes of M6.5–7.5 reported by Makdisi and Seed (1978) and plotted by Jibson (2007).

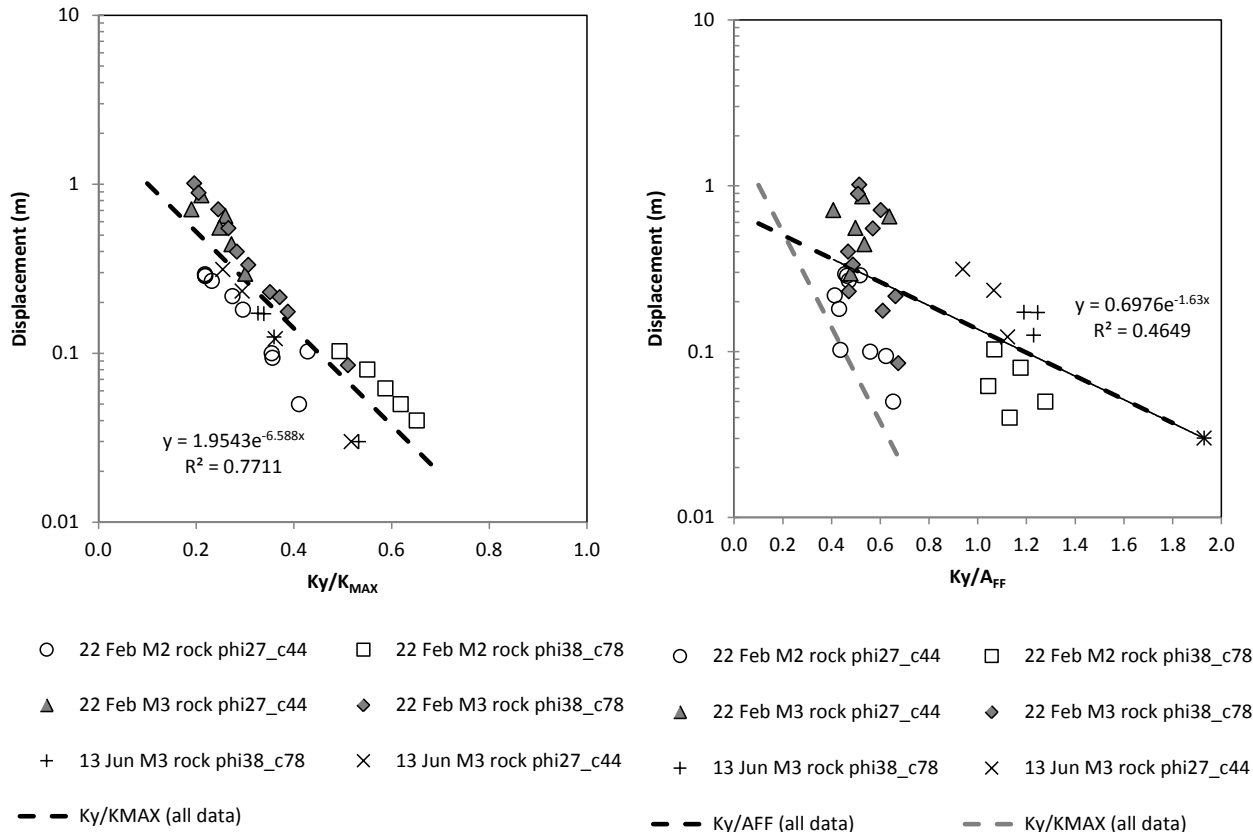


Figure 28 Source area 11B (cross-section 1), decoupled Slope/W displacements calculated for different ratios of yield acceleration to maximum average acceleration of the mass (K_y/K_{MAX}), and maximum acceleration of the mass (K_y/A_{FF}), for selected slide-surface geometries, and given material shear strength parameters. M2 represents slide surfaces associated with failure mechanisms 2 and M3 with failure mechanism 3. A_{FF} is the peak acceleration of the input earthquake time acceleration history. Synthetic rock outcrop time acceleration histories for the 22 February and 13 June 2011 earthquakes were used as inputs for the assessment. ($N = 40$). The dashed lines are exponential trend lines fitted to the semi-log data. The formula and the coefficient of determination (R^2) for the trend lines are shown.

4.2.2.5 Forecast modelling of permanent slope deformation

The results from the decoupled assessment show that the magnitude of permanent slope displacement during an earthquake will vary in response to:

1. the shear strength of the rock mass at the time of the earthquake;
2. pore pressures within tension cracks and the rock mass, at the time of the earthquake; and
3. duration and amplitude of the earthquake shaking.

Given both source areas 11A and 11B have already undergone 1.8 and 0.8 m of permanent slope displacement respectively during the 2010/11 Canterbury earthquakes, it is possible that such displacements have reduced the overall shear strength of the materials in the slope, making them more susceptible to future earthquakes. It is also not known how much more displacement the slopes may be able to undergo before failing catastrophically, i.e., where the magnitude of displacement causes the failure mass to break down, forming a more rapid failure.

For both source areas, the relationship between the yield acceleration and the maximum average acceleration (from Figure 27 and Figure 28) has been used to determine the likely range of displacements of a given failure mass with a range of yield accelerations (K_y) at given levels of maximum average ground acceleration (K_{MAX}). This has been done using the four earthquake event bands, used to represent the range of earthquake events the slopes could be subjected to in the future. The four peak ground acceleration bands are the same as those originally adopted for the cliff collapse risk assessment by Massey et al. (2012a).

The results are shown in Table 11. Conservative yield accelerations have been adopted to take into account the possibility that the current shear strength of the materials is now degraded as a result of the past movement. The geometries of the different failure masses adopted for the assessment are the same as those shown in Figure 20 (source area 11A) and Figure 22 and Figure 23 (source area 11B).

Table 11 Forecast modelling results from the dynamic slope stability assessment for source areas 11A and 11B. Estimated displacements are rounded to the nearest 0.1 m.

Source area	11A				11B			
Adopted yield acceleration (K_y) (g)	0.1				0.4			
PGA band (A_{FF}) ¹	1	2	3	4	1	2	3	4
PGA range of band (A_{FF}) (g)	0.1–0.4	0.4–1.0	1.0–2.0	2.0–5.0	0.1–0.4	0.4–1.0	1.0–2.0	2.0–5.0
Midpoint of PGA (A_{FF}) band (g)	0.25	0.7	1.5	3.5	0.25	0.7	1.5	3.5
Adopted K_{MAX} to A_{FF} ratio	2.1 (mean + 1 standard deviation)				2.3 (mean + 1 standard deviation)			
Equivalent K_{MAX}	0.5	1.5	3.2	7.4	0.6	1.6	3.5	8.2
Estimated displacements (m)	0.4	1.2	1.8	2.2	0.0	0.4	0.9	1.4

¹ A_{FF} represents the peak horizontal ground acceleration of the free field input motion.

² The relationship between the yield acceleration and the average acceleration (from Figure 27 and Figure 28) has been used to determine the likely magnitude of displacement for different yield accelerations (K_y) for a given slide surface at given levels of maximum average ground acceleration (K_{MAX}). The values of K_{MAX} represent the midpoint of each peak ground acceleration band used in the risk assessment. For example, the midpoint peak acceleration of the 0.1–0.4 g band would be 0.25 g.

4.2.3 Slope stability – summary of results

The main results from the static and dynamic stability assessment are:

Source area 11A

1. Under current conditions, it is possible for failure of the trial slide surfaces to occur under either static or dynamic conditions. However, it should be noted that material strengths – and therefore the slope factors of safety – may reduce with time (weathering), water content, and further movement of the slope under either static or dynamic conditions.
2. Based on the dynamic back-analysis of slope stability the minimum values of friction (ϕ) and cohesion (c) of the fill are about 30° and 5 kPa, to achieve the recorded displacements of the slope (during the 2010/11 Canterbury earthquakes) inferred from crack apertures. These are likely to be at the upper end of the range considered to be reasonable as they represent summer water content conditions, i.e., dry. The static factor of safety of the assessed slope is therefore thought to range between 1 and 1.3 for the failure mechanisms and range of material parameters assessed.
3. Given the relatively low static factors of safety, a small increase in pore water pressure (piezometric head levels) within the fill, weak materials underlying the fill and or within open tension cracks, could lead to instability of the slope under static conditions (i.e., short duration high intensity rain, and or longer periods of wet weather). Changes in the water content of the materials, could also lead to a reduction in the cohesion, and therefore the static factor of safety.
4. Given the relatively low yield acceleration of the slope (estimated to be in the range of 0.1–0.2 g) it is likely that future earthquakes could reactivate the slope, leading to permanent displacements that could be quite large. The magnitude of any coseismic permanent displacements will depend upon:
 - a. The shear strength of the materials at the time of the earthquake;
 - b. The pore pressure/water content conditions within the slope at the time of the earthquake as affected by antecedent rainfall; and
 - c. The duration and amplitude of the earthquake shaking at the site.
5. However, rainfall-induced failures are likely to be more mobile, and the return period of the triggering event more frequent, and therefore pose a greater risk than earthquake induced failures.

Source area 11B

1. Given the relatively high static factors of safety (estimated to be in the range of 1.9–5), it would take a relatively large increase in pore water pressures (piezometric head levels) within the rock mass and or within open tension cracks, to trigger instability of the assessed failure mechanisms under static conditions. This is thought to be unrealistic based on the current conditions of the slope.
2. It is possible that small localised failures of the loess and the outer face of the rock slope would occur under static conditions. However, based on the slope geometry these are likely to be relatively small in volume, compared to those failures triggered by earthquakes.

3. The assessed failure mechanisms (failure through the loess, rock mass and weak layer) have relatively high yield accelerations, estimated to be in the range of 0.4–0.5 g. It is possible that future strong earthquakes could reactivate the slope, leading to permanent displacements that could be moderate in magnitude. The magnitude of any coseismic permanent displacements will mainly depend upon:
 - a. The shear strength of the material at the time of the earthquake;
 - b. The pore pressure conditions within the slope at the time of the earthquake as affected by antecedent rainfall; and
 - c. The duration and amplitude of the earthquake shaking at the site.

Source area 11C

1. Given the relatively low static factors of safety (estimated to be in the range of 1.1–1.3), a small increase in pore water pressures (piezometric head levels) within the fill and or within open tension cracks, or an increase in soil water content (reduction in cohesion), could lead to instability of the slope under static conditions (i.e., short duration high intensity rain, and or longer periods of wet weather).
2. Given the relatively low yield acceleration of the slope (estimated to be in the range of 0.05–0.2 g based on the pseudostatic method), it is likely that future earthquakes could reactivate the slope.
3. However, rainfall-induced failures are likely to be more mobile, and the return period of the triggering event more frequent, and therefore pose a greater risk than earthquake induced failures.

4.3 RUNOUT DISTANCE

4.3.1 Potential source volume estimation

The likely locations and volumes of potential sources 11A, 11B and 11C have been estimated based on:

1. Numerical stability analyses results;
2. Field surveys;
3. Mapped crack distributions relating to the 2010/11 Canterbury earthquakes; and
4. Engineering geology and morphology of the slope.

Three possible failure volume estimates – lower, middle and upper range estimates – have been calculated for each potential source area. The variation in failure volumes reflects the uncertainty in the source shape (depth, width and length dimensions) estimated from site conditions and the modelling.

Volumes were calculated by estimating the shape of any future failures as quarter-ellipsoids (half-spoon shaped) (following the method of Cruden and Varnes, 1996) (Figure 29) and estimated volumes are shown in Table 12.

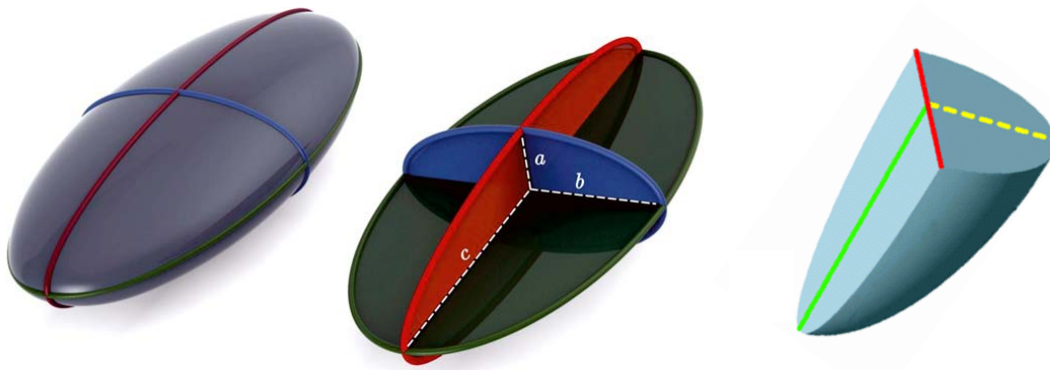


Figure 29 Estimation of landslide volume assuming a quarter-ellipsoid shape.

Table 12 Example of estimated source volumes (the first digit in the number is significant) and Fahrboeschung angles.

Mass movement	Main source material	Source volume estimation					Fahrboeschung angle	
		Source volume	Slice depth (m)	Slice length (m)	Source width (m)	Volume (m ³)	Mean (°)	Mean - 1 STD (°)
11B	Rock talus	MIN	3	13	12	240	50.0	43.4
		MID	4	16	16	540	48.2	41.6
		MAX	8	18	18	1,400	46.1	39.6
	Boulder Roll	MIN	3	13	12	240	44.2	38.4
		MID	4	16	16	540	43.3	37.5
		MAX	8	18	18	1,400	42.1	36.4
11A	Loess-Fill Debris Flow	MIN	2.5	20	30	790	21.4	13.9
		MID	5	30	60	4,700	18.0	11.5
		MAX	7	40	60	8,800	16.9	10.7
11C	Loess-Fill Debris Flow	MIN	1	6	22	70	26.8	17.9
		MID	2	8	32	270	23.7	15.5
		MAX	3	9	43	600	21.9	14.3

For source area 11B, the credibility of the debris avalanche potential source volumes (boulder roll and talus) has been evaluated by comparing them against estimated volumes of individual debris avalanches that fell from the rock slopes at Richmond Hill Road, Shag Rock Reserve and Redcliffs (Massey et al., 2012b) during the 13 June 2011 earthquakes (Figure 30). These volumes were derived from the terrestrial laser scan change models.

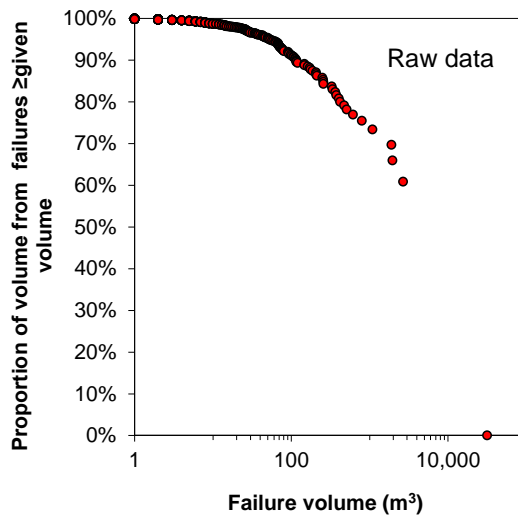


Figure 30 Proportion of volume from debris avalanches in the Port Hills greater than or equal to a given volume. Data from the 2011 landslide volumes triggered by the 13 June 2011 earthquakes, derived from terrestrial laser scan change models of Richmond Hill, Shag Rock Reserve and Redcliffs. Plots represent raw data and binned data.

For source areas 11A and 11C, the credibility of the earth/debris flow potential source volumes has been evaluated by comparing them against estimated volumes of individual landslides in loess and loess derivative materials, such as colluvium in the Port Hills, mapped by Townsend and Rosser (2012). The distribution of the 124 landslides is shown in Figure 31, and the data are well modelled by a log normal distribution, adopting the area depth relationships of Larsen et al. (2010).

The range of estimated volumes in Table 12 is well within the range of these two datasets.

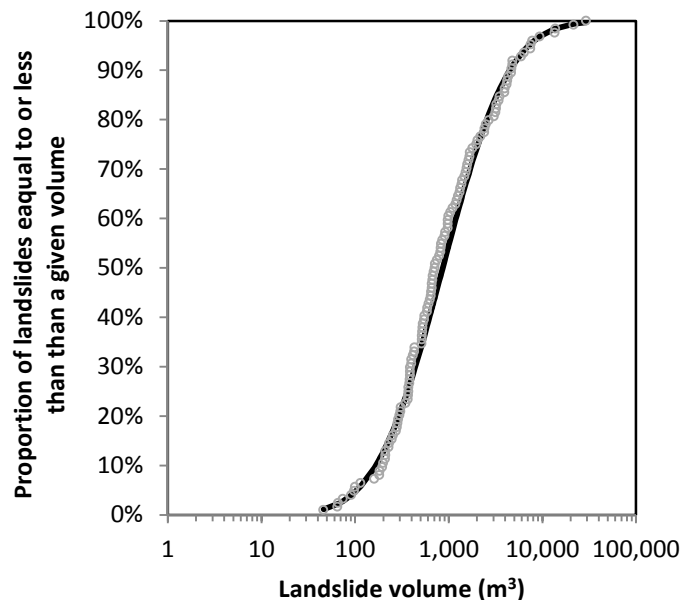


Figure 31 Estimation of landslide volumes in the Port Hills loess from Townsend and Rosser (2012) adopting the area depth relationships of Larsen et al. (2010).

4.3.2 Runout modelling

The debris runout distance from the identified potential source areas has been assessed both empirically and numerically.

4.3.2.1 Empirical method

Debris avalanches (source area 11B)

A total of 45 sections through Port Hills debris avalanches that were triggered by the 22 February and 13 June 2011 earthquakes have been assessed. For each section the fahrboeschung (angles) for debris avalanche: 1) “talus” (where the ground surface is obscured by many boulders); and 2) “boulder roll” (individual boulders) have been defined based on field mapping. The results for each are shown in Figure 32 as ratios of H/L where H is the height of fall and L is the length, or runout distance, of the mapped rockfalls and debris avalanche deposits (talus).

These two fahrboeschung relationships are based on debris avalanches that fell from many cliffs in the wider Port Hills area during the earthquakes. They therefore reflect all of the different types of slope shape that could affect the debris avalanche runout.

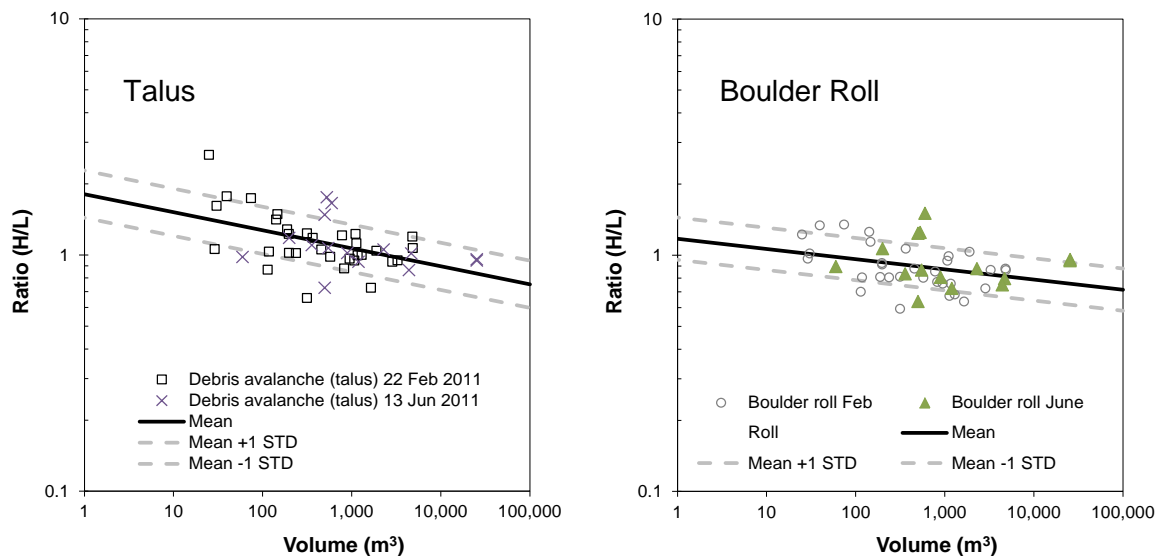


Figure 32 Empirical fahrboeschung angle measurements. The empirical fahrboeschung relationships, expressed as the ratio of height (H) to length (L) for debris avalanche talus and boulder roll (rockfalls), recorded in the Port Hills. N = 45 sections. Errors are expressed as the mean \pm one standard deviation (STD).

The mean and mean minus one standard deviation fahrboeschung angles for debris avalanches (talus and boulder roll) from each potential source volume (lower, middle and upper estimates), are shown in Table 12. The mean and mean minus one standard deviation fahrboeschung angles for the assessed range of potential source volumes (lower, middle and upper estimates) are shown in Figure 33.

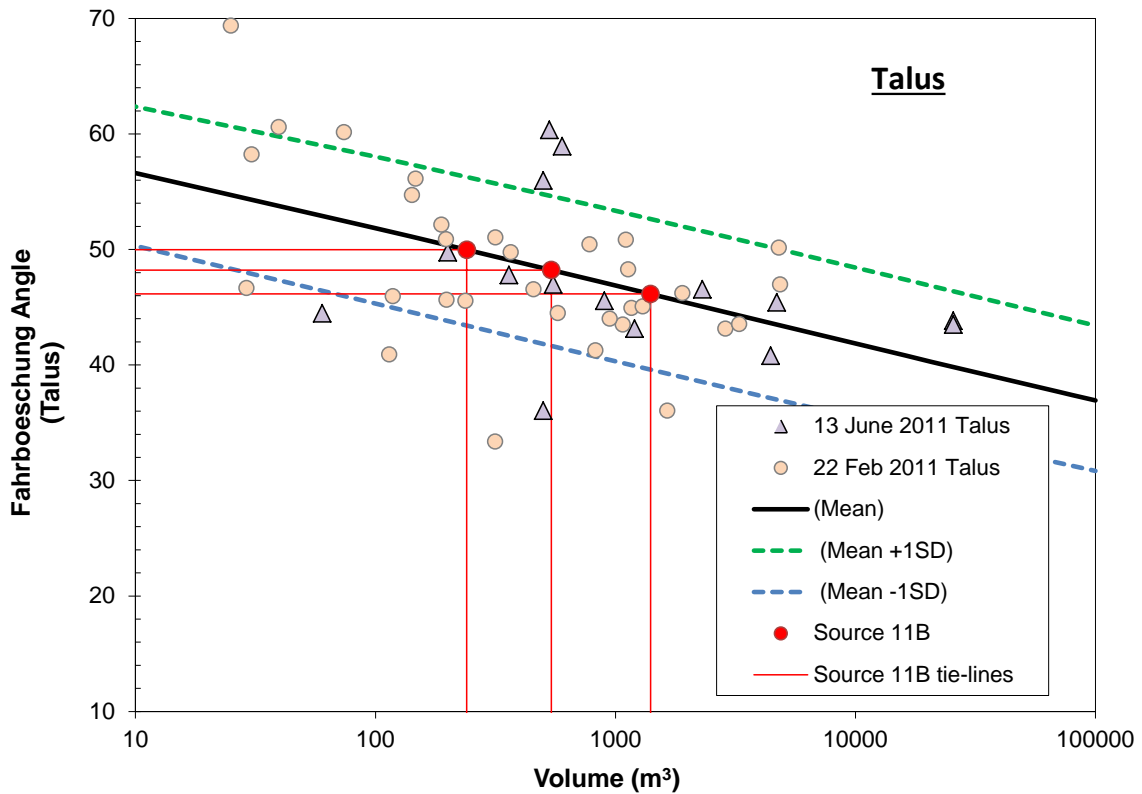
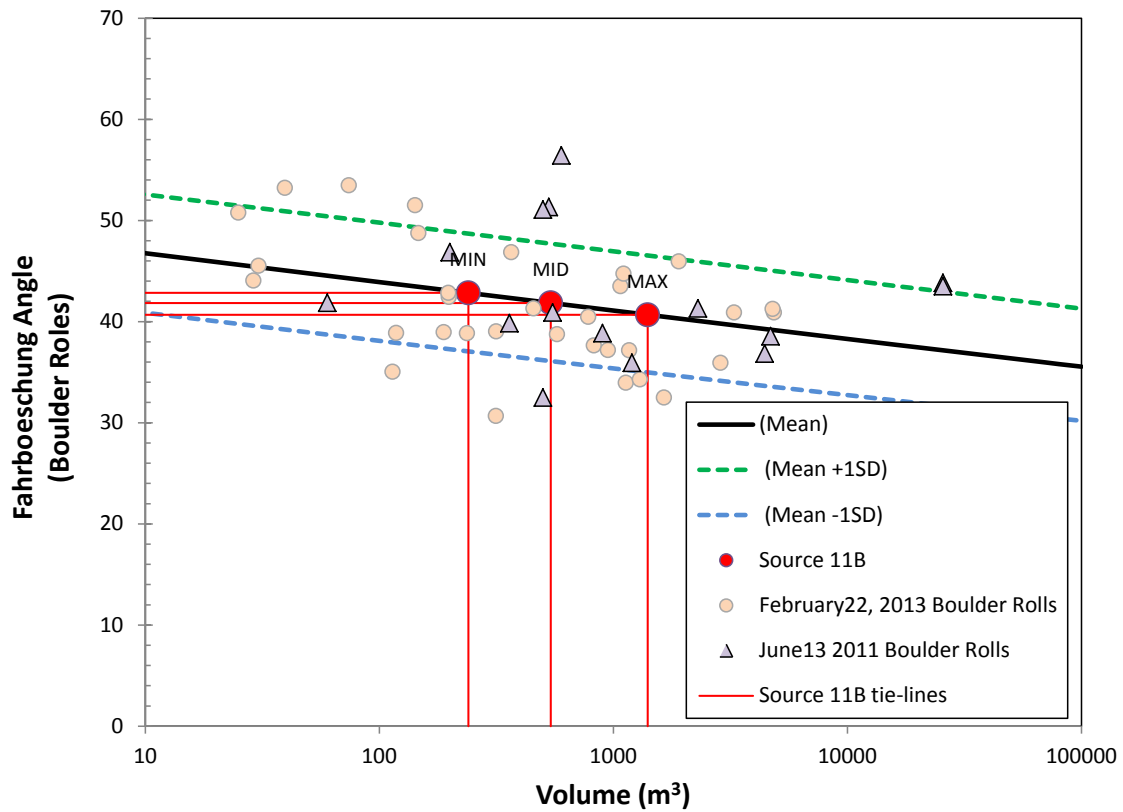


Figure 33 Estimation of boulder roll and talus fahrboeschung angles based on empirical runout data.

Earth/debris flows (source areas 11A & 11C)

For earth/debris flows, the fahrboeschung angles have been defined applying the method described in Massey and Carey (2012) as shown in Figure 33; using published earth/debris flow records reflecting different types of slope shape that could affect the debris runout.

The established empirical relationships are used to estimate the likely run out distances for the upper, middle and lower volume estimates of source areas 11A and 11C.

Figure 34 shows the estimated mean and mean minus one standard deviation earth/debris flow fahrboeschung angles derived for assessed source area areas 11A and 11C. For each source a range in fahrboeschung angles is estimated based on the range in volumes (min, mid, max) as shown in Table 12.

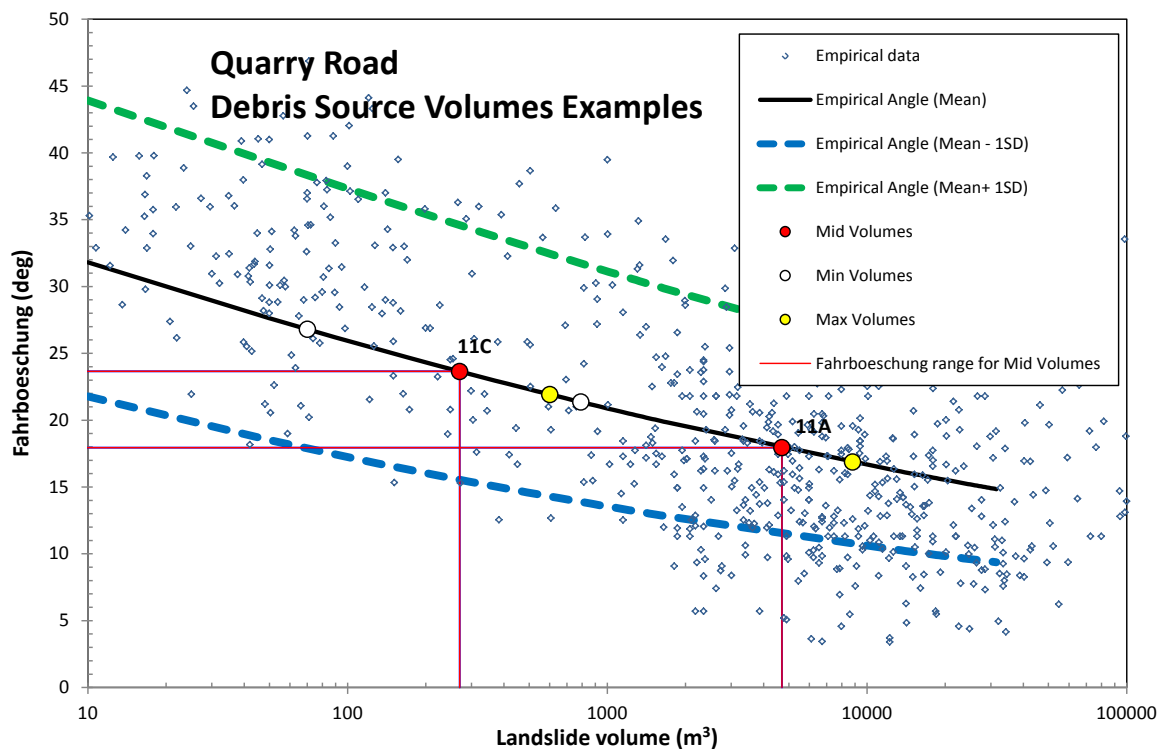


Figure 34 Estimation of debris flow fahrboeschung angles based on empirical runout data presented in Massey and Carey (2012).

4.3.2.2 Numerical method – RAMMS

Debris avalanche (source area 11B)

It is noted, as detailed by Massey et al. (2014), that the fahrboeschung method does not take into account the shape of the slope below the source area, which can have a significant effect on the actual runout of the debris. The RAMMS software (RAMMS, 2011) takes into account the site slope geometry when modelling debris runout. The physical model of RAMMS Debris Flow uses the Voellmy friction law. This model divides the frictional resistance into two parts: 1) a dry-Coulomb type friction (coefficient μ) that scales with the normal stress; and 2) a velocity-squared drag or viscous-turbulent friction (coefficient ξ). The RAMMS model parameters were calculated from the back-analysis of 23 debris avalanches (ranging in volume from 200 to 35,000 m³) that fell from the slopes at Richmond Hill Road, Shag Rock Reserve and Redcliffs during the 22 February and 13 June 2011 earthquakes.

The modelled parameters μ (μ) and ξ were optimised to obtain a good correlation between the modelled versus actual runout and deposited debris heights (Figure 35).

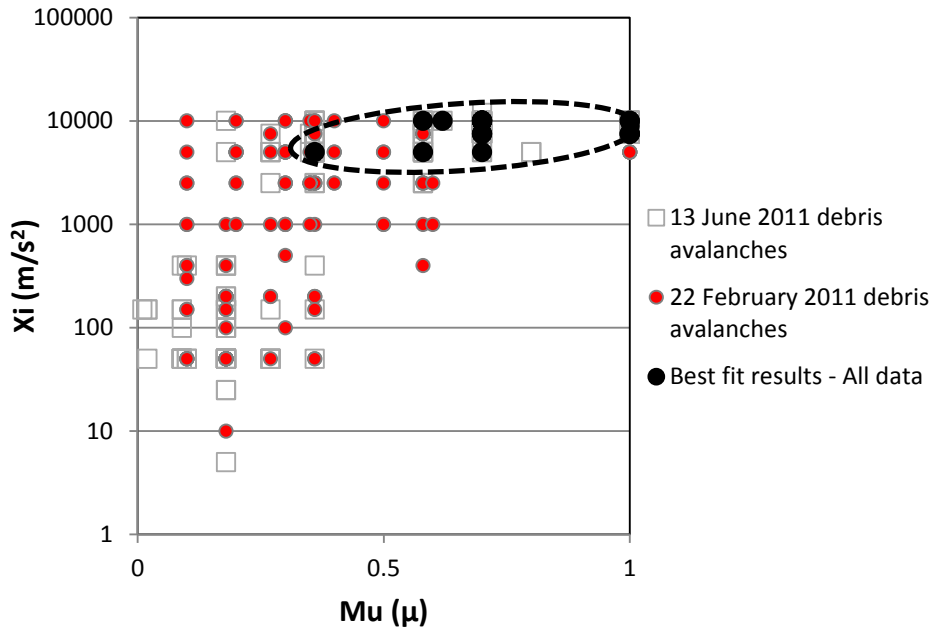


Figure 35 Range of parameters used to back-analyse the runout of debris avalanches in the Port Hills triggered by the recent earthquakes using the RAMMS software (RAMMS, 2011).

The model parameters that gave the “best fits” between modelled and actual runout distances and heights when: $\mu = 0.7$ and $\xi = 7,500 \text{ m/s}^2$. The ξ values are comparable to results from other assessments compiled by Andres (2010) for rockfalls (debris avalanches), but the μ values are larger than those shown by Andres (2010), possibly because the Port Hills debris avalanches are more clast-dominated (Figure 36) and/or the debris was dry at the time of the failure.

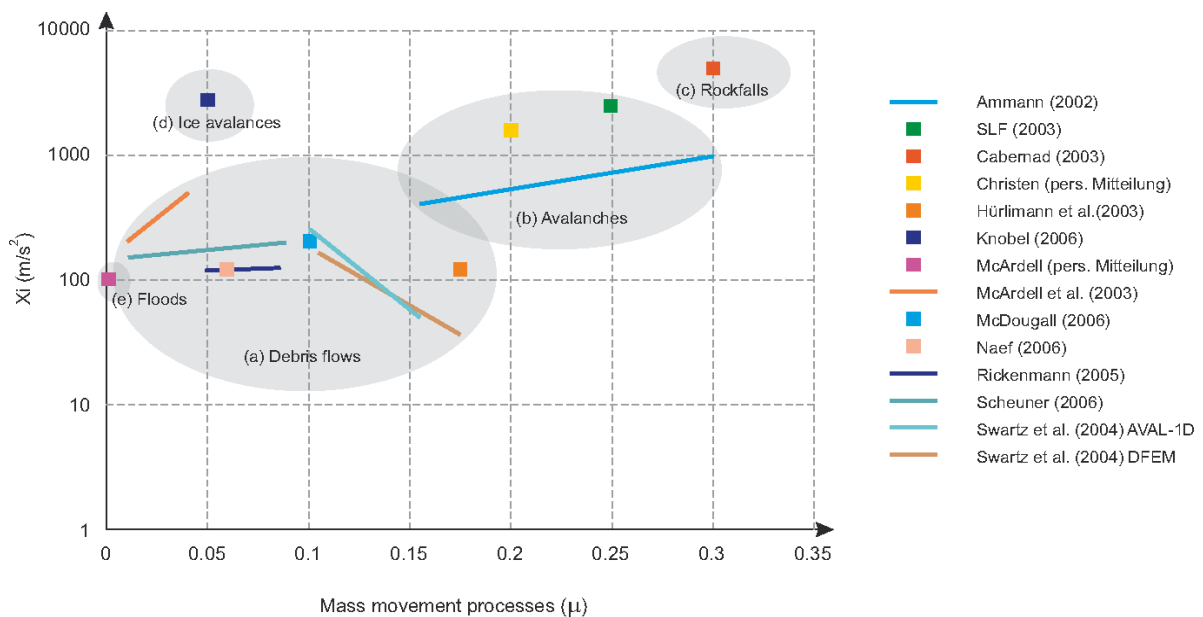


Figure 36 Range of parameters for different mass movement processes: a) debris flows, b) snow avalanches, c) snow avalanches, d) ice avalanches, e) debris floods. Modified from Andres (2010).

For each back-analysed debris avalanche, the modelled final debris thicknesses were compared to the actual deposit thicknesses interpolated from difference models derived from the airborne LiDAR surveys using a 1 m grid. For debris avalanches triggered by the 22 February 2011 earthquakes the deposit thicknesses were estimated from differences between the 2011a (March 2011) LiDAR survey and the 2003 LiDAR survey. For debris avalanches triggered by the 13 June 2011 earthquakes the 2011c (July 2011) and 2011a LiDAR surveys were used. Statistics from the comparison give a mean difference of 0.5 (± 0.4) m³, with a mode of 0.2 m³ (Figure 37) for the 1 m² grid cells.

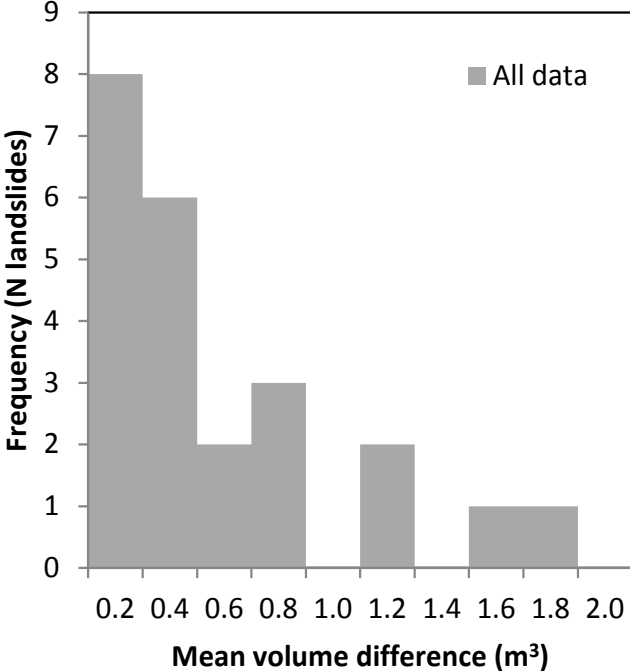


Figure 37 Mean volume difference between the RAMMS modelled volumes and the actual recorded volumes per 1 m² grid cell. N = 23 debris avalanches triggered by 22 February and 13 June 2011 earthquakes.

For the 23 debris avalanches, the performance of the RAMMS and fahrboeschung models (based on the compiled 45 sections shown in (Figure 36) were assessed against the actual field mapped runout distances. The RAMMS model performed well with a gradient of 1.01 (± 0.04) at one standard deviation and coefficient of determination (R^2) of 0.3 indicating the data are scattered. The empirical fahrboeschung model performed about the same as the RAMMS model, where the gradient was 1.06 (± 0.05) at one standard deviation but the coefficient of determination (R^2) of 0.5 indicates less scatter (Figure 38).

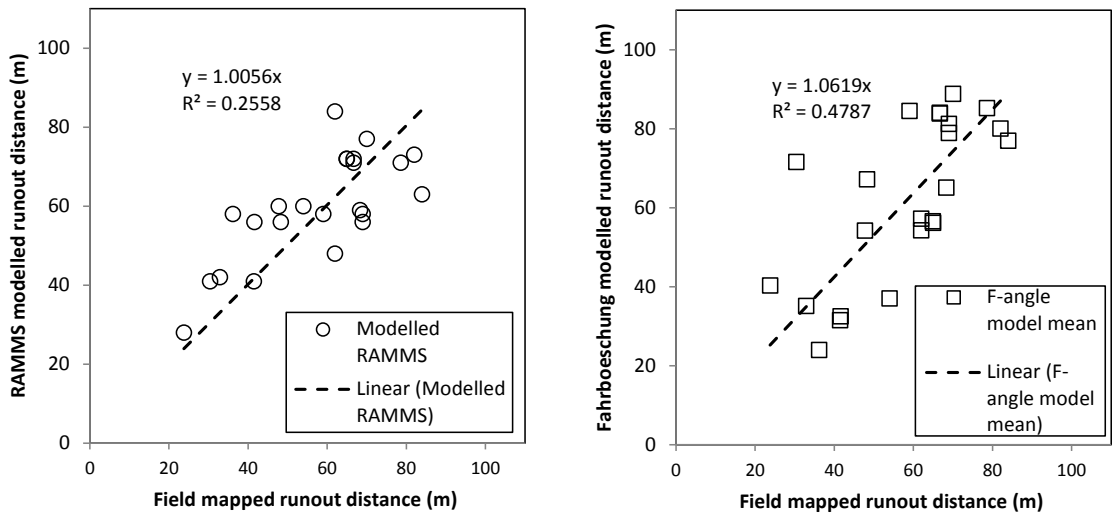


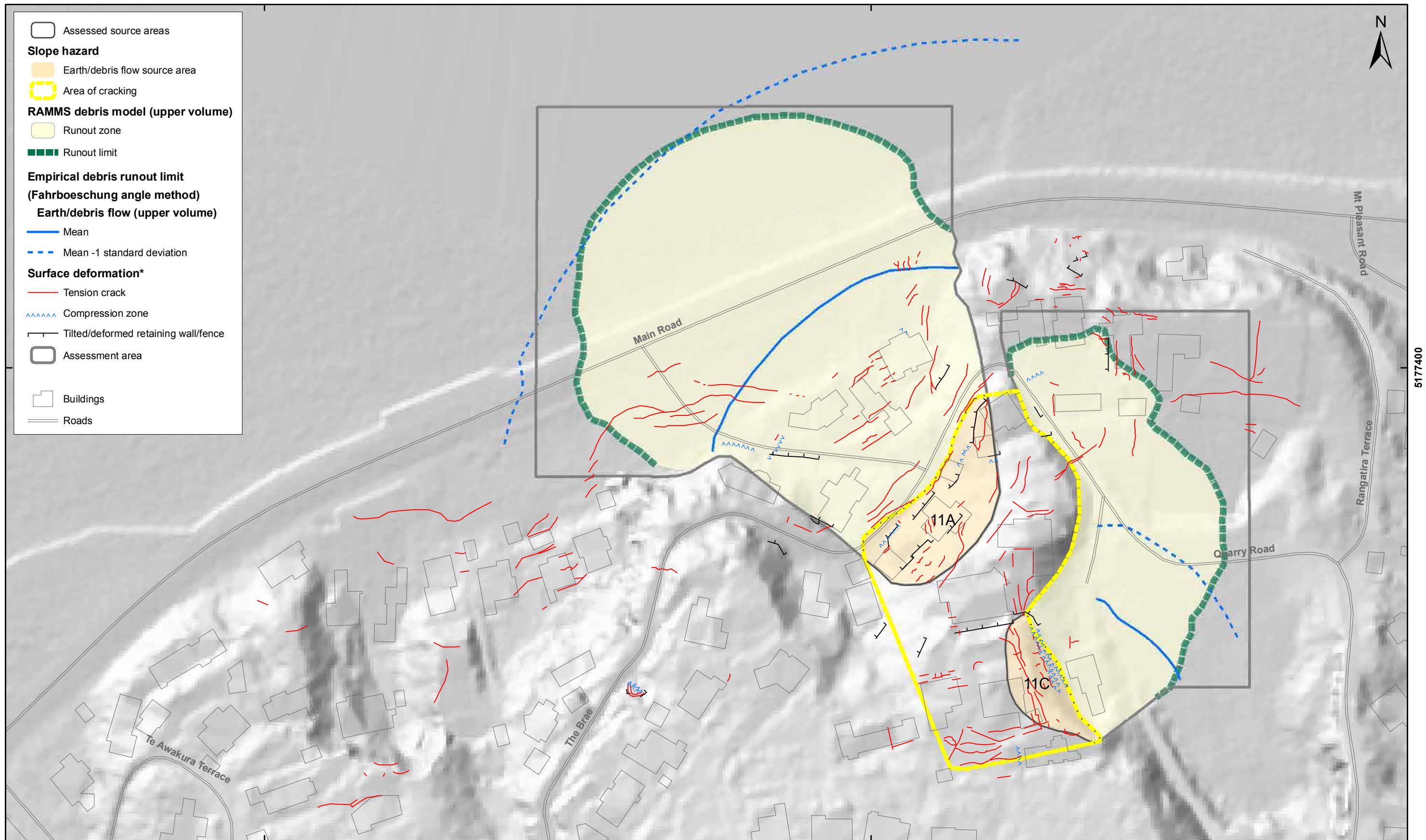
Figure 38 Comparison between the RAMMS modelled and the empirical-modelled debris runout (Figure 36) and the actual recorded runout for debris avalanches triggered by the 22 February and 13 June 2011 earthquakes. N = 23 debris avalanches.

Earth/debris flows (source areas 11A and 11C)

The RAMMS model parameters were calculated from the back-analysis of four Port Hills debris flows. The modelled parameters μ and x_i were optimised to obtain a good correlation between the modelled versus actual runout and deposited debris heights. The model, with calibrated input parameters ($\mu = 0.06$ (7°) and $x_i = 200 \text{ m/s}^2$), were used to estimate the likely velocity and depth of the debris at given locations down the slope for the given failure volumes. The μ and x_i values are comparable to results from other assessments compiled by Andres (2010) for debris flows (Figure 36).

4.3.3 Forecast runout modelling

A hazard map (Figure 39) presents the empirical and numerical runout limits from the modelling. The mean and mean minus one standard deviation fahrboeschung angles for each source area assuming the upper volume estimates, are shown. The estimated runout distances from RAMMS are shown in Appendix 4 (debris height) and Appendix 5 (debris velocity), for sources 11A, 11B and 11C (upper, middle and lower source volume estimates), along with the corresponding mean and mean minus one standard deviation fahrboeschung angles.



SCALE BAR: 0 50 100 m

EXPLANATION:

* Taken from report CR2012/317

Background shade model derived from NZAM post earthquake 2011c (July 2011) LiDAR survey resampled to a 1 m ground resolution. Roads and building footprints provided by Christchurch City Council (20/02/2012). PROJECTION: New Zealand Transverse Mercator 2000

DRW:
BL
CHK:
CM, FDP



**EARTH/DEBRIS FLOW HAZARD MAP
(Source areas 11A and 11C)**

**Quarry Road
Christchurch**

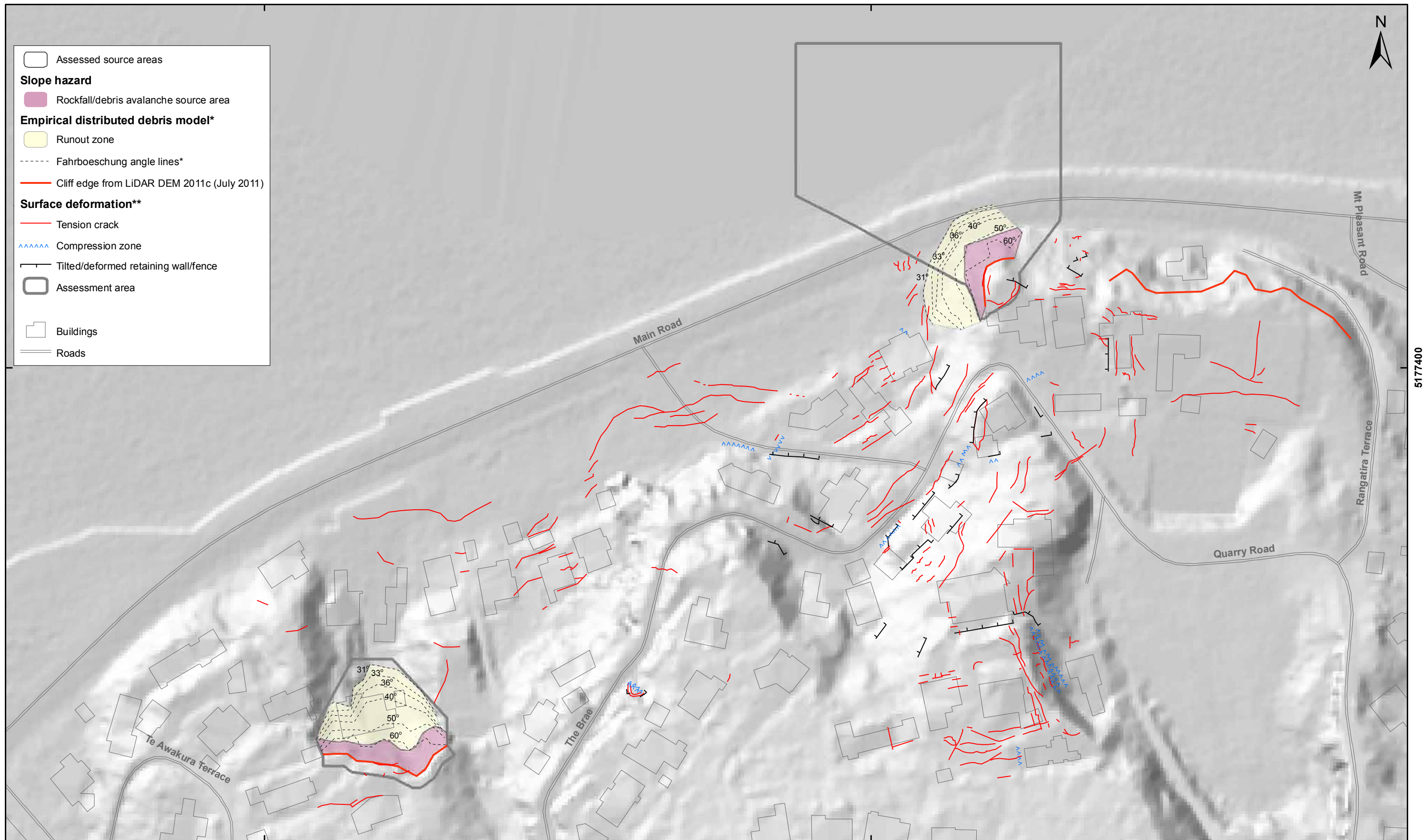
FIGURE 39

Map 1

FINAL

REPORT:
CR2014/75

DATE:
June 2014



1576800

1577000



EXPLANATION:
 * Modified from report CR2012/124
 ** Taken from report CR2012/317
 Background shade model derived from NZAM post earthquake
 2011c (July 2011) LiDAR survey resampled to a 1 m ground resolution.
 Roads and building footprints provided by Christchurch City Council (20/02/2012).
 PROJECTION: New Zealand Transverse Mercator 2000

DRW:
BL
 CHK:
CM, FDP



**CLIFF COLLAPSE HAZARD MAP
 (Randomly distributed debris)**

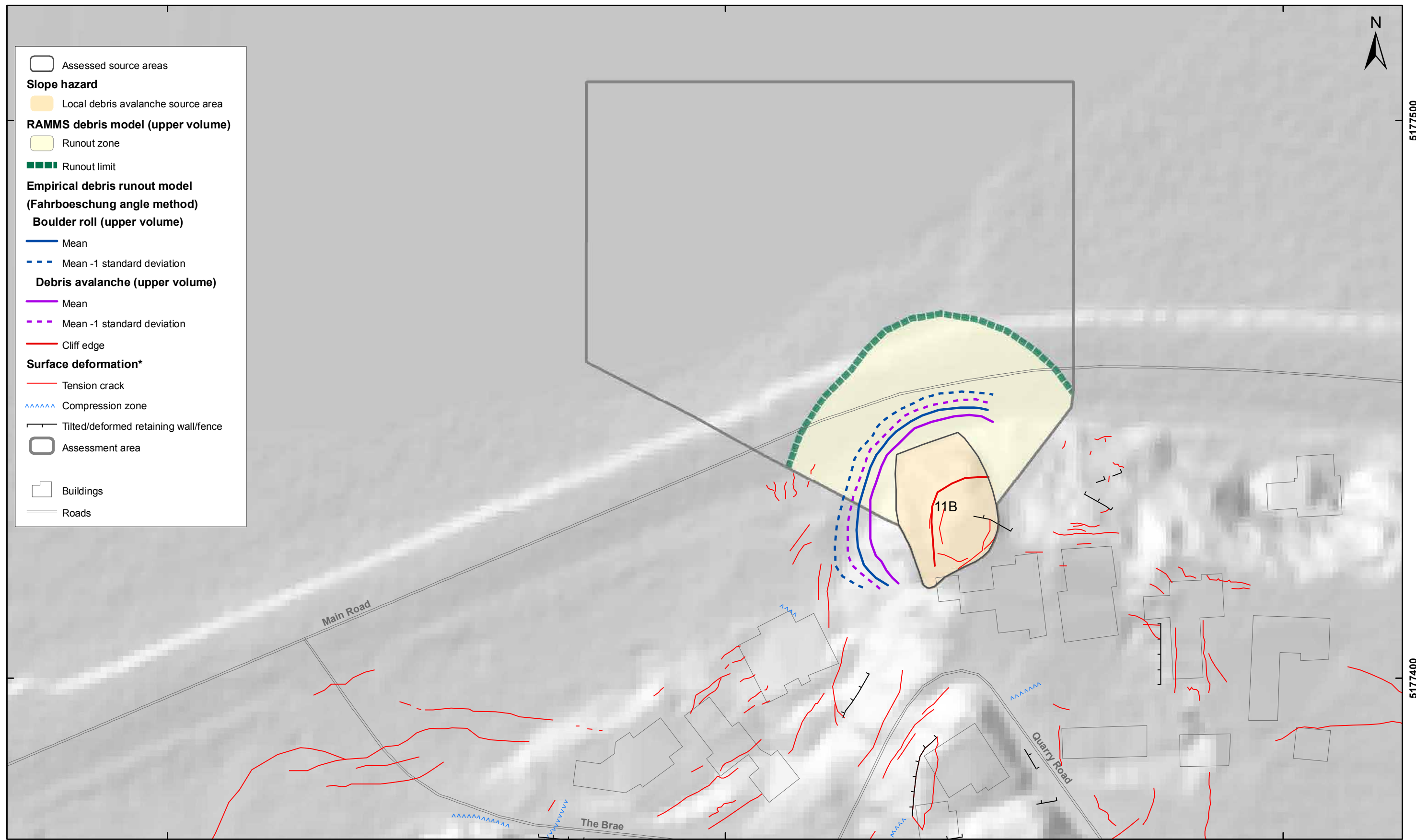
**Quarry Road
 Christchurch**

FIGURE 39

Map 2

FINAL

REPORT: CR2014/75 DATE: June 2014



5177500

5177400

1576900

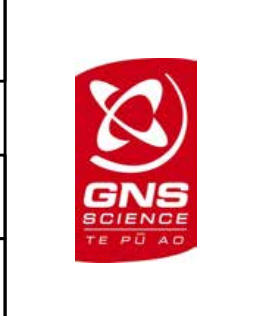
1577000

1577100



EXPLANATION:
 * Taken from report CR2012/317
 Background shade model derived from NZAM post earthquake 2011c (July 2011) LiDAR survey resampled to a 1 m ground resolution.
 Roads and building footprints provided by Christchurch City Council (20/02/2012).
 PROJECTION: New Zealand Transverse Mercator 2000

DRW:
BL
 CHK:
CM, FDP



**DEBRIS AVALANCHE HAZARD MAP
 (Source area 11B)**

**Quarry Road
 Christchurch**

FIGURE 39	
Map 3	
FINAL	
REPORT: CR2014/75	DATE: June 2014

5.0 RISK ASSESSMENT RESULTS

5.1 TRIGGERING EVENT FREQUENCIES

Failure of the assessed source areas could be triggered by earthquakes (dynamic conditions) or by water ingress (static conditions).

5.1.1 Frequency of earthquake triggers

For earthquake triggers, the frequency of a given free-field peak ground acceleration (A_{FF}) occurring is obtained from the New Zealand National Seismic Hazard Model (Table 13) (Stirling et al., 2012). The increased level of seismicity in the Christchurch region is incorporated in a modified form of the 2010 version of the National Seismic Hazard Model (Gerstenberger et al., 2011).

For these assessments, peak ground acceleration is used to represent earthquake-shaking intensity, as peak ground acceleration is the ground-motion parameter considered to be most directly related to coseismic landslide initiation (Wartman et al., 2013).

Table 13 The annual frequency of a given peak ground acceleration (PGA) band occurring on rock (site class B) for different years from the 2012 seismic hazard model for Christchurch (G. McVerry, personal communication 2014). Note: these are free field rock outcrop peak ground accelerations (equivalent to A_{FF}).

Annual frequency of the representative earthquake event in a given PGA band				
PGA band	1	2	3	4
PGA range of band (g)	0.1–0.4	0.4–1.0	1.0–2.0	>>2
Year 2016 annual frequency of representative event in band ¹	0.16	0.03	0.0016	0.00005
Next 50-year average annual frequency of representative event in band ¹	0.08	0.01	0.0007	0.00002

¹ The annual frequency of the representative event in the band – assumed to be the midpoint of the band – is calculated by subtracting the annual frequency of the 0.4 g PGA from the annual frequency of the 0.1 g PGA.

5.1.1.1 Peak ground acceleration and permanent slope displacement

It is difficult to estimate the probability of triggering failure, leading to catastrophic slope collapse, where the debris runs out down slope forming a debris avalanche or flow. It is also possible that permanent slope displacements could cause catastrophic damage to dwellings located in the source area, even if the debris does not leave the source. The level of displacement chosen to differentiate between safe and unsafe behaviour (Abramson et al., 2002) differs between authors. Some examples are:

- Hynes-Griffin and Franklin (1984) suggest that up to 0.1 m displacements may be acceptable for well-constructed earth dams.
- Wieczorek et al. (1985) used 0.05 m as the critical parameter for a landslide hazard map of San Mateo County, California.
- Keefer and Wilson (1989) used 0.1 m for coherent slides in southern California.
- Jibson and Keefer (1993) used a 0.05–0.1 m range for landslides in the Mississippi Valley.

- e. The State of California (1997) finds slopes acceptable if the Newmark displacement is less than 0.15 m. A slope with a Newmark displacement greater than 0.3 m is considered unsafe. For displacements in the “grey” area between 0.15 and 0.3 m, engineering judgement is required for assessment.

The probability of the assessed source areas 11A and 11B being triggered in a given earthquake was based on the calculated permanent displacement, estimated from the decoupled results (Figure 27 and Figure 28 respectively).

5.1.2 Frequency of rainfall triggers

The return period of the rainfall that could initiate failure of the assessed source areas is unknown because:

- There is evidence of historic and prehistoric earth/debris flows at the site,
- The 5 March 2014 rainstorm in Lyttelton (130 mm) triggered several large earth/debris flows. The return period of the rainfall at Lyttelton was about 100 years, but the lower amount of rainfall at the site (89 mm) had a return period of only about 10–20 years.
- It is likely that the slope could fail if the water content of the loess increases, but the likelihood of this happening is not known.
- Even though the slope survived a 10–20 year return period event, the loess water content of the slope was likely to have been seasonally low as the storm occurred at the end of a dry summer.

It is therefore difficult to estimate the annual frequency of the event that could initiate catastrophic failure of the assessed source areas.

5.2 EARTH/DEBRIS FLOWS (SOURCE AREAS 11A AND 11C)

5.2.1 Peak ground acceleration and permanent slope displacement

The probability of a given amount of displacement occurring for source area 11A was based on the estimated permanent slope displacements, calculated from the decoupled assessment results. The permanent displacement of the source area for a representative event within each given peak ground acceleration band was estimated from the relationship between the yield acceleration (K_y) and the maximum average acceleration of the mass (K_{MAX}) Figure 27. The midpoint of each peak ground acceleration band (e.g. the midpoint peak acceleration (A_{FF}) of the 0.1–0.4 g band would be 0.25 g) was used as the representative event within each band, and this was multiplied by the site specific ratio of K_{MAX} to A_{FF} (assuming the mean plus one standard deviation) to estimate the equivalent maximum average acceleration of the mass (K_{MAX}) for the given value of A_{FF} . For example, the A_{FF} for the representative event in band 1 is 0.25 g, the equivalent K_{MAX} would be 0.5 g, assuming a ratio of 2.1.

The probabilistic seismic hazard model used in this assessment provides the annual frequencies of free-field rock outcrop peak horizontal ground accelerations (A_{FF}) and therefore the annual frequencies of the equivalent maximum average acceleration of the mass (K_{MAX}) (Table 14).

Table 14 Probability of failure for source area 11A. Estimated displacements are rounded to the nearest 0.1 m, and are based on the relationship between K_y/K_{MAX} shown in Figure 27.

Free field peak horizontal ground accelerations (A_{FF})¹ (g)	0.2	0.5	0.7	1.0
Year 2016 annual frequency of event (from PSHM)	0.090	0.0157	0.0059	0.00164
Year 2016 return period (years)	11	64	169	610
Next 50-year average annual frequency of event (from the PSHM)	0.042	0.0072	0.0027	0.00076
Next 50-year average return period (years)	24	139	370	1316
Adopted K_{MAX} ² to A_{FF} ratio	2.1 (mean + 1 STD)			
Equivalent K_{MAX} for the given A_{FF}	0.4	1.1	1.5	2.1
Estimated displacements (m) for K_y of 0.1	0.2	0.9	1.2	1.5
Estimated displacements (m) for K_y of 0.2	0.0	0.4	0.6	0.9
Estimated displacements (m) for K_y of 0.3	0.0	0.1	0.3	0.6

¹ A_{FF} represents the peak horizontal ground acceleration of the free field input motion.

² K_{MAX} represents the maximum average acceleration of the failure mass taken from the relationship in Figure 27.

In Table 14, for the peak ground acceleration band 4, K_{MAX} is estimated to be 7.4 g. In reality this is highly unlikely to occur as the slope would fail well before such values could be achieved, and at these ratios of K_y/K_{MAX} , the relationship with displacement (shown in Figure 27) is in the portion of the graph where the data trend upwards, and therefore the results are unreliable.

However, a PGA in this band is also highly unlikely to occur. The return period of such an event is 20,000 years (assuming the year 2016 annual frequency), and is well outside the design considerations usually taken into account for residential dwellings.

Earthquake induced permanent displacements of source area 11C, although not assessed, are also likely to be quite large given the low calculated yield acceleration for the assessed section.

5.2.2 Overall triggering event frequency

Given the previous results, rainfall-induced earth/debris flows are, however, likely to be more mobile and the return period of the triggering event more frequent than earthquake-induced failures, and therefore pose the greatest risk.

For source areas 11A and 11C, for rainfall (static) triggers:

- For the risk assessment, various return periods of 20, 50, 100 and 200 years for the triggering event were assumed, and the sensitivity of the risk estimates to these return periods assessed.
- Failures of the slope could occur from anywhere within the identified source area and could vary greatly in volume. The assessed source areas represent the geometries and volumes of the sources that could potentially fail forming earth/debris flows.

It should be noted that under dynamic conditions (earthquakes) permanent displacement (slumping and cracking) of the currently cracked area could also occur, which could still pose a risk to any dwellings located in this area.

5.3 CLIFF COLLAPSE (SOURCE AREA 11B)

Given the relatively high factors of safety of cross-section 1 (representing source area 11B), earthquakes are thought to be the main trigger for the assessed failure mechanisms.

5.3.1 Peak ground acceleration and permanent slope displacement

The estimated magnitude of permanent slope displacement of the assessed source in a future earthquake was based on the decoupled assessment results. The permanent displacement of the source at a given level of free-field peak ground acceleration (A_{FF}) was estimated from the relationship between the yield acceleration (K_y) and the maximum average acceleration of the mass (K_{MAX}) (Figure 28). Different levels of peak ground acceleration were adopted based on the four earthquake event bands, and each multiplied by the site-specific ratio of K_{MAX} to A_{FF} (assuming the mean plus one standard deviation) to estimate the equivalent maximum average acceleration of the mass (K_{MAX}) for the given value of A_{FF} (Table 15).

5.3.2 Permanent slope displacement and likelihood of catastrophic slope failure

The probability of occurrence of local source area 11B was based on the estimated permanent displacement, estimated from the decoupled results (Figure 28), as follows:

- If the estimated displacement of the source area is ≤ 0.1 m then the probability of catastrophic failure = 0.
- If the estimated permanent displacement of the source area is ≥ 1.0 m then the probability of catastrophic failure = 1.
- If the estimated permanent displacements are between 0.1 m and 1 m then the probability of failure (P) is calculated based on a linear interpolation between $P = 0$ at displacements of 0.1 m, and $P = 1$, at displacements of 1 m.

It should be noted that parts of the slope have already moved more than 0.8 m during the 2010/11 Canterbury earthquakes, and it is not known how much more movement the slope can take, before failing catastrophically.

Table 15 Probability of failure for source area 11B. Estimated displacements are rounded to the nearest 0.1 m, and are based on the relationship between K_y/K_{MAX} shown in Figure 28.

Source area	11B			
Adopted yield acceleration (K_y) (g)	0.4			
Adopted yield acceleration (K_y) (g)	1	2	3	4
PGA band (A_{FF}) ¹	0.1–0.4	0.4–1.0	1.0–2.0	2.0–5.0
PGA range of band (A_{FF}) (g)	0.25	0.7	1.5	3.5
Midpoint of PGA (A_{FF}) band (g)	2.3 (mean + 1 standard deviation)			
Adopted K_{MAX} ³ to A_{FF} ratio	0.6	1.6	3.5	8.2 ³
Equivalent K_{MAX}	0.0	0.4	0.9	1.4
Probability of failure	0.0	0.3	0.9	1.0
Annual frequency of the representative event that could trigger the estimated displacement (Year 2016 seismic hazard model). The return period, in years, is shown in brackets	0.16 (6)	0.03 (33)	0.0016 (625)	0.00005 (20,000)

¹ A_{FF} represents the peak horizontal ground acceleration of the free field input motion.

² K_{MAX} represents the maximum average acceleration of the failure mass taken from the relationship in Figure 27.

³ A K_{MAX} of 8.2 g is highly unlikely to occur as the slope would fail well before such values could be achieved. A PGA in this band is also highly unlikely to occur. The return period of such an event is 20,000 years (assuming the year 2016 annual frequency), and is well outside the design considerations usually taken into account for residential dwellings.

In Table 15, for the peak ground acceleration band 4, K_{MAX} is estimated to be 8.2 g. In reality this is highly unlikely to occur as the slope would fail well before such values could be achieved, and at these ratios of K_y/K_{MAX} , the relationship with displacement (shown in Figure 28) is in the portion of the graph where the data trend upwards, and therefore the results are unreliable.

However, a PGA in this band is also highly unlikely to occur. The return period of such an event is 20,000 years (assuming the year 2016 annual frequency), and is well outside the design considerations usually taken into account for residential dwellings.

5.4 DEAGGREGATION OF THE PROBABILISTIC SEISMIC HAZARD MODEL

The seismic performance of the assessed source areas in future earthquakes (Table 14 and Table 15) were inferred from assessing their performance in past earthquakes, mainly the 22 February, 16 April, 13 June and 23 December 2011 earthquakes, using the relationship established between peak ground acceleration and the amount of permanent slope displacement (Figure 27 and Figure 28). These earthquakes varied in magnitude between M5.2 and M6.3, and were “near-field”, i.e., their epicentres were very close, within 10 km, to the Quarry Road site.

Earthquakes of longer duration will affect the site in different ways. For example, the response of the assessed source areas (at higher water contents representative of winter conditions) may be non-linear, and could lead to larger cumulative permanent displacements. Conversely, the peak amplitudes relating to longer duration earthquakes from more distant sources are likely to be lower and may not trigger displacement of the rock slope.

The annual frequencies of a given level of peak ground acceleration occurring in the area are given by the National Seismic Hazard Model of New Zealand (Stirling et al., 2012). The National Seismic Hazard Model combines all of the various earthquake sources that could contribute to the seismic hazard at a given location. The National Seismic Hazard Model estimates for the Port Hills are based on a combination of different earthquake sources: 1) subduction zone; 2) mapped active faults; and 3) unknown or “background” earthquakes. For the risk assessment it is important to deaggregate the National Seismic Hazard Model to assess which earthquake sources contribute the most to it.

Buxton and McVerry (personal communications 2014) suggest that it is magnitude M5.3–6.3 earthquakes on unknown active faults within 20 km of the site that contribute most to the seismic hazard. These earthquakes are similar to the 22 February, 16 April 13 June and 23 December 2011 earthquakes.

5.5 DWELLING OCCUPANT RISK

Figure 40, Map 1 shows the annual individual fatality risk estimated for earth/debris flows triggered under static conditions from source areas 11A and 11C.

Figure 40, Map 2 shows the original annual individual fatality risk estimated for cliff collapse in Massey et al. (2012a) for source area 11B. The same risk model contained in Massey et al. (2012a) has also been applied to source area 11E and is also shown on Map 2 (Figure 40). This risk model includes the risk from cliff collapses generated under both static and dynamic conditions.

Figure 40, Map 3 shows the annual individual fatality risk for debris avalanches associated with source area 11B.

Figure 40, Map 4 shows the annual individual fatality risk for source area 11B from combining the results shown in Maps 2 and 3, to produce a map showing the total risk from the combined different hazards present at the site.

5.5.1 Variables adopted for the risk assessment

Other variables used in the risk assessment were discussed at a workshop with Christchurch City Council on 18 March 2014. Based on the results from the workshop, the risk estimates presented in Figure 40 adopt the following main variables:

- $P_{(H)}$ for earthquake triggers the annual frequency of the triggering event adopt the 2016 seismic hazard model results, which include aftershocks (this is discussed in Massey et al., 2012b).
- $P_{(S:H)}$ the probability that a person, if present, is in the path of the debris is based on variable (lower, middle and upper) estimates of the debris volume that could be triggered in an event.
- $P_{(T:S)}$ the probability that a person is present at a particular location, as the debris moves thought it, of 67%. Assuming an “average” person spends 16 hours a day at home. For this assessment, GNS Science has assumed the same “average” occupancy rate value adopted by the Canterbury Earthquake Recovery Authority and Christchurch City Council (this is discussed by Massey et al., 2012b).

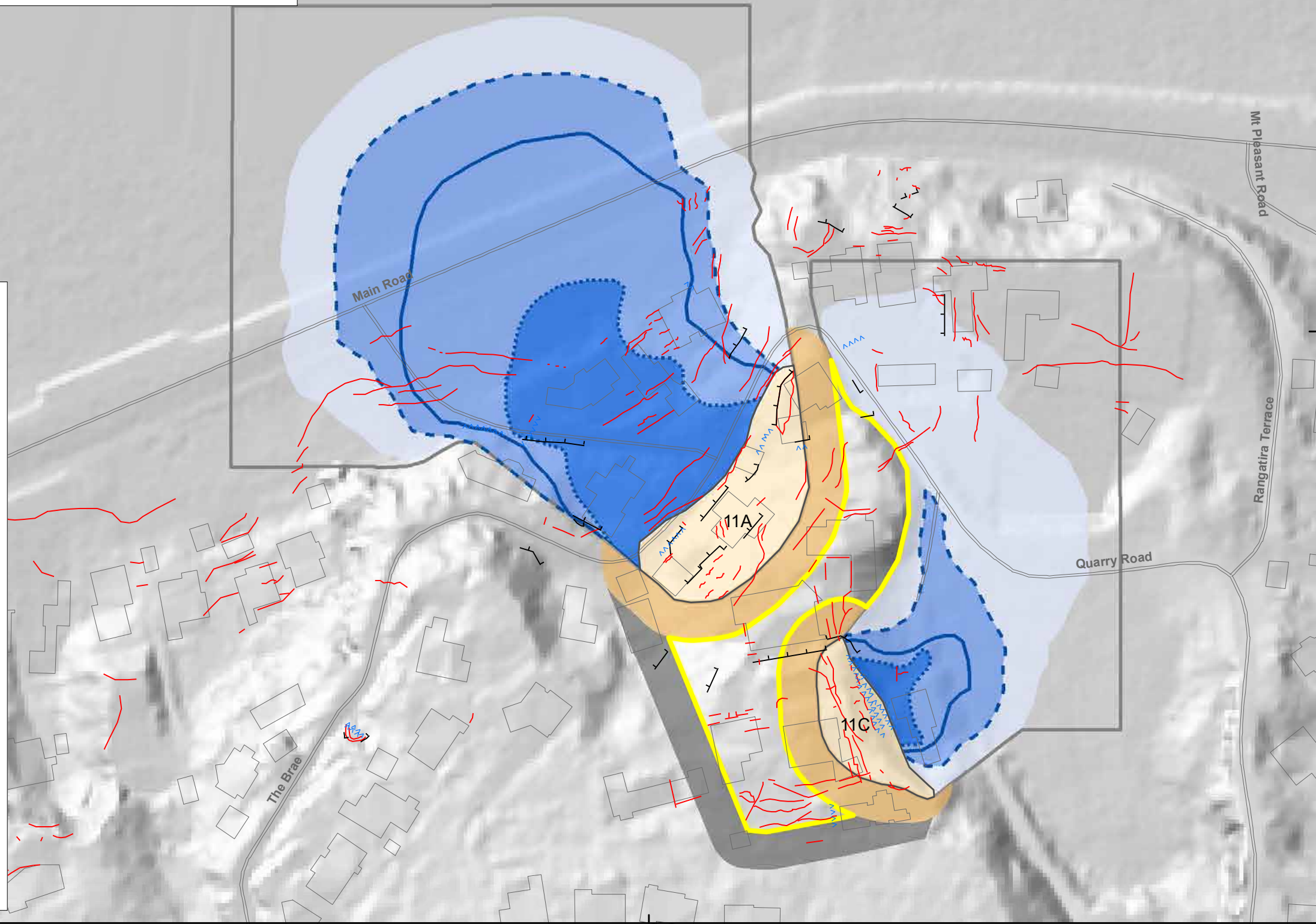
- $V_{(D:T)}$ for debris avalanches hazards, the vulnerability of a person, if present and inundated by debris, is a constant vulnerability factor of 70% has been adopted for this risk assessment. A constant vulnerability value is thought reasonable as the modelled velocity of the boulders, even in the distal runout zone are still relatively high with people unlikely to be able to get out of the way. For earth/debris flow hazards, a variable vulnerability has been used based on the velocity of the debris (Appendix 1).

Annual individual fatality risk bands (e.g. 10^{-3} to 10^{-4}) – The risk of being killed in any one year is expressed as a number such as 10^{-4} (“ten to the minus four”). 10^{-4} can also be expressed as one chance in 10,000 of being killed in any one year.

Earth/debris flow - A type of landslide associated with long runout. They tend to be rapid (> 5 m/sec), liquefied landslides of mixed water and debris (typically loess) that can look like flowing concrete.



Assessed source areas
Slope hazard
 Earth/debris flow source area
 Class III relative hazard exposure area
Potential future enlargement of mass movements
 Earth/debris flow source 10 m enlargement area
 Class III relative hazard exposure 10 m enlargement area
Earth/debris flow annual individual fatality risk
 Greater than 10^{-4} (all volumes)
 10^{-4} uncertainty zone*
 Less than 10^{-4} (all volumes)
 10^{-4} annual individual fatality risk line
 Upper volume
 Middle volume
 Lower volume
Surface deformation**
 Tension crack
 Compression zone
 Tilted/deformed retaining wall/fence
 Assessment area
 Buildings
 Roads



1576800

1577000

SCALE BAR: 0 50 100 m

EXPLANATION:
 * Greater than 10^{-4} for upper volume, greater or less than 10^{-4} for the middle volume but below 10^{-4} for the lower volume
 ** Taken from report CR2012/317
 Background shade model derived from NZAM post earthquake 2011c (July 2011) LiDAR survey.
 Roads and building footprints provided by Christchurch City Council (20/02/2012).
 PROJECTION: New Zealand Transverse Mercator 2000

DRW:
BL
 CHK:
CM, FDP



**EARTH/DEBRIS FLOW
 ANNUAL INDIVIDUAL FATALITY RISK
 (Source areas 11A and 11C)**

**Quarry Road
 Christchurch**

FIGURE 40

Map 1

FINAL

REPORT: CR2014/75 DATE: June 2014

Annual individual fatality risk bands (e.g. 10^{-3} to 10^{-4}) – The risk of being killed in any one year is expressed as a number such as 10^{-4} (“ten to the minus four”). 10^{-4} can also be expressed as one chance in 10,000 of being killed in any one year.

Cliff collapse – Includes debris avalanche and cliff recession hazards.

Debris avalanche - A type of landslide comprising many boulders falling simultaneously from a slope. The rocks start by sliding, toppling or falling before descending the slope rapidly (greater than 5 metres per second) by any combination of falling, bouncing and rolling.

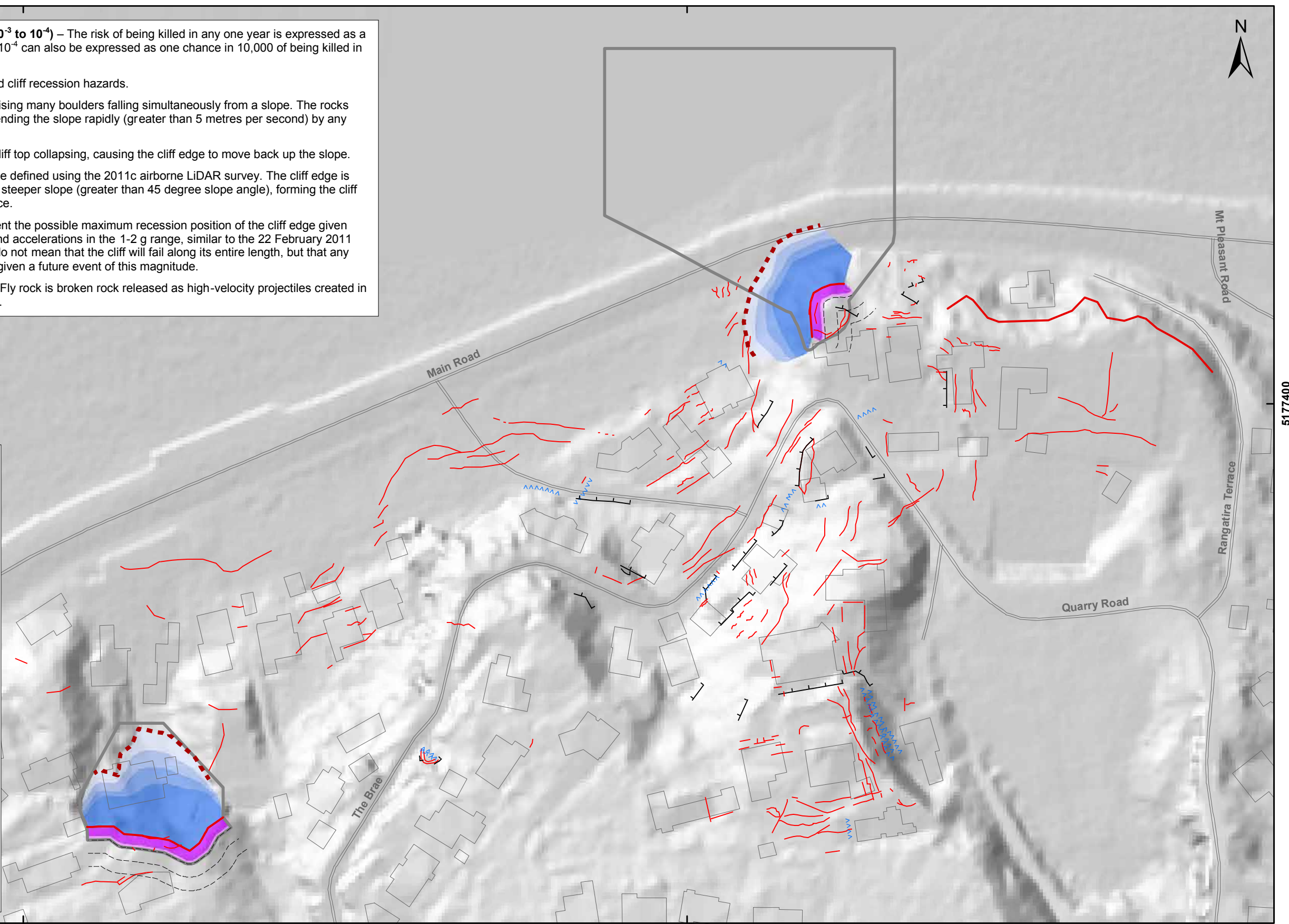
Cliff recession – Is the result of parts of the cliff top collapsing, causing the cliff edge to move back up the slope.

Cliff edge – This is the position of the cliff edge defined using the 2011c airborne LiDAR survey. The cliff edge is defined as the line of intersection between the steeper slope (greater than 45 degree slope angle), forming the cliff face and the shallower slope above the cliff face.

Earthquake event lines - These lines represent the possible maximum recession position of the cliff edge given future earthquakes with associated peak ground accelerations in the 1-2 g range, similar to the 22 February 2011 and 13 June 2011 earthquakes. These lines do not mean that the cliff will fail along its entire length, but that any place along the cliff could fail back to this line given a future event of this magnitude.

Fly rock line – Is the mapped limit of fly rock. Fly rock is broken rock released as high-velocity projectiles created in impacts between rocks and other hard objects.

- Debris avalanche***
annual individual fatality risk
- Greater than 10^{-3}
 - 10^{-3} to 10^{-4}
 - 10^{-4} to 10^{-5}
 - Less than 10^{-5}
- Cliff recession***
annual individual fatality risk
- Greater than 10^{-3}
 - 10^{-3} to 10^{-4}
- Fly-rock line (31 degrees)*
 - Earthquake event line*
 - Cliff edge
- Surface deformation****
- Tension crack
 - Compression zone
 - Tilted/deformed retaining wall/fence
 - Assessment area
 - Buildings
 - Roads



SCALE BAR: 0 50 100 m

EXPLANATION:
 * Modified from report CR2012/124
 ** Taken from report CR2012/317
 Background shade model derived from NZAM post earthquake 2011c (July 2011) LiDAR survey resampled to a 1 m ground resolution.
 Roads and building footprints provided by Christchurch City Council (20/02/2012).
 PROJECTION: New Zealand Transverse Mercator 2000

DRW:
BL
 CHK:
CM, FDP



**CLIFF COLLAPSE
 ANNUAL INDIVIDUAL FATALITY RISK
 (From GNS Science Report CR2012/124)**

**Quarry Road
 Christchurch**

FIGURE 40	
Map 2	
FINAL	
REPORT: CR2014/75	DATE: June 2014

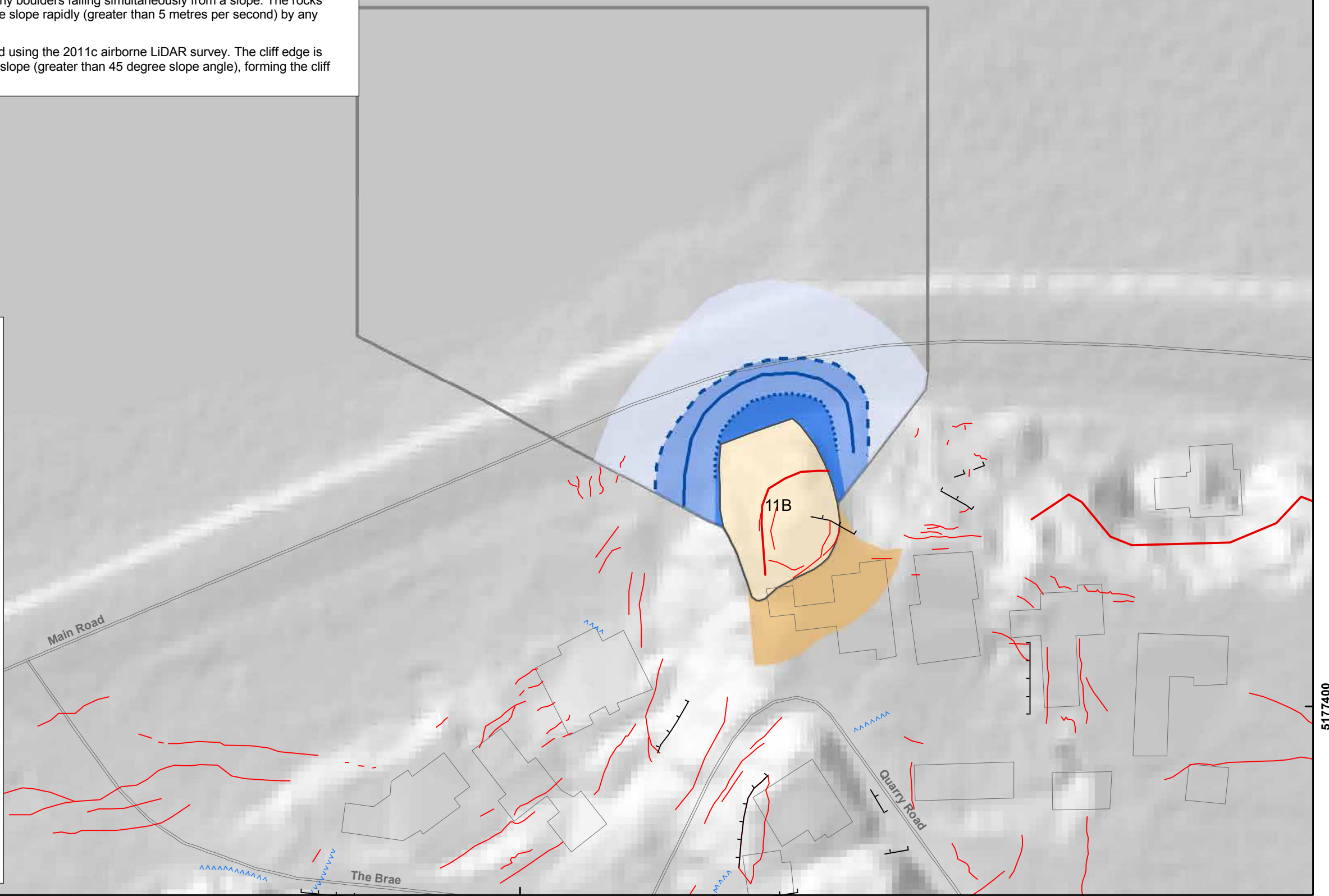
Annual individual fatality risk bands (e.g. 10^{-3} to 10^{-4}) – The risk of being killed in any one year is expressed as a number such as 10^{-4} (“ten to the minus four”). 10^{-4} can also be expressed as one chance in 10,000 of being killed in any one year.

Debris avalanche - A type of landslide comprising many boulders falling simultaneously from a slope. The rocks start by sliding, toppling or falling before descending the slope rapidly (greater than 5 metres per second) by any combination of falling, bouncing and rolling.

Cliff edge – This is the position of the cliff edge defined using the 2011c airborne LiDAR survey. The cliff edge is defined as the line of intersection between the steeper slope (greater than 45 degree slope angle), forming the cliff face and the shallower slope above the cliff face.



- Assessed source area
- Slope hazard**
- Local debris avalanche source area
- Potential future enlargement of mass movements**
- Debris avalanche source 10 m enlargement area
- Debris avalanche annual individual fatality risk**
- Greater than 10^{-4} (all volumes)
- 10^{-4} uncertainty zone*
- Less than 10^{-4} (all volumes)
- Cliff edge
- 10^{-4} annual individual fatality risk line**
- Upper volume
- Middle volume
- Lower volume
- Surface deformation***
- Tension crack
- Compression zone
- Tilted/deformed retaining wall/fence
- Assessment area
- Buildings
- Roads



EXPLANATION:
 * Taken from report CR2012/317
 Background shade model derived from NZAM post earthquake 2011c (July 2011) LiDAR survey resampled to a 1 m ground resolution.
 Roads and building footprints provided by Christchurch City Council (20/02/2012).
 PROJECTION: New Zealand Transverse Mercator 2000

DRW:
BL

CHK:
CM, FDP



**DEBRIS AVALANCHE
 ANNUAL INDIVIDUAL FATALITY RISK
 (Source area 11B)**

**Quarry Road
 Christchurch**

FIGURE 40

Map 3

FINAL

REPORT: CR2014/75 DATE: June 2014

Annual individual fatality risk bands (e.g. 10^{-3} to 10^{-4}) – The risk of being killed in any one year is expressed as a number such as 10^{-4} (“ten to the minus four”). 10^{-4} can also be expressed as one chance in 10,000 of being killed in any one year.

Cliff collapse – Includes debris avalanche and cliff recession hazards.

Debris avalanche - A type of landslide comprising many boulders falling simultaneously from a slope. The rocks start by sliding, toppling or falling before descending the slope rapidly (greater than 5 metres per second) by any combination of falling, bouncing and rolling.

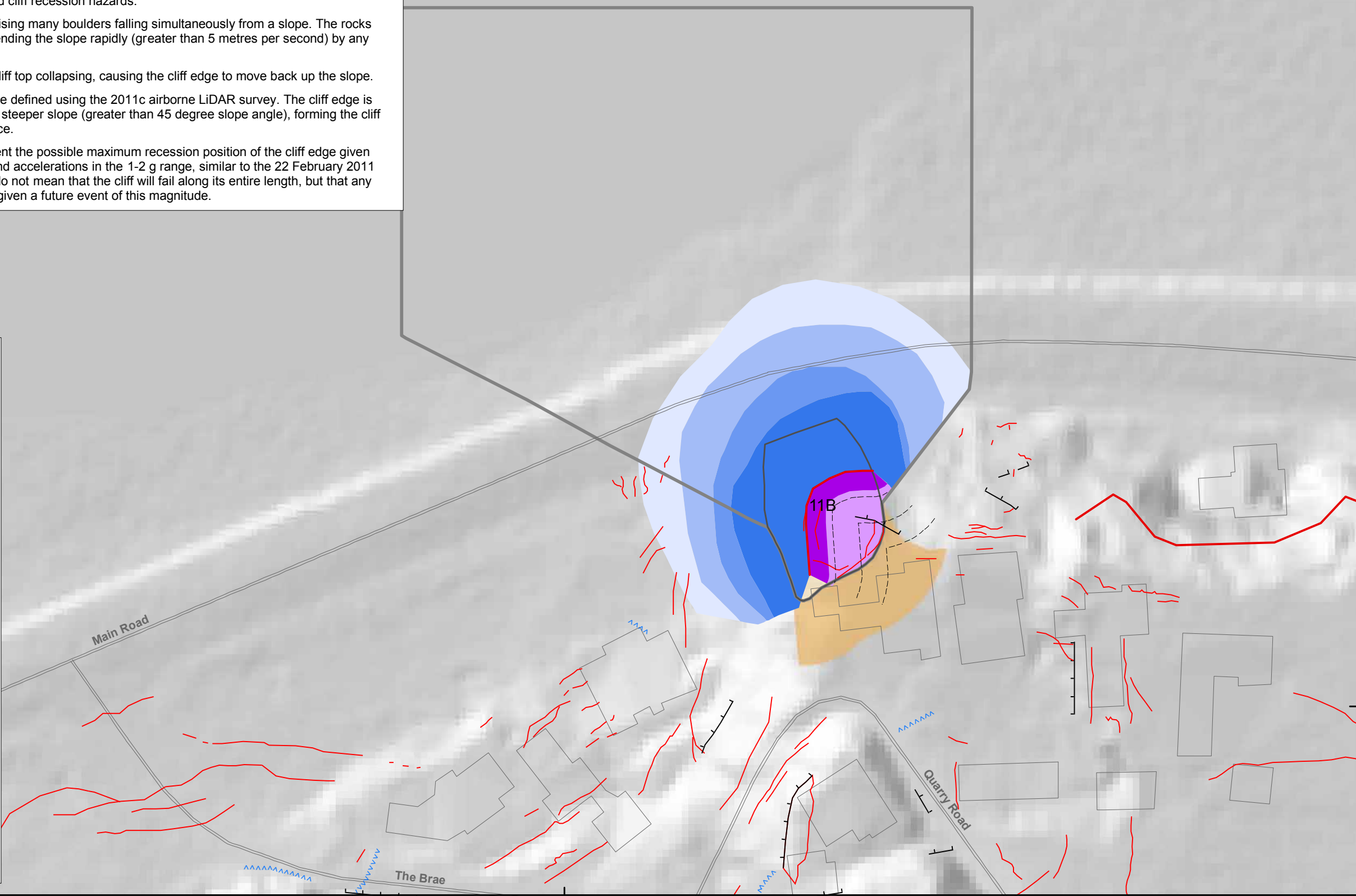
Cliff recession – Is the result of parts of the cliff top collapsing, causing the cliff edge to move back up the slope.

Cliff edge – This is the position of the cliff edge defined using the 2011c airborne LiDAR survey. The cliff edge is defined as the line of intersection between the steeper slope (greater than 45 degree slope angle), forming the cliff face and the shallower slope above the cliff face.

Earthquake event lines - These lines represent the possible maximum recession position of the cliff edge given future earthquakes with associated peak ground accelerations in the 1-2 g range, similar to the 22 February 2011 and 13 June 2011 earthquakes. These lines do not mean that the cliff will fail along its entire length, but that any place along the cliff could fail back to this line given a future event of this magnitude.



- Assessed source area
- Source area
- Source 10 m enlargement area
- Debris avalanche**
- annual individual fatality risk**
- Greater than 10^{-3}
- 10^{-3} to 10^{-4}
- 10^{-4} to 10^{-5}
- Less than 10^{-5}
- Cliff recession***
- annual individual fatality risk**
- Greater than 10^{-3}
- 10^{-3} to 10^{-4}
- Earthquake event line*
- Cliff edge
- Surface deformation****
- Tension crack
- Compression zone
- Tilted/deformed retaining wall/fence
- Assessment area
- Buildings
- Roads



EXPLANATION:
 * Modified from report CR2012/124
 ** Taken from report CR2012/317
 The results combine the annual individual fatality risk modified from report CR2012/124 with the annual individual fatality risk from source area 11B adopting Scenario B
 Background shade model derived from NZAM post earthquake 2011c (July 2011) LiDAR survey resampled to a 1 m ground resolution.
 Roads and building footprints provided by Christchurch City Council (20/02/2012).
 PROJECTION: New Zealand Transverse Mercator 2000

DRW:
BL

CHK:
CM, FDP



**COMBINED CLIFF COLLAPSE
 ANNUAL INDIVIDUAL FATALITY RISK
 (Source area 11B)**

**Quarry Road
 Christchurch**

FIGURE 40

Map 4

FINAL

REPORT:
CR2014/75

DATE:
June 2014

5.5.2 Source areas 11A and 11C

The risk from earth/debris flows from source areas 11A and 11C, adopting the estimated lower, middle and upper source volumes are shown in Figure 40, Map 1.

A 10-m wide zone has been included at the crest of the source areas, to allow for the future retrogression of the source in an up-slope direction, beyond the currently assessed extent. This has been termed an “earth/debris flow source 10 m enlargement area”.

Three annual individual fatality risk lines representing the position of the 10^{-4} risk contour are shown on the map for the upper, middle and lower volumes, assuming a 50-year return period. The area shown as the “greater than 10^{-4} (all volumes)” represents the area of slope where the risk could be greater than 10^{-4} for all assessed failure volumes.

The area shown as the “ 10^{-4} uncertainty zone” represents the area of slope where the risk could be greater than 10^{-4} for the upper source volume, but less than 10^{-4} for the lower source volume and equal to or greater than 10^{-4} for the middle source volume.

The area of slope beyond (further away from the assessed source areas) the 10^{-4} uncertainty zone but within the assessed extent of debris runout represents the area of slope, within the runout zone, where the annual individual fatality risk has been assessed as being less than 10^{-4} for all source volumes.

5.5.2.1 Sensitivity to the annual frequency of the triggering event

The return periods of the event that could initiate failure is unknown. The sensitivity of the risk estimates for source areas 11A and 11C to different event return periods has been assessed. This was done by plotting the location of the 10^{-4} annual individual fatality risk contour, for the upper source volume estimates only, adopting return periods of 20, 50, 100 and 200 years for the triggering event. The results are plotted for source area 11A in Figure 41.

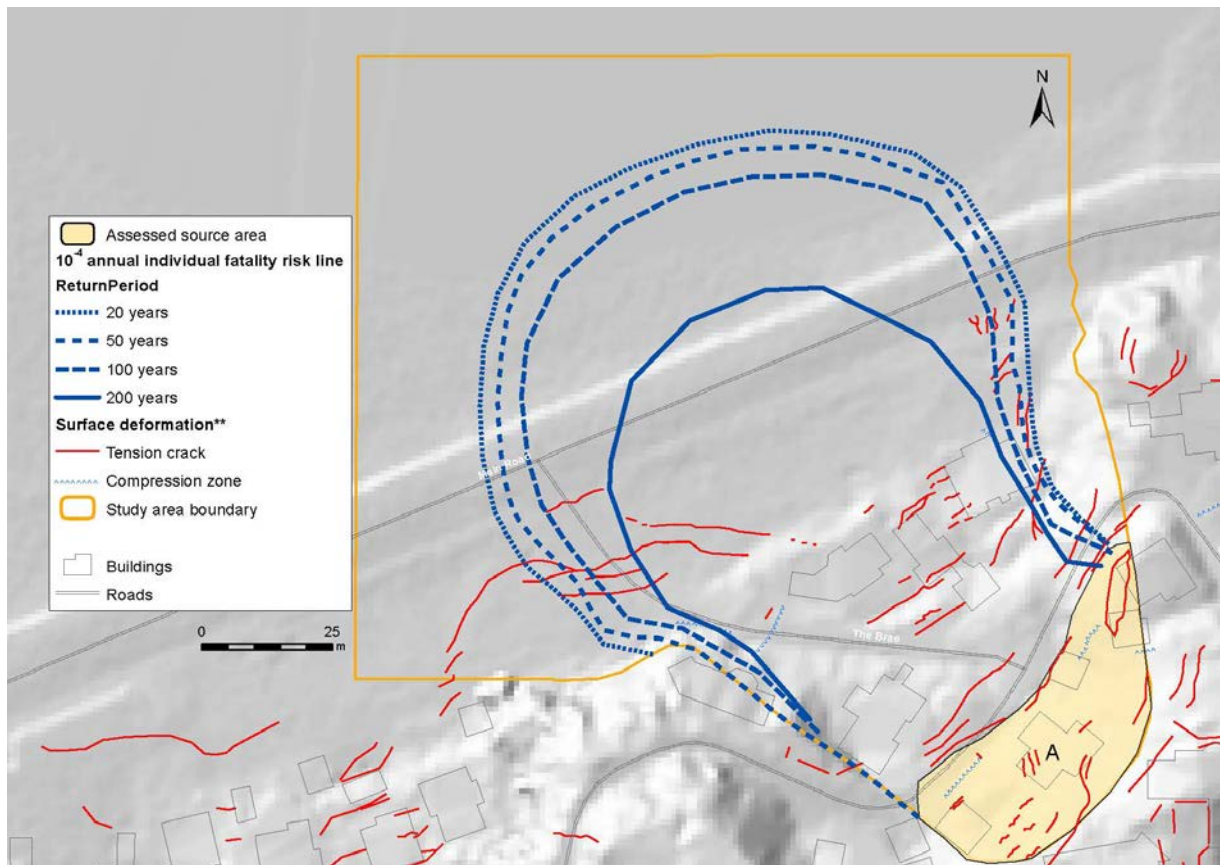


Figure 41 Sensitivity of the risk estimates for source area 11A, upper volume estimates, for triggering event return periods of 20, 50, 100 and 200 years.

The results show that area within the 10^{-4} risk contour reduces between the 20 year and 200 year return periods. This is because the volume of the failure, and therefore runout distance of the debris remains fixed, but the return period of the event increases, leading to a reduction in the risk at the longer return periods.

For source areas 11A and 11C, for the varying return periods assessed, the changing risk has little impact on the numbers of dwellings within the 10^{-4} annual individual fatality risk contour.

For the risk estimates shown in Figure 40, a 50-year return period for the triggering event has been adopted. This is considered reasonable as:

1. The rainfall on 5 March 2014 was equivalent to a 10–20 year return period rain event for this area, and no significant landslides, in this area, were triggered by this storm.
2. There is little difference in the risk estimates adopting the 20 and 100 year triggering event return periods.

5.5.2.2 Slumping and cracking

The area of slope between the cliff-top recession risk zone and the mapped extent of cracking that was highlighted in the Stage 1 report as a Class I area, has now been re-assessed as being in a Class III area. A Class III area is defined in the Stage 1 report (Massey et al., 2013) as:

- Coherent slides and slumps of predominantly loess with associated cumulative inferred displacement of the mass of less than 0.3 m, where dwellings are present within the moving mass. It is possible that renewed movement may have potential to cause only minor damage to dwellings and local infrastructure, if the hazard were to occur. The level of disruption to dwellings is likely to be a function of where they are within the feature. The most hazardous places are the mainly extensional and compressional areas. Given the magnitudes of displacement it is unlikely that damage to dwellings would pose an immediate life risk to their occupants.

A 10-m wide area has been included to take into account any enlargement of the area of slumping and cracking, in an up-slope or lateral direction beyond the currently recognised boundary, which could occur in a future event. This has been termed a “Class III relative hazard exposure 10 m enlargement area”.

5.5.3 Source area 11B

The risk from cliff collapses sourcing from source area 11B, adopting the estimated lower, middle and upper source volumes, and the year 2016 earthquake event frequencies (Table 15) are shown in Figure 40, Map 3.

A 10-m wide zone has been included at the crest of the source areas, to allow for the future retrogression of the source in an up-slope direction, beyond the currently assessed extent. This has been termed a “debris avalanche source 10 m enlargement area”.

Three annual individual fatality risk lines representing the position of the 10^{-4} risk contour are shown on the map for the upper, middle and lower volumes, assuming a 50-year return period. The area shown as the “greater than 10^{-4} (all volumes)” represents the area of slope where the risk could be greater than 10^{-4} for all assessed failure volumes.

The area shown as the “ 10^{-4} uncertainty zone” represents the area of slope where the risk could be greater than 10^{-4} for the upper source volume, but less than 10^{-4} for the lower source volume and equal to or greater than 10^{-4} for the middle source volume.

The area of slope beyond (further away from the assessed source areas) the 10^{-4} uncertainty zone but within the assessed extent of debris runout represents the area of slope, within the runout zone, where the annual individual fatality risk has been assessed as being less than 10^{-4} for all source volumes.

It should be noted that the risk from source area 11B is additional to the risk from the smaller cliff collapses assessed in Massey et al. (2012a).

5.5.3.1 Combined risk

The total risk from the combined hazards is shown in Map 3 of Figure 40. The results combine the risk presented in Massey et al. (2012a) from cliff collapse of the slope with the annual individual fatality risk estimated adopting the middle volume estimates for the cliff collapse hazards (source area 11B) assessed in this report.

The original risk assessment in Massey et al. (2012a) was updated to make it consistent with the input parameters discussed in Massey et al. (2012b) and used in the risk assessments contained in this report and other Stage 2 and 3 reports, these comprised:

1. Annual frequency of an earthquake triggering event: For this assessment GNS Science has adopted the year 2016 national seismic hazard model annual frequencies for earthquake peak ground accelerations.
2. Probability of a person being present: For this assessment, GNS Science has assumed an “average” occupancy rate, i.e., that an average person spends on average 16 hours a day at home ($16/24 = 0.67$ or 67%).
3. Vulnerability of a person if present and hit by debris: For this assessment GNS Science has adopted a constant vulnerability factor of 70%.

It should be noted that the risks presented in Massey et al. (2012a) were estimated for smaller cliff collapse (debris avalanche) source volumes and different failure mechanisms to the deeper seated mechanisms for source area 11B.

5.5.4 Source area 11E

The risk from debris avalanches sourcing from source area 11E are shown in Figure 40, Map 2. Given the lack of detailed site-specific information relating to this slope, GNS Science has applied the cliff collapse risk model (reported by Massey et al., 2012a) to this slope. This was done as the slope is higher than 10 m and the slope angle is greater than 45°, and the slope surface area is greater than 50 m² (the criteria used in the Massey et al., 2012a assessments) and recent failures from the slope have been recorded by Harwood (2011; 2013).

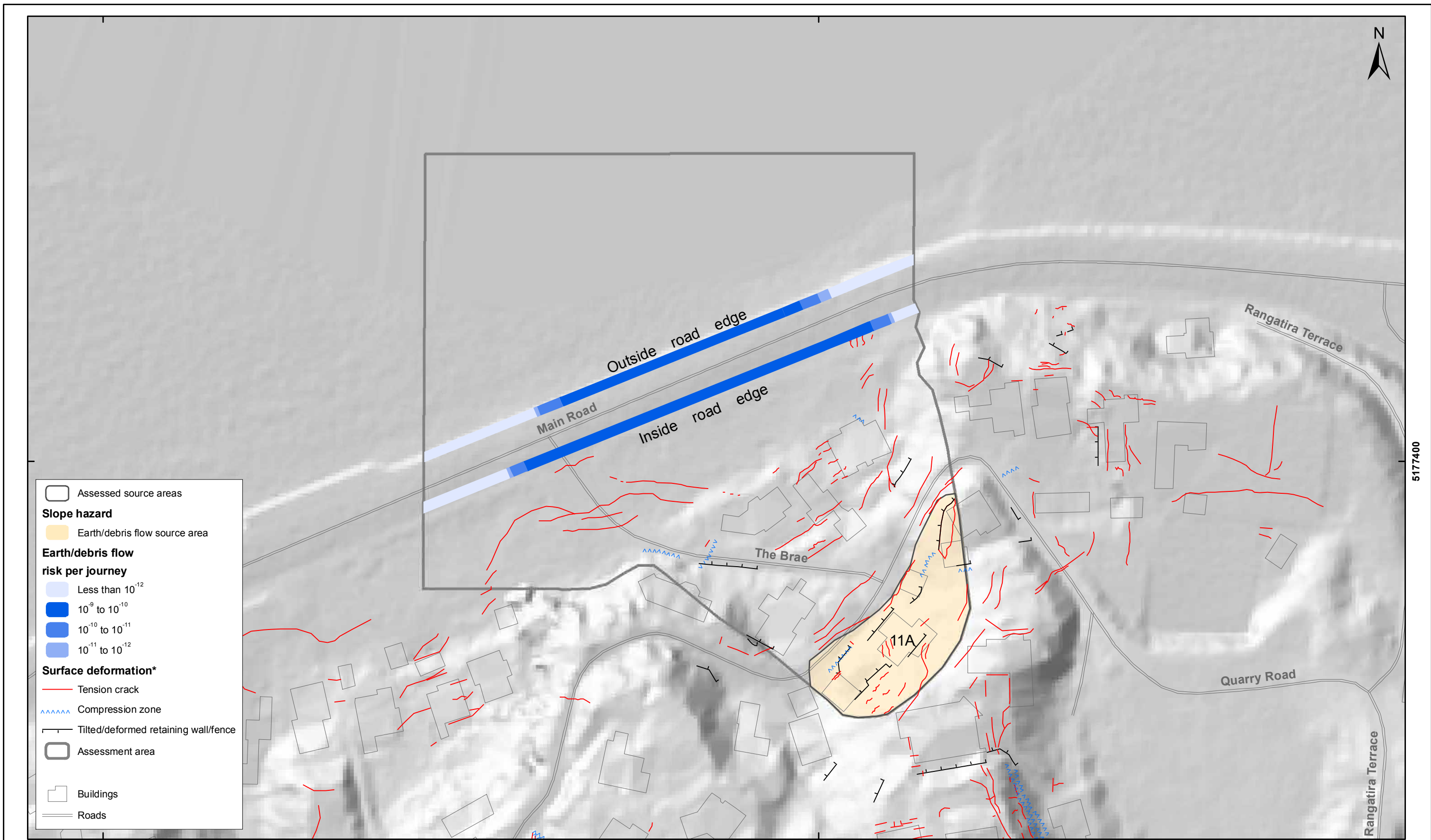
The original risk assessment by Massey et al. (2012a) was updated to make it consistent with the input parameters discussed in Massey et al. (2012b) and used in the risk assessments contained in this report and discussed in Section 5.5.3.1.

5.6 ROAD USER RISK

Figure 42, Maps 1 and 2 show the risk per trip for a pedestrian along the outer and inner edges of Main Road from earth/debris flows originating from source area 11A, for the upper and lower volume estimates respectively.

Figure 42, Maps 3 and 4 show the risk per trip for a pedestrian along the outer and inner edges of Main Road from debris avalanches originating from source area 11B, for the upper and lower volume estimates respectively.

Figure 43 and Figure 44 shows the maximum calculated risks for road users for source areas 11A and 11B respectively. These figures show slope collapse risk per journey at the uphill (southern, landward) and the downhill (northern, seaward) sides of the road in comparison with the risk per journey from motor vehicle crashes that would be expected for journeys of 200 m (the distance from Rantatira Terrace to The Brae – the shortest trip on Main Road that encompasses the study area) on an average New Zealand urban road.



SCALE BAR: 0 50 m

EXPLANATION:

* Taken from report CR2012/317

Background shade model derived from NZAM post earthquake 2011c (July 2011) LiDAR survey resampled to a 1 m ground resolution. Roads and building footprints provided by Christchurch City Council (20/02/2012). PROJECTION: New Zealand Transverse Mercator 2000

DRW:
DH, BL

CHK:
CM, FDP



**ROAD USER RISK : PEDESTRIAN
(Source area 11A)
Higher estimate**

**Quarry Road
Christchurch**

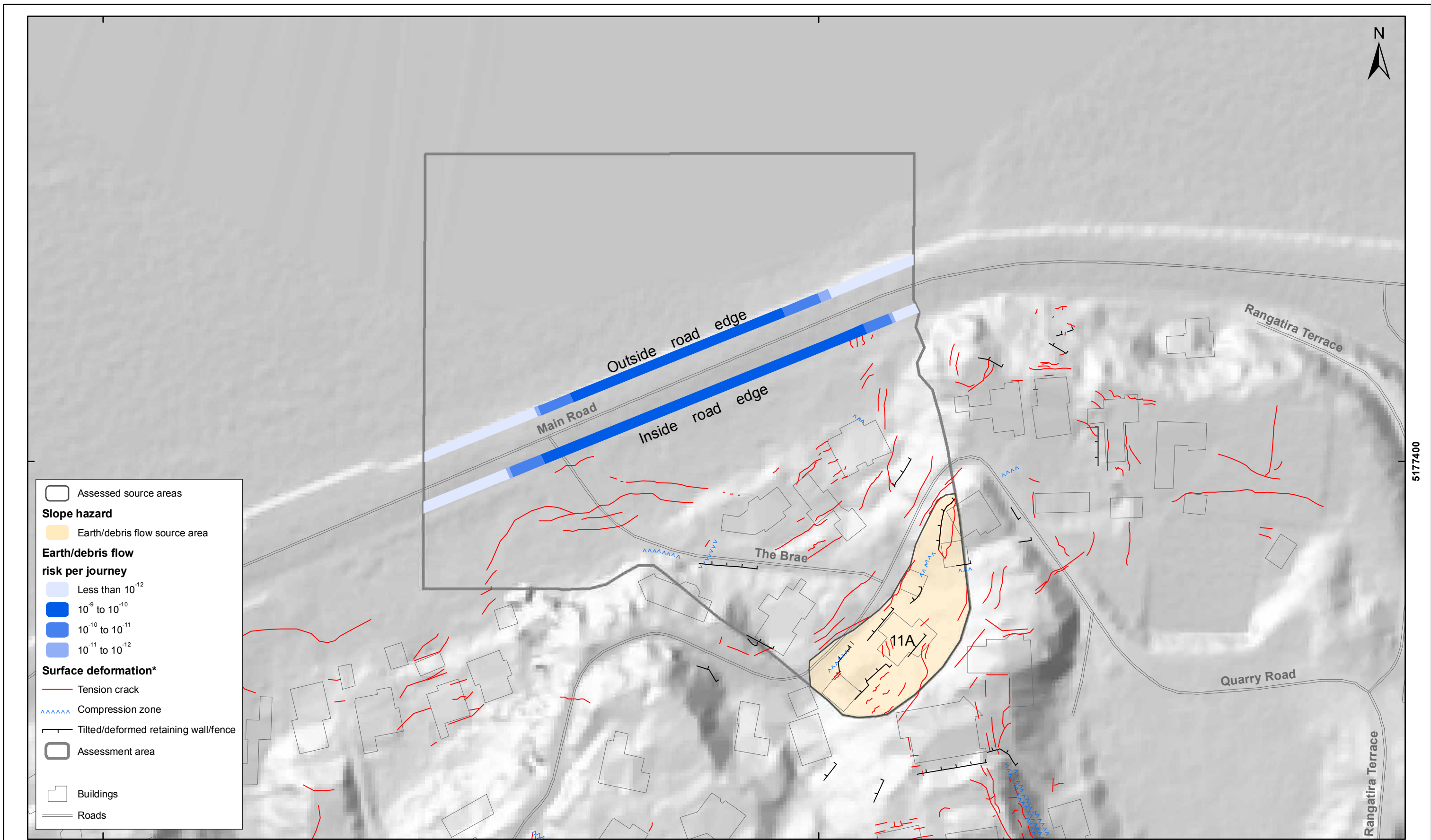
FIGURE 38

Map 1

FINAL

REPORT:
CR2014/75

DATE:
June 2014



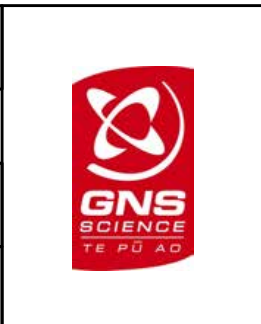
SCALE BAR: 0 50 m

EXPLANATION:
 * Taken from report CR2012/317

Background shade model derived from NZAM post earthquake 2011c (July 2011) LiDAR survey resampled to a 1 m ground resolution.
 Roads and building footprints provided by Christchurch City Council (20/02/2012).
 PROJECTION: New Zealand Transverse Mercator 2000

DRW:
DH, BL

CHK:
CM, FDP



ROAD USER RISK : PEDESTRIAN
(Source area 11A)
Lower estimate

Quarry Road
Christchurch

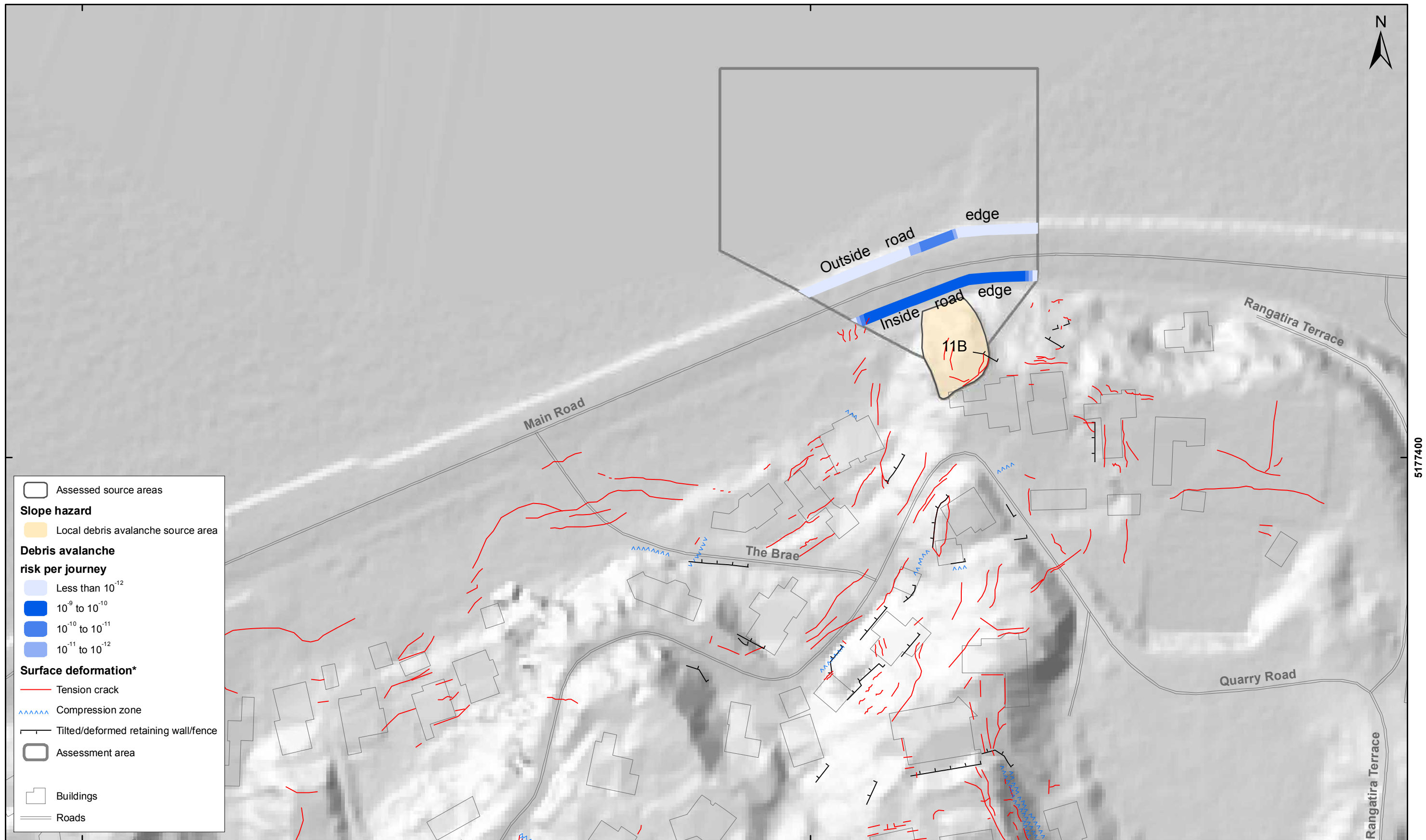
FIGURE 38

Map 2

FINAL

REPORT:
CR2014/75

DATE:
June 2014



- Assessed source areas
- Slope hazard**
- Local debris avalanche source area
- Debris avalanche risk per journey**
- Less than 10^{-12}
- 10^{-9} to 10^{-10}
- 10^{-10} to 10^{-11}
- 10^{-11} to 10^{-12}
- Surface deformation***
- Tension crack
- ~~~~~ Compression zone
- |—|—| Tilted/deformed retaining wall/fence
- Assessment area
- Buildings
- Roads

SCALE BAR:
0
50
m

EXPLANATION:
* Taken from report CR2012/317

Background shade model derived from NZAM post earthquake 2011c (July 2011) LiDAR survey resampled to a 1 m ground resolution.
Roads and building footprints provided by Christchurch City Council (20/02/2012).
PROJECTION: New Zealand Transverse Mercator 2000

DRW:
DH, BL
CHK:
CM, FDP



**ROAD USER RISK : PEDESTRIAN
(Source area 11B)
Higher estimate**

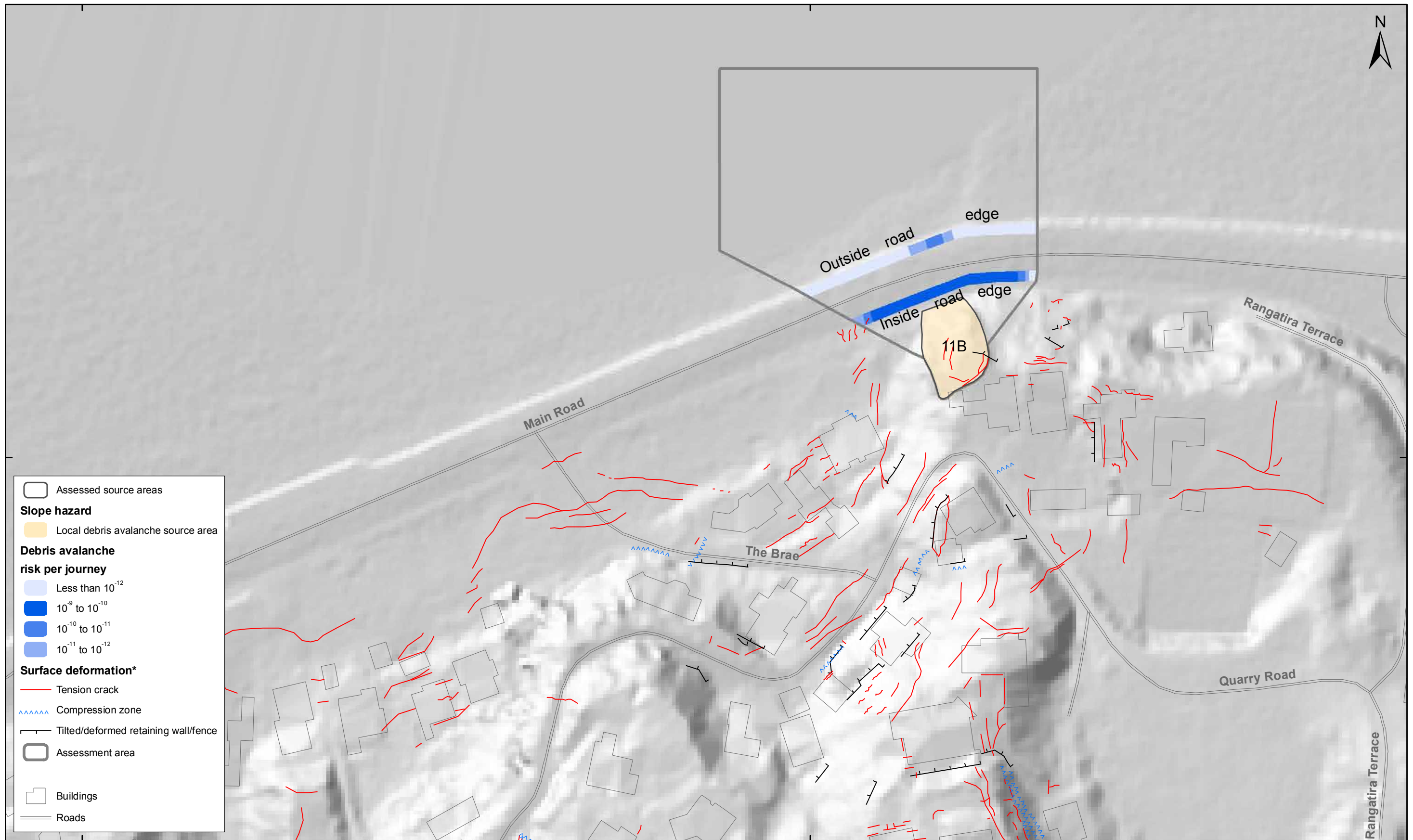
**Quarry Road
Christchurch**

FIGURE 38

Map 3

FINAL

REPORT: CR2014/75 DATE: June 2014



- Assessed source areas
- Slope hazard**
- Local debris avalanche source area
- Debris avalanche risk per journey**
- Less than 10^{-12}
- 10^{-9} to 10^{-10}
- 10^{-10} to 10^{-11}
- 10^{-11} to 10^{-12}
- Surface deformation***
- Tension crack
- - - - - Compression zone
- Tilted/deformed retaining wall/fence
- Assessment area
- Buildings
- Roads

SCALE BAR:
0
50
m

EXPLANATION:
* Taken from report CR2012/317

Background shade model derived from NZAM post earthquake 2011c (July 2011) LiDAR survey resampled to a 1 m ground resolution.
Roads and building footprints provided by Christchurch City Council (20/02/2012).
PROJECTION: New Zealand Transverse Mercator 2000

DRW:
DH, BL
CHK:
CM, FDP



**ROAD USER RISK : PEDESTRIAN
(Source area 11B)
Lower estimate**

**Quarry Road
Christchurch**

FIGURE 38

Map 4

FINAL

REPORT: CR2014/75	DATE: June 2014
----------------------	--------------------

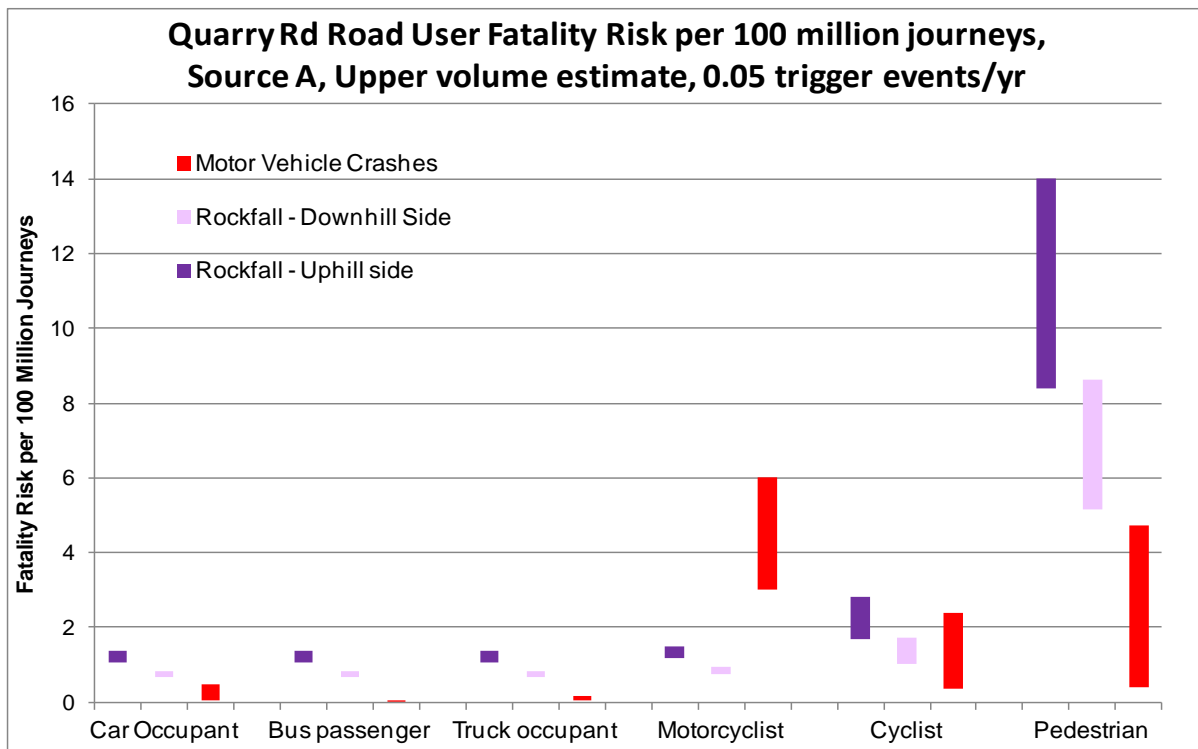


Figure 43 Maximum calculated road user risk per journey, source area 11A.

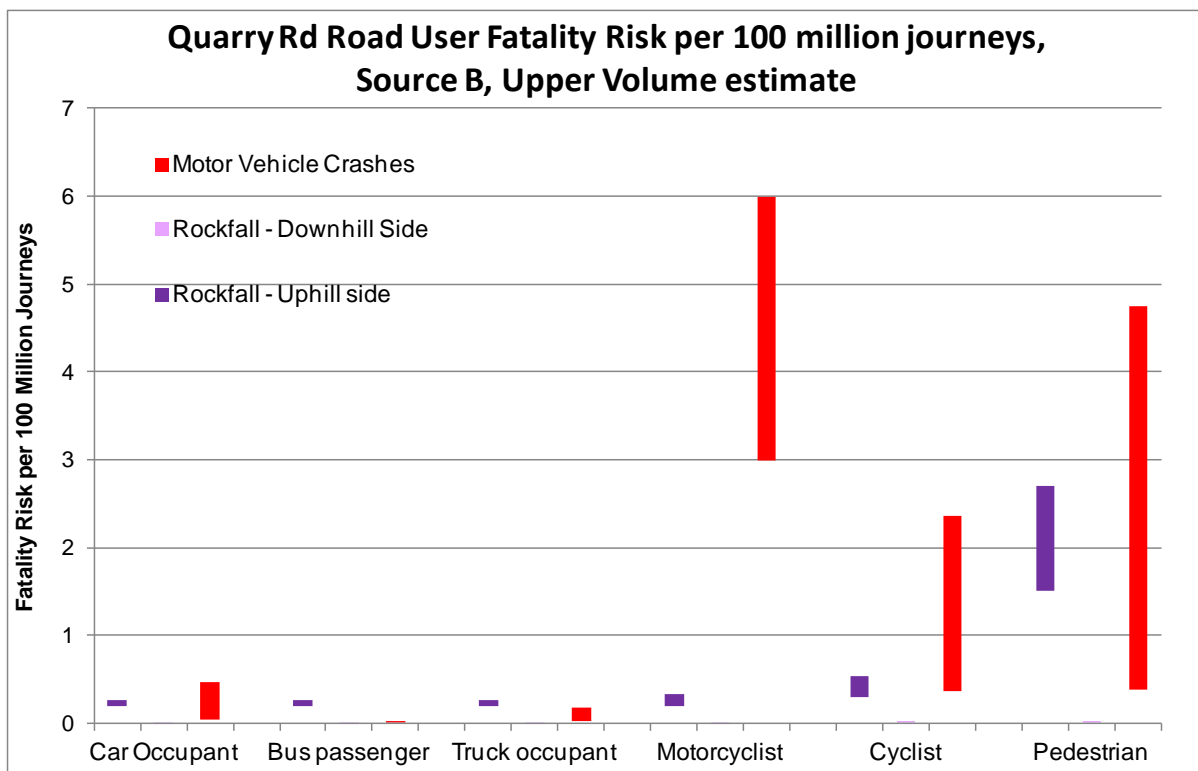


Figure 44 Maximum calculated road user risk per journey, source area 11B.

Notable points include:

1. For source area 11A, the assessed risk for motor vehicle occupants and pedestrians from landslides (upper volume) is considerably greater than that from motor vehicle crashes; that for cyclists is comparable while that for motorcyclists is considerably less than the motor vehicle crash risk. This risk reduces to zero for the lower volume.
2. For source area 11B the assessed slope collapse risk on the southern side of the road for car occupants, cyclists and pedestrians is more comparable with the motor vehicle crash risk. For buses and trucks the slope collapse risk is larger than the crash risk, while for motorcyclists the crash risk is much the larger.
3. The assessed risk on the downhill (seaward) side of the road is about half that on the uphill (landward, southern) side of the road for all users for source area 11A, and disappears altogether on the seaward side of the road for source area 11B (there is in fact a tiny non-zero risk calculated, but it is too small to be visible in Figure 44).
4. The calculated slope collapse risks on the southern side of the road are roughly five to ten times higher for source area 11A than for source area 11B, based on upper volumes of slope failure.

The assessed risk for source area 11A is acutely sensitive to the assumption made as to the source volume – the risk on the road disappears altogether for the lower volume modelled. The risk for source area 11B is much less sensitive, hardly changing at all with source volume. This perhaps reflects the nature of this “all or nothing” hazard – road users are either inundated by a lot of rock or not; it makes little difference whether struck by 3 boulders or 10.

The road usage assumed in this assessment is summarised in Table 16. Main Road, near St Andrews Hill, is classified as a major arterial. A major arterial is ranked the highest out of four road importance types.

It should be noted in comparing landslide risk with motor vehicle crash risk that the vast majority of the latter (certainly in excess of 90%, possibly in excess of 99%) is associated with causes within the control of private road users, as is illustrated by the large variations in car crash risk by sex and age, and the large difference between buses and private cars. The wholly involuntary part of crash risk as a road user (i.e., the residual risk outside one’s own control) is thus well below 10%, possible as little as 1% or less, of the total road crash risk. If slope collapse risk, as an example of a risk outside the control of the person exposed to it, is compared with the involuntary component of motor vehicle crash risk, then slope collapse emerges from this assessment as a substantially higher involuntary risk than motor vehicle crashes for both sources and for all road users with the possible exception of motorcyclists.

Table 16 Main Road usage assumptions.

Road user	Trips/day, heavy user ¹ (combined, E+W)		Trips/year, all users ² (combined E+W)		Average speed ³	
	lower	upper	vehicles	people	lower risk	higher risk
Cars	1	2	6604588	10483318	39.1	30.7
Buses	1	2	39244	598660	39.1	30.7
Trucks	1	2	227582	361236	39.1	30.7
Motorcycles	1	2	121750	121750	39.1	30.7
Cyclists	1	2	365250	365250	25	15
Pedestrians	1	2	36525	36525	5	3

Notes on Table 16:

1. For Wakefield Avenue (Taig and Massey, 2014) we assumed it feasible that some people would travel in and out of Sumner twice per day. For the longer trip along Main Road from Port Hills locations into Christchurch we consider this unlikely. 1 one-way trip per day corresponds roughly to a typical student or commuter making a large majority of their daily (weekdays, excluding holidays) trips by the given mode of transport.
2. Cars, buses and trucks data from Christchurch City Council traffic counts for the Main Road Causeway and through traffic at the Ferrymead/Main Road junction. Bus data corresponds to timetabled No. 3 buses (Sumner to Christchurch Airport) plus school buses. Cyclist data estimated in consultation with GNS Science colleagues who are frequent users of this road (counts at Ferrymead/Main Road junction considered greatly to underestimate actual cycle traffic on this very popular route). Pedestrians and motorcyclists estimated at 1/10 and 1/3 of cyclist traffic respectively. Assumed average vehicle occupancies: for cars 0.58 passengers per vehicle (NZ Travel Survey average passenger km/vehicle km), for trucks as for cars, for school buses 40 persons, for No. 3 buses 15 persons. Motorcycles, cycles, pedestrians all 1 person per "vehicle".
3. Motor vehicle speeds assumed to range from 40 to 50 km/hr in free moving traffic (not a stretch of road where people either wish to or do drive especially slowly). Average speeds assumed to reduce with traffic density from normal speed up to 400 motor vehicles per hour one way, then reducing gradually up to 800 vehicles per hour and more steeply thereafter, reaching 10–15kph above 1100 vehicles per hour. The figures in the table are the weighted averages over every hour of the day/week. Cyclists assumed unaffected by motor vehicle speed (separate lanes for whole of this stretch of road).

Annual individual fatality risk for road users follows the exact same patterns as shown in Figure 43 and Figure 44. The calculated range of risk for regular road users (making 1–2 one-way trips on the road every day) is as follows:

- From source area 11A: between 4 and 10 per million years for motorised road users, rising to between 30 and 100 per million years for pedestrians.
- From source area 11B: between 0.7 and 2.5 per million years for motorised road users, rising to between 6 and 20 per million years for pedestrians.

The aggregated risk over all road users is as follows for the highest risk scenarios assessed (upper source volumes, maximum credible trigger frequency for source area 11A):

- From source area 11A, between 0.07 and 0.14 average expected slope collapse deaths per year (one death every 7–15 years)
- From source area 11B, between 0.008 and 0.017 average expected slope collapse deaths per year (one death every 60–130 years).

For the lower source volumes, the aggregate rate for source area 11A reduces to zero, while that for source area 11B reduces by less than 1%. In all cases (source areas 11A or 11B, any source volume) the casualties are dominated by car occupants (over 80% of all deaths), because the very large numbers of car users outweighs the higher individual risk for more vulnerable road users (cyclists and pedestrians). Taking both sources in combination, the aggregate range of expected deaths per year is estimated to lie in the range:

- 0.008–0.017 for lower source volume assumptions; up to
- 0.08 (=0.008 + 0.07)–0.16 (= 0.14 + 0.017) for upper source volume assumptions.

This corresponds to a range from one fatality in about 130 years up to 1 in 6 years resulting from slope collapse.

6.0 DISCUSSION

6.1 DWELLING OCCUPANT RISK

Important points of note from the results of the hazard and risk assessment undertaken in this study include:

Source areas 11A

1. The risk associated with source area 11A affects the greatest number of dwellings in the area.
2. The annual frequency of the event that could trigger the earth/debris flow is not known, or indeed whether such events could be triggered. However, a 50-year return period (annual frequency of 0.02) has been assumed after considering the uncertainties associated with the fill/loess shear strength parameters and how these may degrade over time.

Source area 11B

The results from the risk assessment, taking into account the debris avalanche hazard assessed in this report, have only increased the level of risk at the dwellings that were already within the original cliff collapse risk areas presented by Massey et al. (2012a). No additional dwellings are within the revised risk zones.

Source area 11C

The annual frequency of the event that could trigger the earth/debris flow (source area 11C) is not known, or indeed whether such events could be triggered. However, a 50-year return period (annual frequency of 0.02) has been assumed after considering the uncertainties associated with the fill/loess shear strength parameters and how these may degrade over time.

Source area 11E

1. There is no site-specific information relating to this abandoned quarry slope, and therefore the levels of risk are uncertain. Geotechnical reports (carried out by Coffeys Ltd. (Harwood, 2011, 2013) provided to GNS Science by Christchurch City Council, indicate that some debris fell from the rock slope during the 22 February 2011 earthquakes, and minor falls of rock and debris had occurred between April 2011 and December 2013 (Harwood, 2011, 2013). Consultants working for the Earthquake Commission confirmed that fallen debris had been removed from behind the dwelling at the toe of the quarry (S. Wallace, personal communication 2014).
2. Given the past performance of the slope and its similarities (height, slope angle and material types) to the slopes assessed by Massey et al. (2012a), it is appropriate to apply the empirical risk model from Massey et al. (2012a) to this slope.
3. There is a dwelling, at the cliff toe, where the rear of the dwelling is in part located within the annual individual fatality risk zone of greater than 10^{-2} , and the front of the dwelling, furthest away from the cliff, is in the 10^{-5} annual individual fatality risk zone.

4. At the slope crest there is a dwelling, which is in part within the 2nd and 3rd earthquake events lines. These lines represent the possible maximum recession position of the cliff edge in future earthquakes with associated peak ground accelerations in the 1–2 g (or greater) range. These lines do not mean that the cliff will fail along its entire length, but that any place along the cliff could fail back to this line given a future event of this magnitude.

6.2 ROAD USER RISK

Source areas 11A and 11B are the only source areas putting users of the Main Road at risk (the Main Road route includes much of the infrastructure that services the urban areas from St Andrews Hill to Scarborough). The two source areas are very different in their characteristics, in particular in their sensitivity to the volumes of slope material assumed to collapse and to the distance the debris travels across the road. Summary findings include:

1. Source area 11A produces risk for road users 5–10 times that of source area 11B for the upper source volumes assessed. However, this drops to zero for the lower volumes assessed, whereas the risk for source area 11B alters by less than 1% between the upper and lower volume scenarios.
2. Risk tapers off with distance from the slope more rapidly for source area 11B than for source area 11A. For source area 11B, risk is barely above zero on the far side of the road, whereas for source area 11A it is about half that on the near-slope (southern) side of the road.
3. For source area 11A (upper volume assumptions) the individual risk per journey or per year from slope collapse is substantially higher than the risk from motor vehicle crashes for all motor vehicles and pedestrians, and is comparable for cyclists but is substantially lower than the crash risk for motorcyclists. For lower volume assumptions the risk is zero for all road users.
4. For source area 11B (any volume assumptions) the individual risk per journey or per year from slope collapse on the near-slope (southern) side of the road is significantly higher than the corresponding motor vehicle crash risk for the same journeys for bus and truck occupants. The risk for car occupants, cyclists and pedestrians is comparable with the crash risk, while that for motorcyclists is significantly lower than the corresponding crash risk. On the northern (seaward) side of the road the risk for all road users is approximately zero.
5. The aggregate risk for all road users from both sources is estimated in terms of average expected number of deaths per year to lie in the range 0.008 up to 0.016 (about one death in 130 years up to 1 death in 6 years) for both sources combined, depending on the failure volume and trigger frequency assumptions used.

6.3 ANNUAL FREQUENCY OF THE EVENT

6.3.1 Source areas 11A and 11C (earth/debris flows)

The frequency of occurrence of the events that could trigger the assessed failure volumes is unknown. Future earth/debris flows at these sites could be more frequent and occur at lower triggering thresholds (e.g. rainfall magnitudes) than those assumed in the assessment.

Source areas 11A and 11C have already undergone more than 2.6 m and 0.4 m of permanent slope displacement respectively, during the 2010/11 Canterbury earthquakes. This displacement may have reduced the shear strength of critical materials, making the source areas more susceptible to future earthquakes. In addition, there may be an unknown amount of further displacement that each source area may be able to undergo before failing catastrophically (i.e., where the magnitude of displacement causes the failure mass to break down to become a mobile failure). At the current time there is no practical means for estimating the numerical value of the “degraded strength”, of the slope.

No permeability or loess water content measurements have been made at the site and ground water records from measurements of the standpipes within the loess have poor temporal resolution and do not cover a full summer and winter cycle. It is therefore not possible to directly assess whether the earthquake-induced cracks have increased the susceptibility of these sites to future failures. However:

- Loess shear strength is critically dependent on water content, and the fill present at the site appears to be, in part, reworked loess.
- At high water contents the range of shear strengths, derived from ring-shear testing, could feasibly represent the strength of the loess in the slope.
- Under such conditions, results from the numerical slope stability back-analysis indicate that failure of the slope is likely.
- It is more likely that failure would occur through specific zones within the fill, e.g. through more permeable zones where water contents are likely to increase more readily, or above permeability boundaries such as soil fragipans.
- Pore pressure above rockhead and the colluvium, within the fill, as well as pore water pressures within the open cracks would also reduce the slope factor of safety.
- Given the now-cracked nature of the slopes, it is feasible that water contents of the fill could increase in response to rainfall, as water can more readily enter the slope via the cracks and broken services.
- Recent, historic landslides have occurred at the site. Reactivation of the slope (source area 11A) was noted in the winter of 2012 (Yetton and Engel, 2014).
- Based on the field evidence it is reasonable to assume that the return period of the event that could trigger failure of the estimated source volumes is somewhere between >10 years and 200 years; 10 years being the return period of the March 2014 rain event and 200 years being the return period of a significant amount of rain.

6.3.2 Source areas 11B and 11E (cliff collapses)

The annual frequency of the representative earthquake event within each band comes from the National Seismic Hazard Model (Stirling et al., 2012), which are time variable (Gerstenberger et al., 2011). The earthquake models used to estimate the seismic hazard through time are based on GNS Science’s “best knowledge” of the cluster-like behaviour of earthquakes. The estimated hazard is highest in the first years, followed by a rapid fall off as the region moves from what can be considered traditional aftershock clustering. The total number of anticipated earthquakes drops by roughly one order of magnitude within the first 5–10 years (Massey et al., 2012b). To take this into account, the sensitivity of the risk estimates, adopting the year 2016 and the 50-year average (from 2012) annual frequencies, were assessed.

6.4 RISK ASSESSMENT SENSITIVITY TO UNCERTAINTIES

In this section, the sensitivity of the risk models for source areas 11A, 11B and 11C, to key uncertainties and reliability of the assessments are discussed. The sensitivity of the risk model used for source area 11E is discussed by Massey et al. (2012a).

The sensitivity of the estimated risk has been assessed to the following risk-contributing factors:

6.4.1 Source volumes

The volumes of debris avalanches and earth/debris flows that could be triggered in future events. This was done by comparing the three volume ranges which account for variation in the likely source volumes. The three volume ranges also took into account variability in the debris runout velocities and inundation heights, as larger volumes of debris tend to travel further down slope at higher velocities.

- Source area 11A: there are quite large differences between the positions of the 10^{-4} annual individual fatality risk contours between the modelled lower and upper source volumes (Figure 40, Map 1). However, the numbers of dwellings inside the 10^{-4} risk contours only reduce by one, between the middle and lower source volume estimates).
- Source area 11B: there is little difference in the position of the 10^{-4} risk contour between the upper and lower volumes (Figure 40, Map 3), indicating that variations in the source volume have a very limited effect on the risk, as the debris does not tend to runout very far – a function of the granular nature of the rock dominated debris.
- Source area 11C: there are quite large differences between the positions of the 10^{-4} annual individual fatality risk contours between the modelled lower and upper source volumes (Figure 40, Map 1). However these changes do not affect the number of dwellings within the greater than 10^{-4} risk zone.

6.4.2 Annual frequency of the triggering event

Changes to the annual frequency of the event that could trigger failure of source areas:

- Source areas 11A and 11C: Risk models were run adopting event annual frequencies of 0.05, 0.02, 0.01 and 0.005, corresponding to return periods of 20, 50, 100 and 200 years respectively, for the upper source volume estimates.
 - a. Results from the assessment show that there is little change between the risk results adopting the 20-year and 100-year return periods. The risk at the dwellings in the greater than 10^{-4} annual individual fatality risk zone decreases by a factor of about 2 (for a return period from 50 to 100 years).
 - b. For return periods greater than 100 years, the greater than 10^{-4} annual individual fatality risk zone reduces incrementally back up slope towards the toe of the source areas. This has little effect for source area 11C as there is only one dwelling at the base of the slope. For source area 11A this reduces the area covered by the greater than 10^{-4} risk zone, but the risk at the dwellings in the zone only reduces by a factor of about 4 (for a return period from 50 to 200 years).
 - c. For return periods of less than 50 years, the greater than 10^{-4} annual individual fatality risk zone increases marginally, and the risk at the dwellings increases by a factor of 2–3 (for a return period from 50 to 20 years).

- d. Source area 11B: the risk model was run adopting the 50-year average annual frequencies from the probabilistic National Seismic Hazard Model for the representative earthquake events in each band. The risk estimates reduce by a factor of 2.2 from adopting the year 2016 estimates to the 50-year average estimates.

6.4.3 Other key uncertainties

- Vulnerability: the probability of death is a function of debris height and velocity. The risk assessment may not adequately take into account the sheltering effect of buildings. Variable vulnerabilities have been adopted linked to debris velocity. However, the vulnerability of a person in a dwelling is related to the nature of the structure, for which there is no New Zealand specific data available for use in the risk assessment. It is possible that the risk could reduce by an order of magnitude or more if the dwelling could withstand inundation by debris without collapsing. This could have a large effect on the risk especially in the distal run out zones where the debris is travelling at lower velocity.
- Changing the probability of failure ($P_{FAILURE}$) of source area 11B in an earthquake from $P_{FAILURE} = 0$ at permanent coseismic displacements of 0.1 m or less, to $P_{FAILURE} = 0$ at 0.3 m of displacement or less. The risk estimates would reduce by a factor of 1.2. Conversely, if $P_{FAILURE} = 0$ at 0 m of displacement the risk would increase by a factor of about 1.1 and if $P_{FAILURE} = 1$ at 0.5 m of displacement, the risk would increase by a factor of about 1.4. These results suggest the risk is insensitive to changes in the probability of failure.

6.4.4 How reliable are the results?

The results (Maps 1–4 in Figure 40) show that largest impact on the risk is from the volumes of material that could be generated in an event, and secondly from the annual frequency of the event that could trigger them.

These uncertainties have little impact on the risk associated with source area 11B as the largest contribution to the risk is from the smaller cliff collapses represented by those in the risk model presented by Massey et al. (2012a). Therefore any reduction in the annual frequencies of the event that could trigger failure of source area 11B would have little impact on the risk.

For source areas 11A and 11C (the earth/debris flows) the uncertainties combine to give slightly more than an order of magnitude uncertainty, in either direction, on the risk estimates. It is therefore possible that the dwellings within the 10^{-4} uncertainty zone are at levels of risk that are less than 10^{-5} , but conversely could be as high as 10^{-3} . Those dwellings in the greater than 10^{-4} risk zone (all source volume estimates), could still be at relatively high levels of risk (10^{-4} or greater) even if the uncertainties are taken into account.

For source areas 11B and 11E (the cliff collapses) the uncertainties combine to give slightly less than an order of magnitude uncertainty, in either direction, on the risk estimates.

Potentially significant uncertainties noted and their likely implications for risk are summarised in Table 17. The sensitivity results are reported in Table 17 as “factors” of 2, 3 etc. These factors represent the estimated variability in the risk value for the given issue. Given that the risk is quoted in numbers of 10^{-4} etc., a factor of 10, would relate to an-order-of magnitude variability, where a risk of 10^{-4} could be 10^{-3} or 10^{-5} .

Table 17 Uncertainties and their implications for risk.

Issue	Direction and scale of uncertainty	Implications for risk
Earth/debris flows (source areas 11A and C)		
a. Choice of whether to use different event annual frequencies other than 0.02 (50-year return period).	Moderate uncertainty between the use of the 50-year and 100-year, return periods. But larger uncertainty between the 50 year and 20 year plus return periods and 50-year and 200-year, return periods.	Longer term risk is potentially 2–4 times lower, but shorter term risk could be 2–3 times higher.
b. Volume of debris produced by a source area.	Largest uncertainty between upper volume and the lower volume, and then the lower volume and middle volume.	About a factor of 6–7 between the upper and lower volume estimates. But a factor of 4 between the lower and middle estimates, and a factor of 2 between the middle and upper estimates.
c. Changing the assumed debris height where probability of inundation = 0 from 0.3 m–0.5 m and 0.1 m.	Small uncertainty in either direction.	Would change modestly by a factor of about 1.2 in either direction.
d. Occupancy (proportion of time people are at home)	Assumption of 100% occupancy instead of 67% would modestly increase the estimated risk.	Would increase modestly by a factor of about 2.
e. Vulnerability (probability of being killed if inundated by debris).	Variable vulnerabilities have been adopted linked to debris velocity. However, the vulnerability of a person in a dwelling is related to the nature of the structure, for which there is no data available for use in the risk assessment. Potentially large uncertainty in either direction but very difficult to quantify.	Could be relatively large depending on the nature of the dwelling construction and age/ability of the person to get out of the way of the debris.
Debris avalanche (source area 11B)		
a. Choice of whether to use different earthquake event annual frequencies from year 2016 to 50-year average.	Moderate uncertainty between the use of the year 2016 and 50-year average earthquake event frequencies.	Longer term risk is potentially 2–3 times lower.
b. Volume of debris produced by the source area.	Largest uncertainty between scenarios.	A factor of about 4 in either direction.

Issue	Direction and scale of uncertainty	Implications for risk
c. Changes to the probability of failure of each source area adopting PFAILURE = 0 = displacement of 0.3 m, and PFAILURE = 1 = 0.5 m of displacement.	Small uncertainty in either direction.	Would decrease by a factor of 1.2 but could increase by a factor of 1.4.
d. Changing the assumed debris height where probability of inundation = 0 from 0.1 m–0.3 m and 0.1 m.	Small uncertainty in either direction.	Would change modestly by a factor of about 1.1 in either direction.
e. Occupancy (proportion of time people are at home).	Assumption of 100% occupancy instead of 67% would modestly increase the estimated risk.	Would increase modestly by a factor of about 2.
f. Vulnerability (probability of being killed if inundated by debris).	Assumption of 100% instead of 70% would modestly increase the estimated risk.	Would increase modestly by a factor of about 2. Dwelling construction and age/ability of the person to get out of the way of the debris have a significant effect on the risk could be factors of 10 or more in the downward direction.

7.0 CONCLUSIONS

With reference to source area boundaries as show in Figure 2, the conclusions of this report are:

7.1 HAZARD

1. There is potential for volumes ranging from several hundreds to thousands of cubic metres of:
 - a. Earth/debris flows (source areas 11A and 11C) of mixed soil, mainly fill (re-worked loess); and
 - b. Cliff collapses of mixed soil and rock, mainly rock (source areas 11B and 11E), which are potentially larger than those cliff collapse failures previously assessed at the site (Massey et al., 2012a).
2. The most likely triggers for these newly identified landslide sources are earthquake ground shaking for the cliff collapses and prolonged heavy rainfall for the earth/debris flows.
3. The frequency of landslide events from these sources is difficult to estimate and could be anything from once in a few tens to once in many hundreds of years.

7.2 Risk

7.2.1 Dwelling occupant

1. Source area 11A: The risk associated with this earth/debris flow hazard affects the greatest number of dwellings, where the annual individual fatality risks are assessed as being 10^{-4} or greater, for some of these dwellings.
2. Source area 11B: The results from the risk assessment, taking into account the cliff collapse hazard assessed in this report, have increased the level of risk (from cliff-top recession) to an annual individual fatality risk of greater than 10^{-4} , at the dwelling that was already within the original cliff-top recession risk area (Massey et al., 2012a).
3. Source area 11C: The hazard associated with this earth/debris flow affects dwellings at the slope crest and at the toe, where the annual individual fatality risks are greater than 10^{-4} .
4. Source area 11E: The hazard associated with this debris avalanche affects a dwelling at the cliff toe, where the risk is assessed as being greater than 10^{-4} .

7.2.2 Road user

1. Source areas 11A and 11B are the only sources putting users of the road (Main Road, one of Christchurch's busiest lifeline routes) at risk.
2. Source area 11A (upper source volume assumptions): the individual risk per journey or per year from earth/debris flows is substantially higher than the risk from motor vehicle crashes for all motor vehicles and pedestrians. The risk is similar for cyclists but is substantially lower than the crash risk for motorcyclists.

3. Source area 11B (for any assessed source volume assumptions): the individual risk per journey or per year from debris avalanches onto the southern side of the road (closer to the slope) is significantly higher than the corresponding motor vehicle crash risk for the same journeys for bus and truck occupants. The risk is comparable to the crash risk for car occupants, cyclists and pedestrians, but is significantly lower than the corresponding crash risk for motorcyclists. The risk falls rapidly with distance from the slope, reaching zero on the far (seaward) side of the road.

7.2.3 Risk management

1. A risk-management option of monitoring rainfall, soil moisture and pore-pressure in the source areas, may be of some value in providing warning of conditions approaching critical levels, but:
 - a. Such early warning could not be assured, as experience in the Port Hills and elsewhere is that water levels in open tension cracks can rise very rapidly to critical values.
 - b. There would be little time to evacuate potentially at-risk residents given the rapid nature of the hazard.
 - c. There is currently no precedent data for rates of change of groundwater or water content of loess to provide reliable alert criteria.
2. It should be noted that slope material strengths, and thus factors of safety, may be expected to deteriorate with time, weathering and any further earthquakes.

8.0 RECOMMENDATIONS

GNS Science recommends that based on the results of this study, Christchurch City Council:

8.1 POLICY AND PLANNING

1. Decide what levels of life risk to dwelling occupants will be regarded as tolerable.
2. Decide how Council will manage risk on land and roads where life risk is assessed to be at the defined threshold of intolerable risk and where the level of risk is greater than the threshold.
3. Prepare policies and other planning provisions to address risk lesser than the intolerable threshold in the higher risk range of tolerable risk.

8.2 SHORT-TERM ACTIONS

8.2.1 Hazard monitoring strategy

1. Include the report findings in a slope stability monitoring strategy with clearly stated aims and objectives, and list how these would be achieved, aligning with the procedures described by McSaveney et al. (2014). In the meantime, establish a survey network on the slope (particularly on source area 11A), so as to maintain awareness of changes in the behaviour of the slope.
2. Ensure that the existing emergency management response plan for the area identifies the dwellings that could be affected by movement and runout, and outlines a process to manage a response.

8.2.2 Risk monitoring strategy

Monitoring the slope for early warning of potentially dangerous trends in groundwater or slope movement as part of a hazard warning system, is not recommended as it is currently not thought to be feasible. Monitoring alerts for slope deformation and groundwater changes cannot be relied upon to provide adequate early warning as experience from Port Hills and elsewhere shows that deformation and groundwater changes can occur rapidly, with little warning, and there is little site-specific information on which to build such a warning system.

8.2.3 Surface/subsurface water control

Reduce water ingress into the slopes, where safe and practicable to do so, by:

- a. Identifying and relocating all water-reticulation services (water mains, sewer pipes and storm water) inside the identified mass-movement boundaries to locations outside the boundary, in order to control water seepage into the slope. In particular, a sewer main currently crosses the edge of source area 11A, and should if possible be relocated away from this area; and
- b. Control surface water seepage by filling the accessible cracks on the slope and providing an impermeable surface cover to minimise water ingress. However, it is not thought that such works alone are sufficient to reduce the risk.

8.3 LONG-TERM ACTIONS

8.3.1 Engineering measures

Assess the cost, technical feasibility and effectiveness of alternative longer term engineering and relocation solutions, for example (but not limited to):

- a. Removal/stabilisation of the slopes in the assessed source areas;
- b. Installation of drainage works;
- c. Relocation of houses to alternative locations within existing property boundaries;
- d. Withdrawal and rezoning of the land for non-residential use; or
- e. Any proposed engineering works would require a detailed assessment and design and be carried out under the direction of a certified engineer, and should be independently verified in terms of their risk reduction effectiveness by appropriately qualified and experienced people.

8.3.2 Reassessment

Reassess the risk and revise and update the findings of this report in a timely fashion, for example:

- a. in the event of any changes in ground conditions; or
- b. in anticipation of further development or land use decisions.

9.0 REFERENCES

- Andres, N. 2010. Unsicherheiten von Digitalen Geländemodellen und deren Auswirkungen auf die Berechnung von Gletscherseeausbrüchen mit RAMMS (Dr. R. Purves, D. Schneider, Dr. C. Huggel).
- Ashford, S.A., Sitar, N. 2002. Simplified method for evaluating seismic stability of steep slopes. *Journal of Geotechnical and Geoenvironmental Engineering* 128: 119–128.
- Australian Geomechanics Society 2007. Practice note guidelines for landslide risk management. *Journal and News of the Australian Geomechanics Society* 42(1): 63–114.
- Bell, D.H., Glassey, P.J., Yetton, M.D. 1986. Chemical stabilisation of dispersive loessical soils, Banks Peninsula, Canterbury, New Zealand. *Proceedings of the 5th International Congress of the International Engineering Geological Society* 1: 2193–2208
- Bell, D.H., Trangmar, B.B. 1987. Regolith materials and erosion processes on the Port Hills, Christchurch, New Zealand: Fifth International Symposium and Field Workshop on Landslides. Lausanne, A.A. Balkema. Volume 1: 77–83.
- Bray, J.D., Rathje, E.M. 1998. Earthquake-induced displacements of solid-waste landfills. *Journal of Geotechnical and Geoenvironmental Engineering* 124: 242–253.
- Bray, J.D., Travasarou, T. 2007. Simplified procedure for estimating earthquake-induced deviatoric slope displacements. *Journal of Geotechnical Engineering and Environmental Engineering*. DOI: 10.1061/(ASCE)1090-0241(2007)133:4(381)
- California, State of. 1977. Analysis and Mitigation of Earthquake-Induced Landslide Hazards, Guidelines for Evaluation and Mitigation of Seismic Hazards in California, Division of Mines and Geology, California Department of Conservation Special Publication 117, Chapter 5, 15 p.
- Carey, J., Misra, S., Bruce, Z., Barker, P. 2014. Canterbury Earthquakes 2010/11 Port Hills Slope Stability: Laboratory testing factual report. GNS Science Consultancy Report CR2014/53.
- Choi, W.K. 2008. Dynamic properties of Ash-Flow Tuffs. PhD Thesis, The University of Texas at Austin.
- Chopra, A.K. 1966. Earthquake effects on dams. PhD Thesis, University of California, Berkeley.
- Craig, R.F. 1997. *Craig's Soil Mechanics*, 6th Edition, Spon Press, London.
- Corominas J. 1996. The angle of reach as a mobility index for small and large landslides. *Canadian Geotechnical Journal* 33: 260–271.
- Corominas, J. Copons, R., Moya, J., Vilaplana, J. M., Altimir, J., Amigo, J. 2005. Quantitative assessment of the residual risk in a rockfall protected area. *Landslides* 2: 343–357. DOI:10.1007/s10346-005-0022-z.
- Cruden, D.M., Varnes, D.J. 1996. Landslide types and processes. *Landslide: investigation and mitigation*. Turner, K.A., Schuster, R.L. (eds.). Special report, Transportation Research Board, National Research Council 247, Chapter 3, 36–75.
- Dawson, E.M., Roth, W.H., Drescher, A. 1999. Slope stability analysis of by strength reduction. *Geotechnique* 122(6): 835–840.
- Del Gaudio, V., Wasowski, J. 2010. Advances and problems in understanding the seismic response of potentially unstable slopes. *Engineering Geology*, doi:10.1016/j.enggeo.2010.09.007.

- Della Pasqua, F., Massey, C.I., Lukovic, B., Ries, W., Archibald, G. 2014. Canterbury Earthquakes 2010/11 Port Hills Slope Stability: Earth/Debris flow risk assessment for Defender Lane. GNS Science Consultancy Report 2014/67.
- Du, J., Yin, K., Nadim, F., Lacaqsse, S. 2013. Quantitative vulnerability estimation for individual landslides. Proceedings of the 18th International Conference on Soil Mechanics and Geotechnical Engineering, Paris 2013. pp. 2181–2184.
- Eurocode 8. EN1998-5. 2004. Design of structures for earthquake resistance Part 5: Foundations, retaining structures and geotechnical aspects.
- Finlay, P.J., Mostyn, G.R., Fell, R. 1999. Landslides: Prediction of Travel Distance and Guidelines for Vulnerability of Persons. Proceedings of the 8th Australia New Zealand Conference on Geomechanics, Hobart. Australian Geomechanics Society, ISBN 1 86445 0029, Vol 1, pp.105–113.
- Geotechnics Ltd. 2014. GNS Science, Port Hills Inclinometers, Christchurch. Job No. 720085.001/REP.
- Gerstenberger, M., Cubrinovski, M., McVerry, G., Stirling, M., Rhoades, D., Bradley, B., Langridge, R., Webb, T., Peng, B., Pettinga, J., Berryman, K., Brackley, H. 2011. Probabilistic assessment of liquefaction potential for Christchurch in the next 50 years. GNS Science Report 2011/15.
- Goldwater, S. 1990. Slope failure in loess. A detailed investigation, Allendale, Banks Peninsula. MSc Thesis, University of Canterbury.
- Griffiths, G., Pearson, C., McKerchar, A.I. 2009. Review of the frequency of high intensity rainfalls in Christchurch. NIWA Client Report: CHC2009-139 for Christchurch City Council. 26 pp.
- Harwood, N. 2011. Geotechnical Walkover Inspection at 11A Te Awakura Terrace, Mt Pleasant. Coffey Geotechnical Report, April 2011. GENZCHR15098_11A Te Awakura Terrace, Mount Pleasant.
- Harwood, N. 2013. Geotechnical Walkover Inspection at 11A Te Awakura Terrace, Mt Pleasant. Coffey Geotechnical Report, December 2013. GENZCHR15635AA.
- Hoek, E. 1999. Putting Numbers to Geology – an Engineer’s Viewpoint. The Second Glossop Lecture, Quarterly Journal of Engineering Geology 32(1): 1–19.
- Holden, C., Kaiser, A., Massey, C.I. 2014. Broadband ground motion modelling of the largest M5.9+ aftershocks of the Canterbury 2010–2011 earthquake sequence for seismic slope response studies. GNS Science Report 2014/13.
- Hynes-Griffin, M.E., Franklin, A.G. 1984. Rationalizing the seismic coefficient method. Miscellaneous Paper No. G.L. 84-13, U.S. Army Engineer Waterways Experiment Station, Vicksburg, Mississippi.
- Ishibashi, I., Zhang, X. 1993. Unified dynamic shear moduli and damping ratios of sand and clay. Soils and Foundations 3(1): 182–191.
- Jibson, R.W. 2007. Regression models for estimating coseismic landslide displacement. Engineering Geology 91: 209–218.
- Jibson, R.W., Keefer, D.K. 1993. Analysis of the seismic origin of landslides: Examples from the New Madrid Seismic Zone. Geological Society of America Bulletin 21: 521–536.
- Keefer, D.K., Wilson, R.C. 1989. Predicting earthquake-induced landslides, with emphasis on arid and semi-arid environments. Proceedings of Landslides in a Semi-Arid Environment, Vol. 2, Inland Geological Society, Riverside, California, pp. 118–149.
- Keylock, D., Domaas, U. 1999. Evaluation of topographic models of rockfall travel distance for use in hazard applications. Antarctic and Alpine Research 31(3): 312–320.

- Kim, J., Jeong, S., Park, s., Sharma, J. 2004 Influence of rainfall-induced wetting on the stability of slopes in weathered soils. *Engineering Geology* 75: 251–262.
- Kramer, S.L. 1996. *Geotechnical earthquake engineering*. Prentice Hall, Upper Saddle River, New Jersey.
- Larsen, I.J., Montgomery, D.R., Korup, O. 2010. Landslide erosion controlled by hillslope material. *Nature Geoscience* 3: 247–251.
- Makdisi, F.I., Seed, H.B. 1978. Simplified procedure for evaluating embankment response. *Journal of Geotechnical Engineering Division. American Society of Civil Engineers* 105(GT12): 1427–1434.
- Massey, C.I., Carey, J. 2012. Preliminary hazard assessment for Lucas Lane, Christchurch. GNS Science Letter Report CR2012/268LR.
- Massey, C., Della Pasqua, F. 2014. Canterbury Earthquakes 2010/11 Port Hills Slope Stability: Working Note 2013/09 on the interim findings from investigation of the Quarry Road mass movement. GNS Science Letter Report 2014/09LR.
- Massey, C.I., McSaveney, M.J., Heron, D. 2012a. Canterbury earthquakes 2010/11 Port Hills Slope Stability: Life-safety risk from cliff collapse in the Port Hills. GNS Science Consultancy Report 2012/124.
- Massey, C.I., Gerstenberger, M., McVerry, G., Litchfield, N. 2012b. Canterbury Earthquakes 2010/11 Port Hills Slope Stability: Additional assessment of the life-safety risk from rockfalls (boulder rolls). GNS Science Consultancy Report 2012/214.
- Massey, C.I., McSaveney, M.J., Heron, D., Lukovic, B. 2012c. Canterbury Earthquakes 2010/11 Port Hills Slope Stability: Pilot study for assessing life-safety risk from rockfalls (boulder rolls). GNS Science Consultancy Report 2011/311.
- Massey, C.I., Yetton, M.J., Carey, J., Lukovic, B., Litchfield, N., Ries, W., McVerry, G. 2013. Canterbury Earthquakes 2010/11 Port Hills Slope Stability: Stage 1 report on the findings from investigations into areas of significant ground damage (assessed source areas). GNS Science Consultancy Report 2012/317.
- Massey, C.I., Taig, T., Della Pasqua, F., Lukovic, B., Ries, W., Archibald, G. 2014. Canterbury Earthquakes 2010/11 Port Hills Slope Stability: Debris avalanche risk assessment for Richmond Hill. GNS Science Consultancy Report 2014/34.
- McDowell, B.J. 1989. Site investigations for residential development on the Port Hills, Christchurch. MSc Thesis, University of Canterbury.
- McSaveney, M.J., Litchfield, N., Macfarlane, D. 2014. Canterbury Earthquakes 2010/11 Port Hills Slope Stability: Criteria and procedures for responding to landslides in the Port Hills, GNS Science Consultancy Report 2013/171.
- Morgenstern, N.R., Price, V.E. 1965. The analysis of the stability of general slip surface. *Geotechnique* XV(1): 79–93.
- Newmark, N. 1965. Effects of earthquakes on dams and embankments. *Geotechnique* 15: 139–160.
- New Zealand Transport Agency (NZTA), 2013. Bridge manual (SP/M/022). 3rd edition. July 2013.
- Page, M.J. 2013. Landslides and debris flows caused by the 15–17 June 2013 rain storm in the Marahau–Motueka area, and the fatal landslide at Otuwhero Inlet. GNS Science Report 2013/44. 35p.
- RAMMS 2011. A modelling system for debris flows in research and practice. User manual v1.4 Debris Flow. WSL Institute for Snow and Avalanche research SLF.

- Schanbel, P.B., Lysmer, J. Seed, H.B. 1972. SHAKE; a computer program for earthquake response analysis of horizontally layered sites. Report No. EERC 72-12, University of California, Berkeley.
- Slope Indicator 2005. Digitilt inclinometer probe. Data sheet. Geo Slope Indicator. <http://www.slopeindicator.com/pdf/digitilt-vertical-inclinometer-probe-datasheet.pdf>
- Slope/W 2012. Stability modelling with Slope/W. An engineering methodology. November 2012 Edition. GEO-SLOPE International Ltd.
- Southern Geophysical Ltd., 2013. Geophysical investigation: Borehole shear-wave testing, Port Hills, Christchurch. Southern Geophysical Ltd. Report for GNS Science.
- Stirling, M., McVerry, G., Gerstenberger, M., Litchfield, N., Van Dissen, R., Berryman, K., Barnes, P., Wallace, L., Bradley, B., Villamor, P., Langridge, R., Lamarche, G., Nodder, S., Reyners, M., Rhoades, D., Smith, W., Nicol, A., Pettinga, J., Clark, K., Jacobs, K. 2012. National Seismic Hazard Model for New Zealand: 2010 Update. Bulletin of the Seismological Society of America 102: 1514–1542.
- Taig, T., Massey, C. 2014. Canterbury Earthquakes 2010/11 Port Hills Slope Stability: Estimating rockfall (boulder roll) risk for the road user along part of Wakefield Avenue. GNS Science Consultancy Report 2013/30.
- Tonkin and Taylor 2012a. Christchurch Earthquake Recovery Geotechnical Factual Report Defender Hill. Report prepared for the Earthquake Commission. Ref 52010.0400.
- Tonkin and Taylor 2012b. Christchurch Earthquake Recovery Geotechnical Factual Report Kinsey / Clifton. Report prepared for the Earthquake Commission. Ref 52010.0400.
- Tonkin and Taylor 2012c. Christchurch Earthquake Recovery Geotechnical Factual Report Vernon / Rapaki. Report prepared for the Earthquake Commission. Ref 52010.0400.
- Tonkin and Taylor 2012d. Christchurch Earthquake Recovery Geotechnical Factual Report Maffey's / LaCosta. Report prepared for the Earthquake Commission. Ref 52010.0400.
- Tonkin and Taylor 2012e. Christchurch Earthquake Recovery Geotechnical Factual Report Balmoral / Glendever. Report prepared for the Earthquake Commission. Ref 52010.0400
- Townsend, D.B., Rosser, B. 2012. Canterbury Earthquakes 2010/2011 Port Hills slope stability: Geomorphology mapping for rockfall risk assessment. GNS Science Consultancy Report 2012/15.
- Wartman, J., Dunham, L., Tiwari, B., Pardel, D. 2013. Landslides in eastern Honshu induced by the 2011 Tohoku Earthquake. Bulletin of the Seismological Society of America 103: 1503–1521, doi: 10.1785/0120120128.
- Wieczorek, G.F., R.C. Wilson, Harp, E.L. 1985. Map showing slope stability during earthquakes in San Mateo County, California. Miscellaneous Investigations Map I-1257-E, U.S. Geological Survey.
- Yetton, M.D. 1992. Engineering Geological and geotechnical factors affecting development on Banks Peninsula and surrounding areas – Field guide. Bell, D.H. (ed.): Landslides - Proceedings of the Sixth International Symposium, Christchurch, 10–14 February 1992, Rotterdam, A.A. Balkema, Vol. 2(3).
- Yetton, M., Engel, M. 2014. Port Hills Land Damage Studies Quarry Road Field Investigations. URS Limited report for Christchurch City Council.

10.0 ACKNOWLEDGEMENTS

GNS Science acknowledges: Mark Yetton (Geotech Consulting Ltd.) for advice during the assessment. The authors also thank Nicola Litchfield, Mauri McSaveney, Danielle Mieler, and Rob Buxton (GNS Science) for reviewing this report; and Dr Laurie Richards and Dr Joseph Wartman for their independent reviews.

APPENDICES

A1 APPENDIX 1: METHODS OF ASSESSMENT

A1.1 ENGINEERING GEOLOGY ASSESSMENT METHODOLOGY

The findings presented in this report are based on engineering geological models of the site developed by URS New Zealand Ltd. (Yetton and Engel, 2014), in consultation with GNS Science. The Christchurch City Council engaged URS New Zealand Ltd. (hereafter referred to as URS Ltd.), to provide further geotechnical data to allow GNS Science to fully assess any potential life risks and lifeline impacts from assessed source area at Quarry Road. The URS Ltd. work commenced in mid-August 2013 and results were delivered to GNS Science in October–November 2013. The final report is contained in Appendix 1.

The scope of the URS Ltd. investigation works comprised: 1) engineering geological and geomorphological mapping of the site at a scale of 1:1000; 2) construction of four cross-sections through the site area at a scale of 1:500; 3) interpretation of aerial photographs ranging from 1946–2011; and 4) assessment of available LiDAR data for the site and the construction of a digital terrain model. Other investigations included review and assessment of movement monitored since 6 June 2013 to present (by M. Yetton at the request of Christchurch City Council).

Subsurface investigations carried out by URS Ltd. also included:

- Four cored drillholes at source area 11A (drillholes QR1, QR2 and QR3) and source area 11B (drillhole QR4).
- Piezometers were installed in drillholes QR1, QR2 and QR3.
- Inclinometers were installed in drillholes QR1, QR2 and QR4.

A1.2 HAZARD ASSESSMENT METHODOLOGY

The purpose of the hazard assessment was to assess the likelihood of failure under:

1. static (non-earthquake) conditions (e.g. rain); and
2. dynamic (earthquake) conditions.

The hazard assessment method followed three steps:

Step 1 comprises assessment of the static stability of the slope under non-earthquake (static) conditions, and an assessment of the dynamic (earthquake) stability of selected cross-sections to determine how likely debris avalanches and earth/debris flows are, and whether these can/cannot be triggered under static and/or dynamic conditions.

Step 2 uses the results from step 1 to define the likely failure geometries (source areas) of potential failures, which are combined with the crack patterns and slope morphology and engineering geology mapping to estimate their likely volume. Three volumes are defined for each source area (upper, middle and lower volumes), which represent the range of uncertainties on the estimated dimensions of the potential source areas.

Step 3 models: 1) the distance the debris travels down the slope (runout); and 2) the volume of debris passing a given location, should the failure occur. Modelling is done for each source area, and for the upper, middle and lower volume estimates.

The results from this characterisation are then used in the risk assessment.

A1.2.1 Slope stability modelling

The key output from the static stability assessment is a factor of safety of the given volume, while the key output from the dynamic assessment is the magnitude of permanent slope displacement expected at given levels of earthquake-induced ground acceleration. These two assessments are then used to determine the likely volumes of material that could be generated under the different conditions.

A1.2.1.1 Static slope stability

If a slope has a static factor of safety of one or less, the slope is assessed as being unstable. Slopes with structures designed for civil engineering purposes are typically designed to achieve a long-term factor of safety of at least 1.5 under drained conditions, as set out in the New Zealand Transport Agency (NZTA) 3rd edition of the bridge manual (NZTA, 2013).

Static assessment of the slope was carried out by limit equilibrium using the Rocscience SLIDE[®] software and the General Limit Equilibrium method (Morgenstern and Price, 1965). The failure surfaces were defined using the path search feature in the SLIDE[®] software, and a zone of tension cracks was modelled corresponding to mapped crack locations on the surface and in exposures. As the depth of tension cracks is unknown, the simulated tension cracks depth was defined based on the relationship of Craig (1997), in order to satisfy the thrust line verification method in the numerical model.

Models were run on selected cross-sections and the critical slide surfaces were determined as those which resulted in the lowest calculated factor of safety. Probabilistic and sensitivity analyses were run assuming a range of geotechnical material strength parameters based on the estimates of their strength to test model sensitivity. These were derived from in-house laboratory testing on samples of similar materials taken from other sites in the Port Hills and published information on similar materials. Strength parameters were also assessed by back-analysis in the limit equilibrium and dynamic analyses.

The finite element modelling adopts the shear strength reduction technique for determining the stress reduction factor or slope factor of safety (e.g. Dawson et al., 1999). Finite element modelling was undertaken on the same cross-sections adopted for the limit equilibrium modelling assessment, using the Rocscience Phase² finite element modelling software. This was done to check the outputs from the limit equilibrium modelling, because the finite element models do not need to have the slide-surface geometries defined.

A1.2.1.2 Dynamic stability assessment

In civil engineering, the serviceability state of a slope is that beyond which unacceptably large permanent displacements of the ground mass take place (Eurocode 8, EN-1998-5, 2004). Since the serviceability of a slope after an earthquake is controlled by the permanent deformation of the slope; analyses that predict coseismic (slope displacement under earthquake loading), slope displacements provide a more useful indication of seismic slope performance than static stability assessment alone (Kramer, 1996).

The dynamic (earthquake) stability of the slope was assessed with reference to procedures outlined in Eurocode 8 (EN-1998-5, 2004) Part 5. For the Quarry Road assessed source areas, the magnitude of earthquake-induced permanent displacements was assessed for selected cross-sections adopting the decoupled method and using different synthetic earthquake time-acceleration histories as inputs.

The decoupled seismic slope deformation method (Makdisi and Seed, 1978) is a modified version of the classic Newmark (1965) sliding block method that accounts for the dynamic response of the sliding mass. The “decoupled” assessment is conducted in two steps: 1) a dynamic response assessment to compute the “average” accelerations experienced by the slide mass (Chopra, 1966); and 2) a displacement assessment using the Newmark (1965) double-integration procedure with the average acceleration time history as the input motion. The average acceleration time history is sometimes expressed as the horizontal equivalent acceleration time history (e.g. Bray and Rathje, 1998), but they are both the same thing. The average acceleration time history represents the shear stress at the base of the potential sliding mass, as it captures the cumulative effect of the non-uniform acceleration profile in the potential sliding mass.

1. Dynamic response assessment steps:

- a. Two-dimensional dynamic site response assessment using Quake/W was carried out adopting synthetic time acceleration histories for the four main earthquakes known to have triggered debris avalanches, cliff-top deformation and cracking in the Port Hills. Modelled versus actual displacements were compared to calibrate the models.
- b. Synthetic free-field rock-outcrop time acceleration histories for the site – at 0.02 second intervals for the 22 February, 16 April, 13 June and 23 December 2011 earthquakes – were used as inputs for the assessment (refer to Holden et al. (2014) for details).
- c. The equivalent linear soil behaviour model was used for the assessment assuming drained conditions, as no permanent water table has, to date, been recorded in the fill slope (11A and 11C) and the rockslope (11B). Strain-dependent shear-modulus reduction and damping functions for the rock materials were based on data from Schanbel et al. (1972) and Choi (2008). At present, GNS Science does not have dynamic test data for the loess of fill – dynamic testing is currently being carried out by GNS Science as part of a research project. Therefore for loess and fill (where the fill is predominantly re-worked loess) the shear modulus and damping ratio functions from Ishibashi and Zhang (1993) were adopted assuming a plasticity index of five (Carey et al., 2014) and variable confining (overburden) stress, based on the overburden thickness of the fill and loess at each cross-section assessed.
- d. Shear wave velocity surveys were carried out by Southern Geophysical Ltd. for GNS Science. These works comprised the surveying of a surface-generated shear wave signal at 2 m intervals between the surface and the maximum reachable depth inside the drillholes. The loess shear wave velocities were then verified against the results from the dynamic *in situ* probing carried out by Tonkin and Taylor (2012a,b,c,d,e) at nearby sites in the Port Hills.

2. Displacement assessment steps:

- a. The dynamic stresses computed with Quake/W – from each input synthetic earthquake time history – were assessed using Slope/W to examine the stability and permanent deformation of the slope subjected to earthquake shaking using a procedure similar to the Newmark (1965) method (detailed in Slope/W, 2012).
- b. For the Slope/W assessment, a range of material strength parameters was adopted for the rock, loess and fill (based on the results from laboratory strength testing, published information and static back-analysis of slope stability), to assess the sensitivity of the modelled permanent deformation to changing material strength.
- c. For each trial slide surface, Slope/W uses the initial stress condition to establish the static strength of the slope and the dynamic stress (from Quake/W) at each time step to compute the dynamic shear stress of the slope and the factor of safety at each time step during the modelled earthquake. Slope/W determines the total mobilised shear arising from the dynamic inertial forces. This dynamically driven mobilised shear is divided by the total slide mass to obtain an average acceleration for a given slide surface at a given time step. This average acceleration response for the entire potential sliding mass represents one acceleration value that affects the stability at a given time step during the modelled earthquake.
- d. For a given trial slide surface Slope/W:
 - i. Computes the acceleration corresponding to a factor of safety of 1.0. This is referred to as the yield acceleration. The critical yield acceleration of a given slide mass is the minimum pseudostatic acceleration required to produce instability of the block (Kramer, 1996). The average acceleration, at each time step, is then calculated for each slide surface.
 - ii. Integrates the area of the average acceleration (of the trial slide mass) versus time graph when the average acceleration is at yield acceleration. From this it then calculates the velocity of the slide mass at each time interval during the modelled earthquake.
 - iii. Estimates the permanent displacement, by integrating the area under the velocity versus time graph when there is a positive velocity.
- e. To calibrate the results, the permanent displacement of the slide mass for a given trial slide surface geometry (for a given cross-section) was compared with crack apertures and survey mark displacements, and also with the geometry and inferred mechanisms of failure that occurred during the 2010/11 Canterbury earthquakes. Those soil strength parameters that resulted in modelled displacements of similar magnitude to the recorded or inferred slope displacements were then used for forecasting future permanent slope displacements under similar earthquakes.

A1.2.1.3 Forecasting permanent slope displacements

To forecast likely displacement of the slope as a result of future earthquakes, the relationship between the yield acceleration (K_y) and the maximum average acceleration (K_{MAX}) was used. Using the results from the decoupled (Slope/W) assessment, the maximum average acceleration (K_{MAX}) was calculated for each selected slide surface (failure mass), from the average acceleration versus time plot – where the average acceleration versus time plot is the response of the given slide mass to the input time history. The decoupled assessment uses the 22 February and 13 June 2011 synthetic earthquake time histories, as inputs (Holden at al., 2014), and the calibrated material strength parameters derived from back-analysis (bullet 2. e. above).

The K_y/K_{MAX} relationship was used to determine the likely magnitude of permanent displacement of a given failure mass – with an associated yield acceleration (K_y) – at a given level of average acceleration within the failure mass (K_{MAX}) (Figure 27 and Figure 28).

Permanent coseismic displacements were estimated for a range of selected trial slide surfaces from each cross-section. These results were then used in the risk assessment to assess the probability of failure of a given range of slide surfaces.

A1.2.2 Estimation of slope failure volumes

The results of the URS Ltd. engineering geological assessments (Yetton and Engel, 2014; Appendix 1) and the slope stability modelling carried out by GNS Science have modified the shapes of the originally identified mass movements, to characterise several potential landslide source areas, in particular:

1. In assessed source areas 11A and 11C there is potential for local failures of loess and fill, particularly in areas where the bulk strength of the slope could be degraded as a result of earthquake-induced cracking.
2. In assessed source areas 11B and 11E there is potential for failure of the rock slope (cliff collapse), where displacement could occur either through the rock mass (11B and 11E) or along a potential weak layer at the base of the slope (11B only).

The most likely locations and volumes of potential failures were estimated based on the numerical analyses, current surveyed displacement magnitudes, material exposures, crack distributions and slope morphology. The purpose of this was to constrain the likely depth, width and length of any future failures. This was done by linking the main cracks and pertinent morphological features, in combination with the width, length and depth of the failure surfaces derived from the finite element and limit equilibrium modelling.

Three failure volumes (upper, middle and lower) were estimated for each potential source area to represent a range of source volumes. The variation in failure volume reflected the uncertainty in the results from the modelling and mapping, e.g. the depth, width and length dimensions.

The credibility of these potential failure volumes was evaluated by comparing them against: 1) the volumes of relict failures recognised in the geomorphology near the site and elsewhere in the Port Hills; 2) historically recorded failures; and 3) the volumes of material lost from the Quarry Road assessed source area slope and other similar slopes, during the 2010/11 Canterbury earthquakes.

There are four main sources of information on historical non-seismic failures for the Port Hills:

1. archived newspaper reports from between 1870 and 1945 (a selection of which is presented in Appendix 2);
2. the GNS Science landslide database, which is “complete” only since 1996;
3. insurance claims made to the Earthquake Commission for landslips which are “complete” only since 1996; and
4. information from local consultants (M. Yetton, Geotechnical Consulting Ltd. and D. Bell, University of Canterbury) which incompletely covers the period from 1968 to present (McSaveney et al., 2014).

A1.2.3 Debris runout modelling

The potential runout of debris from the slope was assessed empirically by the fahrboeschung method and also by numerical modelling.

1. Fahrboeschung method:
 - a. The fahrboeschung model is based on a relationship between topographical factors and the measured lengths of runout of debris (Corominas, 1996). The fahrboeschung^{2F}¹ (often referred to as the “travel angle”) method (Keylock and Domaas, 1999) uses the slope of a straight line between the top of the source area (the crown) and the furthest point of travel of the debris. The analysis is based on failure points starting at the cliff crest.
 - b. The volume of debris/earth flows and debris avalanches passing a given location within the study area is based on an empirical relationship established from a compilation of run out distances from published international and local (in the Port Hills) earth/debris flows and debris avalanches. Two different empirical models were used based on the dominant type of debris movement.
 - For earth/debris flows, which tend to be fluid, the empirical relationship is based on a data set of over 700 earth/debris flows from New Zealand (including the Port Hills and Banks Peninsula) and overseas, compiled by Massey and Carey (2012).
 - For debris avalanches, which tend to be less fluid and do not run out as far as flows, the empirical relationship is based on data from about 45 debris avalanches that fell from Port Hills slopes during the 2010/11 Canterbury earthquakes. The empirical relationship separated “talus” (where the debris comprises many boulders that cover the entire ground surface) from “boulder roll” (where the debris comprises a few individual boulders that extend further out from the cliff toe than the talus).

¹ Fahrboeschung is a German word meaning “travel angle” adopted in 1884 by a pioneer in landslide runout studies, Albert Heim. It is still used in its original definition.

2. Numerical methods:

- a. Numerical modelling of landslide runout was carried out using the RAMMS® debris-flow software. This software, developed by the Snow and Avalanche Research Institute based in Davos, Switzerland, simulates the runout of debris flows and snow and rock avalanches across complex terrain. The module is used worldwide for landslide runout analysis and uses a two-parameter Voellmy rheological model to describe the frictional behaviour of the debris (RAMMS, 2011). Two different sets of parameters were used depending on whether the failure was assessed to be a flow or avalanche.
 - *Earth/debris flows*: The model was calibrated by “back-analysing” the runout of five Port Hills and Banks Peninsula debris flows and the modelled parameters optimised to obtain a good correlation between the modelled versus actual runout.
 - *Debris avalanches*: The model was calibrated by “back-analysing” the runout of 24 Port Hills debris avalanches that fell during the 2010/11 Canterbury earthquakes, and the modelled parameters optimised to obtain a good correlation between the modelled versus actual runout.
- b. The modelling results give likely debris runout, area affected, volume, velocity and the maximum and final height of debris in a given location at any moment in the runout - refer to Section 4.3 for details of the calibration.
- c. The RAMMS modelling uses a “bare earth” topographic model, and so the runout impedance of buildings and larger trees was not considered.

A1.3 RISK ASSESSMENT

During the 2010/11 Canterbury earthquakes a few boulders and relatively small volumes of fill and loess (less than 50 m³) fell from the slopes at Quarry Road. During the earthquakes the slopes also moved, causing cracks to open, although the soil and rock mass did not leave the source area.

The slopes are now cracked and water can more readily infiltrate the slope. This is particularly important for fill (re-worked loess) and loess, as its strength is largely governed by its moisture content (McDowell, 1989). The strength of the rock mass forming the slope at Quarry Road has been reduced by earthquake-induced fractures and movement and it will continue to degrade with time due to factors such as weathering, rainfall and material strength fatigue. Larger-volume failures from the slopes are now more likely in future earthquakes and when subjected to non-earthquake triggers such as rain.

Details of the failure mechanisms and landslide hazards assessed in this risk assessment at each source area are contained in Table A1.1.

Table A1.1 Failure mechanisms and landslide hazard types included in this risk assessment

Source area	Failure mechanism (from Yetton and Engel, 2014)	Landslide hazard type assessed	Assessed main triggering conditions
11A	Fill slope failure	Earth/debris flow	Static
11B	Rock slope failure	Debris avalanche	Dynamic and static
11C	Fill and loess cut slope failure	Earth/debris flow	Static
11E	Rock slope failure of quarry face	Debris avalanche	Dynamic and static

The risk from cliff collapses falling from the slope at source area 11B was originally assessed by Massey et al. (2012a). In addition to the identified rockfall risk at this site, the potential for larger failures from the same slope has also been assessed.

A1.3.1 Fatality risk for dwelling occupants

The risk assessment is based on the following method and assumptions:

A1.3.1.1 Source areas 11A and C (earth/debris flows):

1. Divide the entire study area into a series of 1 m by 1 m grid cells.
2. Consider the possible range of triggering events from non-earthquake triggers (mainly rain). The annual frequency of the event (rainfall) that could trigger failure of any of the identified source areas (source area 2) is difficult to estimate. The variation of risk across the slope has, therefore been assessed using a range of event frequencies and earth/debris flow source volumes:
 - It has been assumed that the return period of the event (mainly rainfall) that could trigger failure of the assessed source area is unlikely to be less than 20 years (event annual frequency of 0.05), as the rainfall recorded in the Port Hills 3–5 March 2014, which did not cause substantial failures, was equivalent to a 20–50 year return period rain event for the north facing slopes of the Port Hills.
 - Event annual frequencies ($P(H)$) of 0.05, 0.02, 0.01, and 0.005 corresponding to return periods of 20, 50, 100 and 200 years, were used for the assessment.
 - The main source area was characterised based on the evidence and assessment collected to date, and estimates of the likely failure volumes were made.
 - Three scenarios were considered based on: 1) lower; 2) middle; and 3) upper estimates of the source volume.
 - Each volume scenario was assessed as having an equal probability of failure in a given event, but that only one source area was likely to fail in that event.
3. For each representative event, and for each scenario, estimate:
 - a. The frequency of the event and the volume of debris, for a given source scenario, produced in that event ($P_{(H)}$)
 - b. The height of the debris reaching/passing a given grid cell and the probability of a person at that location being inundated (buried) by the debris ($P_{(S,H)}$).

- c. The probability that a person is present at a given location in their dwelling as the debris moves through it, ($P_{(T:S)}$), which has been linked to landslide intensity (Du et al., 2013).
 - d. the probability that a person is killed if present and inundated by debris ($V_{(D:T)}$)
4. Combine 3(a)–(d) for each source area scenario to estimate the annual individual fatality risk at different locations below the slope at different event annual frequencies.
 5. These values were then modelled using ArcGIS®. ArcGIS is used to interpolate between the risks calculated at given grid cells so as to produce contours of equal risk. A single contour was presented for each scenario (lower, middle and upper source volumes) for each event annual frequency, representing the estimated risk of 10^{-4} (ten to the minus four, or 1 chance in 10,000 of dying per year).
 6. The annual individual fatality risk value of 10^{-4} was chosen as this has been used previously by Christchurch City Council and the Canterbury Earthquake Recovery Authority to delineate existing dwellings that are exposed to potentially unacceptable levels of risk from rockfalls.

A1.3.1.2 Source area 11B (debris avalanches)

Only the part of source area 11B described by Yetton and Engel (2014) as “potential rock bluff collapse” has been assessed in this risk assessment. This is in addition to the original risk estimates presented in Massey et al. (2012a), which have been updated to make them consistent with the input parameters used in the risk assessments contained in this report. These are discussed in the risk assessment section for source area 11E. The risk from the “potential small-scale soil slope failures” (Yetton and Engel, 2014), have not been assessed.

For source area 11B:

1. Divide the entire study area into a series of 1 m by 1 m grid cells.
2. Consider the possible range of triggering events, in terms of a set of earthquake triggers, and choose a small set of representative earthquake events spanning the range of severity of events from the smallest to the largest:
 - Results from the numerical assessments suggest that it is unlikely that large failure of the rock slope would occur during rainfall events – although smaller rockfalls could still occur, which are included in the original risk assessment for the site (Massey et al., 2012a).
 - Four earthquake peak ground acceleration (PGA) event bands were adopted (0.1–0.4 g, 0.4–1 g, 1–2 g and 2–5 g), as per those in the original risk assessment (Massey et al., 2012a).
 - The main source area (source area 11B) was characterised based on the evidence and assessment collected to date, and estimates of the likely failure volumes were made.
 - Three scenarios were considered based on: 1) lower; 2) middle; and 3) upper estimates of the source volume, and the relative stability (yield acceleration, K_y) of the slope.

3. Estimate the probability of occurrence of the characterised source area 11B debris avalanche for each representative earthquake peak ground acceleration band, as a function of the magnitude of permanent slope displacement estimated from the decoupled results, as follows:
 - If the estimated displacement of the source is ≤ 0.1 m then the probability of catastrophic failure = 0. This means that the source area is unlikely to fail catastrophically if permanent displacements are ≤ 0.1 m. This was based on measurements of slopes that underwent permanent displacement (i.e., cracking), but where the displacement magnitudes were < 0.1 m and where catastrophic failure did not occur.
 - If the estimated permanent displacement of the source ≥ 1.0 m then the probability of catastrophic failure = 1. This means that the source area is likely to fail catastrophically if displacements are ≥ 1 m.
 - If the estimated permanent displacements are between 0.1 m and 1 m then the probability of failure (P) is calculated based on a linear interpolation between P = 0 at displacements of 0.1 m, and P = 1, at displacements of 1 m.
4. For each representative event, within each scenario, estimate:
 - a. The frequency of the event, the probability of failure and the volume of debris produced in that event, for a given source scenario ($P_{(H)}$).
 - b. The height of the debris reaching/passing a given grid cell and the probability of a person at that location being inundated (buried) by the debris ($P_{(S:H)}$).
 - c. The probability that a person is present at a given location in their dwelling as the debris moves through it, ($P_{(T:S)}$).
 - d. The probability that a person is killed if present and inundated by debris ($V_{(D:T)}$)
5. Multiply 4(a)–(d) for each source area scenario to estimate the annual individual fatality risk at different locations below the slope.
6. These values were then modelled using ArcGIS®. ArcGIS is used to interpolate between the risks calculated at given grid cells so as to produce contours of equal risk. A single contour was presented for each scenario (lower, middle and upper source volumes) for each event annual frequency, representing the estimated risk of 10^{-4} (ten to the minus four, or 1 chance in 10,000 of dying per year).
7. The annual individual fatality risk value of 10^{-4} was chosen as this has been used previously by Christchurch City Council and the Canterbury Earthquake Recovery Authority to delineate existing dwellings that are exposed to potentially unacceptable levels of risk from rockfalls.

A1.3.1.3 Source area 11E (debris avalanches)

There is no site-specific information relating to this abandoned quarry slope. Geotechnical reports (carried out by Coffeys Ltd.) provided to GNS Science by Christchurch City Council, indicate that some debris fell from the rock slope during the 22 February 2011 earthquakes, and minor falls of rock and debris had occurred between April 2011 and December 2013 (Harwood, 2011, 2013). Consultants working for the Earthquake Commission confirmed that fallen debris had been removed from behind the house at No. 36 Main Road at the toe of the quarry (S. Wallace, personal communication 2014).

Given the lack of detailed site-specific information relating to this slope, GNS Science has applied the cliff collapse risk model (Massey et al., 2012a) to this slope. This was done as the slope is higher than 10 m and the slope angle is greater than 45° (the criteria used in the Massey et al. (2012) assessments) and recent failures from the slope have been recorded.

The original risk assessment by Massey et al. (2012a) was updated to make it consistent with the input parameters used in the risk assessments contained in this report, these comprised:

1. Field mapping and verification of cliff crest (edge).
2. Annual frequency of an earthquake triggering event: For this assessment GNS Science has adopted the year 2016 probabilistic national seismic hazard model annual frequencies for earthquake peak ground accelerations.
3. Probability of a person being present: For this assessment, GNS Science has assumed the same “average” occupancy rate value adopted by the Canterbury Earthquake Recovery Authority, i.e., that an average person spends on average 16 hours a day at home ($16/24 = 0.67$ or 67%).
4. Vulnerability of a person if present and hit by debris: For this assessment GNS Science has adopted a constant vulnerability factor of 70% as it was the factor adopted by the Canterbury Earthquake Recovery Authority for the previous risk assessments.

A1.3.2 Probability of inundation

$P_{(S:H)}$ is the probability of a person at a given location being inundated (buried) by the debris, should the person be present in that location as the debris moves through it. The height of debris passing a given location was estimated using the RAMMS model outputs. The maximum height of the debris reaching/passing a given grid cell at any time step during the modelled earth/debris flow was used. These were combined with simple models of probability (of inundation) as a function of the height of debris reaching/passing a given grid cell, where:

Source areas 11A and C (earth/debris flows)

1. Probability of inundation $P_{(INUN)} = 0$ if the maximum height of the debris reaching/passing the grid cell is ≤ 0.3 m.
2. Probability of inundation $P_{(INUN)} = 1$ if the maximum height of the debris reaching/passing a given grid cell is ≥ 1 m.
3. Probability of inundation $P_{(INUN)}$ is between 0 and 1 for debris heights greater than 0.3 m but less than 1.0 m, adopting a linear interpolation.

Source area 11B (debris avalanche)

- Probability of inundation $P_{(INUN)} = 0$ if the maximum height of the debris reaching/passing the grid cell is ≤ 0.1 m.
- Probability of inundation $P_{(INUN)} = 1$ if the maximum height of the debris reaching/passing a given grid cell is ≥ 1 m.
- Probability of inundation $P_{(INUN)}$ is between 0 and 1 for debris heights greater than 0.1 m but less than 1.0 m, adopting a linear interpolation.

The difference between the inundation height probabilities adopted for the assessments reflects the dominant movement mechanism and nature of the debris associated with the different hazards. Debris avalanches, sourcing from the rock slopes, comprise multiple boulders of rock, rather than a fine-grained deposits of soil as per the debris derived from the earth/debris flows sourcing from the soil slopes. An earth/debris flow with a flow height 0.3 m or less is unlikely to inundate a person, as the debris is quite fluid and would likely flow around a person, regardless of the debris velocity. On the other hand a debris avalanche with a debris height of 0.3 m or less could still inundate a person, as the rock debris has significantly more mass than soil, and could knock a person over.

A1.3.3 Probability of a person being present

$P_{(T:S)}$ is the probability an individual is present in the portion of the slope when the debris moves through it. It is a function of the proportion of time spent by a person at a particular location each day and can range from 0% if the person is not present, to 100% if the person is present all of the time.

For planning and regulatory purposes it is established practice to consider individual risk to a “critical group” of more highly-exposed-to-risk people. For example, there are clearly identifiable groups of people (with significant numbers in the groups) who do spend the vast majority of their time in their homes – the very old, the very young, the disabled and the sick.

The assumption used in the previous risk assessment (Massey et al., 2012a) for judging whether risk controls should be applied to individual homes was thus that most-exposed individuals at risk would be those who spend 100% of their time at home.

In other international rockfall risk assessments (e.g. Corominas et al., 2005), values ranging from 58% (for a person spending 14 hours a day at home) to 83% (for a person spending 20 hours a day at home), have been used to represent the “average” person and the “most exposed” person, respectively. However, in reality the most exposed person is still likely to be present 100% of their time.

For the land zoning assessments carried out by the Canterbury Earthquake Recovery Authority – with regards to rockfall and debris avalanche risk – their policy adopted an “average” occupancy rate, to assess the average annual individual fatality risk from rockfall across the exposed population in order to estimate the risk to the average person.

For this assessment, GNS Science has assumed the same “average” occupancy rate value adopted by the Canterbury Earthquake Recovery Authority, i.e., that an average person spends on average 16 hours a day at home ($16/24 = 0.67$ or 67%).

When a person is at home they tend to spend more time in their home than in their garden. Whilst in their home they cannot occupy every part of it at the same time. To proportion the person across their home, GNS Science has assumed that Port Hills homes have a footprint area (assuming a single story dwelling) of $A_F = 100 \text{ m}^2$. The probability that a person will be occupying a given area within their home at any one time can be expressed as:

$$P_{(T:S)} = \frac{(0.67)}{(A_F / P_A)} \quad \text{Equation 2}$$

Where 0.67 (67%) is the proportion of time a person spends in their home and P_A is the area of home occupied by a person at any one time. For this assessment, GNS Science has adopted a 2 m by 2 m (4 m^2) area to represent P_A . Therefore the probability of a person being present in a given 4 m^2 area within their home is 0.03 (3%) for the average person. No distinction is made between single versus multiple storey dwellings.

A1.3.4 Probability of the person being killed if inundated by debris

This is the probability of a person being killed if present and inundated (buried) by debris. Vulnerability (V) depends on the landslide intensity, the characteristics of the elements at risk, and the impact of the landslide (Du et al., 2013).

This probability is expressed as vulnerability, the term used to describe the amount of damage that results from a particular degree of hazard. Vulnerability ranges between 0 and 1 and for fatality risk represents the likelihood of an injury sustained by the individual being fatal (1) and the possibility of getting out of the way to avoid being struck. For earth/debris flows people tend to be killed because they are inundated (buried) by debris, and if the velocity of the debris is rapid, it is possible that a person could be knocked off their feet and buried.

Studies from Hong Kong (e.g. Finlay et al., 1999) summarised the vulnerability ranges and recommended likelihood of death “if buried by debris”. The vulnerability of an individual in open space if buried by debris is given as 0.8–1.0 but if only hit by debris (and not buried) the vulnerability is 0.1–0.5, with recommended values of 1 and 0.3 respectively, assuming that it may be possible to get out of the way. For people in homes, it would be unlikely that a person would be able to take evasive action as they would not see the debris coming. However, this argument is counterbalanced by the level of protection a house may provide by stopping debris from entering it.

There is scant data on the performance of New Zealand homes when inundated by debris. However, in one such recent case of a home being impacted by earth/debris flow, the building offered little protection and the person was killed (Page, 2013). Finlay et al. (1999) recommend using a vulnerability factor of 0.9–1.0 if a person is in a building and if the building is hit by debris and collapses, but ranging to 0.0–0.1 if the debris strikes the building only.

However, Du et al. (2013) recommend that vulnerability and landslide intensity are also a function of the velocity of the debris when it impacts a person or building. Given that debris flows are triggered by rain it is most likely that people would be inside homes when debris flows trigger and therefore some protection is likely. However, for debris avalanches triggered by earthquakes people may be outside in gardens (where two deaths occurred from falling rocks triggered by the 22 February 2011 earthquake).

Source areas 11A and 11C (earth/debris flows)

For fill and loess earth/debris flows where the debris tends to be very fluid, it is likely that homes (even wooden ones) would provide some protection from the debris. In this risk assessment the probability of being inundated has been calculated separately as $P_{(S:H)}$. Therefore it would be appropriate to apply different vulnerabilities to different parts of the debris trail based on debris velocity.

For the risk assessment, the velocity ranges given in Australian Geomechanics Society (2007) were used, and these were linked to the vulnerabilities reported by Finlay et al. (1999) and Du et al. (2013), as no specific information on how Zealand buildings perform when impacted by debris was available (Table A1.2). The RAMMS model outputs were used to calculate debris velocity at different locations along the earth/debris flow trail, using the ranges given in Table 3.

Table A1.2 Vulnerability factors for different debris velocities used in the risk assessment.

Velocity (m/s)	Description	Vulnerability
>5 m/s	Building collapse or building inundated with debris, death almost certain	1
0.5–5	Inundated building with debris, but person not buried	0.6
0.5–0.05	Building is hit but the person not buried and escape possible	0.2
<0.05	Debris strikes building only	0

Source area 11B (debris avalanche)

The probability of a person being killed if hit by a boulder is related to the boulder flux, which in turn is a function of the number and velocity of boulders passing through a given location. In this risk assessment the probability of a person being hit by N boulders within the debris (should a person be present) has been calculated separately as $P_{(S:H)}$.

Debris velocities derived from RAMMS model outputs are typically >5 m/s for most of the runout areas assessed. However, the velocity rapidly drops to <0.05 m/s in the distal limits of runout over a relatively short distance of several metres. These calculations are similar to field observations made from video footage although, some boulders within the distal debris fringe (mainly individual boulders) travelled at higher velocities, i.e., “fly rock”. Fly-rock may occur when moving blocks impact and fracture resulting in high velocity rock fragments being released.

Based on these observations, a constant vulnerability factor of 70% has been adopted for this risk assessment as it was the factor adopted by the Canterbury Earthquake Recovery Authority (CERA) for the previous risk assessments. A constant vulnerability value is thought reasonable as the velocity of the boulders, even in the distal runout zone are still relatively high with people unlikely to be able to get out of the way. The protective effects of buildings have not been taken into account, this is because most people killed by falling boulders during the 22 February 2011 earthquake were outside and therefore not protected by buildings. However, it is noted that buildings do have a sheltering effect as only 45% of buildings hit by boulders were penetrated (Massey et al., 2012c).

A1.3.5 Road-user risk assessment

The risk to road users of Main Road has been assessed. Main Road is a major lifeline. The risk to road users along Quarry Road and any other ancillary road in the study areas has not been assessed.

The road user risk has been expressed in multiple terms including: 1) annual individual fatality risk, based on an assumed number of trips per year; and 2) the risk per trip, for different types of road user, namely car occupant, bus passenger, truck occupant, motor cyclist, pedal cyclist and pedestrian. The risk method is similar to the one detailed by Taig and Massey (2014) for Wakefield Avenue, but here also includes the possibility of earth/debris flows and debris avalanches occurring at specific locations on the site. An illustration of road user risk assessment methodology is contained in Section A1.3.6.

Road users are susceptible to multiple hazards in the event of debris avalanches:

1. Direct impact of rockfall onto them or their vehicles;
2. Crashing into rockfall debris on the road, or crashing (into other vehicles that stop or swerve violently) while trying to avoid rockfall debris; and
3. Being carried away in the collapse of a roadway during cliff-top recession or falling into an area of missing roadway.

For Wakefield Avenue the first two were potentially significant as there were numerous potential sources of obstruction along a long stretch of road; even in this situation risk from the first hazard greatly exceeded that from the second. As at Wakefield Avenue, the third hazard is not relevant at the Quarry Road study area as there are no lengths of road susceptible to cliff-top recession.

As regards the second hazard, the Quarry Road slope collapse sources considered here are considered to present significantly lower risk relative to the first hazard than was the case for Wakefield Avenue because:

- a. the length of road at risk is much shorter;
- b. the slope collapses of concern (from source areas 11A and 11B) involve coherent debris flows or avalanches rather than randomly scattered boulders; and
- c. the traffic on the road at risk (Main Road) is much heavier, meaning that the chance of any one road user being the first to encounter debris on the road is much reduced.

The second hazard is not considered significant in risk terms, and the risk assessment has focused purely on the first hazard – of being impacted or inundated by rockfall or loess debris.

Main Road is a busier road with a wider range of regular users than Wakefield Avenue, and road user risk has been assessed for:

- a. Car occupants;
- b. Bus occupants;
- c. Truck occupants;
- d. Motorcyclists;
- e. Cyclists; and
- f. Pedestrians.

The event tree model shown in Figure A1.1 was applied, using only the top chain of events in view of the low assessed significance of the “drive into or swerve avoiding debris on the road” hazard. Consideration was given to modelling the “swerve avoiding debris” hazard for Main Road in view of the possibility of swerving into the sea immediately next to the road, but in light of: 1) the shallow slope down from the road; 2) the shallowness of the water; and 3) the very localised nature of the hazard from source areas 11A and 11B (the risk falls off sharply across the road and from source area 11B in particular is minimal on the seaward side), the considerable additional effort involved in modelling this particular hazard was not considered worthwhile.

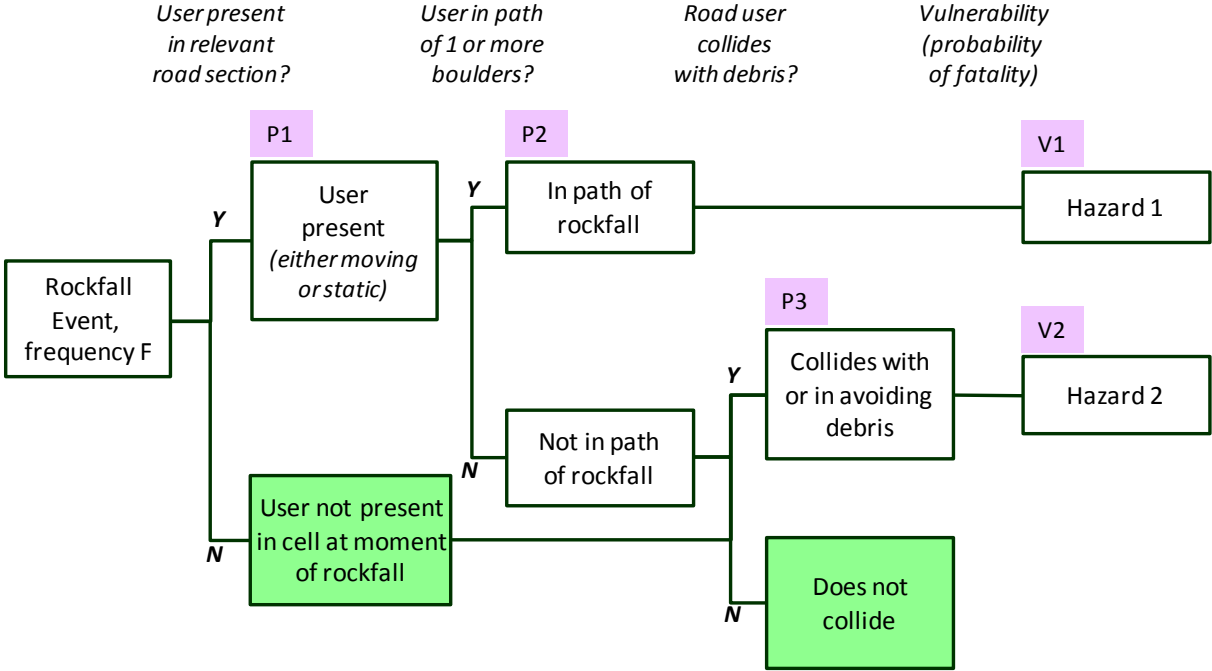


Figure A1.1 Event tree model for road user risk assessment.

Given that the length of Quarry Road passing through the study area is unconfined, it is unlikely that road users would be trapped by debris, and therefore potentially at risk from secondary failures onto the road. A summary of the derivation of the key input probabilities P1, P2, and V1 is given in Tables A1.3 and A1.4.

Table A1.3 Definition and derivation of key road risk parameters.

Parameter	Definition	Value/Formula	Basis of calculation
P ₁	Years per journey that road user is present within relevant cell, per single journey	$P1 = (\text{time in hours in cell per jny}) / (\text{hrs per yr})$ $= (L/v) / (365.25 \times 24)$ where $v = \text{speed (m/hr)}$ $= V \times 1000$ PLUS annual time spent stationary / no. journeys	Time spent within cell length L metres, given average speed of travel V kph plus any time spent stationary (per year, divided by no. of journeys)
P ₂	Probability that a road user, if present within a given cell, will be in the path of one or more boulders in the event of a rockfall incident	$P2 = 1 - (1-P)^N$, (N \geq 1) or $P2 = N \cdot P$ (N $<$ 1), where P = prob in path of 1 boulder passing through cell, and N = no. boulders passing thru cell in given scenario <i>(calculated for each cell individually)</i>	Basis is that probability of NOT being in the path of each of N boulders is 1-P. In turn $P = (d+D)/L$ (or 1 if $d+D > L$)
V ₁ (Source 11B)	Probability of death if in path of one or more boulders <i>Significant change from previous (Wakefield Ave) model; vulnerability is assessed for the PERSON as the target of debris, rather than first for the VEHICLE</i>	Simple assumptions (compatible with those used in dwelling risk assessments)	Road users are outdoors and looking ahead so have a considerably advantage over people in their homes in terms of ability to take evasive action, particularly at this site where risk falls off very sharply with distance so it is only a few metres to safety
V ₁ (Source 11A)	Probability of death in the event of inundation of the road by a (largely loess in character) debris flow	Adaptation of model used for people in dwellings. As for Source 11B, vulnerability is considered at the level of the PERSON rather than the VEHICLE	Vulnerability for different road users is modified to account for a) the possible protective effect of the vehicular 'shell', and more importantly b) to reflect the different ability of a road user to take evasive action

Table A1.4 Assumptions used in quantifying road user risk for Quarry Road.

Parameter	Definition	Key Inputs	Road User	Key Input/Output Values				Important Assumptions
				V kph - lower risk	V kph - higher risk	P1 - lower risk	P1 - higher risk	
P ₁	Years per journey that road user is present within relevant cell, per single journey	Ave speed V kph	Car occupant	39.1	30.7	2.92E-09	3.72E-09	Delays on Main Road are frequent. These have been modelled using hour by hour traffic count data, matching average speed to traffic density, and then taking the weighted average speed over all hours of day and days of the week for motor vehicle users. This has the effect of reducing average speeds from 40-50kph to about 30-40kph.
			Bus passenger	39.1	30.7	2.92E-09	3.72E-09	
			Truck occupant	39.1	30.7	2.92E-09	3.72E-09	
			Motorcyclist	39.1	30.7	2.92E-09	3.72E-09	
			Cyclist	25	15	4.56E-09	7.61E-09	
			Pedestrian	5	3	2.28E-08	3.80E-08	
				Effective road user diameter D (m)		P(in path of single boulder)		
				lower risk	higher risk	lower risk	higher risk	
P ₂	Probability that a road user, if present within a given cell, will be in the path of one or more boulders in the event of a rockfall incident	Effective road user diameter D metres	Car occupant	1	1	1.00	1.00	Rockfall behaves as a random set of discrete boulders of a given diameter; when working (as here) with 1x1m grid cells the probability of being in the path of a boulder passing through the cell is taken as 1. For loess debris flows, the probability of inundation is evaluated exactly as for dwelling occupants; vulnerability is then related to debris velocity.
			Bus passenger	1	1	1.00	1.00	
			Truck occupant	1	1	1.00	1.00	
			Motorcyclist	1	1	1.00	1.00	
			Cyclist	1	1	1.00	1.00	
			Pedestrian	1	1	1.00	1.00	
			Road User	V1 - lower risk	V1 - higher risk			
V ₁ (Source 11B)	Probability of death if in path of one or more boulders <i>Significant change from previous (Wakefield Ave) model; vulnerability is assessed for the PERSON as the target of debris, rather than first for the VEHICLE</i>	P(death) if within path of a single boulder	Car occupant	0.3	0.5	There appears to be little net effect of a vehicular shell in modifying the chance of a person in the path of a boulder being killed - several recent incidents show people surviving massive impacts on cars unless they were in the direct path of the boulder. Buses & trucks may provide some protective effect but are also more at risk of multiple boulder impacts, and might be worse in terms of escape if knocked into the sea. Cyclists & pedestrians are particularly vulnerable if hit, but are also best placed to get early warning (aural and visual) and take evasive action. Pros & cons for motor vehicle occupants, cyclists & pedestrians are considered to balance out. Motorcyclists have the worst mix of (noise insulation from outside) plus (vulnerability if struck) plus (combination effect of fall at road speed if struck)		
			Bus passenger	0.3	0.5			
			Truck occupant	0.3	0.5			
			Motorcyclist	0.4	0.7			
			Cyclist	0.3	0.5			
			Pedestrian	0.3	0.5			
				Debris velocity (m/s), where inundation occurs				
			Road User	> 5	0.5 to 5	0.05 to 0.5	< 0.05	
V ₁ (Source 11A)	Probability of death in the event of inundation of the road by a (largely loess in character) debris flow	P(death) if inundated with debris travelling at speed shown	Car occupant	1	0.4	0.1	0	Similar observation apply to those above for rockfall. Motor vehicles (particularly the more massive trucks and buses) would be expected to provide significant protection for low loess flow heights and speeds, but this may be countered by the possibility of more difficult escape if swept into the sea by higher and faster loess flows. As for rockfall, cyclists' and pedestrians' higher vulnerability if hit is considered balanced by greater ability to take evasive action, while motorcyclists have the worst mix of vulnerability factors.
			Bus passenger	1	0.4	0.1	0	
			Truck occupant	1	0.4	0.1	0	
			Motorcyclist	1	0.6	0.2	0	
			Cyclist	1	0.4	0.1	0	
			Pedestrian	1	0.4	0.1	0	

Note: Cells shaded yellow are user input assumptions.

The parameters shown in Table A1.4 are uncertain. As in our previous work on road user risk from rockfall, inputs and outputs are presented as ranges from “reasonable lower” to “reasonable upper” values. No statistical significance is attached to these ranges; the results are regarded as providing a sensible range, given the associated uncertainties, within which to assume the actual risk might lie. Perhaps the single largest uncertainty is in the volume of material which flows from the debris sources; as for the dwelling risk assessments this has been explicitly considered by carrying out all assessments three times, for upper, central and lower estimates of debris source volumes.

The risk equation is evaluated for each cell in the grid for each rockfall scenario considered, based on a number of boulders calculated as the ratio of the volume of rock passing through the cell (from RAMMS output) to average boulder volume (based on the assumption of average boulder size of 0.5 m diameter). The grid used was simplified relative to that used in modelling dwelling risk by excluding cells that did not form part of the roadway in order to streamline the calculation process; in all other respects the rockfall modelling used to estimate individual road-user risk was identical to that used to estimate individual dwelling occupant risk.

As in the dwelling occupant assessment, the set of scenarios modelled for source B covers:

- Four seismic trigger scenarios ranging from 0.1–0.4 g up to 2–5 g peak ground acceleration, with an increasing probability as shaking increases that debris source area 11B will be triggered, and
- Four non-seismically triggered rockfall scenarios (corresponding to different severities of weather-induced rockfall).

For source area 11A, the likely trigger is extreme rainfall, but the frequency of the event required to trigger the slope collapse is not known. As for dwelling occupants, risk has been calculated for road users on the basis of four different plausible frequencies of collapse (0.05, 0.02, 0.01 and 0.005 – covering a range from once in 20 to once in 200 years).

For source area 11B, the overall risk per journey contributed by each cell is calculated as the sum of (frequency of triggering event scenario) x (probability of death per journey if the triggering scenario occurs) for all four seismic and four non-seismic event triggers. This risk is in addition to that calculated in previous work (Massey et al., 2012a) from cliff collapse. The risks per journey for each cell were thus summed over all contributory trigger scenarios, and added to the corresponding road user risk calculated from cliff collapse to produce the maps shown at Figure 42.

For both source areas 11A and 11B the overall risks per journey were calculated by summing over all cells making up the southern (landward) side of Main Road and the northern (seaward) side of Main Road, allowing the change in risk across the width of the road readily to be compared with each other and with the existing motor vehicle crash risk (based on average statistics for New Zealand urban roads, from Ministry of Transport publications on road crashes and casualties and on number of journeys and distance travelled by different road user groups).

A1.3.6 Road user risk assessment illustration

The calculation process is illustrated for a single grid cell and seismic event in Table A1.5 (hazard 1) and Table A1.6 (hazard 2, noting that at this particular site the risk from hazard 2 is not quantified as it is considered insignificant relative to that from hazard 1). Table A1.7 then shows how various risk outputs of interest are calculated from the probabilities per journey for individual cells and for the whole length of road.

Table A1.5 Calculation process for risk from hazard 1 (single cell, per journey).

Example Calculation:	R1 - Risk from Hazard 1 (hit by falling rocks)					
Grid Cell no. 29805 (cell width L = 2m)						
Seismic scenario	Band 2, 0.3 to 0.5g PGA					
Contributing sources	Localised sources 1 & 2, plus distributed sources					
Formula for R1: =	F x P₁ x P₂ x V₁					
<i>where</i>						
F = frequency of Band 2 EQ =	0.032153 events per year					
P ₁ = time in cell/journey	from table XX2 (road user dependent)					
V ₁ = P _{death} if in path of 1+rocks	from table XX2 (road user dependent)					
P ₂ = P _{in path of 1 or more rocks}	from all sources (cell & scenario dependent, see below)					
Calculation of P2					Notes/Formulae	
Boulders passing	Source 1	Source 2	Distributed sources			
Volume rockfall passing, m ³	0.648	1.173	0.000833	V ₁ from RAMMS		
Equivalent no. 0.5m boulders	9.90	17.92	0.0127	N = V / (4/3 π r ³)		
<i>which is combined with</i>						
P(in path of single boulder)	lower	upper				
Car	0.75	1.00	P _{one} = (d+D)/L (see Tables XX1 & XX2)			
Motorcycle	0.75	1.00				
Pedal cycle	0.75	1.00				
Pedestrian	0.50	0.75				
<i>to calculate</i>						
P(in path of 1 or more of N boulders, if source triggered)	Source 1	Source 2	Distributed sources	Upper value only shown		
Car	1	1	0.012733	for N>1		
Motorcycle	1	1	0.012733	P _N = 1 - (1 - P _{one}) ^N		
Pedal cycle	1	1	0.012733	for N<1		
Pedestrian	0.999999	1	0.00955	P _N = N.P _{one} (see Table XX1)		
<i>which is combined with</i>						
P(source triggered)	0.444	0.278	1.000	in Band 2 earthquake		
<i>to calculate, for sources individually, then in combination</i>						
P₂, = P(in path of 1 or more of N boulders - UPPER, Band 2 EQ)	Source 1	Source 2	Distributed sources	P2 (Any Source)		
Car	0.444	0.278	0.013	0.6039	P _(any source) = 1 - (1 - P _{source1}) x (1 - P _{source2}) x (1 - P _{sourceN}) etc.	
Motorcycle	0.444	0.278	0.013	0.6039		
Pedal cycle	0.444	0.278	0.013	0.6039		
Pedestrian	0.444	0.278	0.010	0.6026		
<i>this can now be combined with the other parameters to calculate R1</i>						
Calculation of R1	F	P_{1, upper}	P_{2, upper}	V_{1, upper}	R1_{upper}	R1 is dimensionless, P(death per journey)
Car	0.032153	6.5E-09	0.6039	0.3	3.8E-11	
Motorcycle	0.032153	6.5E-09	0.6039	0.8	1.0E-10	
Pedal cycle	0.032153	1.5E-08	0.6039	0.7	2.1E-10	
Pedestrian	0.032153	9.1E-08	0.6026	0.7	1.2E-09	

Table A1.6 Calculation process for risk from hazard 2 (single cell, per journey).

Example Calculation:	R2 - Risk of crashing into (or in avoiding) rockfall debris on road					
Grid Cell no. 29805 (cell width L = 2m)						
Seismic scenario	Band 2, 0.3 to 0.5g PGA					
Contributing sources	Localised sources 1 & 2, plus distributed sources					
Formula for R2: =	F x P₃ x V₂					
<i>where</i>						
F = frequency of Band 2 EQ =	0.032153 events/year					
P ₃ = time/journey within which collision will occur	= Debris factor x Collision Factor x Braking Factor (see below)					
V ₂ = P(death if collision occurs)	from table XX2 (road user dependent)					
Calculation of P3					Notes/Formulae	
(a) Debris factor	Source 1	Source 2	Distributed			
Boulders on or passing the road	9.90	17.92	0.0127		Debris factor = (1 if > 0.2 boulders on or passing road, 0 otherwise) x P(source triggered in Band 2 EQ)	
Debris factor if source triggered	1	1	0			
P(source triggered)	0.444	0.278	1.000			
Debris factor for each scenario	0.444	0.278	0.000			
Overall Debris factor	0.599				Overall debris factor = 1 - (1-P _{source1}) x (1-P _{source2}) x (1-P _{distrib sources})	
(b) Collision factor						
Current assumptions	0.500	for all road users except pedestrians			See text for derivation	
(c) Braking factor						
	lower	upper				
Car	2.08	3.98			= braking time (seconds)	
Motorcycle	1.82	3.48				
Pedal cycle	1.41	3.12			(see text & Appendix X for derivation)	
Pedestrian	0.00	0.00				
<i>Combination of (a) x (b) x (c) (converted from seconds to years) gives P3 values as follows</i>						
P3 values	Debris factor	Collision factor	Braking factor (upper)	P_{3,upper}		Upper values only shown
Car	0.599	0.500	3.98	3.78E-08		Note: braking factor is converted to years in order to use P3 with annual event frequencies to calculate R2
Motorcycle	0.599	0.500	3.48	3.30E-08		
Pedal cycle	0.599	0.500	3.12	2.97E-08		
Pedestrian	0.599	0.000	0.00	0.00E+00		
<i>this can now be combined with the other parameters to calculate R2</i>						
Calculation of R2	F	P_{3, upper}	V_{2, upper}	R2_{upper}		R2 is dimensionless, P(death per journey)
Car	0.032153	3.8E-08	0.0100	1.2E-11		
Motorcycle	0.032153	3.3E-08	0.0250	2.7E-11		
Pedal cycle	0.032153	3.0E-08	0.0170	1.6E-11		
Pedestrian	0.032153	0.0E+00	0.0000	0.0E+00		

Table A1.7 Calculation of risk parameters of interest from single cell risk per journey.

Aggregation of Risk Parameters for Cells			
(a) Risk per journey			
Risk R_{ij} for road user j within cell i =	$R1_{ij} + R2_{ij}$		
Risk R_j per journey to road user j =	sum of R_{ij} for all relevant i (all cells on uphill side or downhill side of road, as appropriate)		
(b) Other key risk parameters			
Annual Individual Fatality Risk for user j	$= R_j \times M_{j,ind}$	$M_{j,ind}$ = Journeys/year by individual heavy road user of type j	
Average expected fatalities per year, user j	$= R_j \times M_{j,tot}$	$M_{j,tot}$ = Journeys/year by ALL road users of type j	
Probability of 1 or more fatal accidents/year (road user type j)	$= P_j = 1 - (1-R_j)^{M_{j,tot}}$		
Probability of 1 or more fatal accidents/year (among ALL road users)	$= 1 - (1-P_{car}) \times (1-P_{motorcycle}) \times (1-P_{cycle}) \times (1-P_{pedestrian})$		

Because the road is significantly wider than a single gridcell, gridcells were tagged on the upslope (landward) and downslope (seaward) sides of the road. The risk per journey is then aggregated for each side of the road, enabling the risk to be compared for journeys on either side. It is noted that the pavement runs on the upslope side of the road (though is currently closed for part of its length), while there are dedicated cycleways on both side of the road throughout the area assessed here.

As for the dwelling risk assessment, the calculations were repeated for three sets of rockfall scenarios to explore sensitivity to the key issue of how far rockfall will reach out from the slope toe. Scenario B uses central estimates of debris volume and runout. Scenario A uses upper estimates of debris volume and runout, while scenario C uses lower estimates of debris volume and runout.

Current New Zealand road traffic accident statistics were used to provide comparison information on the risk road users would face in their ordinary travel up and down Wakefield Avenue for a journey of the same length (540 m) as that covered in the risk assessment model.

A1.3.7 Road user risk – Additional discussion on main assumptions

The parameters used in quantifying the event tree described in the main report, and the values or models appropriate for Wakefield Avenue, are briefly discussed in turn. Throughout, tables highlight in yellow the key user input assumptions which can readily be altered in our risk assessment model to explore sensitivities and uncertainties.

A1.3.7.1 P_1 – proportion of a year which a road user spends in an individual model cell, per journey

The average time at risk for a road user is simply the distance travelled (in this case 2 m is the length of each cell) divided by the average journey speed (converted into appropriate units). In calculating risk, P_1 is to be converted into a risk per journey by multiplying by the initiating event frequency. Thus if that frequency is expressed in events per year (P_1) needs to be expressed as a proportion of a year (then years/journey x events/year = events/journey).

For roads in general the average journey speed needs to take into account both “normal” journeys when traffic flows smoothly, “congested” journeys where there is some speed reduction, and “delay events” when traffic is actually stopped. The impact of journey delay is greatest for motorised road vehicles; for pedestrians traffic congestion has minimal impact. In some cases it may be possible reliably to estimate the average journey time, taking all these factors into account. In others it may be appropriate to estimate the proportion of journeys falling into each category (normal, congested, subject to a delay event) and the journey time associated with each.

For the section of Main Road assessed here, delays are a regular daily occurrence at the peak hours when traffic volumes are heaviest. Traffic volumes by hour of day and day of the week are available for the Causeway (the section of Main Road to the east of the section of interest here) and for the junction of Ferrymead Road and Main road (to the west of the section of interest). These were used to estimate motor vehicle traffic volumes as shown in Table A1.8 for the section of Main Road of interest.

Table A1.8 Traffic volumes for Main Road (from Rantatira Terrace to The Brae), interpolated from Causeway and Ferrymead Road/Main Road junction values.

Total Motor Vehicles - Westbound (towards CC)									
Period	Mon	Tues	Wed	Thur	Fri	Sat	Sun	Averages	
Ending								4Day	7Day
01:00	6	5	7	9	12	22	30	7	13
02:00	4	5	6	5	8	18	26	5	10
03:00	3	3	4	7	8	16	23	5	9
04:00	8	8	6	8	11	17	25	8	12
05:00	22	18	19	22	20	21	31	20	22
06:00	81	79	71	72	83	40	32	76	65
07:00	290	282	345	283	293	130	78	300	243
08:00	1140	1165	1141	1082	1039	265	162	1132	856
09:00	1191	1243	1181	1161	1107	535	327	1194	964
10:00	847	849	861	894	907	827	657	863	835
11:00	739	711	659	786	760	968	875	724	785
12:00	708	705	662	764	802	974	981	710	799
13:00	593	572	583	627	651	788	872	594	669
14:00	554	529	533	611	608	722	920	557	640
15:00	535	520	515	603	610	658	900	543	620
16:00	577	579	583	676	639	602	870	604	647
17:00	575	565	591	638	625	551	713	592	608
18:00	459	473	493	494	453	346	414	480	447
19:00	407	459	463	473	464	357	366	450	427
20:00	282	316	338	366	371	308	239	326	317
21:00	146	166	172	187	178	133	141	168	161
22:00	99	118	113	129	130	105	84	115	111
23:00	49	56	62	60	92	84	39	57	63
00:00	15	19	20	28	49	53	13	21	28
TOTALS									
12hr 19:00	8324	8371	8265	8808	8665	7591	8058	8442	8297
24hr 24:00	9330	9446	9427	9987	9920	8540	8819	9547	9353

Total Motor Vehicles - Eastbound (towards Sumner)									
Period	Mon	Tues	Wed	Thur	Fri	Sat	Sun	Averages	
Ending								4Day	7Day
01:00	34	30	37	53	67	124	167	39	73
02:00	13	15	17	15	25	55	79	15	31
03:00	7	6	8	15	16	31	45	9	18
04:00	8	8	6	8	11	17	24	7	12
05:00	6	5	5	6	5	6	8	5	6
06:00	22	21	19	19	22	11	8	20	18
07:00	78	75	92	76	78	35	21	80	65
08:00	284	290	284	270	259	66	40	282	213
09:00	424	442	420	413	394	190	116	425	343
10:00	322	323	327	340	345	314	250	328	317
11:00	354	340	316	376	364	463	419	346	376
12:00	415	413	387	447	469	570	574	416	468
13:00	607	586	597	642	666	807	893	608	686
14:00	678	647	652	747	744	884	1126	681	782
15:00	720	699	693	811	820	885	1211	731	834
16:00	835	838	843	977	925	871	1259	873	935
17:00	947	931	974	1051	1031	908	1175	976	1002
18:00	1122	1158	1205	1208	1108	847	1013	1173	1094
19:00	662	748	754	770	755	582	596	734	695
20:00	367	411	439	476	482	401	311	423	413
21:00	286	325	337	367	348	261	276	329	314
22:00	259	308	295	339	341	276	220	300	291
23:00	177	202	223	215	331	302	140	204	227
00:00	73	93	98	139	239	260	65	101	138
TOTALS									
12hr 19:00	7368	7415	7453	8053	7880	7387	8673	7572	7747
24hr 24:00	8696	8914	9030	9782	9845	9164	10039	9106	9353

The 7-day, 24-hour average figures used in this study are shown in the blue shaded cells at the bottom right of Table A4. Traffic was partitioned between cars (including light vans) and trucks based on the counts taken at the Ferrymead Road/Main Road junction. Bus traffic was deduced from the timetable for the No. 3 bus which runs from Sumner to Christchurch Airport, and from the school buses which run over this stretch of this road during term times.

Motor traffic generally travels at or close to the speed limit when possible along this stretch of road (40–50 km/hr speeds have been assumed here). To estimate the (significant) average delays experienced over this section, a correlation between one-way traffic volume and average speed has been used as shown in Table A1.9 (based on the authors' personal experience and judgement). The table shows implied vehicle spacings for traffic not flowing smoothly at lower volume levels.

Table A1.9 Traffic density and average journey speeds along Main Road

1-way vehicles/hr	Speed range (kph)		Average separation (m)	
	Lower speed (kph)	Upper speed (kph)	lower speed	upper speed
<400	40	50		
400-600	38	48	95	120
600-800	36	45	60	75
800-900	32	40	40	50
900-1000	22	30	24	33
1000-1100	15	20	15	20
>1100	10	15	9	14

A1.3.7.2 P₂ – Probability a road user is in the path of one or more boulders, should a rockfall triggering event occur

As in previous studies (Taig and Massey, 2014) this is calculated from the assumed effective dimensions of road users and of boulders, and from the modelled flux of boulders into/through each cell. Our recent work for Wakefield Avenue (Massey et al, 2014) adapted that methodology to deal with cell sizes comparable to the largest “target” vehicles under consideration. In this (Quarry Road) study, the cell size has been further reduced from 2 x 2 m to 1 x 1 m, while the range of vehicles considered has been extended to include trucks and buses. This means the cell size is now small relative to most of the vehicles under consideration.

In order to avoid the complexities of integrating probabilities over multiple small units within a motor vehicle, the assessment approach used here focuses on the individual PERSON as the target of rockfall or debris flow, rather than the VEHICLE. The dimensions used for all road users are thus the same, regardless of their mode of transport. The vehicle is treated as having no effect on the probability of the person being in the path of one or more boulders; its effect IS, though, considered in estimating the person’s vulnerability (probability of death if in the path of the debris flow or rockfall).

A1.3.7.3 V_1 – Probability of death if in the path of one or more boulders.

The probability of death depends on two factors:

- a. Whether the road user is able to avoid the rockfall, despite being in its path; and
- b. The severity of injury if the rockfall cannot be avoided and strikes the vehicle or road user themselves.

The approach used here to estimate vulnerability is based on that developed in our earlier work in this area (Taig and Massey, 2014; Massey et al., 2014), except that the “target” is now treated as the individual person rather than as the vehicle in which they are travelling. Vulnerability is thus now defined as probability of death if the PERSON is within the path of rockfall, rather than if the VEHICLE is in the path of rockfall. The general effect is to reduce values of P_1 but to increase values of V_1 in comparison with our most recent work for Wakefield Avenue (Massey et al., 2014).

Vulnerabilities have been estimated in this study as shown in Table A1.10. Vulnerability in the event of inundation by N boulders where N is greater than 1 (the number of boulders is estimated from the volume of debris inundating a cell divided by the average boulder volume for a 0.5m diameter spherical boulder) is calculated as

$$\text{Vulnerability (N)} = 1 - [1 - \text{Vulnerability}(1)]^N$$

The vulnerabilities in the event of loess inundation are adapted from those used for dwellings, with the key difference being that ALL road users are already out of doors and facing forwards, so should have a much better chance of being aware of debris falling towards them than an average person in a dwelling. The rapid fall-off of risk across the road is also an important consideration here, as it means that if a road user becomes aware of debris coming towards them, they should have a good chance – particularly for smaller, nimbler road users – of being able successfully to take evasive action as the distance to a place of relative safety is small.

Table A1.10 Vulnerabilities estimated for different road users, for loess inundation and for rockfall.

					Road User	V1 - lower risk	V1 - higher risk					
V ₁ (Source 11B)	Probability of death if in path of one or more boulders <i>Significant change from previous (Wakefield Ave) model; vulnerability is assessed for the PERSON as the target of debris, rather than first for the VEHICLE</i>	P(death) if within path of a single boulder	Car occupant	0.3	0.5	There appears to be little net effect of a vehicular shell in modifying the chance of a person in the path of a boulder being killed - several recent incidents show people surviving massive impacts on cars unless they were in the direct path of the boulder. Buses & trucks may provide some protective effect but are also more at risk of multiple boulder impacts, and might be worse in terms of escape if knocked into the sea. Cyclists & pedestrians are particularly vulnerable if hit, but are also best placed to get early warning (aural and visual) and take evasive action. Pros & cons for motor vehicle occupants, cyclists & pedestrians are considered to balance out. Motorcyclists have the worst mix of (noise insulation from outside) plus (vulnerability if struck) plus (combination effect of fall at road speed if struck)						
			Bus passenger	0.3	0.5							
			Truck occupant	0.3	0.5							
			Motorcyclist	0.4	0.7							
			Cyclist	0.3	0.5							
			Pedestrian	0.3	0.5							
Debris velocity (m/s), where inundation occurs												
			Road User	> 5	0.5 to 5	0.05 to 0.5	< 0.05					
V ₁ (Source 11A)	Probability of death in the event of inundation of the road by a (largely loess in character) debris flow	P(death) if inundated with debris travelling at speed shown	Car occupant	1	0.4	0.1	0	Similar observation apply to those above for rockfall. Motor vehicles (particularly the more massive trucks and buses) would be expected to provide significant protection for low loess flow heights and speeds, but this may be countered by the possibility of more difficult escape if swept into the sea by higher and faster loess flows. As for rockfall, cyclists' and pedestrians' higher vulnerability if hit is considered balanced by greater ability to take evasive action, while motorcyclists have the worst mix of vulnerability factors.				
			Bus passenger	1	0.4	0.1	0					
			Truck occupant	1	0.4	0.1	0					
			Motorcyclist	1	0.6	0.2	0					
			Cyclist	1	0.4	0.1	0					
			Pedestrian	1	0.4	0.1	0					

**A2 APPENDIX 2: PAST LANDSLIDES IN THE PORT HILLS AND BANKS
PENINSULA**

Past Landslides in the Port Hills and Banks Peninsula

Introduction

Not many landslides in loess occurred during the 2010/11 Canterbury earthquakes, and where they did occur they generally comprised small (<100 m³) disrupted falls and avalanches of loess from steep slopes (adopting the terminology of Keefer 1984).

Several of the mass movements being investigated by GNS Science for Christchurch City Council are areas where the 2010/11 earthquakes caused significant cracking in loess, where the cracks are thought to relate to landslide processes, mainly coherent soil slides/slumps (Keefer, 1984) rather than shallow inelastic behaviour of the ground during shaking.

It is not well understood how these mass movements in loess will perform in the future, especially in the Class I areas (where the landslide, if it were to occur, could cause loss of life). The findings of work presented in this report suggest there is potential for earth/debris flows (a very mobile type of landslide where the debris resembles wet concrete) to occur from the loess slopes in these Class I areas.

Recent (past few decades experience) suggests such landslides are relatively small (< 100 m³), but there is good geomorphological and historical evidence of much larger landslides, including some that have killed people in Banks Peninsula. This appendix presents a summary of the historical and pre-historic evidence of landslides in the Port Hills and Banks Peninsula.

Landslide types

Historical landslides in the Port Hills and Banks Peninsula have mainly been due to rainfall (Harvey, 1976; Bell and Trangmar, 1987; Goldwater, 1990; Elder et al., 1991; Udell, 2013; and McSaveney et al. 2014). There have been five deaths from landslides, (mainly earth/debris flows in loess or loess derivative materials) in Banks Peninsula reported in newspaper articles 1870-1938 (compiled by E. McSaveney 2012). Two people were killed while walking or camping; and the other three people were killed in their homes.

One well documented landslide event that affected the larger area of the Port Hills was reported by Harvey (1976). A total of 519 landslides, mainly earth/debris flows in loess in the Port Hills were mapped after a rainstorm. The rain occurred over 5 days between 19-23 August 1975. A total rainfall of 126 mm was recorded at the Christchurch Gardens Gauge, with a maximum daily rainfall of 69 mm on 21 August 1975. A daily rainfall of 69 mm has an annual frequency of once every 5 years and the 5-day rainfall occurs about once every 2 years (based on McSaveney et al, 2014), indicating the rain was unexceptional.

A study of landslides in the Akaroa area by Tonkin and Taylor (2008) identified three main types of landslide affecting the area: 1) bedrock landslides; 2) Active gullies encompassing tunnel erosion, surface erosion and small- to medium-scale landslides (about 1 to 5 m deep and 3-10 m wide); and 3) large loess/bedrock landslides (5 to 15 m in depth and 100-300 m wide/long). Tonkin and Taylor (2008) suggest that the generally accepted ideas on slope instability on the Port Hills include: 1) soil creep/shallow landslides triggered by rainfall; 2) tunnel gully erosion; 3) large-scale landslides are absent and 4) bedrock landslides are

absent. Large-scale landslides and bedrock landslides were thought to be absent from the Port Hills, but present in the Akaroa area, because the climate in Akaroa is slightly wetter, and the materials more weathered than the Port Hills.

Landslide volumes

Harvey (1976) noted that most of the 519 landslides from August 1975 occurred in loess and mixed colluvium. Landslide volumes estimated using the mean data reported by Harvey (1976), range from a few tens to many hundreds of cubic metres. Estimated volumes of individual relict landslides (pre 1940) in loess and loess-derivative materials, such as colluvium in the Port Hills, were mapped by Townsend and Rosser (2012) from aerial photographs and field assessments. The distribution of 124 relict landslides, adopting the area depth relationships of Larsen et al. (2010) range from a few tens to tens of thousands of cubic metres. No landslides in the tens of thousands of cubic metres range have been documented in the Port Hills since European settlement

More recently, claims made to the earthquake Commission for landslip damage, over the period 1997 to 2012, were mainly triggered by rainfall (Udell, 2013; McSaveney et al., 2014). These claims generally relate to landslides with volumes of less than 100 m³.

A large earth/debris flow, predominantly in loess, occurred in Lyttelton during the 5 March 2014 rainstorm. The volume of this landslide is estimated to be 1,000-2,000 m³.

Factors contributing to past landslides

Bell and Trangmar (1987), based in part on the work by Harvey (1976), state that: i) most of the rainfall-induced landslides in the Port Hills area occurred on slopes inclined between 25° and 31°; ii) the angle of the back scarp varied between 31° and 45°; iii) most failures had rupture surfaces that corresponded to hydraulic boundaries e.g. loess/colluvial loess boundary; iv) the depth of failure was typically between 0.6 and 2.5 m deep (Bell and Trangmar, 1987) with a mean depth of about 1.0 m and length of 15-20 m (Harvey, 1976); and v) the landslides were generally translational in shape and their basal slide surfaces were sub parallel to the ground surface (Harvey, 1976).

Harvey (1976) found that slopes with relatively sunny (inferred to be drier) aspects had the lowest average failure slope angles, and shady (inferred to be wetter) aspects had steeper failure slope angles. However, most of the displaced debris (about 67%) came from landslides on the shady slope aspects. Results from slope stability back-analysis carried out by Elder et al. (1991) of several of the landslides mapped by Harvey (1976) suggest that the difference in slope angle between the sunny versus shady aspects was not particularly significant. The higher total volume of debris from landslides occurring on shady slope aspects would suggest that these landslides were larger in volume than those occurring on sunny slope aspects.

Elder et al., (1991) note that loess failures tend to trigger in the upper "S" (lower surface layer including topsoil, 0.2-0.7 m below ground surface) and "C" (compact layer 0.4 m to 1.3 m below ground level) layers. This is because the upper horizons are relatively weaker (in shear strength) than the underlying parent material, but principally this reflects a loss of capillary tension "suction" and the build-up of pore water-pressure above the relatively impermeable lower layers (Elder et al., 1991).

Potential earthquake effects contributing to future landslides

An initial assessment of the effects of seismically induced ground deformation and cracking caused by the 2010/11 earthquakes on the occurrence of localised landslides following rainfall, in the Port Hills was carried out by Udell (2013). Udell (2013) reports that there has been little difference in the numbers of claims made to the EQC for rainfall-induced landslide damage to dwellings following the 2010/11 earthquakes compared to those made before the earthquakes. This assessment is based on the number of claims made to the EQC for landslides triggered during the August 2012 rainstorm being comparable to those numbers made in response to pre-earthquake rainstorms in October 2000 and August 2006. These three rain events had 96-hour rainfalls with annual frequencies of about once every 5 years. The results reported by Udell (2013) are somewhat limited as:

- The August 2012 rainfall was unexceptional.
- There is no information relating to the volumes of the landslides that initiated the claims, and therefore the severity of the landslide hazards cannot be assessed, i.e. pre-2010/11 earthquake claims could have been made for relatively minor damage from relatively small landslides.
- Many areas of the Port Hills were not cracked during the 2010/11 earthquakes, and many areas only suffered superficial cracking and deformation unrelated to mass movement processes. Therefore, it would be unlikely that rainfall following the 2010/11 earthquakes would trigger more landslides and therefore claims in these areas. It is likely that the loess slopes in these areas were already cracked and fissured before the earthquakes, as such features, in loess, are quite common in loess.
- People were evacuated from the main areas where cracking caused by the 2010/11 earthquakes was thought to relate to mass movement processes (Massey et al., 2013). In the most affected areas (the Class I areas, Massey et al., 2013) many dwellings were purchased by the Canterbury Earthquake Recovery Authority and so it would be unlikely that claims would be made to the EQC in respect of land movement occurring after the 2010/11 earthquakes.
- It is too early after the 2010/11 earthquake to assess the long-term performance of the Class I mass movements with regards to rainfall. Initial inspections following the March 2014 rainstorm identified many small (less than 50 m³) landslides, of predominantly loess, had occurred in these areas, even though the rainfall in these areas was unexceptional.

Summary of landslides in the Port Hills

Most recorded historical landslides in the Port Hills have comprised relatively shallow (less than 5 m deep) and small (less than 100 m³ in volume) earth/debris flows, which have occurred in loess and loess-derived materials. Such landslides have occurred frequently and have resulted in many landslide claims to the EQC.

Results from geomorphological mapping suggest that large volume (>1,000 m³) relict landslides have occurred in the Port Hills, but that these have been relatively infrequent – one recorded since European settlement in c. 1840.

Such large landslides have occurred historically in the wider Banks Peninsula area, and have killed five people (in four landslides).

It is too early to assess how the slopes that were significantly cracked, as a result of earthquake-induced mass movement (particularly the Class I areas) during the 2010/11 earthquakes, will perform in the future.

References

Bell, D.H., Trangmar, B.B. 1987. Regolith materials and erosion processes on the Port Hills, Christchurch, New Zealand: Fifth International Symposium and Field Workshop on Landslides. Lausanne, A.A. Balkema. Volume 1: 77-83.

Elder, D. McG., McCahon, I. F., Yetton, M. D. 1991. The earthquake hazard in Christchurch a detailed evaluation. Report for the New Zealand Earthquake Commission. March 1991.

Goldwater, S. 1990. Slope Failure in Loess. A detailed Investigation, Allendale, Banks Peninsula. MSc Thesis, University of Canterbury.

Harvey, M.D. 1976. An analysis of the soil slips that occurred on the Port Hills, Canterbury, between 10-25 August 1975. Soil Science Society of New Zealand, Palmerston North, August 1976.

Keefer, D. K., 1984, Landslides caused by earthquakes: Geological Society of America Bulletin, v. 95, no. 4, p. 406-421.

McSaveney, M.J., Litchfield, N., Macfarlane, D. 2014. Canterbury Earthquakes 2010/11 Port Hills Slope Stability: Criteria and procedures for responding to landslides in the Port Hills. GNS Science Consultancy Report 2013/171.

Tonkin and Taylor Ltd. 2008. Slope hazard susceptibility assessment. Akaroa Harbour Settlements. A report prepared for Christchurch City Council. March 2008.

Udell, H. L. 2013. An initial assessment of the effects of seismically induced ground deformation on the occurrence of localised instability following rainfall in the Port Hills, Christchurch. Proceedings of 19th NZGS Geotechnical Symposium. Ed. CY Chin, Queenstown.

Locations of early landslides on Banks Peninsula reported in newspapers (1870-1923)

Eileen McSaveney

Landslides with fatalities

August 1870 – Little River road, somewhere near Akaroa (1 death)

July 1879 – bush at Pigeon Bay (1 death) (rain)

September 1904 - French Farm, Akaroa (1 death) (rain)

January 1923 - at Puaha, four miles from Little River (2 deaths) (flood/debris flow from breached landslide dam) (rain)

Other landslides

September 1870 – rockfall from cliff, Lyttelton Harbour, bay opposite the Pilot Station (Earthquake)

June 1881 – Tikau Bay, Akaroa (failure of landslide dam) (rain)

January 1884 – upper road to Lowry Bay and in gully three-quarters of a mile from Lowry Bay (rain)

May 1886 – small slip closed Sumner road traffic for a time

August 1886 – 1,000 ft high slip on headland between Port Levy and Pigeon Bay

August 1886 – wrecked Annandale Station at Pigeon Bay (eastern side of bay had many smaller slips) (rain)

July 1895 – Pigeon Bay (Holme's Bay side) (caused tsunami) (rain)

August 1895 – Pigeon Bay (wrecked house of Knudson) (landslide near wharf?) (rain)

July 1896 – house wrecked at Lyttelton (rain)

May 1899 – between Lyttelton and Governor's Bay? (boy trapped during attempted crossing of track of recent landslide)

July 1906 – house damaged at Little Akaroa Bay [NB There is no "Little Akaroa Bay", did they mean Little Akaloa Bay?]

March 1907 – rockfall - Sumner Road cliffs between Shag Rock and Middle Rock

July 1923 – slips at Lyttelton and at Salt's Gully (Lyttelton township) (rain) (eight years earlier at same location a landslide covered a cowshed, smothering eight cows)

Newspaper articles from 1870 to c. 1938

Banks Peninsula landslides

Papers Past online archive – compiled by Eileen McSaveney

LANDSLIDES WITH FATALITIES

Grey River Argus, Volume IX, Issue 717, 23 August 1870, Page 2

A man named Duerden has been killed by a landslip on the Little River road, near Akaroa. When found, his body was fearfully mutilated, both legs being broken in several places, his ribs smashed, and numerous other injuries, which must have caused instantaneous death. A man named Walker, living at Little River, had a narrow escape. He was conversing with Duerden, and saw the slip coming, but was overtaken by it, and buried up to the hips, fortunately receiving no injuries.

Timaru Herald, Volume XXXI, Issue 1491, 2 July 1879, Page 2

Christchurch, June 29. A man named William Bamford, while working in the bush at Pigeon Bay, was killed last night by a landslip. He was asleep in his tent at the time and was completely buried. A terrific easterly gale was experienced here last night, but fortunately no particular damage was done.

Wanganui Herald, Volume XXXVIII, Issue 11366, 23 September 1904, Page 7

THE WEATHER.

Gales in the South.

Landslip Fatality.

(Per United Press Association.)

CHRISTCHURCH, September 22.

A very severe south-west gale, with heavy showers of rain, raged last night and this morning, doing minor damage to trees and fences. The low-lying parts of the city and surrounding country were temporarily flooded. A landslip at French farm, Akaroa, killed a resident, Mr William Giddens, 70 years of age.

Auckland Star, Volume LIV, Issue 23, 27 January 1923, Page 7

BURIED UNDER LANDSLIP.

ONE KILLED TWO INJURED.

AN EXTENSIVE SLIDE.

(By Telegraph—Press Association.)

CHRISTCHURCH, this day. A big landslip occurred at Puaha, four miles from Little River, shortly after midnight, owing to heavy rain. A party of grass seeders was caught in the slips, and Griffiths Pidgeon, a married man, 30 years of age, was killed, and his brother, Frederick Pidgeon, a single man, and James Howard were injured. Howard had to be dug out, and was seriously injured.

The constable at Little River, in telephoning for assistance to dig the men out, stated that the debris extended for two miles. A party of constables has gone out.

Auckland Star, Volume LIV, Issue 24, 29 January 1923, Page 4

CANTERBURY LANDSLIDE.

HOWARDS BODY FOUND. MAN WASHED INTO LAKE.

(By Telegraph - Own Correspondent)

CHRISTCHURCH, Saturday.

The landslide at Puaha near Little River, dammed the waters of the creek, which follows the course of the Puaha Valley. This torrent broke through and swept everything before it. A whare containing a camping party which had been engaged in grass-seeding, was swept down the valley for a mile. One man was killed outright and his brother was seriously injured and had a very narrow escape from death. The third man is still missing, and is believed to have been carried into the flood waters of Lake Forsyth.

The names of the campers are as follows: Griffiths Pidgeon, aged 30, married, killed; Fred Pidgeon, brother—seriously injured; James Howard—missing. Howard's wife is living at Westport, from which place Howard arrived only yesterday.

The slide took place from the top the hill, and blocked the valley below, damming up the creek, which by that time was swollen into a roaring river. The force of the pent waters gradually broke down the resistance of the fallen earth, and with a tremendous rush and roar, the angry torrent swept down the valley.

The force of the current lifted the whare in which the camping party was sleeping and rushed it down the valley for a mile. The body of Griffiths Pidgeon was recovered this morning, and his brother was found to be very seriously injured. He managed to struggle to a whare situated further down the valley, the light from which had attracted his notice. The body of Howard has not yet been recovered. Possibly it is buried or the raging stream may have carried it into Lake Forsyth.

HEAVY FLOODS REPORTED

BRIDGES WASHED TO SEA. (By Telegraph.—Press Association)
CHRISTCHURCH, this day

The body of James Howard, the second man lost in the Little River landslide, was found on Sunday evening, covered with debris, in the centre of Puaha Creek, two miles from the camp and eight chains from the spot where Pidgeon's body was found. Howards was badly mutilated and almost unrecognisable. Howard's wife resides at Westport.

Rain was very heavy throughout Bank's Peninsula and floods are reported at various places, washing bridges out to sea. Over five inches in 24 hours were recorded at Akaroa.

OTHER LANDSLIDES

Cave near Sumner? – July 1875

Timaru Herald, Volume XXIII, Issue 1232, 21 July 1875, Page 3

The Lyttelton Times says:—The excavations that have lately been made have brought to light many curiosities, such as greenstone tomahawks, skeletons of Maoris, and different kinds of bones. The other day, on Dr Turnbull's section, was found amongst the soil, a bone of the Moa, which was pronounced by Dr Von Haast to be the right metatarsal (or lower leg bone) of a very small species of Dinornis. During the process of removing the soil from the base of the hills, skeletons of Maoris were found in different positions, one with his head on his knees, another with his arms stretched out; remains of what apparently were cooking utensils and places where fires, had been made. The general opinion of those who examined it was, that the locality had been originally a Maori camp, and that the people had been buried alive, probably through a landslip. The bones of young children were also found. There were four of five tomahawks, one a beautiful specimen of greenstone, which is now in the possession of the finder, Mr Murphy.

The Christchurch Star, Sunday Sept 3 1870

In a letter published in a morning paper, Dr Haast requests that all who have any information regarding the recent earthquake will communicate with him. We hear that the chimneys in Mr Rhodes' house on the Papanui Road will have to be rebuilt. Mr Rhodes' house at Purau has also been considerably damaged. Colonel de Renzie Brett writes as follows from Kirwee, Courtenay, on Sept. 1: "About a quarter-past six o'clock yesterday evening we experienced a severe shock of earthquake. It produced a rocking motion, which caused the dwelling house built of wood and roofed with galvanised iron to make a noise as if a heavy piece of ordnance were passing by over a pavement. I feel confident that had the house been built of stone or brick it would have been seriously damaged. The motion lasted about three seconds, and appeared to be from east west."

A Leeston correspondent gives the direction of the wave there as about south or south-easterly. He also notes that previous to the shock there was a low rumbling sound, which was followed by a vibratory motion. The time is given as about 25 minutes past six o'clock. No damage is recorded beyond a few breakages at the Irwell and Leeston hotels, and a few shaken chimneys.

The recent earthquake was very severely felt in the neighbourhood of the Pilot Station, Lyttelton Harbour. **It appears that several tons of loose overhanging rock were seen to fall into the sea on the side of the bay opposite the Pilot Station.**

A South Rakaia correspondent writes: On Wednesday evening at 19 minutes past six (by our time) we were visited by a very severe shock of earthquake, which seemed to pass from N.W. by W. to S.E. by E., and lasted nearly one minute, and could distinctly be heard for a considerable time afterwards. It was preceded by a rumbling or roaring, which became almost deafening, and then died away slowly. It shook the store belonging to Mr Middleton so severely as to stop the clock and displace a

quantity of goods, pitching jars,pots, and parcels from the shelves, and shifting bags of grain from the stacks. The horses which were feeding outside started away affrighted, and the whole neighbourhood was thrown into a state of confusion for some time. The evening was fine and moonlit, but a heavy gale rose about 9.30, which lasted till morning.

An Ashburton correspondent writes; "A severe shock of earthquake was felt here on Wednesday evening last at 25 minutes past 6. It was preceded by a loud rumbling noise, and resembled the earthquake of Saturday, June 5, 1869. It appeared to pass in an E.or S.E. direction. It caused much fear among the inhabitants here, for hitherto they had not felt any of the shocks that have been experienced farther north. I have not heard of any damage being done. Some two or three clocks were stopped at the time mentioned. A smart shock was felt at Waimate, about 6.15 p.m. It appeared to take a southwesterly direction.

The following items are from the Timaru and Gladstone Gazette of Friday last: A severe shock of earthquake was felt in Timaru on Wednesday evening last at about twenty minutes past six. The direction appeared to be from north to south. Several buildings appeared to be shaken, but no material damage has fortunately been done. At the Brown street brickyard several men were employed at the time in stacking bricks Preparatory to their being burnt; they were, however, disturbed in their work by some of the bricks falling down, and hearing the bricks knocking together, and afraid that there might be danger in their remaining in the kiln, speedily left it. A shed about fifty feet long, belonging to Mr Barnfrede, was also much shaken. The vessels in the roadstead also felt the shock. On board the Ottawa the vessel was thought to be dragging, but on observations being taken, it was found not to be so. As soon as the shock was over, groups were observed collected in various parts of the town, evidently expecting a repetition of the shock, and as might be supposed, rumours were rife as to several buildings being injured, but as is generally the case, turned out to be mere idle reports. We have heard of several extraordinary freaks having taken place, but which are hardly worth enumerating.

Our Temuka correspondent reports as follows: "This morning the inquiry was, Did you feel the earthquake?" and there was no mistake hut it was felt, and that pretty severely last night. About half-past six p.m. a tremendous rumbling noise was heard, and in a very few seconds the houses and buildings began to shake about in a manner that was certainly anything but pleasant. The motion lasted some seconds, giving unmistakeable evidence as to what it was, and causing the occupiers of houses to vacate the same with all possible speed. The first observation I heard on reaching the road was evidently from a son of the Sister Isle who observed "Faith, this is the first earthquake I ever saw, and I never saw such a big one in my life." But joking apart, the shock was pretty severe, and caused considerable alarm. Most of the brick buildings have sustained damage, and the new store erected by Mr Mendleson has been cracked in many places, rendering it necessary to secure the same by bracing it with iron; and Mr Collins shop felt the effects of the shock. A picture in Dr. Rayner's house was shaken from the wall and the glass broken to pieces, but I do not hear of any real serious injury being the result. A variety of Opinions are expressed as to the direction from which the earthquake proceeded, but I should imagine it was from the north-west and proceeded south east.

Our Waihi Crossing correspondent says: At about a quarter to seven p.m. a severe shock was felt in the neighbourhood of the Waihi Crossing, causing great alarm to the

inhabitants, and a sickening sensation was felt by them after the shock, as was plainly visible on their countenances as they flocked together to relate the circumstances. At the Clarendon Hotel the bottles and glasses rattled together on the shelves. It was preceded with a loud rumbling noise, and appeared to move from north-west to southeast. From Oamaru we learn that two very perceptible shocks were felt at about half-past six. Several substantial buildings the Bank of New Zealand among others were visibly shaken, but we have not heard of any actual damage. From Dunedin we learn that there was a smart shock at twenty minutes past six. It lasted for several seconds. The direction was from north to south. No damage done only rang bells and jingled glasses.

Landslide dam failure at Tikau Bay, Akaroa – June 1881

Otago Witness, Issue 1546, 25 June 1881, Page 9

A rather distressing occurrence in connection with the late storm (says the Christchurch Press) took place on the property of Mr A. C. Knight, Tikau Bay, Akaroa. An employe of Mr Knight was living with his wife in a small house near the creek, which it seems had been blocked up with a landslip, thereby causing a stoppage and allowing a large pool of water to get together. The heavy rain of Friday night swelled the creek into a raging torrent, and, the dam giving way, carried the house down the gully, breaking it to pieces with all its contents, the occupants barely escaping with their lives. The poor man not only lost all his clothes and furniture, but £18 in money, which was in his purse. While searching amongst the debris for his money, he discovered his watch, which he had left on a nail in the house, hanging on the branch of a tree, And, strange to say, the watch was going.

Landslides – Lowry Bay – January 1884

Evening Post, Volume XXVII, Issue 19, 23 January 1884, Page 2

[Wellington]

A very heavy landslip is reported on the upper road to Lowry Bay, entirely blocking it up, and compelling all traffic to deviate to the lower or tidal road. Our informant estimates that the work of clearing a passage must occupy several days even if a strong staff of men should be employed.

Two Italian fishermen had a very narrow escape from sudden death yesterday. They live in a small hut erected at the mouth of a deep gully about three quarters of a mile from Lowry Bay. Owing to the excessive rain of Monday, a heavy landslip occurred during the night in the gully just above this hut. The men were awakened by the rush of the earthy and rocky avalanche that was descending and absolutely brushing past their hut, but, strange to say, without injuring it, although had it been struck fair by any one of the massive boulders, several feet in diameter, which came down in regular volleys, it is morally certain that the building and its inmates would have been crushed to jelly. The two men listened in the utmost terror to the appalling sounds, which they supposed to indicate a tremendous earthquake, and momentarily expected to be dashed into atoms, but the landslip left them unhurt. In the morning they found

the face of the immediately adjacent country extraordinarily changed, and were devoutly thankful for their hairbreadth escape.

Star, Issue 5619, 15 May 1886, Page 3

Sumner.

TRAFFIC STOPPED BY A SLIP. [Special to the Star.]

SUMNER, May 15.

A slight slip has taken place on the Sumner road, which has stopped traffic for a time. It is still raining here (12.30 p.m.) Some parts of the township are completely flooded.

**Pigeon Bay landslide – August 1886
(NB Produced large wave)**

North Otago Times, Volume XXXI, Issue 6132, 19 August 1886, Page 2

CHRISTCHURCH.

August 19.

A serious landslip has occurred at Pigeon Bay, completely wracking Mr Hay's house, which afterwards caught fire. No lives were lost, all the family managing to make their escape. Every assistance was rendered by the settlers. The roads on the Peninsula are impassable, and to-night great damage was feared unless the rain abated.

Timaru Herald, Volume XLIII, Issue 3708, 20 August 1886, Page 2

THE PIGEON BAY LANDSLIP.

(By Telegraph.) Christchurch, Aug. 19.

Further details to hand with reference to the landslip at Pigeon Bay show that the whole of Messrs Hay Bros., Annandale Station, has been swept away. Mr Thomas Hay heard the slip coming about 9.15 a.m. on Wednesday. He called his men to take out the four children. Mrs Hay also had to be carried. They ran as fast as they could for the road. Thomas Hay stayed to see all out of the house, and then ran himself, the slip nearly overtaking him. Another slip followed, shifting the chimneys and setting fire to the house, and some time afterwards a third slip carried away the whole of the buildings into the sea and creek. The slips came from the top of the range about 1 1/2 miles from the house. The beach and the bed of the creek are strewn with debris, and about twenty men were working today picking up what they could out of the silt. Mr Hay estimates his loss at £8000. The weather is again thick and reigning. [sic]

Messrs Hay Bros. house, woolshed, and outbuildings, which were destroyed by landslip and fire at Pigeon Bay, were insured in the South British Office for £2600.

THE LAND-SLIP IN CANTERBURY.
(Christchurch Press)

The late continuous rain has been the cause of a disaster at Pigeon Bay, the result of which in a small way reminds one forcibly of the late eruptions in the North Island. Fortunately, however, no loss of life occurred, though had the accident happened at night or earlier in the morning, it is probable we should have had to chronicle a sad disaster. As it was the escape of Mr. Thomas Hay and his family from death may be regarded as almost miraculous. There are few of the older settlers who do not know the homestead of Annandale well. Here it was that some forty-three years ago Mr. Ebenezer Hay settled down, and it has since become one of the most noted of the estates of Canterbury. The house itself, which has been added to and modernised, as it were, since its first building, stood back from the road a little, the mountain spur rising at the back. It was not far from the shores of the bay, and when seen, as it was, by the writer not many months ago, was the beau ideal of a peaceful and happy rural retreat. Now all is desolation, not a vestige either of the house itself or the outhouses surrounding it being left. The destruction is complete, and so sudden was the calamity which overtook the family that it was with the utmost difficulty that they made their escape, merely with the clothes they were wearing at the time.

The letter sent by the messenger from Mrs. Hay to her relatives here contained a most graphic account of the disaster. Between eight and nine on Wednesday morning the men who were working on the farm heard a roar, and looking towards the hills which rise up at the back of Annandale, saw the mountain, as it were, rending in two over their heads, and a gigantic landslip coming down. The alarm was at once given, with praiseworthy promptitude and coolness, each one seized a child and rushed down the path from the house to the road. As they fled along in terror a second slip came down, crushing the house to atoms, and the debris fell all round the flying fugitives, so close to them that the fall of earth was, as it were, upon them. Fortunately, they were enabled to gain the road in safety, and ultimately took refuge in the store. In the meanwhile, the house, which had been flattened to the earth by the fall of the slip, took fire. This was caused by fires in different parts of the house, which were log fires, the one in the kitchen being raised up above a large colonial oven. So soon as the debris crushed on to the house the fire was thrown out in contact with the boards, and the remains of Annandale were destroyed altogether in this way. The family passing, scantily clad, through torrents of rain, ultimately managed to reach the hotel, wet through and almost exhausted from the terrible scene through which they had passed.

We were working in the creek," said Mr. James Hay, whom I met up to the knees in soft mud superintending the work of picking out the relics from the soil, "when I heard a most tremendous roar. We had been on the look-out for slips, and therefore were to some extent prepared. Those in the house ran for their lives, and as I went at top speed towards the house to aid I looked up. There above me, coming down the mountain side at railroad speed was a wall of earth some forty or fifty feet high throwing up as it came high in the air a kind of spray. I thought at first it was an

eruption. We all got out of the house and down to the bottom by the fence. As the mass of earth came on it struck a very strong fence which we had put up above the house, breaking the 6 x 4 posts about off like matches. This I think prevented it carrying away the house. I then rushed up to the house to see if all were out, and supposing they were so turned to leave, when just then I saw the little head of one of the children. This was a little boy about two years old who had been into the store room taking the sugar. I grabbed him and turned to run. As I did so I heard a second slip coming, and had hardly got away when it came with a rush and a roar, right on to the house crushing it as one would an eggshell. So close was it behind me that I felt the spray of the earth striking me in the back as I ran. The house then took fire, and burned for quite two hours. The two eldest of the youngsters ran themselves, and we managed to get the rest out and away on to the bridge over the creek only just in time to see our home disappear as if it had never existed. The gardener had a narrow escape. He was in a small shanty in the garden and heard the roar. He started out and had hardly gone a chain before the shanty was buried under ten feet of earth. We lost nine dogs and about fifty sheep. Some of the carcasses of the latter we have found in the soil. By the way a most singular occurrence took place with regard to one of the dogs. The first slip buried him completely, but after the second one I was surprised to see him join us on the bridge. To give you an idea of the way in which the various things in the house were scattered, continues Mr. Hay, "We found my brother's purse containing £18 down by low water mark. This had been placed in a drawer in one of the rooms. The heavy safe was also carried down, to low water mark, and stranger than all we found the kitchen store and the kettle on it near the safe."

The insurances amount in the whole to £2620, distributed as follows :— £1500 on the dwellinghouse, £400 on the woolshed, £65 on the dairy and cheese house, £135 on the slaughter-houses, £20 on the men's house, and £500 on the furniture. All these insurances are in the South British Company.

Te Aroha News, Volume IV, Issue 169, 11 September 1886, Page 5

A TERRIBLE LANDSLIP

DESTRUCTION OF A CANTERBURY HOMESTEAD.

Narrow Escape of Sixteen Persons.

The late continuous rain has been the cause of a disaster at Pigeon Bay, which has swept away completely one of the oldest residences in Canterbury, and converted what was a charming spot into perfect desolation. Fortunately, however, no loss of life occurred, though, had the accident happened at night or earlier in the morning, it is probable we should have had to chronicle a sad disaster. As it was the escape of Mr Thomas Hay and his family from death may be regarded as almost miraculous. There are few of the older settlers who do not know the homestead of Annandale well. Here it was that some forty-three years ago Mr Ebenezer Hay settled down, and it has since become one of the most noted of the estates of Canterbury. The house itself which has been added to and modernised, as it were, since its first building, stood back from the road a little, the mountain spur rising at the back. A letter sent by Mrs Hay to her relatives in Christchurch contained a most graphic account of the disaster. Between eight and nine on Wednesday morning, 18th August the men who were working on the farm heard a roar, and looking toward the hills which rise up at the back of

Annandale, saw the mountain, as it were, rending over their heads, and a gigantic land slip coming down. The alarm was at once given, and with praiseworthy promptitude and coolness, each [each] one seized a child and rushed down the path from the house to the road. As they fled along in terror a second slip came down crushing the house to atoms, and the debris fell all around the flying fugitives, so close to them that the fall of earth was as it were upon them. Fortunately they were enabled to gain the road in safety, and ultimately took refuge in the store. In the meanwhile the house, which had been flattened to the earth by the fall of the slip, took fire. This was caused by the fires in different parts of the house which were log fires, the one in the kitchen being raised up above a large colonial oven. So soon as the debris crushed on to the house, the fire was thrown out in contact with the boards and the remains Annandale [Annandale] were destroyed altogether in this way. The force of the slip may, be imagined when it is stated that the remains of the furniture, &c, were swept right out into the bay.

The family than [sic] made an attempt to get round to the hotel, but owing to the large land slips which had fallen on the road between the hotel and the store, they were unable to do so. The only method by which they could reach the shelter of the hotel was by boats. This, owing to the sea running in the bay, was a work of some danger. Added to this the rain was descending in torrents, and they possessed little or nothing in the shape of covering to keep out the wet. Ultimately they managed to reach the hotel, wet through and almost exhausted from the terrible scene through which they had passed. Once at the hotel Mr and Mrs Bridges did all in their power to make them comfortable. It may be noted that there were at the time of the accident some sixteen persons at Annandale including Mr and Mrs Hay and family and those employed on the farm. The other settlers in the Bay were so much alarmed after the calamity that they too left their houses and sought refuge in the hotel.

Otago Witness, Issue 1814, 27 August 1886, Page 15

THE PIGEON BAY LANDSLIP.

EXTRAORDINARY EXPERIENCES.

An interesting account of the landslip in the Pigeon Bay district is given by the special reporter of the Christchurch Press, who says : —

The scene along the coast was exceedingly fine, the waves beating against the rockbound shore with great force, and sending up clouds of spray. An excellent view of what is known as " The Blow Hole," close to Port Levy rocks, was obtained. This is a cavity in the rocks open to the sea, with an orifice on the landward side, through which the spray is sent high in air with great violence. Yesterday it was in full operation, and resembled one of the geysers in the North Island, the column of spray being some 30ft or 40ft high.

As we steamed slowly down Pigeon Bay the effects of the late rains were noticeable on either side. The face of the mountains sloping down to the sea were scarred deeply in numerous places with heavy slips, many tons of earth, in parts taking with them trees, having fallen on the beach. Of course the scene of the late disaster was the one to which the eyes of all on board turned at once, and as we drew near the full extent of what had occurred was enabled to be realised. Where once was a beautiful garden,

with well-appointed house, stables, dairy, wool shed, and the usual outbuildings of a large farm, was now a blank. The steamer having moored to the wharf, I set off on an

INSPECTION OF THE SCENE.

To reach this by way of the road was, as I subsequently found out, a work not only of difficulty but also in parts of danger. Once on terra firma, my troubles were by no means over, as the rain had almost entirely demolished the road, and what was left was simply quagmire. However, after a little trouble, I reached the bridge over the creek, the creek opposite where Annandale once was, and I will now endeavour to describe

WHAT THE SLIP LOOKED LIKE.

From where I stood looking up the mountain, some 1300 ft or 1400 ft high, the whole of the centre of the face, from top to bottom, was scarred with a great wide rent. At the top was a cup-like crater, as if the top of the mountain had fallen in and pushed out the soil underneath. With the cloud of mist hovering about the top of the hill, and the wide rent made more conspicuous by the chocolate colour of the soil, there seemed to me to be a singular resemblance to the rent in Tarawera — a resemblance which the steam-like appearance of the mist made more complete. This rent, down which the hundreds of tons of soil which overwhelmed Annandale travelled on that eventful morning with lightning speed, is about 100 or 150 ft wide. The hill rises behind the spot where the house is, but is not particularly steep until near the top. A clump of bluegums slightly to the right of the track of the slip, and therefore not exposed to the full force of it, one solitary walnut tree, and another bluegum near the bottom of the garden facing the road, are all that remains of a highly cultivated fruit and flower garden and 10 buildings, including a thirteen - roomed house and large wool shed. The site occupied by these now resembles nothing so much as a newly ploughed field with fragments of debris of all kinds mixed in the soil. At the spot where the house stood there is now from 12ft to 15ft of earth piled up, and at the bottom by the road it is some 3ft or 4ft above the 6ft fence. Beyond this latter, and covering the 8ft stone wall which divided the garden, the debris of the slip has gone right out into the bay, reclaiming the land from the sea for some yards below low water mark. Some idea of the force with which the mass of earth came down the hill may be gathered from the fact that the large wool shed referred to was taken bodily some chains and hurled into the creek, the massive timbers being splintered up, and the whole fabric dispersed like a house of cards. The creek is now filled with remnants of timber, iron, &c, whilst the shores of the bay from opposite Annandale to Holmes' Bay is also strewn with the wreckage of the house, furniture, &c. The scene is one of the utmost desolation. At one part was to be seen a quantity of household goods, books, and clothing, heaped together amidst the soil; in another, scattered along the beach was a mass of every conceivable article, strewn far and wide, as though some demon in a fit of destructive rage had hurled them right and left. When it is remembered that the house stood some 40ft above low water mark, and some four or five chains distant therefrom, some idea may be formed of the enormous amount of earth which fell in so short a time. Having endeavoured to convey an idea of the scene as it presented itself to me, let me note some of the

INCIDENTS OF THE EVENT.

"We were working in the creek," said Mr James Hay, whom I met up to the knees in soft mud superintending the work of picking out the relics from the soil, " when I

heard a most tremendous roar. We had been on the look-out for slips, and therefore were to some extent prepared. Those in the house ran for their lives, and as I went at top speed towards the house to aid I looked up. There, above me coming down the mountain side at railroad speed, was a wall of earth some 40 or 50 feet high, throwing up, as it came, high in the air, a kind of spray. I thought at first it was an eruption. We all got out of the house and down to the bottom by the fence. As the mass of earth came on it struck a very strong fence which we had put up above the house, breaking the 6 by 4 posts short off like matches. This, I think, prevented it carrying away the house. I then rushed to the house to see if all were out, and supposing they were so, turned to leave, when just then I saw the head of one of the children. This was a little boy about two years old, who had been into the store-room taking the sugar. I grabbed him and turned to run. As I did so I heard a second slip coming, and had hardly got away when it came with a rush and a roar, right on to the house, crushing it as one would an egg shell. So close was it behind me that I felt the spray of the earth striking me in the back as I ran. The house then took fire and burned for quite two hours. The two eldest of the youngsters ran themselves, and we managed to get the rest out and away on to the bridge over the creek only just in time to see our home disappear as if it had never existed. The gardener had a narrow escape. He was in a small shanty in the garden and heard the roar. He started out, and had hardly gone a chain before the shanty was buried under ten feet of earth. We lost nine dogs and about fifty sheep. Some of the carcasses of the latter we have found in the soil. By-the-bye, a most singular occurrence took place with regard to one of the dogs. The first slip buried him completely, but after the second one I was surprised to see him join us on the bridge. He was so coated with the soil that until we washed him we had no idea which of the dogs it was. What was the roar like? " says Mr Hay in answer to a question. "Well, I can hardly say. It was a most unearthly noise, and so loud that all the people in the bay heard it and ran out of their houses, thinking there was an eruption on the mountain and that an earthquake was about to take place. To give you an idea of the way in which the various things in the house were scattered," continued Mr Hay, " we found my brother's purse, containing £18 down by low water mark. This had been placed in a drawer in one of the rooms. The heavy safe was also carried down to low water mark, and stranger than all, we found the kitchen stove and the kettle on it ! near the safe."

Later.

The following additional particulars of the extraordinary landslip at Pigeon Bay were supplied by a resident to the Lyttelton Times :—

The women and children hurried down the lane, and over the bridge, to the store, and all were safe there before the fourth and dreadful avalanche. Mr Scott now rode down the main road. He saw the wreck. He heard the roar. He spurred his horse, and just cleared the bridge as the fourth avalanche came down with deafening sound, carrying the large wool shed, borne on cubic yards of liquid mud, right across the main road, into the creek above the big bridge, and hurling the burning house over the sea wall on to the sea beach below, obliterating every trace of the once extensive Annandale. The main road was now impassable. A pedestrian climbed up the hillside, just above the dreadful gully, and describes the scene as being awful. He climbed to the hilltop, above the slip, and I came down on the Holmes' Bay side, only to find himself hemmed in there. He describes the starting place as being like what he pictures the crater of a volcano to be. A huge precipice, about 80ft long and 30ft deep, opens down to a small table land, about the eighth of an acre in extent. The hillsides are all

worn bare by the water. There are several smaller slips into the large one. A roaring sound like Niagara preluded a stream of liquid mud. The force of the fourth avalanche may be imagined, when it shook the store, 400 yards away, like an earthquake. At that moment several people were being conveyed from Feirrie Glen to the hotel in a boat, and the amount of mud forced into the sea on this occasion caused quite a tidal wave to sweep over the bay, and if the boat had not just reached the island it would probably have been swamped. The beach presented a most lamentable appearance. Timber, trees, grass seed, &c, were piled up and floating about as if two vessels had been wrecked in the bay.

Taranaki Herald, Volume XXXV, Issue 7152, 24 August 1886, Page 2

HEAVY FLOODS DOWN SOUTH.

THE LANDSLIP AT PIGEON BAY. Tue [sic] floods in Canterbury have done enormous damage, and the roads will not be passable for the coach for some time. There are tremendous slips everywhere, and though fifty or sixty men are at work they can make little head way. Tho disaster at Pigeon Bay is the most serious one. The whole top of the hill above Messrs Hay Bros. homestead slipped on to the house, woolshed, and offices, carrying them out to sea.

Sergeant Brooks, who had visited the scene of the landslip at Pigeon Bay, supplied the following :—About 915 on Wednesday morning Mr. Thomas O. Hay, Mr. Robert Hay, Mr. Husband, and three station hands were cleaning away the mud that had washed into the house on the previous night, when they heard a noise, and looking up the hill at a distance of about a mile they saw a landslip coming straight towards the house, and Thomas Hay sang out, "All hands clear and run." Some ran into the house, where were Mr. James Hay and Mrs. Robert Hay with four children. The station hands carried a child each. Mr Robt. Hay and Mr Husband carried Mrs. Hay out of the house, making all haste to get clear of the slip. Mr. T. Hay was the last to leave, staying to see that there were no people left in the house. The slip was close on to his heels when he got to the road. For a short time the slip stopped, a portion of it resting against the house, but only for a minute, when it started a second time, twisting the chimneys of the house, which then took fire. A short time after, and while the house was still burning, a third slip came, carrying the large woolshed, stables, outbuildings and dwelling-houses of the station hands with the burning residence of the Messrs Hay Bros, a distance of 200 yds from where they originally stood, across a road and a creek on to the sea beach, leaving the whole corner section quite bare, the only thing left to mark the spot being part of the fowl house. The sea beach is all strewn with wreckage from the buildings, from amongst which was found the iron safe containing the papers of the Messrs Hay Bros. Some sacks of cocksfoot which were stored in the shed were found on another section 400 yards away. The Messrs Hay Bros. reckon their loss at fully £8000. The house and furniture were insured in the South British for £2000.

Mr. Ebenezer Hay, who was the first settler in Pigeon Bay, came to Wellington from Scotland in 1840, and after living for three years in Wellington, went to Pigeon Bay, where he built his first hut near the creek. He afterwards built a house on the site of that which has just been destroyed, which was erected about 14 years ago. The latter was a large two-storeyed building, and was surrounded by all the buildings required for carrying on the work of the station — a wool-shed, stable, slaughter-house, dairy, wash-house, and other structures, forming almost a small township. These stood on a

slope about 120 yards from the Bay Creek, which ran past the front of the house, and about 180 yards from the sea, above which they stood 50ft. At the back of the House the ground ascended with a gradual slope to a precipitous knob, about a mile distant from which a small creek found its way to the sea. The slip was evidently caused by the breaking off of a portion of this knob, which rolled down the water-course, destroying everything in its path.

From the situation of the house, it might have been supposed to be entirely safe from all danger of landslips, while Mr. James Hay's residence, the Glen, which has escaped, appeared to be in a far more dangerous location. It is fortunate that the catastrophe did not occur at night, when the occupants of Annandale were sleeping. Had it done so, not a single person would have escaped with life.

The startling event seems to have caused quite a panic in Pigeon Bay, as none of the residents could be sure that their houses were safe from a similar fate. No particulars are to hand as to any loss of live-stock that may have been occasioned, but it is supposed that this was not very great.

The rains have caused an immense amount of damage to the public roads and to private properties there. In some places the main road has been carried away bodily, pedestrians having to cross private properties to continue their journey. Many of the settlers were on watch all night dreading landslips. Many chains of fencing and acres of good land have been destroyed. Several narrow escapes of loss of life have occurred.

Wellington, August 24. — It is still raining here more heavily than usual. There has only been one day without rain this month, and not three that could be called fine. No damage has been reported as yet, but the streets of the town are in fearful condition, and great complaints are being made against the city authorities.

Taranaki Herald, Volume XXXV, Issue 7153, 25 August 1886, Page 2

The stormy weather which has prevailed during the past month has been very severely felt in the South Island, and the accounts in our exchanges of the destruction there is to property are very sad to read. There have been several land slips, but the one in Canterbury has been the worst. Ordinarily, when a landslip is referred to, is [sic] is supposed to represent a fall of so many tons of earth, but the Pigeon Bay landslip, which, last week destroyed Annandale, the homestead of Mr. Thomas Orr Hay, cannot be estimated by the number of tons— it can only be adequately measured by its number of acres. To give some idea of the power of the landslips, Mr. Hay states that he picked up his safe on the beach, half-way high and low -water marks, and about a couple of chains from the creek. It weighs half a ton, would take four or five men to roll it over. The big posts of the stock-yard, which were as thick as a man's body, were cut off at the ground as pieces are cleared off a chess-board. Mr. Hay in describing the landslip says. "My brother timed the fall of the third slip. I reckon that the hill is 1300 or 1400 ft high and a mile away, and my brother found the slip was just a minute and a-half from the time it started till it reached the sea. The biggest fall came even quicker than that. I don't know how many acres of the sea must have been filled up, but it must be three or four acres, and besides there is all the stuff that is left round the house."

Hawera & Normanby Star, Volume VIII, Issue 1412, 30 August 1886, Page 2

TELEGRAMS.

(PER UNITED PRESS ASSOCIATION.)

CHRISTCHURCH, August 30.

On Friday the captain of the steamer Akaroa, when passing the headland between Port Levy and Pigeon Bay, discovered a big slip on the northern side of the mountain, extending from the summit to the base, a height of 1000 feet. A strange rumbling heard at Lyttelton on Friday morning is supposed to have been caused by the slip.

Hawera & Normanby Star, Volume VIII, Issue 1414, 1 September 1886, Page 2

"Puff," in the Wellington Press : — "

Great landslip between Port Levy and Pigeon Bay ! The face of the mountain 1000 feet high tumbled into the sea ! Why skip ye so, ye little hills ! Banks Peninsula on the rampage ! Flopping about anyhow ! What does it mean ? There's been nothing like it since the first settlers arrived ! No ; the fact is there have been the heaviest spring rains for 25 years, and the Peninsula being stripped of the bush, the steep places have given way ! That's what will happen periodically in all the mountainous parts of the colony ! Only another of the evil results of wanton destruction of natural forests ! Oh yes, the colonists will have to pay pretty dear for their folly before they have done with it !"

Many years later

Evening Post, Volume CXXXV, Issue 59, 11 March 1943, Page 5

MR. EBENEZER HAY

(P.A.) CHRISTCHURCH, This Day.

The death has occurred of Mr. Ebenezer Hay, of Annandale, Pigeon Bay, at the age of 67. A well-known runholder and sportsman, he was a son of Mr. and Mrs. T. O. Hay, and was named after his grandfather, who sailed from Glasgow in the ship Bengal Merchant in 1839. Arriving in Wellington in January, 1842, his grandfather, with Captain Sinclair, built a small vessel on the Petone beach, and in it they set out to explore the South, Island, finally deciding to settle at Pigeon Bay. The old Annandale homestead, including the woolshed and outbuildings, was carried away by a huge landslide and the present homestead was erected in 1884. Originally the estate comprised some 7500 acres, carrying upwards of 10,000 sheep and 1500 head of cattle.

Caves at Moncks Bay - Report: April 1890

New Zealand Tablet, Volume XVII, Issue 51, 11 April 1890, Page 19

WATSONVILLE, SUMNER.

(From an occasional Correspondent.)

About two miles from Sumner proper, and opposite the rough-level tract of land, about forty-five acres in extent and known as Monck's Flat, there is a bay or broad flat valley that contains close upon fifty acres. The estuary formed by the union of the river Heathcote and the river Avon fronts this valley, and the hills on each side shade it completely from the east and south-west winds. The valley formerly formed one property and then belonged to the late Mr. Watson.The next valley towards Sumner belongs to Mr. Monck. Several months ago, when some men were getting stones for the roads from the face of a steep rock that is on Mr. Monck's property, and at the end of the spur that divides the two valleys, a cave consisting of two dome-shaped compartments, was suddenly and unexpectedly discovered. The apex of the outer cave, which now consists of but half a dome, is about eighteen feet high, and the apex of the inner cave is from eight to nine feet. The outer cave is also about twenty feet long, and fifteen broad, while the inner cave is nigh forty-two feet long and twenty-four wide. To advance into the inner cave—inside of which it is so intensely dark that to see anything a person must be provided with one or more candles — it was necessary to crawl on the knees, as the entrance is not more than two feet high. But Mr. Monck has cut a deep central trench, and there is now a walk from one end of the cave to the other. On the floor there was an accumulation of ashes and shells several yards in depth. This accumulation proves that the cave must have been a famous camping place for a very long time before the entrance to the outer cave was centuries ago accidentally covered and concealed by an earthquake or a landslip. The cave, like the larger one known as the Maori Point Cave, was originally simply an air bubble in a stream of lava, and it is very probable that there are several undiscovered caves at Sumner. Many articles of interest, such as a canoe paddle, and a bailer fashioned from a solid block of wood were found in the caves. Sinkers, fishing-hooks, and spears, parts of wooden combs, knots of skinned native flax, greenstone chisels and axes and a variety of bones were also discovered. In one place a large quantity of beautiful black curled glossy, human hair was found. This hair seemed as perfect as hair recently cut from the head of some Maori. Mr. Monck was anxious to preserve the caves as when first found, but when their discovery became known a whole army of persons rushed from the city of the plains, and these Cockney geologists soon destroyed what centuries had spared.

Another landslip at Pigeon Bay (large wave) July 1895

Grey River Argus, Volume XXXVII, Issue 9182, 11 July 1895, Page 3

NEW ZEALAND TELEGRAMS

(PER PRESS ASSOCIATION)

Dunedin, July ,9.

Reports from Banks Peninsula state that most of the roads are blocked with landslips, caused by recent heavy rains.

A landslip of extraordinary dimensions at Pigeon Bay started at six o'clock, and rushed into the sea with such force as to raise a tremendous wave, which swept across Pigeon Bay (from Holme's Bay side), and swamped the road to a distance of nearly a mile. A number of families living in Pigeon Bay locality have left their homes; fearing further slips, the hills being dangerously fissured.

Timaru Herald, Volume LVIII, Issue 1803, 11 July 1895, Page 3

Reports from Bank's Peninsula state that most of the roads are blocked by a landslip caused by the recent heavy rains. Last night there was a slip of extraordinary dimensions at Pigeon Bay. The slip started at 6 o'clock and rushed into the sea with such force as to raise a tremendous wave which swept across Pigeon Bay (from the Holmes Bay side) and swamped the road for a distance of half a mile. A number of families in the Pigeon Bay locality are leaving their homes, fearing further slips, the hills being dangerously fissured.

Yet another landslip at Pigeon Bay August 1895

Star , Issue 5326, 2 August 1895, Page 3

LANDSLIP.

A HOUSE CARRIED AWAY.

[from our own correspondent]

AKAROA, August 2,

This morning another large landslip occurred at Pigeon Bay, which carried away Mr Knudsen's house and completely blocked the road to the wharf, to which communication can only be made at present by boat at high tide.

Wanganui Herald, Volume XXIX, Issue 8615, 3 August 1895, Page 2

Christchurch. 2nd August.

By a landslip at Pigeon Bay this morning the house of Knudson was swept away, and the road to the wharf completely blocked. No lives were lost, Knudson having removed his furniture and family about three weeks ago, when fissures appeared in the hillside above his place.

Star, Issue 5328, 5 August 1895, Page 4

The Landslip.

FURTHER PARTICULARS.

The steamer Jane Douglas ran an excursion trip to Pigeon Bay yesterday for the purpose of affording anyone sufficiently interested a view of the huge landslip which took place in the bay on Friday morning last. Between 80 and 100 persons, including a representative of this journal, availed themselves of the opportunity. The slip was not altogether a surprise to the residents, for during the heavy and continued rains of last month deep fissures had been noticed on the hill, and the settlers whose houses were below these had removed their belongings and left their homes. When the weather broke it was considered that all was then safe, and that the ground would settle down, as it has done in many other places, but last week's heavy rain and snow caused the worst fears of the residents to be realised. Steaming up Pigeon Bay harbour, numerous small slips, chiefly on the eastern side of the bay, were observable, and on nearing the wharf the heavy slips of three weeks ago came within sight. That which occurred almost abreast of the wharf, when the debris was hurled into the sea with sufficient force to create the huge wave which swept across the harbour (a distance of fully half a mile), was viewed with considerable interest. The site of the disastrous slip of nine years ago, when Messrs Hay's fine homestead was completely wrecked, also attracted attention, for on the same spot another slip had recently occurred. Here a portion of a plantation of gums had been uprooted and swept with the debris into the sea. All these huge slips, large as they undoubtedly were, pale with utter insignificance when compared with

LAST FRIDAY'S DISASTER.

Reaching the wharf, the majority of the party at once commenced the work of inspecting the ruins. The writer was fortunate in early obtaining the assistance of Mr Frank Dunkley, the young man who narrowly escaped losing his life by the slip. With the idea of obtaining a better view, the high hill from where the slip started was scaled, and on the climb up it was observed that for several chains on the northern side of the slip the earth showed deep fissures, which might at any time come away, and probably would do so in the event of heavy rain or frost. Arriving at the uppermost end of the slip, the sight well nigh baffles description. From here right into the sea, a distance of probably 850 or 900 yards, is one mass of ruin, fences being swept away, great slumps of trees lying strewn about, growing trees being uprooted and hurled in every direction amongst the clay. It is only in looking down into the great gulf which has been formed that any idea can be got of the magnitude of the disaster. Fully 900 feet wide; with an average depth of 50 feet, and for a length of about 2000 feet is the extent of the country that has suffered. In some places the depth extends to 70 feet, and in many places marks resembling huge plough furrows are visible where the volume of earth has forced its way down the hill. Little hillocks with their accompanying valleys have been formed here and there, while in many places the surface soil and even the snow are still visible, having simply slid perhaps a hundred yards from their previous position.

MR KNUDSON'S HOUSE,

which was a substantially built dwelling of five rooms, was situate on a spur dividing two gullies. The slip started on Mr Hay's land, and coming on into Mr Knudson's section, divided at the top of the spur behind the house. The volume was of such extent, however, and moved with such rapidity that a portion of it swept over the spur, and in its course demolished the house and garden. A portion only of the matchwood left was to be seen, for some of the timbers and sheets of galvanised iron were swept into the sea below. Just below where the house stood the debris again left the spur and

joined the main volume in the gullies, and crossing the road swept into the sea close to what residents of the Bay call The Island. At its entrance into the water the face of clay, &c, was estimated to be fully seventy feet high, and fences, trees, &c, have been forced over the mud flats of the bay for hundreds of yards, so that at low tide it is almost possible to reach the other shore on dry land.

AN EYE WITNESS.

The Rev A. Blakiston, who was an eye witness to this awe-inspiring scene, has kindly supplied a few particulars. He states that at about 9.15 a.m. his attention was directed to sheep, horses and cattle running out of the gullies. He then saw that a slip was taking place. The surface about half-way up what subsequently turned out to be the slip appeared to be sliding down the hill, taking with it trees, just as they stood. Mr Blakiston called to one or two neighbours, and as they stood watching the scene, the whole hill appeared to tremble and shake, and then immediately, with a loud rumbling noise, the millions of tons of earth commenced to move. With one terrific rush the whole mass of earth, taking before it anything which came within its course, was hurled into the sea. The young man Dunkley was standing close to the water's edge, watching the small slip, when Mr Blakiston and others called to him. He had "a distance of fifty or sixty yards to run, and only just managed to get away from the line of the avalanche when it swept; at a great rate over the ground where a second or two before he had stood. The debris appeared comparatively dry, and residents of the Bay, who can now claim a good deal of experience of these matters, state that all previous slips have been much more sloppy.

Great sympathy is felt for Mr Knudson and his family. Mr Knudson has resided at the Bay for thirty-one years. He has a family of nine—five daughters and four sons—and the homestead which was so quickly demolished on Friday has been his home for over a quarter of a century.

Messrs A. Cuff and Co. very generously devoted the net proceeds of yesterday's trip of the Jane Douglas to the fund which is being organised for the assistance of the sufferers by the slip.

Star , Issue 5329, 6 August 1895, Page 3

The Pigeon Bay Landslip — The special trip run by the Jane Douglas for the benefit of the sufferers by the landslip at Pigeon Bay resulted in the sum of 8£ 2s 6d being taken. The whole of this will be handed over to the relief fund by the Lyttelton and Peninsular Steamship m Company.

Landslide at Lyttelton – July 1896

Poverty Bay Herald, Volume XXIII, Issue 7689, 29 July 1896, Page 2

Friday's Christchurch Press gives an account of the landslip at Lyttelton, briefly mentioned in our telegrams last week. A two-storied semi-detached house, containing about six rooms in each division, the property of Mr John McIntosh, of the Peninsula, had the back wall smashed in by a heavy slip. One division of the house was occupied by Mrs Adams and her family, and the other division by Mrs Fenton and a large family, including several grown-up daughters. The hill behind the house is very steep,

and, as it faces the south-west, small slips have been frequent, but hitherto they have not done much damage beyond piling up against the back wall of the house and smothering whatever happened to be in the back yard. On Thursday morning, however, a considerable area of the surface, which had become sodden with water, slipped off, and coming down with great force smashed in the back of the house and carrying all before it broke through into the front room. As may be imagined the inmates received a great fright. Every article of furniture in the back rooms was smashed and many of those in the front part of the house. The back rooms of the houses are frequently occupied as bedrooms, but on this occasion they were fortunately unoccupied. Had anyone been sleeping there they must have been killed as the back wall was driven in and the rooms filled to the ceiling with heavy wet clay. All exit from the house by the back way was cut off, and, as the stairs were smashed and filled up with, earth, the inmates had considerable difficulty in making their escape. Eventually a rope was obtained, and the occupants were lowered out of the top windows. The morning was pitch dark and the rain coming down in torrents, and, as may be imagined, the experience was a most unpleasant one. Added to the wretchedness was the doubt that at any moment another and larger slip might come down and hurl the building out on to the street or possibly over the cliff on the other side. At the first appearance of daylight carts were obtained, and the remains of the wrecked furniture were removed elsewhere, that from upstairs having to be lowered through the windows by ropes.

Star, Issue 6493, 23 May 1899, Page 2

AN ALARMING EXPERIENCE.

A young man, one of a party that walked from Christchurch to Governor's Bay on Sunday, had an alarming experience. When nearing the main road leading from Lyttelton to the bay the party left the Pass Road, and intended taking a short cut on to the road below. They ran down the hill near the spot where the recent landslip occurred, and one of the party attempted to cross the clay surface over which the slip had passed. He had not gone far when he began to sink, till nothing, but his head remained in view. His mates went in search of assistance, and found a resident, who accompanied them to the spot. By the aid of clods placed as stepping-stones the rescuers were able to reach the entombed youth. Their efforts to pull him out of the semiliquid clay were unsuccessful, and it was only by the aid of a large fork that the unfortunate man was dug out of the trap into which he had fallen. But for the loss of one of his boots he was none the worse for his adventure.

Northern Advocate - 7 July 1906, Page 2

A Landslip Ruins a Home.

TONS OF EARTH AND ROCK.

Christchurch, July 7.

A rather serious landslip occurred at Little Akaroa Bay, Banks Peninsula, on Tuesday night, about seven o'clock. Some tons of earth slid down the mountain side and came in contact with a dwelling-house and some refreshment rooms kept by an elderly couple named Bennett, their home being completely ruined. One part of the house was turned round, and the other was driven partly over some rocks. Tons of mud, stone, and other matter were accumulated round the house and garden.

Auckland Star, Volume LIV, Issue 179, 28 July 1923, Page 7

LANDSLIDES IN LYTTTELTON.

SLIPS IN THE HILLS.

(By Telegraph.—Special to "Star.")

CHRISTCHURCH, this day.

Continuous rains during the month have caused a number of land slips of varying sizes in Lyttelton. On Thursday a portion of a clay bank over Captain S. S. Horn's house gave way, and about four tons of earth fell perilously close to the back door just after a previous fall of two tons had been cleaned away.

Water surging from the hills disappeared under the foundations of the house and found an outlet at the garden gate several feet below. At the same level the undercurrent made a cave about twelve feet deep, something like a shell hole in the lawn adjoining the house.

Yesterday a land slip of several tons occurred in Salts Gully. Starting on the hill side it swept all before it for about eighty yards, carrying away two fowl houses, overturning a substantially built shed, and uprooting a number of fruit trees. Later a further slide of soft mud covered the side entrance to the house. It is recalled that about 3 four years ago in the same locality a large landslide occurred in the early hours of the morning completely covering a cowshed and smothering eight cows.

Sumner Road rockfalls - 1907

Star, Issue 8891, 30 March 1907, Page 7

GREAT LANDSLIP.

SUMNER CLIFFS "TAILING."

TRAFFIC COMPLETELY BLOCKED.

POSSIBLE DANGER TO CLIFTON RESIDENCES.

The cliffs on the Sumner Road have been a source of anxiety to the authorities and the public ever since the road was first opened by the Provincial engineer, and periodically there have been falls of rock, more or less serious. The cliff, of course, is constantly "tailing." That is to say, the steep face tends to wear down with the weather, and if the falling debris were left undisturbed it would, in course of time,

form a moderately easy slope. The process is for the most part a very slow one, but the heavy rains of the past few days, with rather severe changes of temperature, apparently hastened the breaking-away, and last evening an enormous mass of rock and earth came down without warning.

The locality is familiar to everyone who has journeyed to Sumner, and the overhanging rocks always look threatening. The slip occurred just beyond the Shag Rock corner, between the Shag Rock and what is called the Middle Rock, and according to the estimate of the Sumner engineer, Mr W. J. O'Donnell, between 3000 and 5000 tons of stuff came down.

The fall occurred just before the seven o'clock tram from Christchurch reached the Shag Rock. Indeed, the tram is said to have been within a chain or two of the Rock when the enormous mass came thundering down on to the road. Fortunately there was no one very near, but Mr O'Donnell's son and daughter, who were on the road, saw the fall in the moonlight. The debris buried the roadway for perhaps a couple of chains, in places to a depth of fifteen or twenty feet. It smashed the water mains which supply the borough of Sumner, carried away the overhead gear of the electric tramway and played havoc with the permanent way. One mighty rock lies on the outer side of the road, and in its fall it has torn up rails and sleepers. The lines are bent and broken, and the permanent way will have to be reconstructed.

So many false alarms have been, raised in connection with the cliffs that the report of a great slip did not at once receive credence. But the non-arrival of the seven o'clock tram made it clear to Sumner folk that the line was blocked, and news was sent through promptly to Christchurch. Vigorous measures were demanded, and emergency gangs were hastily organised at both ends. The Sumner Borough Council, concerned for the road, but more immediately still for its water supply, engaged five and twenty men forthwith, to connect the upper reservoir with the lower main, so that a supply might be available at the earliest moment. At the Christchurch end, the tramway authorities at once sent down a gang of men to clear the line. It was hopeless to think of getting trams through, however, and arrangements were hastily made to carry passengers between Sumner and Monck's by motor launch. This service worked very well, the last batch of passengers getting through to Sumner by midnight.

In the meantime Mr F. H. Chamberlain, the Tramway Board's engineer, went down to investigate. He returned late last night, and it was understood that a gang of thirty men would be put on at once to clear the line and carry out repairs. The Sumner Borough Council expected last night that a dray might be able to get through by midday to-day, but there seems to be no prospect of tramway communication being restored before to-night at the earliest. A fervent hope was expressed, however, that daylight would prove the obstacles to be less formidable than they appeared by moonlight. Still, there are some enormous pieces of rock in the debris, and these will not easily be shifted, even with the appliances available to the Tramway Board's staff.

It was rumoured last night that one of the houses on the hill-top was unsafe, but inquiry showed that the fall had occurred from the face of the cliff, and there was no reason to suppose that the ground at the back was affected.

Star , Issue 8892, 2 April 1907, Page 2

[Editorial]

THE SUMNER ROAD.

The recent landslip on the Christchurch-Sumner road has naturally directed public attention to the need for protection against similar accidents. It is felt that Friday's slip might, under different circumstances, have been attended by loss of life, and that unless a repetition of it is prevented the next fall may be much more serious in its consequences. The public confidence is indeed gravely disturbed, and it rests with the authorities to take immediate steps to restore it. The precise nature of the action to be taken is not, of course, for a layman to decide. It should be left for the decision of expert engineers, and the engineers should be the cleverest procurable. And when the experts have given their opinion as to the nature of the measures to be taken to render the road absolutely secure against further falls, it will be the duty of the authorities to carry them into effect without loss of time. If there is any difference of opinion as to the local body or which the responsibility of doing the work rests, it should be settled at once. There may not be another fall for years but on the other hand the cliff may give way again at any moment, and it is the duty of the authorities to make provision for the possibilities of the immediate, not the distant future. Considerations of expense should not be allowed to stand in the way. The safety of the public is of more important than saving the rates, and no expense in reason should be spared to ensure the public safety. The mere removal of the debris that fell last week, and the widening of the road under the cliffs though necessary for the convenience of traffic, would be of little avail as permanent solution of the problem. It is possible that the top of the cliffs will have to be removed or the estuary bridged and the road diverted from under the cliffs. It is possible, even, that still more drastic measures will be necessary to ensure the safety of traffic. But whatever steps are shown to be expedient must be taken no matter what the cost may be. Sumner is the principle watering-place of North and Mid-Canterbury; it has a large resident population, and it is patronised by hundreds of visitors daily. To leave the road in its present position would be to set up a perpetual menace to life and limb, and to endanger the popularity of the borough both as a place of residence and as a holiday resort. We have no desire to be alarmist, but we certainly think that the various authorities interested ought to co-operate in providing a safe access to the borough with as little loss of time as possible.

Wanganui Herald, Volume XXXXI, Issue 12130, 2 April 1907, Page 5

THE SUMNER LANDSLIP.

A Dangerous Cliff.

(Per United Press Association.)

CHRISTCHURCH, April 2.

The work of clearing the Sumner landslip was suspended yesterday, there being ample room for vehicles to pass. Large rocks have to be blasted, and it will five or six days to clear the road altogether. The general opinion is that the upper overhanging cliff will have to be brought down and the face sloped back, but even though the road and the tramline be moved further out into the estuary there is still the danger of a fall from the cliff, which at present seems as if hanging just over the road. If something be not done a terrible accident may happen.

Evening Post, Volume LXXIII, Issue 79, 4 April 1907, Page 6

There is a difference of opinion whether the Sumner Borough Council or the Christchurch Tramway Board is responsible for the roadway running under the Cliffs, the scene of the recent landslip. The board maintains that its duty is to make tramlines and not to form roadways. Meanwhile no steps have been taken to remove the source of a very great danger from the overhanging rocks.

A3 APPENDIX 3: RESULTS FROM THE TWO-DIMENSIONAL SITE RESPONSE ASSESSMENT FOR CROSS-SECTIONS 1 AND 2

The results from the two-dimensional site response modelling are shown for source areas 11A (cross-section 2) and 11B (cross-section 1). The maximum acceleration (A_{MAX}) at the cliff crest derived from the modelling of each synthetic earthquake time history has been plotted in Figure A3.1. Each point on the graph represents the response of the slope crest to a given synthetic free field rock outcrop earthquake input motion (Table A3.1). The modelling for cross-sections 1 and 2 adopt the same synthetic earthquake time acceleration histories.

Source area 11A (cross-section 2)

The fundamental frequency of the slope varies from 3.8 to 10 Hz based on the equation in Bray and Travasarou (2007), where frequency = $1/(4 \times H/V_s)$, and H = slope height of 20 m, and V_s = average shear wave velocity for the slope of 300–800 m/s. The dominant frequency of the input motions is between 3.6 Hz and 5.7 Hz. The “tuning ratio” defined as the ratio between the dominant frequency of the input motion and the fundamental frequency of the slope (Wartman et al., 2013), is about 1.0–1.5 for a shear wave velocity of 300 m/s, and 0.4–0.6 for a shear wave velocity of 800 m/s.

Results from the seismic response assessment suggest that the peak ground acceleration amplification factors (S_T) for source area 11A are about 2.6 (± 0.2) for horizontal motions, and 3.7 (± 0.2) for vertical motions – errors at one standard deviation (Figure A3.1). The amplification factor at higher input peak ground accelerations is about 1.9 (13 June 2011 earthquake) to 2.7 (22 February 2011 earthquake) compared to 4.4 and 4.5 for lower input ground accelerations (16 April and 23 December 2011 earthquakes respectively), indicating a non-linear amplification factor.

Source area 11B (cross-section 1)

The fundamental frequency of the slope varies from 5 to 10 Hz based on the equation in Bray and Travasarou (2007), where frequency = $1/(4 \times H/V_s)$, and H = slope height of 15 m, and V_s = average shear wave velocity for the slope of 300–600 m/s. The dominant frequency of the input motions is 3.6 Hz and then 5.7 Hz. The “tuning ratio” is about 0.7–1.1 for a shear wave velocity of 300 m/s, and 0.4–0.6 for a shear wave velocity of 600 m/s.

Results from the seismic response assessment suggest that the peak ground acceleration amplification factors (S_T) for source area 11B (cross-section 1) are about 2.8 (± 0.2) for horizontal motions and 2.4 (± 0.1) for vertical motions – errors at one standard deviation (Figure A3.1).

Table A3.1 Results from the two-dimensional site response assessment for cross-section 1 (source area 11B) and cross-section 2 (source area 11A), using the synthetic free-field rock outcrop motions for the Quarry Road site by Holden et al. (2014) as inputs to the assessment. PGA is peak ground acceleration.

Earthquake (2011)	Free-field input PGA (horizontal) – A_{FF} (g)	Free-field input PGA (vertical) – A_{FF} (g)	Maximum PGA (horizontal) at slope crest – A_{MAX} (g)		Maximum PGA (vertical) at slope crest – A_{MAX} (g)	
			Cross-section 1	Cross-section 2	Cross-section 1	Cross-section 2
22 February	1.03	0.69	2.99	2.74	1.64	2.61
16 April	0.04	0.04	0.12	0.18	0.06	0.12
13 June	0.42	0.24	0.91	0.80	0.63	0.75
23 December	0.17	0.13	0.46	0.78	0.28	0.45

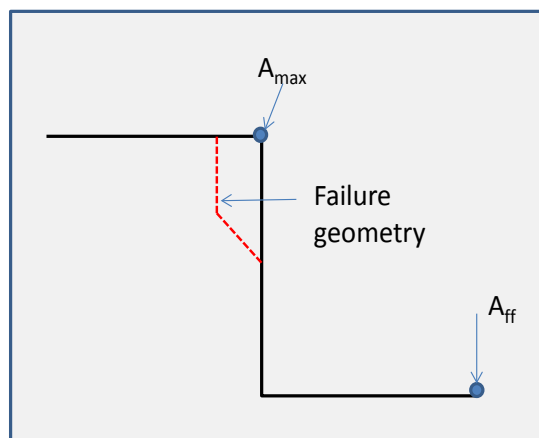
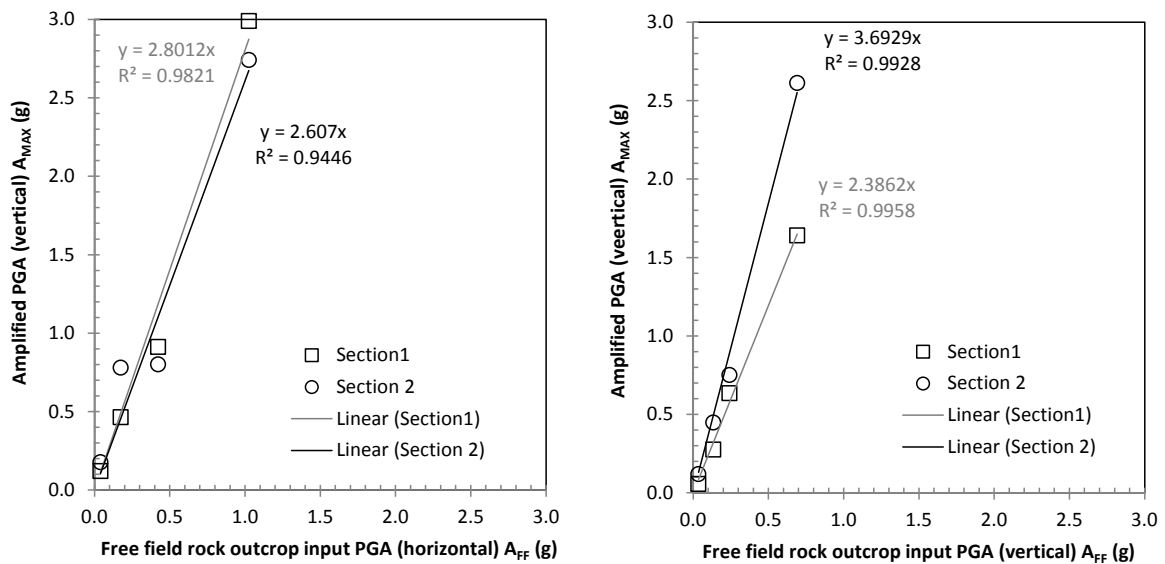


Figure A3.1 Amplification relationship between the synthetic free-field rock outcrop input motions (A_{FF}) and the modelled cliff crest maximum accelerations (A_{MAX}) for cross-sections 1 and 2. A schematic diagram showing the locations of the various recorded accelerations is shown.

Amplification of peak ground accelerations

Results from this assessment have shown that the relationship between the peak ground acceleration of the free-field input motion and the corresponding modelled peak acceleration at the slope crest (A_{MAX}), is non-linear for the soil site (source area 11A) and approximately linear for the rock site (source area 11B). In the range of modelled peak horizontal accelerations, the horizontal amplification factor (S_T) is typically in the order of about 2.6 (source area 11A) and 2.8 (source area 11B) times the input free-field peak horizontal acceleration.

Although the amplification factors are similar between the two sites, the geology of the sites is different, where source area 11A is predominantly a soil site while source area 11B is predominantly a rock site. Source area 11A comprises about 10 m of fill (loess) overlying loess, basalt breccia and lava, where the mean shear wave velocities of the materials change from 1,100 m/s in the basalt breccia and lava to 300 m/s in the fill (Figure A3.2). The results suggest that the impedance contrasts between the materials contribute most to the amplification of shaking, but that the peak horizontal accelerations (for all modelled earthquakes) concentrate around the convex break in slope, corresponding to where the largest permanent slope displacements were recorded. These results are similar to those reported by others (e.g. Del Gaudio and Wasowski, 2010), where material impedance contrasts have been shown to have a significant effect on the amplification of shaking, which could explain the localised displacements of the surface material mapped and described by Yetton and Engel (2014) and the significant shaking damage to those dwellings at the slope crest (4 and 6 Quarry Road) above the area of mapped cracks.

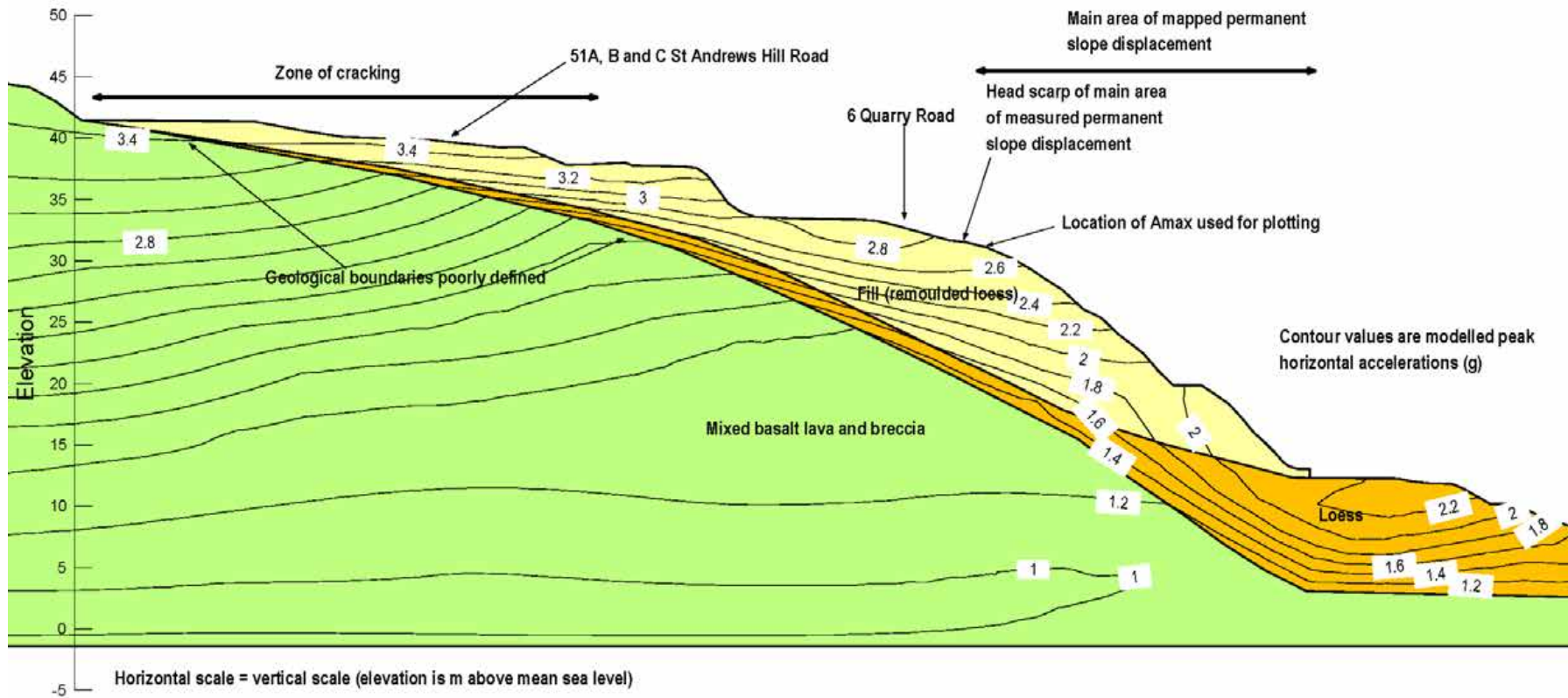


Figure A3.2 Modelled peak horizontal ground acceleration contours for the 22 February 2011 earthquake at Quarry Road, source area 11A (cross-section 2). Note: the high peak horizontal ground accelerations shown at the left of the drawing are not thought realistic as the geological boundary conditions in this area are unknown and have been inferred.

In contrast, source area 11B (cross-section 1) comprises about 2–3 m of loess (mean shear wave velocity of 300 m/s) overlying basalt breccia and lava (mean shear wave velocity of 600 m/s). The results show that there is little change in the modelled peak horizontal ground accelerations between the rock and the loess, possibly because the layer of loess is relatively thin and the shear wave velocities, and therefore impedance contrasts, are not as different as those at cross-section 2. It should be noted that the down-hole shear wave velocities were recorded after the main 2010/11 Canterbury earthquakes and so represent the current shear wave velocities of the ground, which are likely to have deteriorated from pre-earthquake conditions.

At low to moderate acceleration levels (less than 0.4 g, input motion) peak modelled accelerations (A_{MAX}) at source area 11A (soil site) are greater than those at source area 11B (rock site). While at higher input accelerations the peak accelerations (A_{MAX}) at source area 11B (rock site) are larger than those at source area 11a (soil site).

The relationship between the modelled vertical and horizontal peak ground accelerations recorded at the slope crest (A_{MAX}) is shown in Figure A3.3. The gradient of the linear fit is 0.56 (± 0.02) for source area 11B (cross-section 1) and 0.93 (± 0.1) for source area 11A (cross-section 2) – errors at one standard deviation. The relationship between horizontal and vertical peak ground accelerations appears linear.

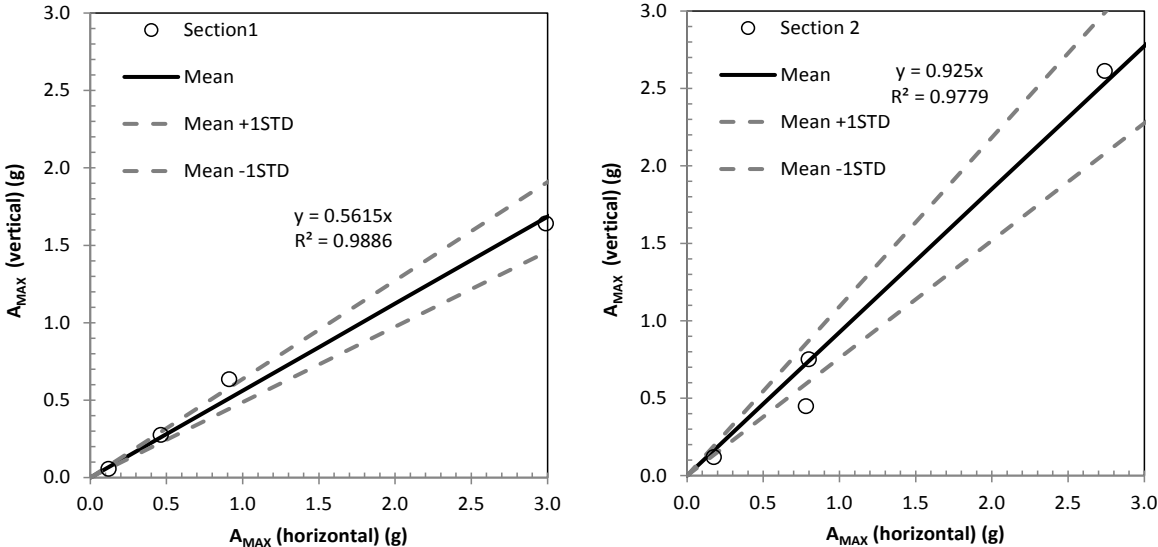


Figure A3.3 Relationship between the modelled horizontal and vertical maximum accelerations modelled at the slope crest (A_{MAX}) for cross-sections 1 and 2, using the synthetic free-field rock outcrop motions for the Quarry Road site by Holden et al. (2014) as inputs to the assessment. The mean and standard deviation trend lines are fitted for A_{MAX} all data. Errors are shown as the mean \pm one standard deviation (1 STD).

Eurocode 8, Part 5, Annex A, gives some simplified amplification factors for the seismic action used in the verification of the stability of slopes. Such factors, denoted S_T , are to a first approximation considered independent of the fundamental period of vibration and, hence, multiply as a constant scaling factor.

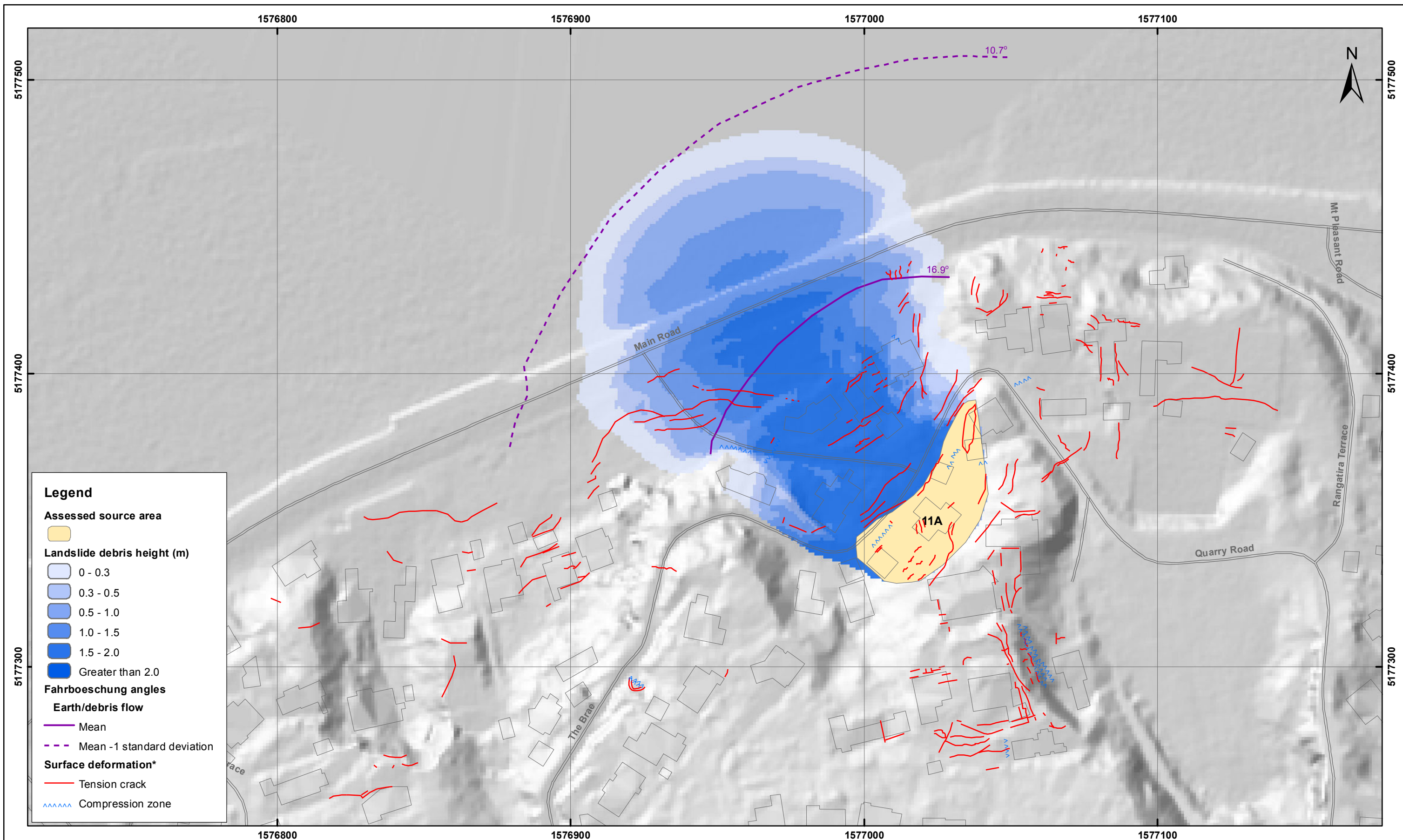
Eurocode 8, Part 5, Annex A recommends:

1. Isolated cliffs and slopes. A value $S_T \geq 1.2$ should be used for sites near the top edge.
2. Ridges with crest width significantly less than the base width. A value $S_T \geq 1.4$ should be used near the top of the slopes for average slope angles greater than 30° and a value $S_T > 1.2$ should be used for smaller slope angles.
3. Presence of a loose surface layer. In the presence of a loose surface layer, the smallest S_T value given in a) and b) should be increased by at least 20%.
4. Spatial variation of amplification factor. The value of S_T may be assumed to decrease as a linear function of the height above the base of the cliff or ridge, and to be unity at the base.
5. These amplification factors should in preference be applied when the slopes belong to two-dimensional topographic irregularities, such as long ridges and cliffs of height greater than about 30 m.

Ashford and Sitar (2002) recommend an S_T of 1.5 be applied to the maximum free-field acceleration behind the crest based on their assessment of slopes typically $>60^\circ$ to near vertical and of heights (toe to crest) of typically >30 m. This factor is based on the assessment of slopes that failed during the 1989 Loma Prieta M_W 6.9 earthquake.

Results from the seismic response assessment suggest that the peak ground acceleration amplification factors (S_T) for Quarry Road are about 2.8 (source area 11B, cross-section 1) and 2.6 (source area 11A, cross-section 2) times for horizontal motions.

**A4 APPENDIX 4: RAMMS MODELLING RESULTS FOR SOURCE AREAS
1 AND 2. ESTIMATED LANDSLIDE RUNOUT HEIGHT**

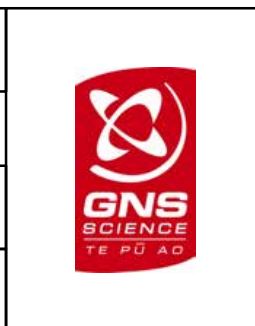


SCALE BAR: 0 25 50 m

EXPLANATION:
 * Taken from report CR2012/317
 Background shade model derived from NZAM post earthquake 2011c (July 2011) LiDAR survey resampled to a 1 m ground resolution.
 Roads and building footprints and types provided by Christchurch City Council (20/02/2012).
 PROJECTION: New Zealand Transverse Mercator 2000

DRW:
BL, WR

CHK:
CM, FDP



ESTIMATED LANDSLIDE RUNOUT HEIGHT
Source 11A - Upper Volume (8,800 m³)

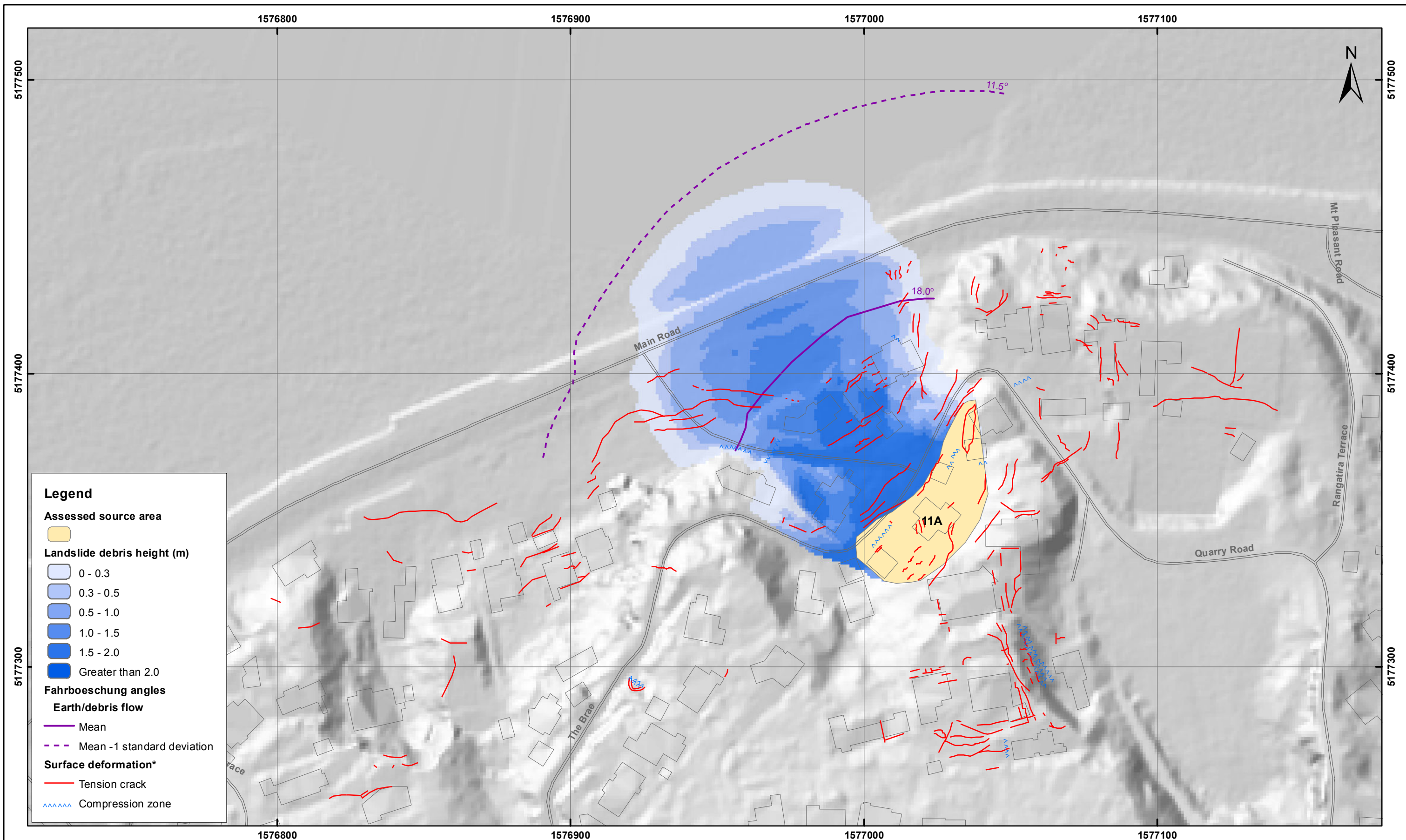
Quarry Road - Port Hills
Christchurch

APPENDIX 4

Map 1

FINAL

REPORT: CR2014/75 DATE: June 2014



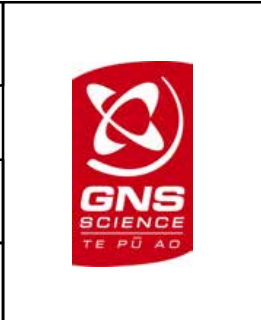
- Legend**
- Assessed source area**
 - Landslide debris height (m)**
 - 0 - 0.3
 - 0.3 - 0.5
 - 0.5 - 1.0
 - 1.0 - 1.5
 - 1.5 - 2.0
 - Greater than 2.0
 - Fahrboeschung angles**
 - Earth/debris flow**
 - Mean
 - Mean -1 standard deviation
 - Surface deformation***
 - Tension crack
 - Compression zone

SCALE BAR: 0 25 50 m

EXPLANATION:
 * Taken from report CR2012/317
 Background shade model derived from NZAM post earthquake 2011c (July 2011) LiDAR survey resampled to a 1 m ground resolution. Roads and building footprints and types provided by Christchurch City Council (20/02/2012).
 PROJECTION: New Zealand Transverse Mercator 2000

DRW:
BL, WR

CHK:
CM, FDP



ESTIMATED LANDSLIDE RUNOUT HEIGHT
Source 11A - Middle Volume (4,700 m³)

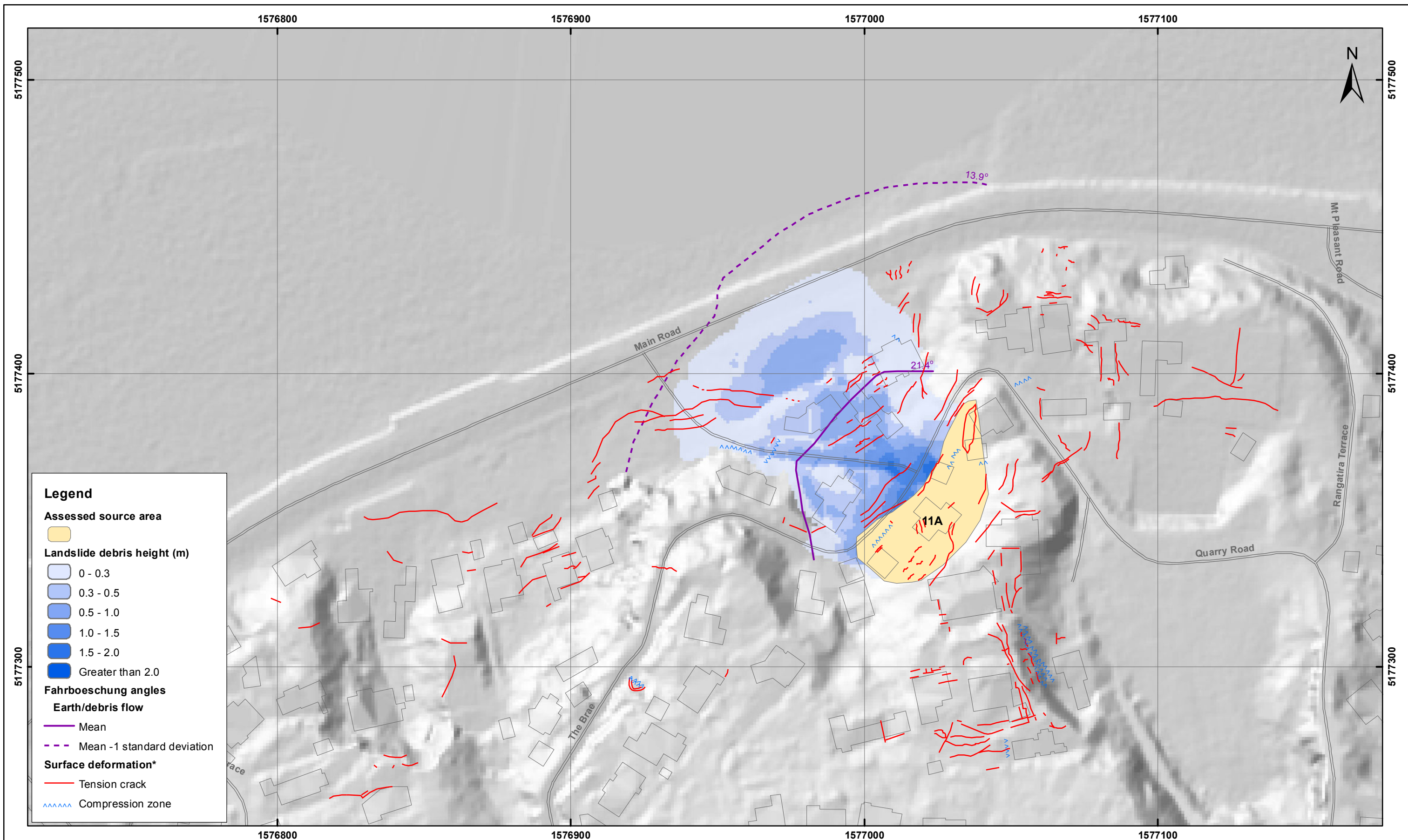
Quarry Road - Port Hills
Christchurch

APPENDIX 4

Map 2

FINAL

REPORT: CR2014/75 DATE: June 2014

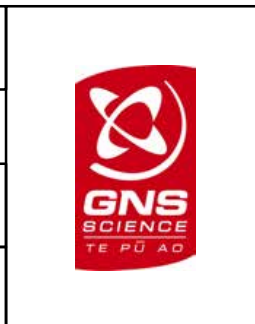


SCALE BAR: 0 25 50 m

EXPLANATION:
 * Taken from report CR2012/317
 Background shade model derived from NZAM post earthquake 2011c (July 2011) LiDAR survey resampled to a 1 m ground resolution.
 Roads and building footprints and types provided by Christchurch City Council (20/02/2012).
 PROJECTION: New Zealand Transverse Mercator 2000

DRW:
BL, WR

CHK:
CM, FDP



ESTIMATED LANDSLIDE RUNOUT HEIGHT
Source 11A - Lower Volume (800 m³)

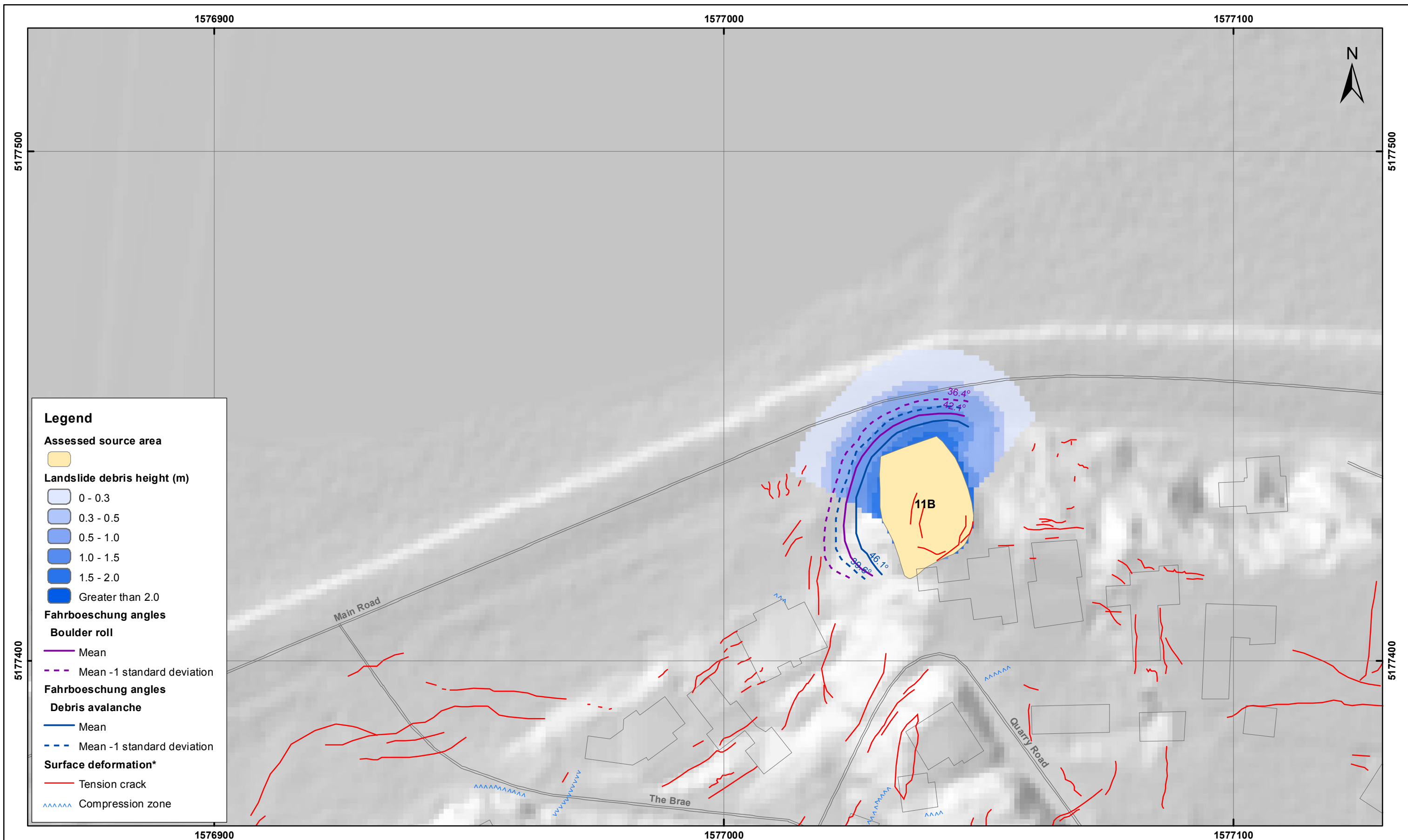
Quarry Road - Port Hills
Christchurch

APPENDIX 4

Map 3

FINAL

REPORT: CR2014/75 DATE: June 2014

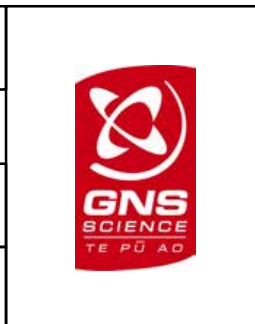


SCALE BAR: 0 25 50 m

EXPLANATION:
 * Taken from report CR2012/317
 Background shade model derived from NZAM post earthquake 2011c (July 2011) LiDAR survey resampled to a 1 m ground resolution.
 Roads and building footprints and types provided by Christchurch City Council (20/02/2012).
 PROJECTION: New Zealand Transverse Mercator 2000

DRW:
BL, WR

CHK:
CM, FDP



ESTIMATED LANDSLIDE RUNOUT HEIGHT
Source 11B - Upper Volume (1,400 m³)

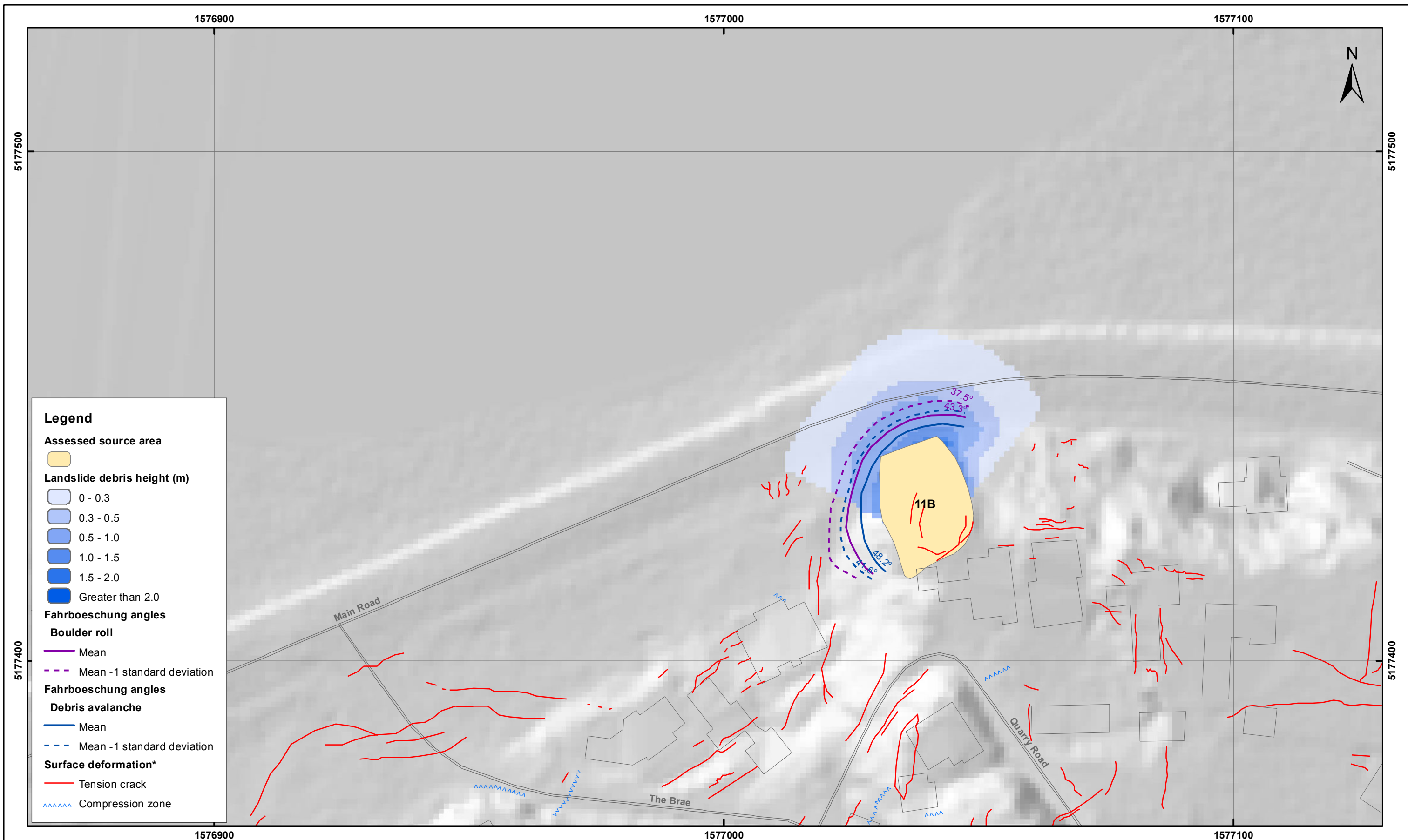
Quarry Road - Port Hills
Christchurch

APPENDIX 4

Map 4

FINAL

REPORT: CR2014/75 DATE: June 2014

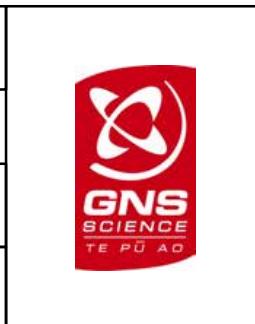


SCALE BAR: 0 25 50 m

EXPLANATION:
 * Taken from report CR2012/317
 Background shade model derived from NZAM post earthquake 2011c (July 2011) LiDAR survey resampled to a 1 m ground resolution.
 Roads and building footprints and types provided by Christchurch City Council (20/02/2012).
 PROJECTION: New Zealand Transverse Mercator 2000

DRW:
BL, WR

CHK:
CM, FDP



ESTIMATED LANDSLIDE RUNOUT HEIGHT
Source 11B - Middle Volume (540 m³)

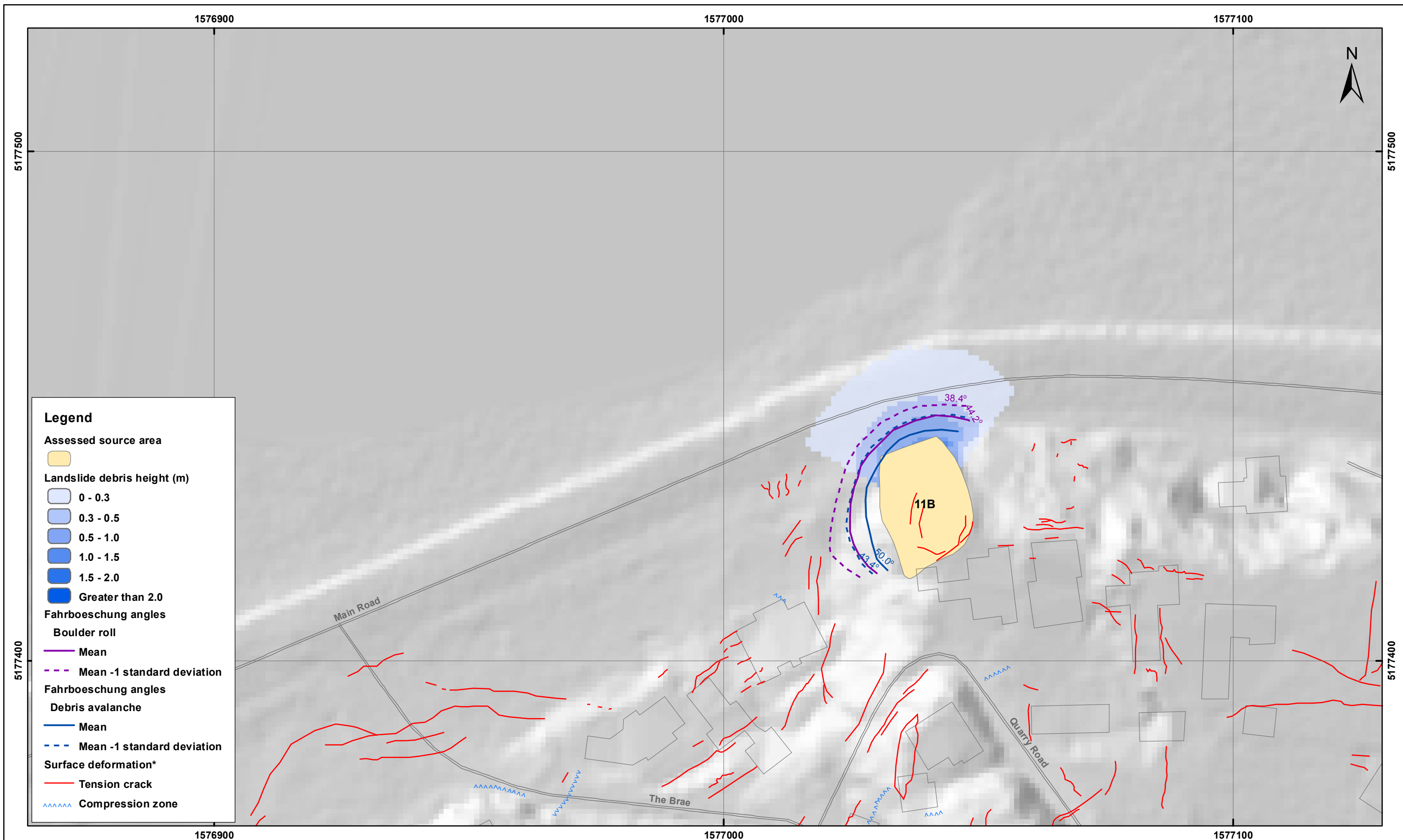
Quarry Road - Port Hills
Christchurch

APPENDIX 4

Map 5

FINAL

REPORT: CR2014/75 DATE: June 2014

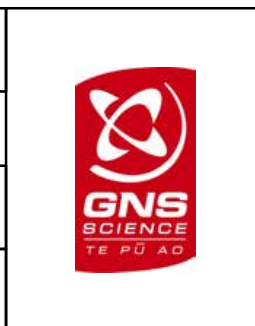


SCALE BAR: 0 25 50 m

EXPLANATION:
 * Taken from report CR2012/317
 Background shade model derived from NZAM post earthquake 2011c (July 2011) LiDAR survey resampled to a 1 m ground resolution.
 Roads and building footprints and types provided by Christchurch City Council (20/02/2012).
 PROJECTION: New Zealand Transverse Mercator 2000

DRW:
BL, WR

CHK:
CM, FDP



ESTIMATED LANDSLIDE RUNOUT HEIGHT
Source 11B - Lower Volume (240 m³)

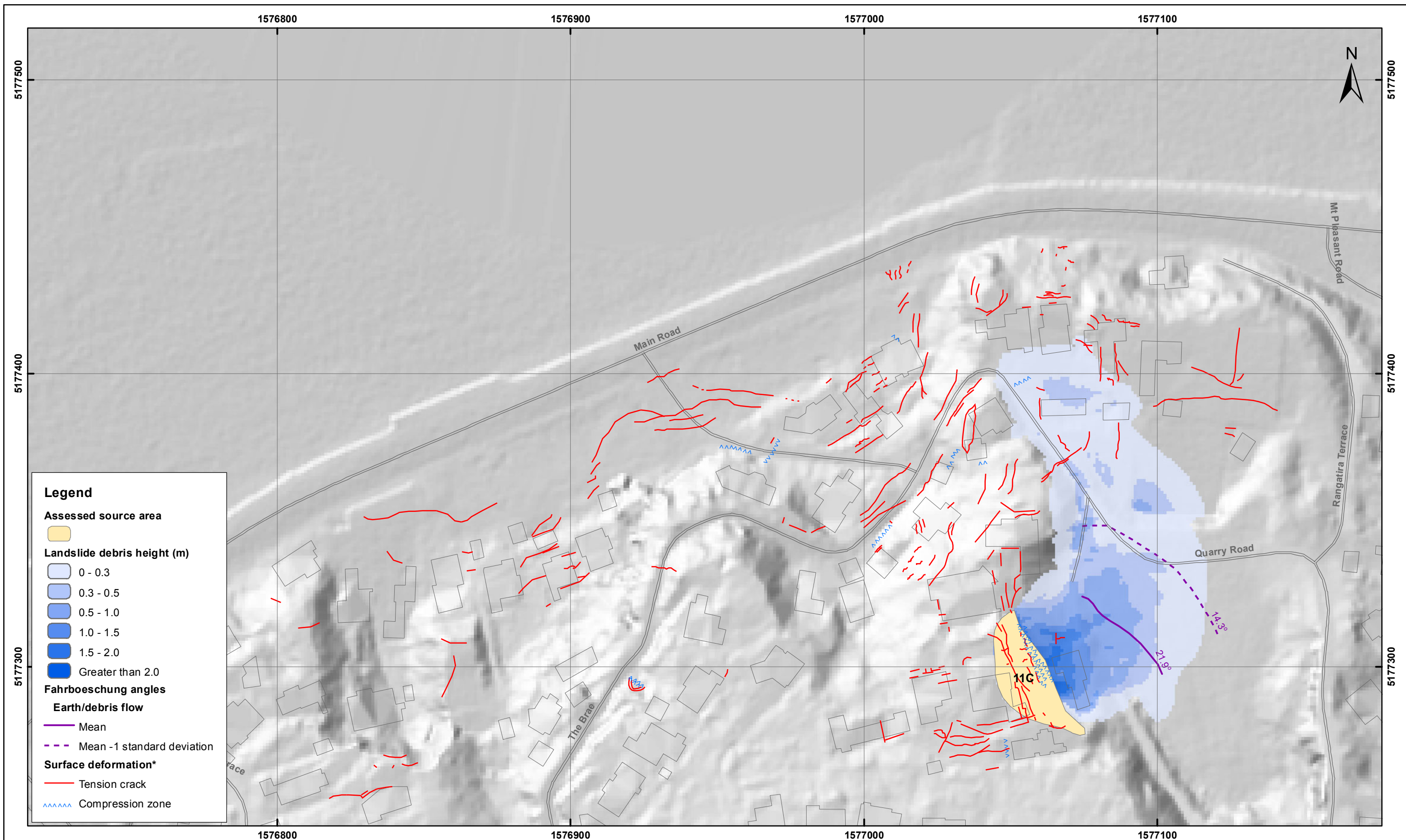
Quarry Road - Port Hills
Christchurch

APPENDIX 4

Map 6

FINAL

REPORT: CR2014/75 DATE: June 2014

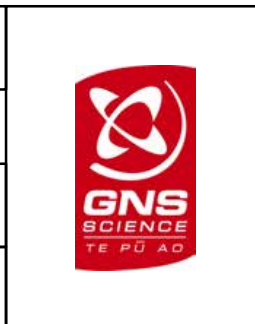


SCALE BAR: 0 25 50 m

EXPLANATION:
 * Taken from report CR2012/317
 Background shade model derived from NZAM post earthquake 2011c (July 2011) LiDAR survey resampled to a 1 m ground resolution.
 Roads and building footprints and types provided by Christchurch City Council (20/02/2012).
 PROJECTION: New Zealand Transverse Mercator 2000

DRW:
BL, WR

CHK:
CM, FDP



ESTIMATED LANDSLIDE RUNOUT HEIGHT
Source 11C - Upper Volume (600 m³)

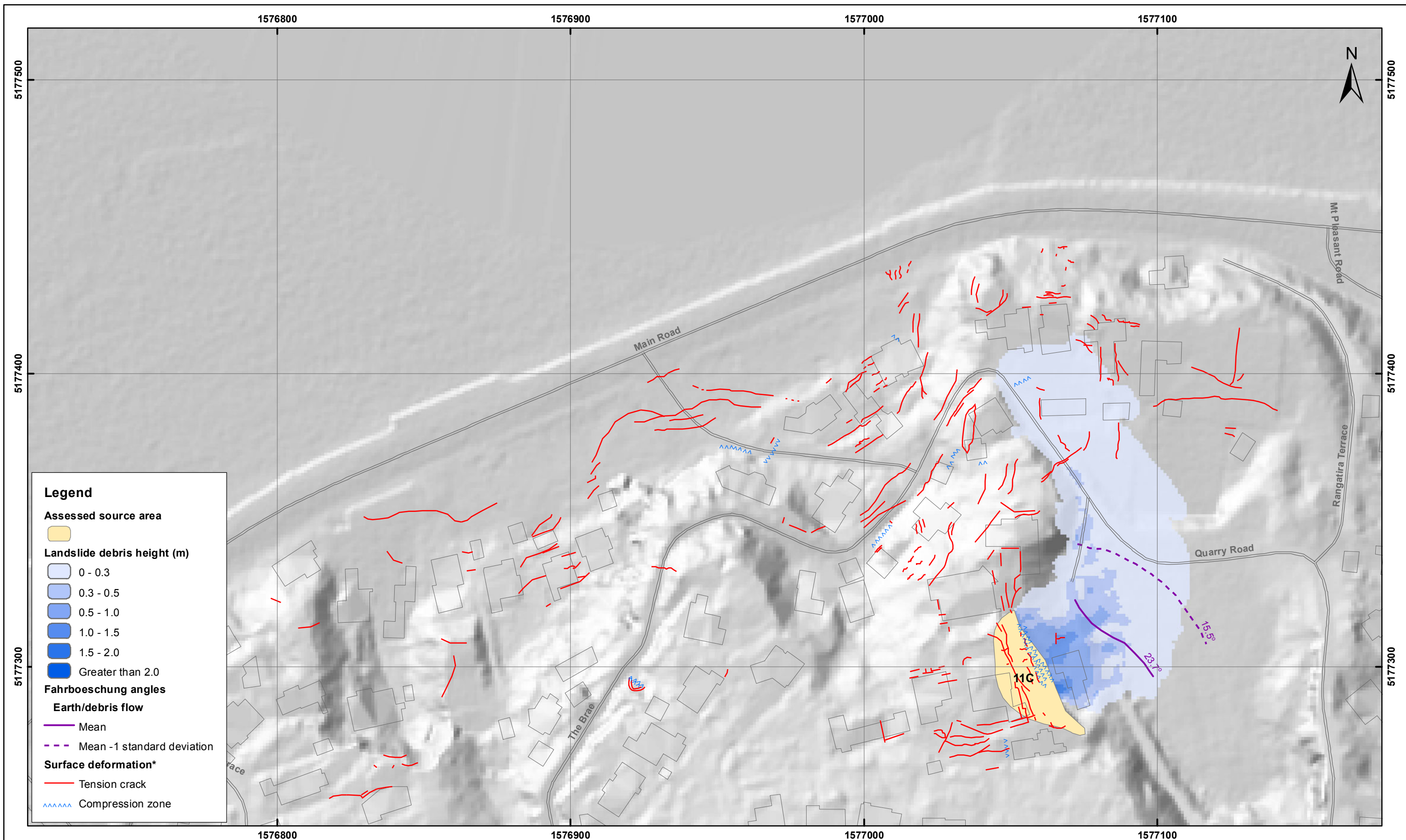
Quarry Road - Port Hills
Christchurch

APPENDIX 4

Map 7

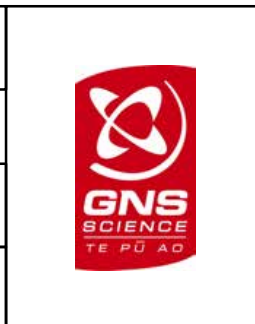
FINAL

REPORT: CR2014/75 DATE: June 2014



EXPLANATION:
 * Taken from report CR2012/317
 Background shade model derived from NZAM post earthquake 2011c (July 2011) LiDAR survey resampled to a 1 m ground resolution.
 Roads and building footprints and types provided by Christchurch City Council (20/02/2012).
 PROJECTION: New Zealand Transverse Mercator 2000

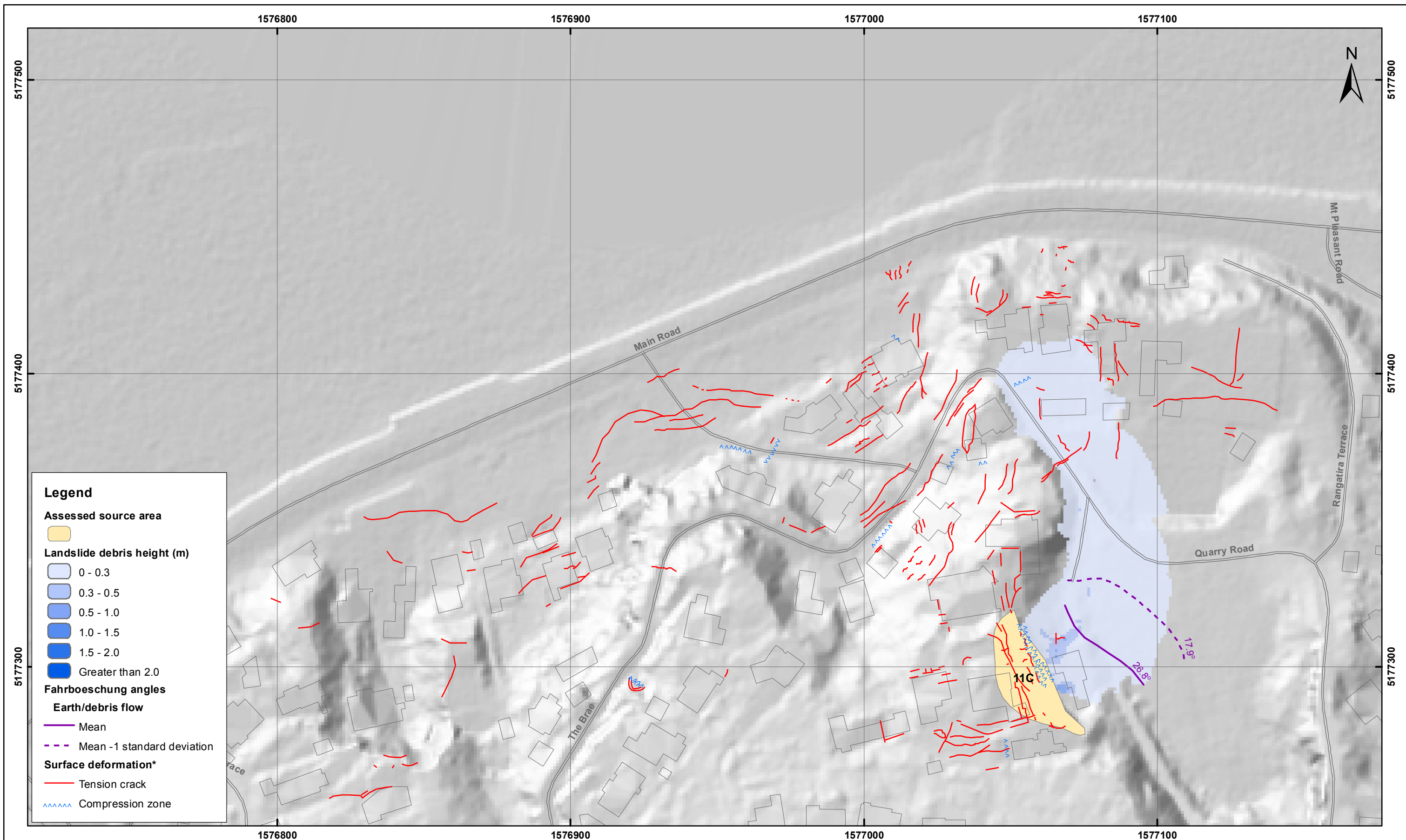
DRW:
BL, WR
 CHK:
CM, FDP



ESTIMATED LANDSLIDE RUNOUT HEIGHT
Source 11C - Middle Volume (270 m³)

Quarry Road - Port Hills
Christchurch

APPENDIX 4
 Map 8
FINAL
 REPORT: CR2014/75 DATE: June 2014



Legend

Assessed source area

Landslide debris height (m)

- 0 - 0.3
- 0.3 - 0.5
- 0.5 - 1.0
- 1.0 - 1.5
- 1.5 - 2.0
- Greater than 2.0

Fahrboeschung angles

Earth/debris flow

- Mean
- Mean -1 standard deviation

Surface deformation*

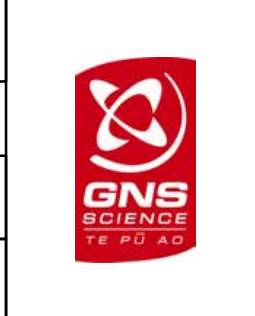
- Tension crack
- Compression zone



EXPLANATION:
 * Taken from report CR2012/317
 Background shade model derived from NZAM post earthquake 2011c (July 2011) LiDAR survey resampled to a 1 m ground resolution. Roads and building footprints and types provided by Christchurch City Council (20/02/2012).
 PROJECTION: New Zealand Transverse Mercator 2000

DRW:
BL, WR

CHK:
CM, FDP

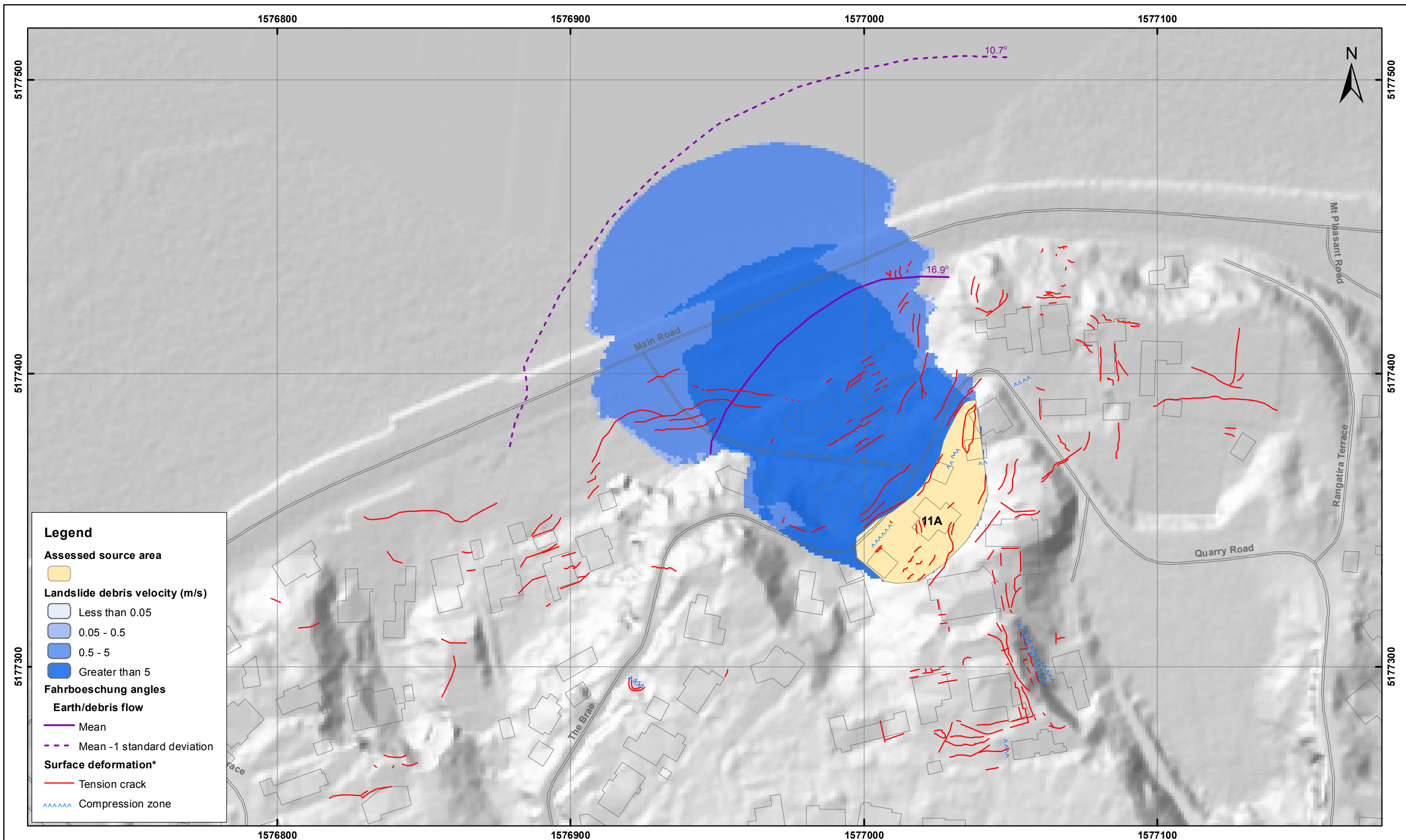


ESTIMATED LANDSLIDE RUNOUT HEIGHT
Source 11C - Lower Volume (70 m³)

Quarry Road - Port Hills
Christchurch

APPENDIX 4	
Map 9	
FINAL	
REPORT: CR2014/75	DATE: June 2014

A5 APPENDIX 5: RAMMS MODELLING RESULTS FOR SOURCE AREAS 1 AND 2. ESTIMATED LANDSLIDE RUNOUT VELOCITY



SCALE BAR: 0 25 50 m

EXPLANATION:
* Taken from report CR2012/317

Background shade model derived from NZAM post earthquake 2011c (July 2011) LiDAR survey resampled to a 1 m ground resolution. Roads and building footprints and types provided by Christchurch City Council (20/02/2012).

PROJECTION: New Zealand Transverse Mercator 2000

DRW:
BL, WR

CHK:
CM, FDP



ESTIMATED LANDSLIDE RUNOUT VELOCITY
Source 11A - Upper Volume (8,800 m³)

Quarry Road - Port Hills
Christchurch

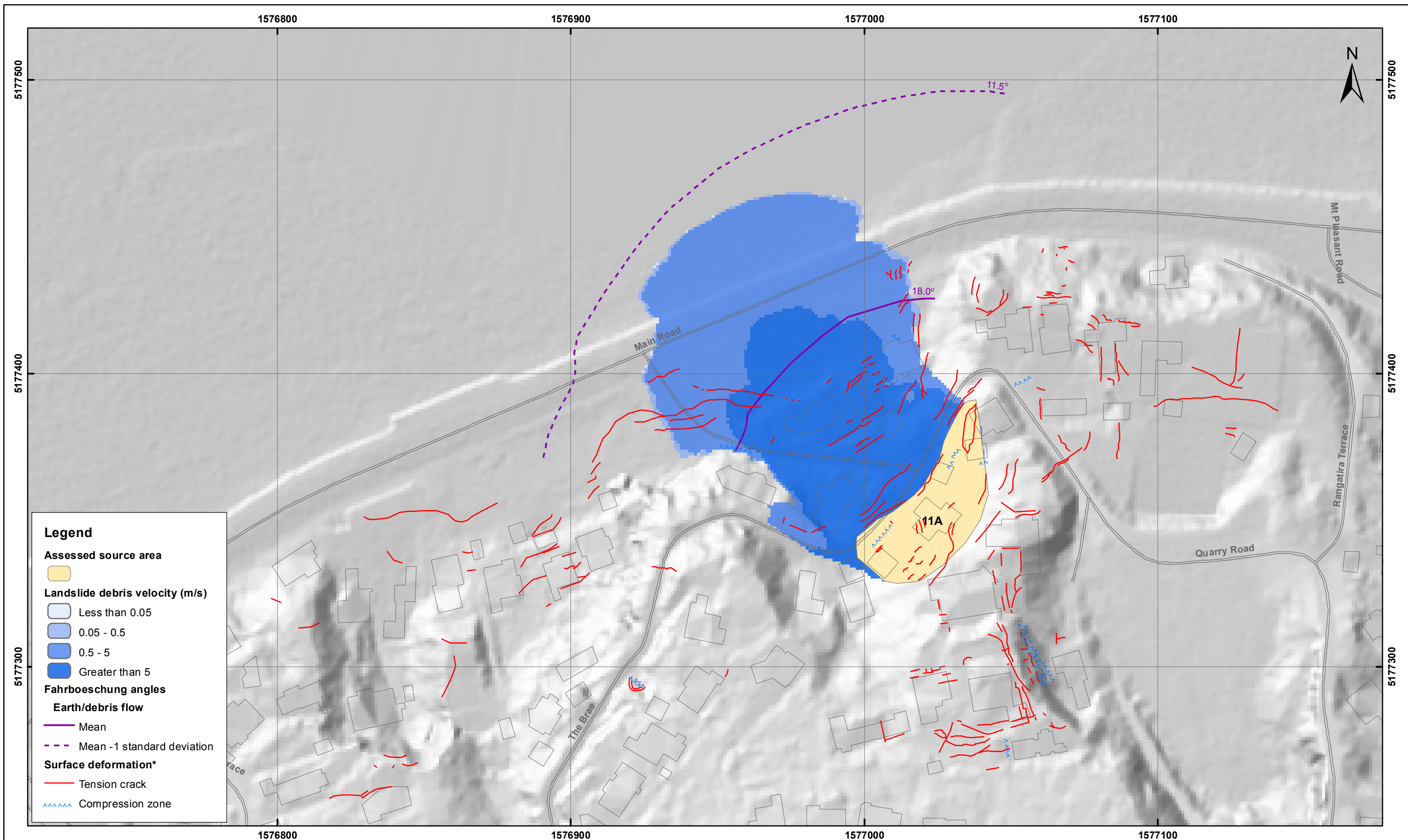
APPENDIX 5

Map 1

FINAL

REPORT:
CR2014/75

DATE:
June 2014

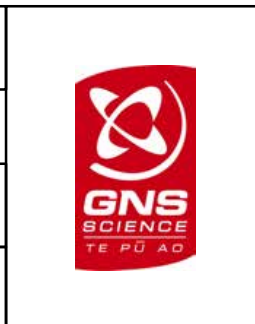


SCALE BAR: 0 25 50 m

EXPLANATION:
 * Taken from report CR2012/317
 Background shade model derived from NZAM post earthquake 2011c (July 2011) LiDAR survey resampled to a 1 m ground resolution.
 Roads and building footprints and types provided by Christchurch City Council (20/02/2012).
 PROJECTION: New Zealand Transverse Mercator 2000

DRW:
BL, WR

CHK:
CM, FDP



ESTIMATED LANDSLIDE RUNOUT VELOCITY
Source 11A - Middle Volume (4,700 m³)

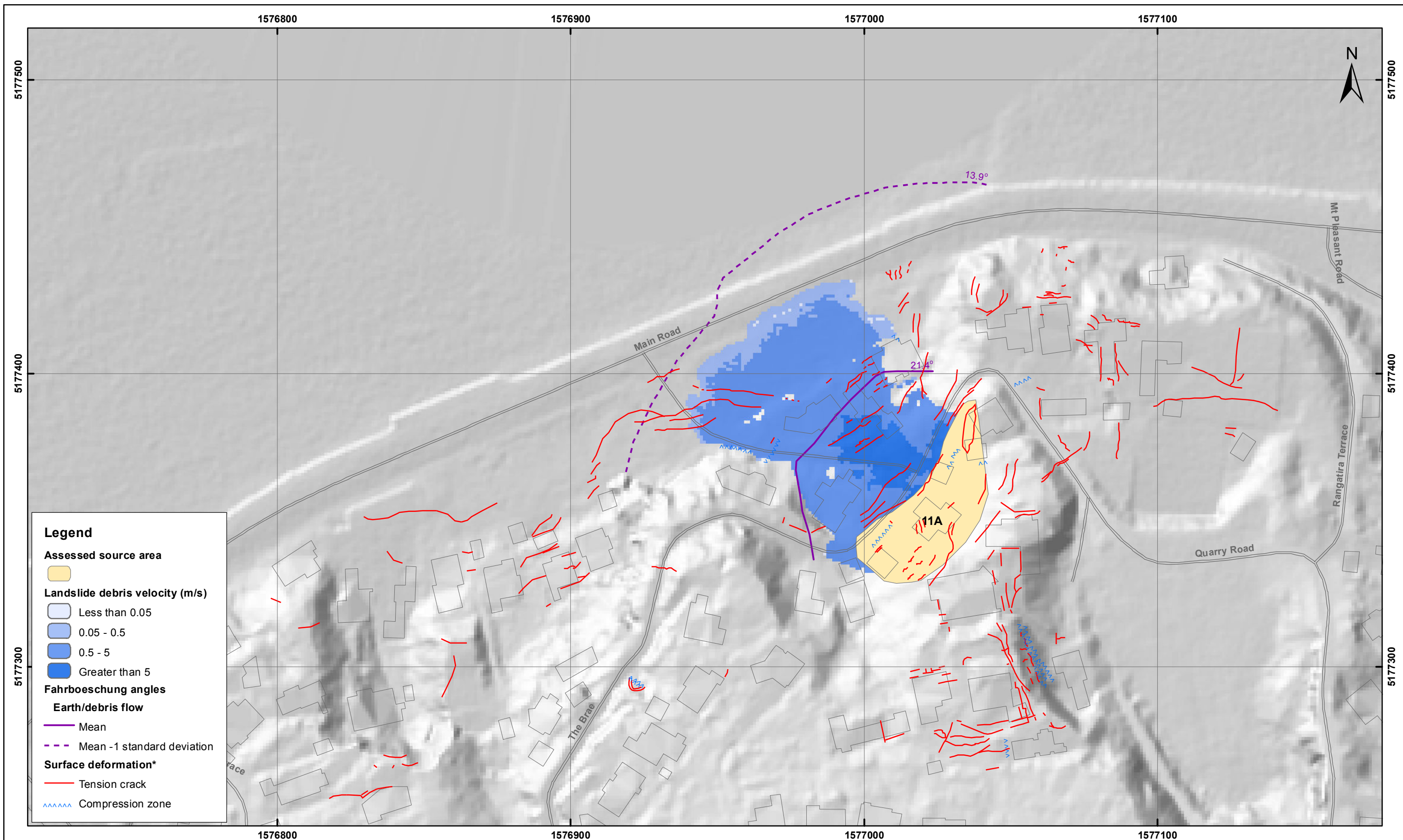
Quarry Road - Port Hills
Christchurch

APPENDIX 5

Map 2

FINAL

REPORT: CR2014/75 DATE: June 2014

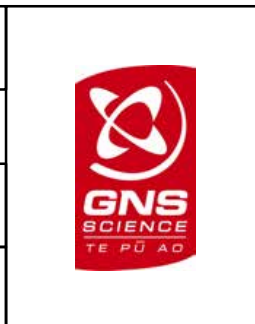


SCALE BAR: 0 25 50 m

EXPLANATION:
 * Taken from report CR2012/317
 Background shade model derived from NZAM post earthquake 2011c (July 2011) LiDAR survey resampled to a 1 m ground resolution.
 Roads and building footprints and types provided by Christchurch City Council (20/02/2012).
 PROJECTION: New Zealand Transverse Mercator 2000

DRW:
BL, WR

CHK:
CM, FDP



ESTIMATED LANDSLIDE RUNOUT VELOCITY
Source 11A - Lower Volume (790 m³)

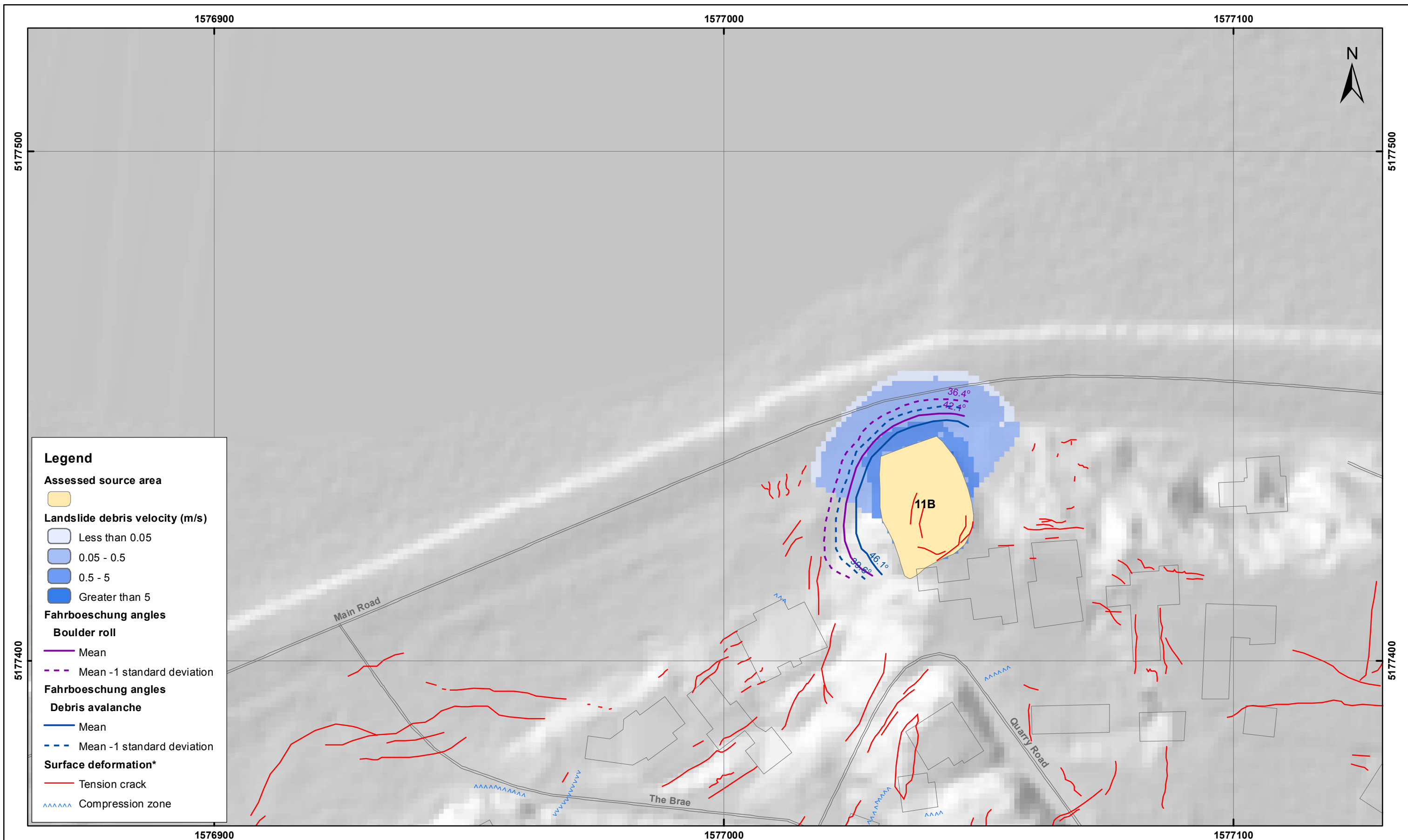
Quarry Road - Port Hills
Christchurch

APPENDIX 5

Map 3

FINAL

REPORT: CR2014/75 DATE: June 2014

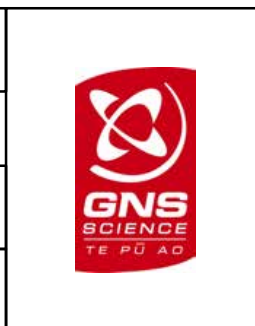


SCALE BAR: 0 25 50 m

EXPLANATION:
 * Taken from report CR2012/317
 Background shade model derived from NZAM post earthquake 2011c (July 2011) LiDAR survey resampled to a 1 m ground resolution.
 Roads and building footprints and types provided by Christchurch City Council (20/02/2012).
 PROJECTION: New Zealand Transverse Mercator 2000

DRW:
BL, WR

CHK:
CM, FDP



ESTIMATED LANDSLIDE RUNOUT VELOCITY
Source 11B - Upper Volume (1,400 m³)

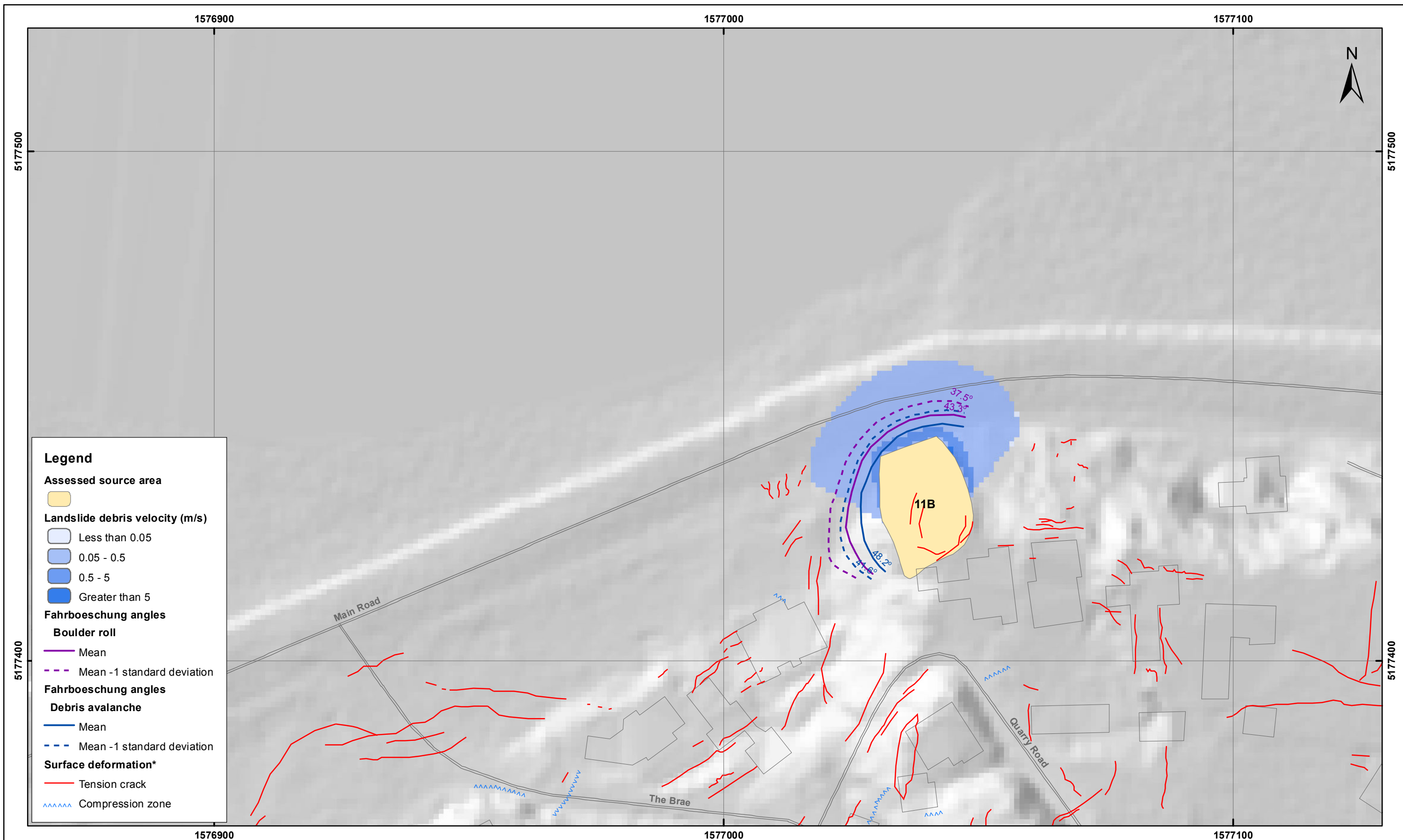
Quarry Road - Port Hills
Christchurch

APPENDIX 5

Map 4

FINAL

REPORT: CR2014/75 DATE: June 2014



SCALE BAR: 0 25 50 m

EXPLANATION:

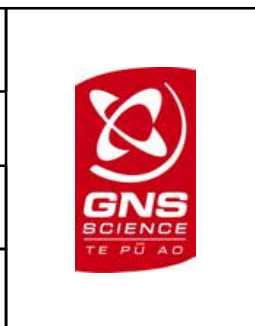
* Taken from report CR2012/317

Background shade model derived from NZAM post earthquake 2011c (July 2011) LiDAR survey resampled to a 1 m ground resolution. Roads and building footprints and types provided by Christchurch City Council (20/02/2012).

PROJECTION: New Zealand Transverse Mercator 2000

DRW:
BL, WR

CHK:
CM, FDP



ESTIMATED LANDSLIDE RUNOUT VELOCITY
Source 11B - Middle Volume (540 m³)

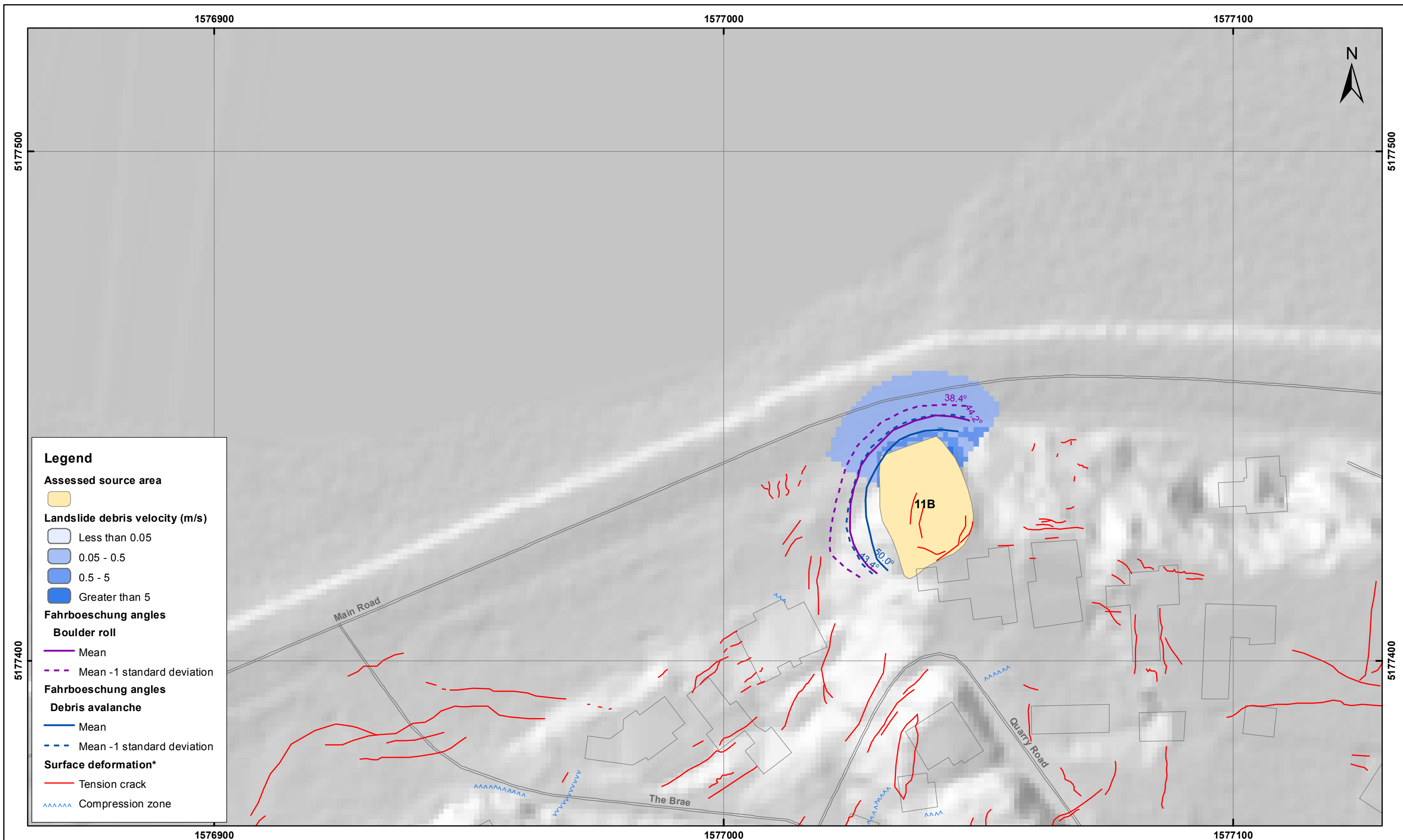
Quarry Road - Port Hills
Christchurch

APPENDIX 5

Map 5

FINAL

REPORT: CR2014/75 DATE: June 2014



SCALE BAR: 0 25 50 m

EXPLANATION:

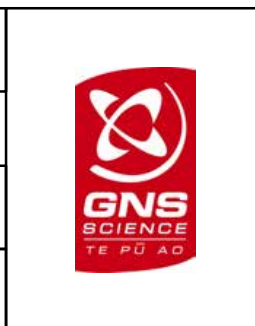
* Taken from report CR2012/317

Background shade model derived from NZAM post earthquake 2011c (July 2011) LiDAR survey resampled to a 1 m ground resolution. Roads and building footprints and types provided by Christchurch City Council (20/02/2012).

PROJECTION: New Zealand Transverse Mercator 2000

DRW:
BL, WR

CHK:
CM, FDP



ESTIMATED LANDSLIDE RUNOUT VELOCITY
Source 11B - Lower Volume (240 m³)

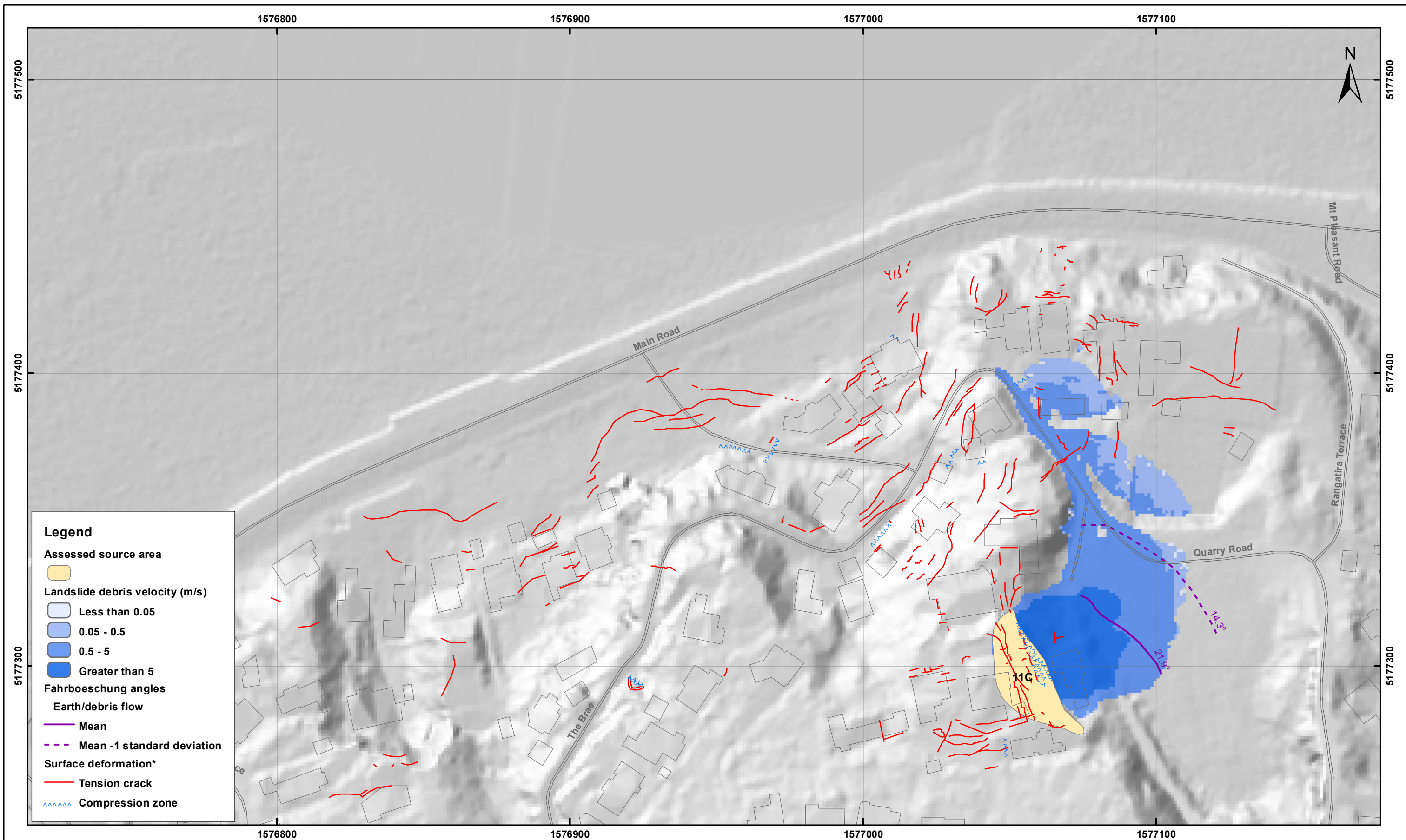
Quarry Road - Port Hills
Christchurch

APPENDIX 5

Map 6

FINAL

REPORT: CR2014/75 DATE: June 2014

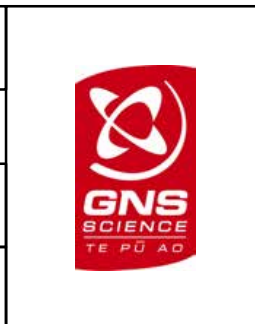


SCALE BAR: 0 25 50 m

EXPLANATION:
 * Taken from report CR2012/317
 Background shade model derived from NZAM post earthquake 2011c (July 2011) LiDAR survey resampled to a 1 m ground resolution.
 Roads and building footprints and types provided by Christchurch City Council (20/02/2012).
 PROJECTION: New Zealand Transverse Mercator 2000

DRW:
BL, WR

CHK:
CM, FDP



ESTIMATED LANDSLIDE RUNOUT VELOCITY
Source 11C - Upper Volume (600 m³)

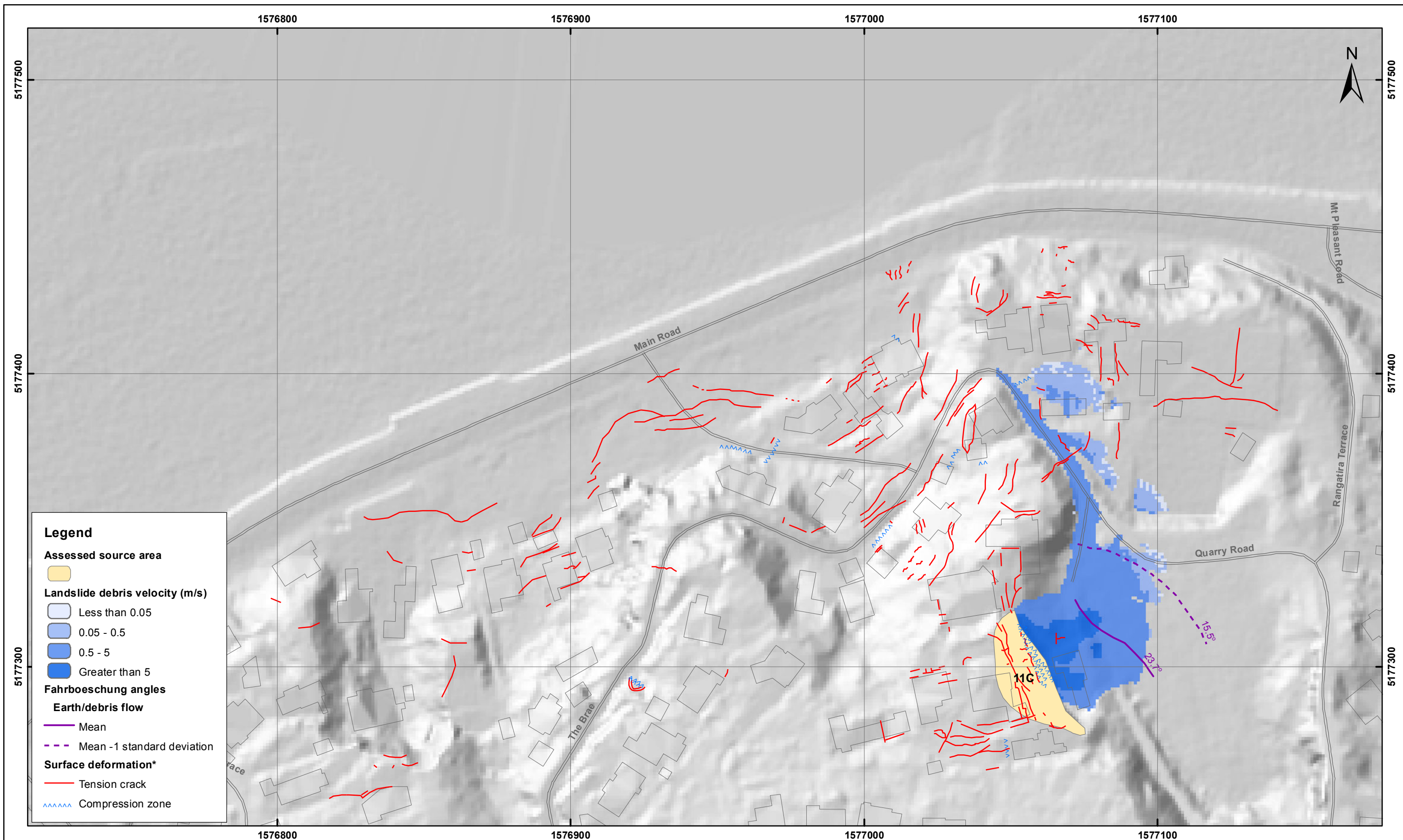
Quarry Road - Port Hills
Christchurch

APPENDIX 5

Map 7

FINAL

REPORT: CR2014/75 DATE: June 2014

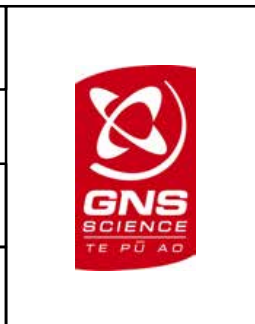


SCALE BAR: 0 25 50 m

EXPLANATION:
 * Taken from report CR2012/317
 Background shade model derived from NZAM post earthquake 2011c (July 2011) LiDAR survey resampled to a 1 m ground resolution. Roads and building footprints and types provided by Christchurch City Council (20/02/2012).
 PROJECTION: New Zealand Transverse Mercator 2000

DRW:
BL, WR

CHK:
CM, FDP



ESTIMATED LANDSLIDE RUNOUT VELOCITY
Source 11C - Middle Volume (270 m³)

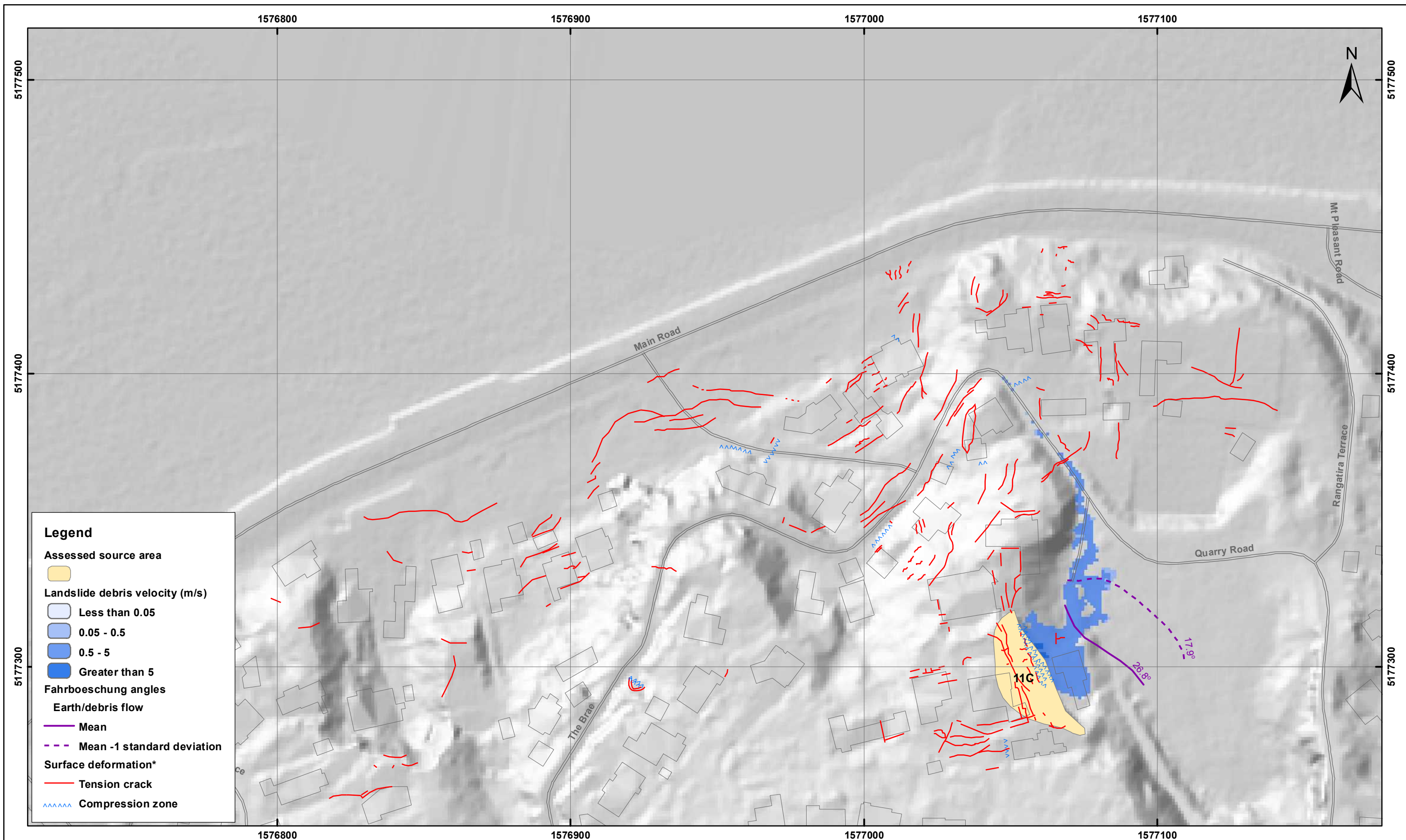
Quarry Road - Port Hills
Christchurch

APPENDIX 5

Map 8

FINAL

REPORT: CR2014/75 DATE: June 2014

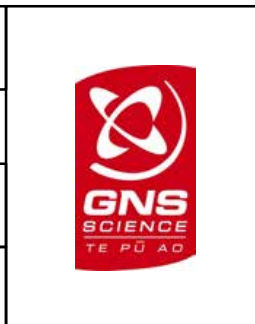


SCALE BAR: 0 25 50 m

EXPLANATION:
 * Taken from report CR2012/317
 Background shade model derived from NZAM post earthquake 2011c (July 2011) LiDAR survey resampled to a 1 m ground resolution.
 Roads and building footprints and types provided by Christchurch City Council (20/02/2012).
 PROJECTION: New Zealand Transverse Mercator 2000

DRW:
BL, WR

CHK:
CM, FDP



ESTIMATED LANDSLIDE RUNOUT VELOCITY
Source 11C - Lower Volume (70 m³)

Quarry Road - Port Hills
Christchurch

APPENDIX 5

Map 9

FINAL

REPORT: CR2014/75 DATE: June 2014



www.gns.cri.nz

Principal Location

1 Fairway Drive
Avalon
PO Box 30368
Lower Hutt
New Zealand
T +64-4-570 1444
F +64-4-570 4600

Other Locations

Dunedin Research Centre
764 Cumberland Street
Private Bag 1930
Dunedin
New Zealand
T +64-3-477 4050
F +64-3-477 5232

Wairakei Research Centre
114 Karetoto Road
Wairakei
Private Bag 2000, Taupo
New Zealand
T +64-7-374 8211
F +64-7-374 8199

National Isotope Centre
30 Gracefield Road
PO Box 31312
Lower Hutt
New Zealand
T +64-4-570 1444
F +64-4-570 4657